Scuola Normale Superiore_Pisa

Regulation of TMEM16A Alternative Splicing

Thesis Submitted for the Degree of Doctor of Philosophiae in Life Sciences

Candidate: Ifeoma Ubby

Supervisor: Prof. Franco Pagani, M.D. Ph.D

Pisa, 2011/2012

Keep moving forward…

TABLE OF CONTENTS

ABSTRACT

TMEM16A/Anoctamin1 is a novel calcium-activated chloride channel involved in neuronal and cardiac excitation, vascular tone, pain perception and olfactory and sensory signal transduction and GI tract motility. It is also associated to diverse type of cancer including breast cancer malignancy. Alternative splicing (AS) of exons 6b, 13 and 15 generates functionally distinct TMEM16A isoforms with different electrophysiological properties. To study their splicing regulation, I performed in minigene system a systematic analysis of exonic and intronic regulatory elements followed by co-transfection of a panel of splicing regulatory factors. Analysis of TMEM16A pre-mRNA splicing supports a model in which each exon is regulated by different *cis*- and *trans*-acting elements. Exon 6b inclusion is regulated primarily by SRSF9 and TRA2B, through a unique GAA-rich ESE element. Exon 15 is enhanced only by TIA1 and FOX1 and this effect is mediated by downstream intronic sequences. On the other hand, the small exon 13, included in most human tissues, was mainly skipped in the minigene and only FOX1 and U2AF65 enhanced its inclusion.

To understand if there is any preferential association between three AS exons, I have evaluated TMEM16A isoforms using a long range RT-PCR assay that amplifies transcripts across the AS events. Coordination between distant alternative spliced exons in the same gene has been suggested to be an important mechanism to regulate gene expression but very few genes have been studied in detail. I observed that the selection of exons 6b and 15 is preferentially coordinated in several human normal tissues: mature transcripts that predominantly include exon 6b tend to exclude exon 15. Unexpectedly, this coordination was not conserved in mouse tissues. This was mainly due to the fact that exon 15 was largely and predominantly excluded in the mouse, a fact that suggest a peculiar evolutionary conservation of AS in this gene.

To explore if changes in splicing coordination of the two major AS events are associated to cancer development I evaluated normal mammalian tissue and corresponding breast tumors of the same cohort, obtained from surgical excision

(n=18). The distribution of individual AS events did not change between normal and tumor tissues. However, the TMEM16A splicing coordination increased significantly in tumors. Indeed, the splicing coordination was present in 50% of normal mammalian breast tissues and in 84% in tumors. In conclusion this study identifies several *cis*-acting elements and *trans*-acting factors involved in the regulation of TMEM16A Alternative Splicing and provides evidence of its intragenic splicing coordination. The increase of TMEM16A splicing coordination observed in breast tumor, might represent a common event in genes with multiple AS events.

INTRODUCTION

The genetic information is stored in DNA, which is transferred from one generation to the next. During the life of a cell, this DNA information is regained as RNA. Whereas DNA is chemically very stable and therefore well suited to archive the genetic information, RNA is chemically more reactive, and thus unstable. Therefore, with the exception of RNA viruses, RNA does not store the genetic information but rather acts as an intermediate between DNA and proteins.

However, RNA does not simply copy the genetic information, as the primary RNA transcript generated from DNA undergoes processing. Most human polymerase II transcripts contain exonic sequences that are finally exported into the cytoplasm, whereas the intervening sequences (introns) remain in the nucleus. The removal of the introns and the joining of the exons is known as pre-mRNA splicing (Berget and Sharp 1977). Almost all human protein-coding genes undergo alternative splicing (AS) (Pan, Shai et al. 2008); this means that, depending on the cellular conditions, an alternative exon can be either included or removed from the final messenger RNA (mRNA).

RNA is more than just a copy of the genetic code: RNA can “interpret” the genetic information depending on environmental cues that the cell receives. Alternative splicing is a central mechanism in this interpretation process, as it allows the expression of selected parts of gene.

Due to its role as a flexible “interpreter”, AS strongly enhances the number of proteins that can be encoded by the genome. For example, by combining one exon out of four alternatively spliced regions that contain 12, 48, 33, and 2 alternative exons each, the *Drosophila Dscam* gene can generate 38016 protein isoforms (Celotto and Graveley 2001). Alternative splicing can thus generate from a single gene a number of protein isoforms that is larger than the total number of protein coding genes. The ability to change the output of the genetic information depending on cellular states, and the ability to expand the information content of the genome, makes AS a central element in gene expression.

Gene Expression and RNA Splicing

In higher eukaryotes, splicing constitutes a critical mode for the regulation of gene expression at the level of RNA processing (Black 2003). The large majority of eukaryotic protein coding genes are transcribed as precursors of messenger RNAs (pre-mRNAs), in which exons are separated from each other by intervening regions of non-protein coding information (introns), which have to be correctly spliced out to produce a mature mRNA. Splicing of pre-mRNAs occurs in a two-step reaction (figure 1A). In the first step, the 2'OH of a specific branch-point nucleotide performs a nucleophilic attack on the first nucleotide of the intron at the 5' splice site forming the lariat intermediate. In the second step, the 3'OH of the released 5' exon performs a nucleophilic attack at the last nucleotide of the intron at the 3' splice site thus joining the exons and releasing the intron lariat (Black 2003).

Signals that specify exon–intron junctions are located at the termini of introns. cis-Acting nucleic-acid elements are: located at the 5'spice site (5'SS AG/GURAGU), the branch point (BP) sequence (CURAY), the polypyrimidine (Py) tract (a run of polypyrimidines located between the 3' splice site and the branch point), and the 3' splice site (3'SS, YAG). These four canonical intronic sequences are recognized by specific components of the spliceosome or associated splicing factors. Indeed, the 5'SS, BP and 3'SS of nuclear pre-mRNA introns are defined by very short consensus sequences that, in metazoans, are very poorly conserved (figure 1B). Unlikely most other enzymes, the spliceosome does not have a preformed active site; on the contrary, the catalytic center must be assembled anew on each pre-mRNA intron in a stepwise interaction of five uridine-rich (U-rich) small nuclear ribonucleoproteins particles (snRNPs) called U1, U2, U4/U6 and U5, and a large number of protein splicing factors (Kramer 1996), and participate in several RNA-RNA and RNA-protein interactions. Human spliceosome also interact with a large number (from 150 to 300) of non-snRNP proteins, including heterogeneous nuclear RNPs (hnRNPs) and serine-arginine (SR) proteins (Wahl, Will et al. 2009).

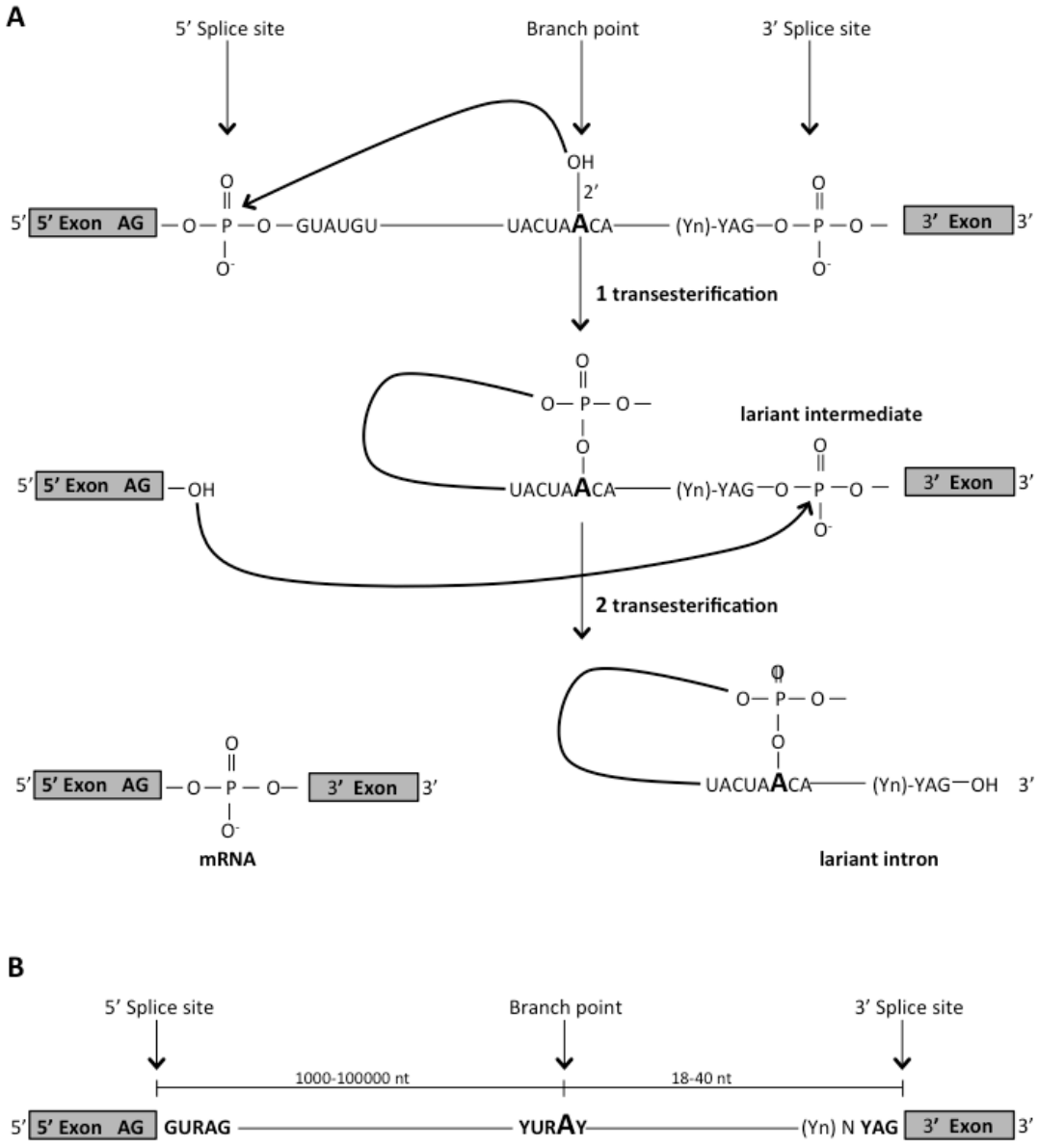

Figure 1. Schematic representation of the two step splicing pathway of nuclear pre-mRNA. *A,* two successive phosphoester transfer reactions. In the first step, a specific adenine nucleotide in the intron sequence (indicated in *bold)* attacks the 5' splice site and cuts the sugar-phosphate backbone of the RNA at this point. The cut 5' end of the intron becomes covalently linked to the adenine nucleotide, thereby creating a loop in the RNA molecule. The released free 3'-OH end of the exon sequence then reacts with the start of the next exon sequence, joining the two exons together and releasing the intron sequence in the shape of a *lariat.* The two exon sequences thereby become joined into a continuous coding sequence; the released intron sequence is then degraded i. *B,* two exons are separated by an intron. Between them are reported the consensus sequences present within an intron. The arrows indicate the position of the 5' (GU) and 3' (AG) splice sites and the branch point (A), shown in bold, the polypirimidine-tract is represented by (Yn). There are several conserved nucleotides near the sequences surrounding the intron-exon junctions that act as essential splicing signals. N means any base. To note only the universally conserved nucleotides are the dinucleotide cores of the 5' and 3' splice together with the branch point (A) showed 100% of frecquency of occurrence.

Each snRNA have a U-rich RNA molecule and a variable number of associated proteins, which make up more than two-thirds of its mass. The U snRNPs undergo a complex maturation process before becoming functional in the spliceosome. All U snRNAs contain a so-called “Sm” binding site that serves as a binding platform for Sm proteins. Sm proteins (B/B', D1, D2, D3, E, F and G) are common factors of U1, U2, U4 and U5, which bound to a conserved Sm motif on the each snRNA. Besides Sm and Sm-like proteins, other particle-specific proteins associate with snRNAs. The number of specific associated proteins vary greatly among the U snRNAs, from only 3 for U1 snRNP to more than 20 for U2 snRNP (Stanek and Neugebauer 2006). The association of the U snRNP-specific proteins is believed to happen in the nucleus since it is known that import of some of them (U1A and U1C for U1 snRNP; U2A' and U2B''for U2 snRNP) occurs independently of snRNA nuclear import ((Feeney and Zieve 1990); (Jantsch and Gall 1992); (Kambach and Mattaj 1994)).

The RNA and protein component of the snRNPs play critical roles in splice site recognition and spliceosome assembly follows a carefully orchestrated stepwise pathway (Will and Luhrmann 2001). The basic steps of the splicing cycle, whereby a single intron is removed from the pre-mRNA being processed, are shown in figure 2. Initially, the U1snRNP interacts with the 5’SS of the pre-mRNA to form the so-called E complex (E –*early*- complex or commitment complex). U1 snRNP-associated proteins U1-70k and U1C stabilize this transient interaction. The U2 Auxiliary Factor snRNP (U2AF65/35) identifies the AG dinucleotide at the 3’ intron/exon junction together with the polypyrimidine tract $(Py)_n$. Mutual stabilization of contacts with the U2AF bound to the 3' SS and the upstream U1 snRNP at the 5' SS can be mediated by members of the serine/arginine-rich (SR) protein family, generating the A complex (figure 2). The establishment of multiple weak interactions from the 3' SS to the 5' SS defines an exon, and constitutes the commitment step towards the splicing pathway ((Robberson, Cote et al. 1990); (Berget 1995)). The transition from A to B complex is marked by the ATP-dependent addition of the U4/U6 and U5 snRNP, preassembled in U4/U6.U5 tri-snRNP. At this level all snRNPs are present, but the spliceosome is catalytically inactive and requires a conformational and compositional rearrangement to come

active and to promote the first transesterification step of splicing. During spliceosome activation, U1 and U4 are destabilized or removed, leading to a B* complex (B activated complex) (Turner, Norman et al. 2004). Eight evolutionarily conserved DExD/H-type RNA-dependent ATPase/helicases act at specific steps of the splicing cycle to catalyze RNA-RNA rearrangements and RNP remodelling events (Valadkhan, Mohammadi et al. 2009). The C complex is then formed, and the spliceosome undergoes the first catalytic step. Subsequently additional rearrangements in the RNPs network are necessary prior to undergo the second transesterification reaction ((Wahl, Will et al. 2009); (Konarska, Vilardell et al. 2006)). Complex C catalyzes the second step, after which the spliceosome dissociates. The mRNA product is then released, while the excised intron remains bound to U2, U5 and U6. Finally, these snRNPs also dissociate and the next round of splicing can then take place.

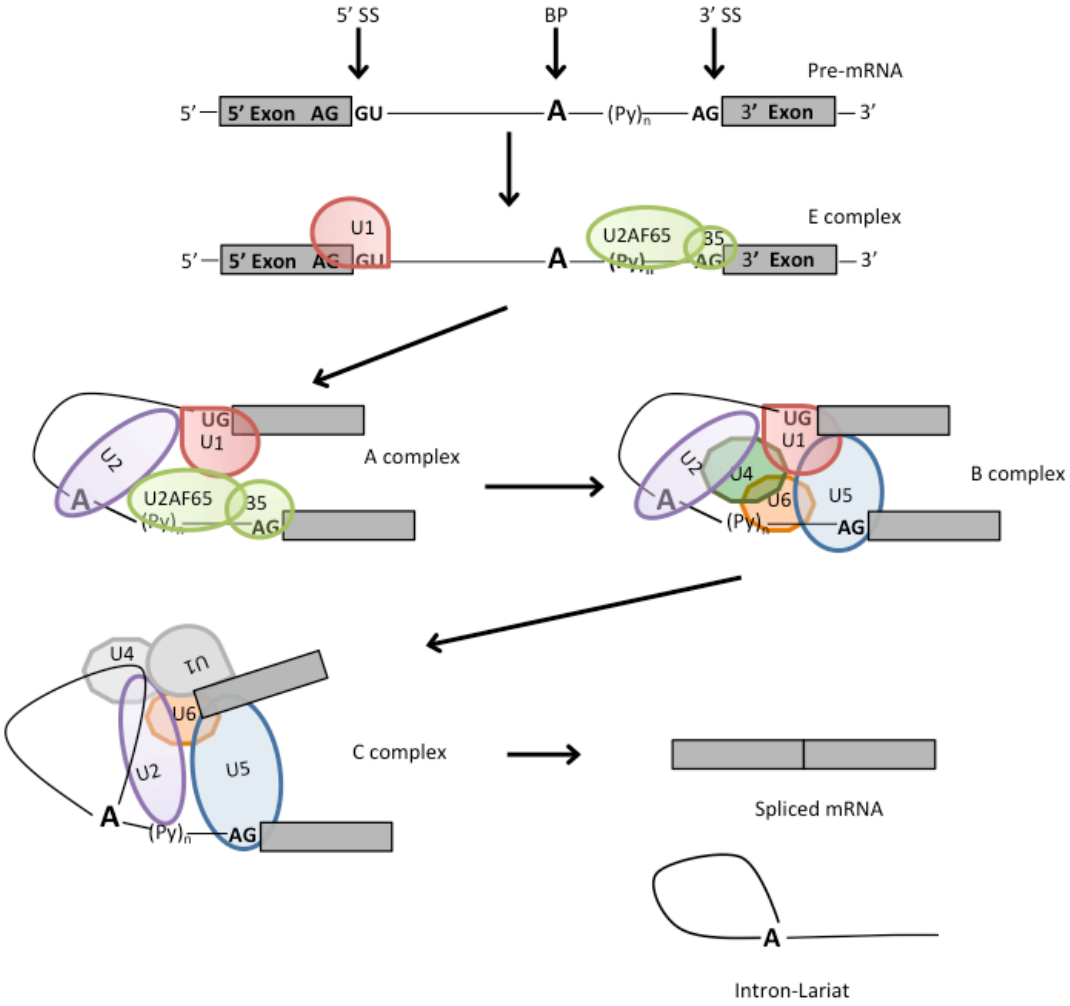

Figure 2. Basic exon recognition and spliceosome assembly. The spliceosome assembles onto the pre-mRNA in a stepwise manner. A consensus sequences that define exon/intron boundaries. Exons are noted by grey *boxes*, and introns by *lines*. Consensus nucleotides are indicated above the line, and the term for sequence is shown below. *5'ss,* splice site; *bp*, the branch point; *3'ss*, splice site; *Py*, polypyrimidine tract. In the E complex, U1 binds the 5′ splice site, U2AF65 binds the polypyrimidine tract, and U2AF35 binds the 3′ splice site. U2AF65 recruits U2 to the branch point, forming the A complex. The B complex forms when the U4/U6-U5 tri-snRNP joins, and then rearragement of the components forms the C complex. U4/U6 base pairing is destabilized, allowing U6 to displace U1 at the 5′ splice site and base pair with U2. U1 and U4 are displaced from the complex. U5 interacts with the 5′ and 3′ splice sites, bridging the exons. It is in the final complex where the two sequential transesterification reactions occur. The end result is the fully spliced mRNA and the intron lariat, which is debranched and degraded.

Signals for Splicing Specificity

Splice Site Sequence

The excision of the introns from a pre-mRNA and the joining of the exons are directed by special consensus sequences at the intron/exon junctions called splice sites.

The 5'SS, also referred to as the donor site, is defined as a single sequence element, with a length of nine nucleotides (nt) (figure 3A). In mammals only the first two bases of the intron GU are universally conserved although they are not the only important bases (Aebi, Hornig et al. 1987). Indeed, this site follows a degenerate consensus sequence YAG/GURAGU (where Y is a pyrimidine, R is A or G) (Sun and Chasin 2000), that base pairs with U1 snRNA in the early spliceosomal E complex.

At the other end of the intron, the 3' splice site region, also referred to as the acceptor site, has three conserved sequence elements: the branch point (BP), the polypyrimidine tract $(Py)_n$ or PPT, and a terminal AG at the extreme 3' end of the intron, as figure 3B shows (Reed 1989). The BP is characterized by the presence of a conserved "A" surrounded by a highly degenerated motif YNYURAY (Y=pyrimidine and R= purine) (Reed and Maniatis 1985). It is commonly found about 18-40 nucleotides upstream of the AG dinucleotide ((Ruskin, Krainer et al. 1984); (Reed and Maniatis 1985)) although some exceptions can be found hundreds of nucleotides away (Reed 1989). The recognition of the branch site involves a base-pairing with the U2 snRNP auxiliary factor (U2AF) in order to form the spliceosome A complex (Berglund, Chua et al. 1997). The 3'SS is functionally coupled with the PPT located between the branch site and the terminal AG at the intron/exon junction (Reed 1989). $(Py)_n$ can display a high percentage of pyrimidines, it varies in length and distance to the BP and the AG. It is essential for efficient branch-point utilisation and correct AG recognition as it has been shown that progressive deletion of the polypyrimidine tract impairs splicing while elongating its length can improve its efficiency (Roscigno, Weiner et al. 1993). The terminal AG dinucleotide or acceptor site defines the 3' border of the intron. This site is characterized by the short YAG/G sequence (Y pyrimidines; the slash is the

intron-exon boundary and the underlined nucleotides are conserved). Even if it is essential for the second step of splicing reaction no base-pairing interactions with snRNAs are involved in recognizing this sequence (Wu, Romfo et al. 1999). The sequences between the branch-point and the acceptor site are commonly devoid of AG dinucleotides (Gooding, Clark et al. 2006).

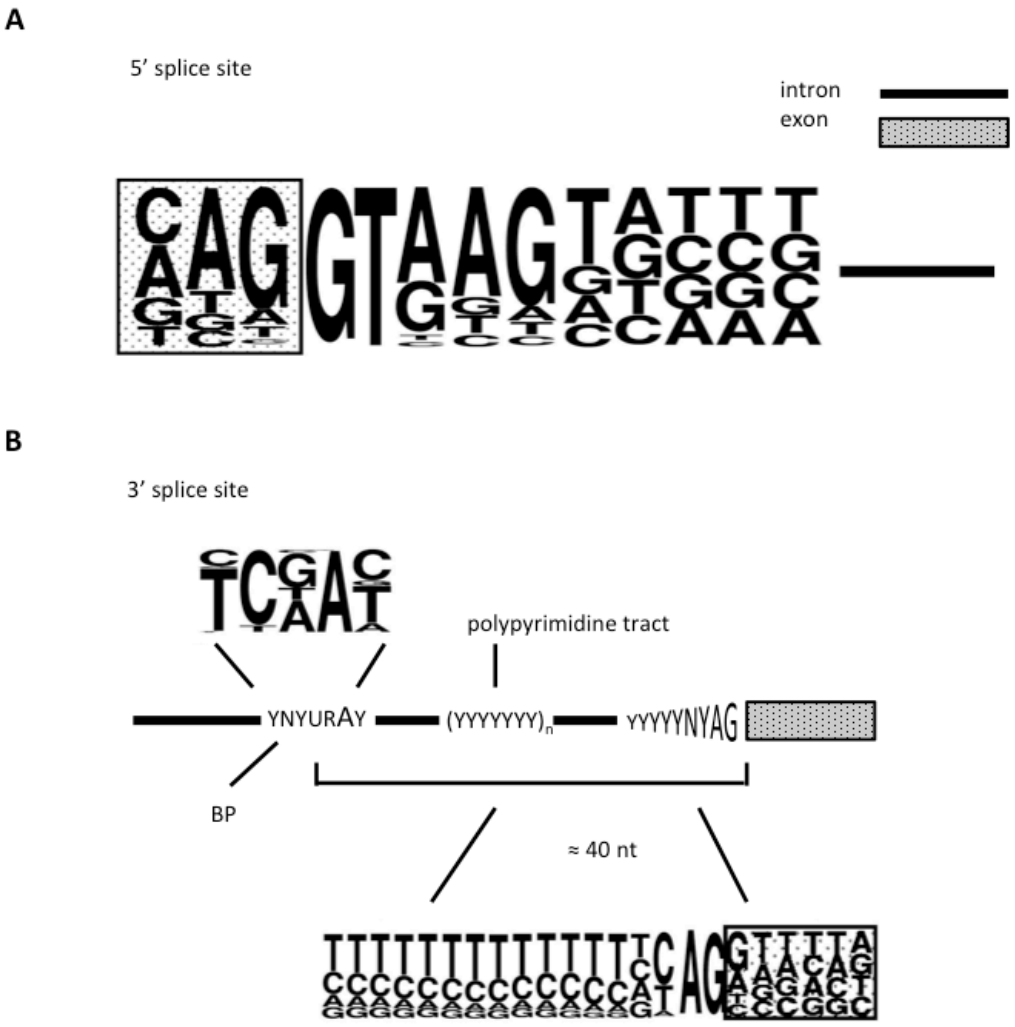

Figure 3. Consensus sequences of splice sites. Below the consensus sequences for each canonical signals are shown. *A,* Diagram of the 5' end of the intron, recognized initially recognized by U1 snRNP, is identified by 9 nt consensus sequences shown. *B,* Diagram of the 3' splice site. The 3 elements within approx. 40 nt of the intron's 3' end are shown.

The role of these RNA sequence elements is of such importance that the sequence complementarity of the 5'SS to U1 snRNA and the extent of the $(Py)_n$ at the 3' SS are used to determine the strength of splice sites. A greater complementarity to U1 snRNA and a longer uninterrupted $(Py)_n$ is translated into higher-affinity binding sites for spliceosomal components and, thus, a more efficient splice site recognition (Hertel 2008).

Splicing Regulatory Elements

The information content of 5'SS, 3'SS, and BP signals is less and less preserved with an increasing number of introns ((Lim and Burge 2001); (Irimia, Penny et al. 2007)), and in higher eukaryotes it is often insufficient to ensure correct RNA splicing. This intrinsic feature of the splice sites allows for a great degree of regulation of the splicing process in the form of alternative splicing. It has also an undesired consequence: *pseudo* splice sites largely outnumber real splice sites and in many cases their strength can surpass that of correct splice sites. Thus, the growing degeneracy, in turn, opens up the possibility for making alternative splice sites choices, and additional signals become necessary (Wang, Rolish et al. 2004), in particular when weak splice sites are involved.

In addition to the conventional splicing signals located at exon-intron boundaries, other *cis*-elements in pre-mRNA increase exon inclusion by serving as binding sites for the assembly of multicomponent splicing enhancer complexes (Cartegni, Chew et al. 2002). These elements, localized both in exon and intron sequences, act by stimulating or inhibiting the use of specific splice sites. Depending on their location and their function, these elements are referred as exonic splicing enhancers (ESE), that facilitate the process of exon definition, thus helping exon inclusion in the mRNA ((Mardon, Sebastio et al. 1987); (Lam and Hertel 2002)). Although originally discovered in regulated exons, ESEs are today also known to be components of constitutively spliced exons ((Mayeda, Screaton et al. 1999); (Schaal and Maniatis 1999)). ESEs assist early spliceosomal complex formation by interacting with components of the splicing machinery that make up previously described the E complex (Reed 1996). This is done generally through the

serine/arginine-rich proteins, SRs, and SR related proteins that generally assemble on ESEs elements to promote both regulated and constitutive splicing by forming networks of interaction with each other (Blencowe 2000) and are also involved in recruitment of spliceosomal components such as U1 snRNP to the 5'SS, or U2AF to the 3'SS to the regulated splice site ((Black 2003); (Graveley 2000)). Thus, SR proteins bound to ESEs function as general activators of exon definition (Lam and Hertel 2002) (figure 4). Several algorithms have been constructed to predict splicing enhancing or silencing regions (Chasin 2007). These computational tools have been helpful in identifying putative exonic splicing enhancers (PESEs) and putative exonic splicing silencers (PESSs).

While the positive regulation of splicing is thought to occur as a result of protein-protein interaction strengthening the recognition of the splice site, negative regulation of splice site choice often result from the prevention of the splice site to be recognized. These negative regulatory sequences, within an exon, are called exonic splicing silencer, ESSs, and in the majority of cases are bound by particular hnRNP family proteins. *Cis-acting* regulatory elements in the intronic sequences have being studied to a lesser extent than those present in exons. Like exonic regulation, there are both positive and negative *cis-acting* sequences in the intron, so called intronic splicing enhancer (ISE) and intronic splicing silencer (ISS). Some of the best characterized ISSs include binding sites for hnRNP A1 protein (described below) ((Hui, Hung et al. 2005); (Matlin, Clark et al. 2005); (Wagner, Baraniak et al. 2005); (Kashima, Rao et al. 2007)); hnRNP I, also called PTB and PTBP1. PTB has strong RNA binding activity, and its preferred binding site is UCUU, often flanked by pyrimidines (Perez, Lin et al. 1997). Initially it was hypothesized that PTB is a positive splicing regulator, but later studies revealed that PTB is rather a splicing repressor ((Garcia-Blanco, Jamison et al. 1989); (Valcarcel and Gebauer 1997)). Early models of PTB repression suggested that it may compete with U2AF65 for polypirimidine tract, however regulation by PTB often requires additional PTB binding elements.

There are several elements known to act as intronic splicing enhancers, ISE's, but the proteins that mediate their effects are less well characterized than for ESE's. One well characterized ISE element is the triplet (GGG) which often

occurs in clusters and can enhance recognition of adjacent 5’ or 3’ splice sites ((McCullough and Berget 1997)). Intronic (CA) repeats in several cases can enhance splicing of upstream exons, probably through binding of hnRNP L protein ((Hui and Bindereif 2005); ((Hung, Heiner et al. 2008)). TIA-1 is an important ISE protein that binds pyrimidine-rich sequences that binds downstream of exon 9, of the CFTR (cystic fibrosis transmembrane conductance regulator) gene (Zuccato, Buratti et al. 2004); (Venables 2007)). Another example in which TIA-1 regulates splicing via ISE elements is Fas exon 6 that can be included or skipped to generate mRNA encoding, respectively, a membrane boud form of the receptor that promotes apoptosis or a soluble isoform that prevents programmed cell death. TIA-1 protein promotes U1 snRNP binding to the 5’ splice site of intron 6, by binding to the ISE element in the +6 to 20 position downstream of Fas exon 6, which in turn facilitate exon inclusion (Izquierdo, Majos et al. 2005).

Two RNA-binding proteins with family members expressed specifically in nervous system and/or muscle tissues are the muscleblind-like (MBNL) and CUGBP/ETR-like (CELF; also known as Bruno-like) factors ((Barreau, Paillard et al. 2006); (Pascual, Vicente et al. 2006)). These factors have been implicated in neurological disorders and in CUG trinucleotide expansion diseases such as myotonic dystrophy (Gallo and Spickett 2010). These factors are also involved in several aspects of mRNA metabolism, including alternative splicing ((Ladd, Charlet et al. 2001); (Ho, Charlet et al. 2004)). Several studies using model pre-mRNA substrates have demonstrated that MBNL and CELF bind intronic CUG-repeat and UG-rich elements respectively. At least some members of this family activate splicing through intronic enhancer elements ((Charlet, Logan et al. 2002); (Ho, Charlet et al. 2004)).

Another common ISE element is the hexanucletide (U)GCAUG motif that represents highly specific recognition element for the Fox family proteins. This element strongly enhances the splicing.

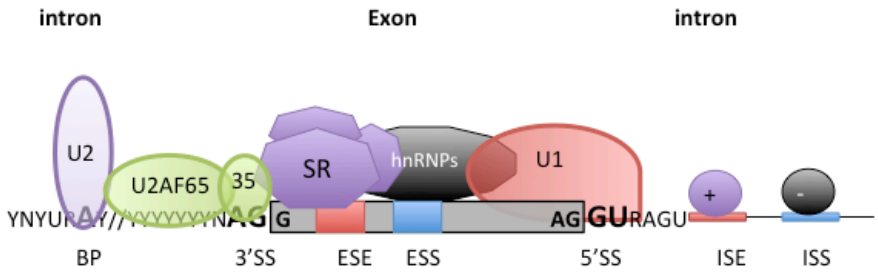

Figure 4. Regulatory elements in pre-mRNA splicing. Schematic representation of the possible distribution of canonical and additional splicing cis-acting elements. The canonical splicing signals that define the exon boundaries are relatively short and poorly conserved sequences. Only the GU at 5' end and the AG at 3' end together with the the branch-point adenosine are conserved (the consensus nucleotides are bold). The polypyrimidine tract of variable length (represented by "y", cytosine or thymine) is reported upstream of the 3'-splice site. The basal components of the splicing machinery bind to the consensus sequences and promote assembly of the splicing complex. The U1 snRNP binds to the 5'-splice site, the U2 snRNP recognizes the branch site and the U2AF localizes to polypirimide tract and 3'splice site sequences. Additional enhancer and silencer elements in the exons (ESE; ESS) and/or introns (ISE; ISS) allow the correct splice sites to be distinguished from the many cryptic splice sites that have identical signal sequences. Trans-acting splicing factors can interact with enhancers and silencers and can accordingly be divided into two main groups: members of the serine arginine (SR) family of proteins and of the heterogeneous nuclear ribonucleoprotein particles (hnRNPs). In general, SR protein binding at ESE facilitates exon recognition whereas hnRNPs are inhibitory. Figure adapted from Pagani and Baralle (Pagani and Baralle 2004).

It has to be noticed that a *cis*-acting element can have overlapping functions as reported for the cystic fibrosis transmembrane conductance regulator gene (CFTR) exons 9 and 12 (Pagani, Buratti et al. 2003; Pagani, Stuani et al. 2003).

In this case, it may be more appropriate to talk about composite exonic regulatory elements of splicing (CERES) (Figure 6). Moreover, different regulatory elements can act in a cooperative fashion. The exonic UAGG motif and intronic GGGG motif overlapping the 5'ss can function cooperatively in the silencing of the

brain-specific cassette exon of the glutamate NMDA R1 receptor gene (Han, Yeo et al. 2005). All these different types of auxiliary *cis*-acting elements contribute significantly to recognition of the correct exons as pointed out by their known role in alternative splicing, contribute significantly to the regulation of constitutive splicing (Cartegni, Chew et al. 2002; Black 2003).

Proteins involved in splicing regulation

The two main players of splicing regulation are: proteins with arginine-serine-rich (RS) domain, and RNA-binding proteins without RS domain. Within the first category, the most important family is the one of SR (serine/arginine-rich) proteins ((Graveley 2000); (Zhong, Wang et al. 2009)), while the second category includes many of the common heterogeneous nuclear ribonucleoproteins (hnRNPs). These proteins can act either positively or negatively depending on where they are binding. Particularly, hnRNPs and SRs have been found as components of distinct regulatory complexes with functional specificity in splicing (David and Manley 2008).

The SR proteins are nuclear phosphoproteins that are concentrated, together with most other splicing factors, in nuclear subregions termed speckels, which are believed to be sites of storage or assembly of splicing factors. It has been proposed that SR proteins and other splicing factors are recruited from the speckles to the sites of active transcription (Lamond and Spector 2003). Thus, certain SR proteins shuttle continuously between the nucleus and cytoplasm (Caceres, Screaton et al. 1998). The SR proteins have a common domain structure of one or two N-terminal RNA-recognition motifs (RRM) followed by an RS domain containing repeated arginine/serine dipeptides (Birney, Kumar et al. 1993) (figure 5).

The RNA binding and the RS domain are modular structures and they can be exchanged between different SR proteins. Differences among SR protein structures depend on the length of the RS domain and the presence or absence of the second RRM domain; when the second RRM domain is present, the sequence is often divergent from the canonical consensus sequence (Graveley 2000). In addition to SR proteins other factors involved in pre-mRNA metabolism can

contain a RS domain. These proteins are usually referred as SR-related proteins and they include both subunits of U2AF, the U1-70K protein and several ATPases (Boucher, Ouzounis et al. 2001). The structural organization of SR proteins suggests a model for their function. The RRM mediates sequence-specific binding to the mRNA, whereas the RS domain seems to be involved mainly in protein-protein interactions (Graveley 2000; Cartegni, Chew et al. 2002).

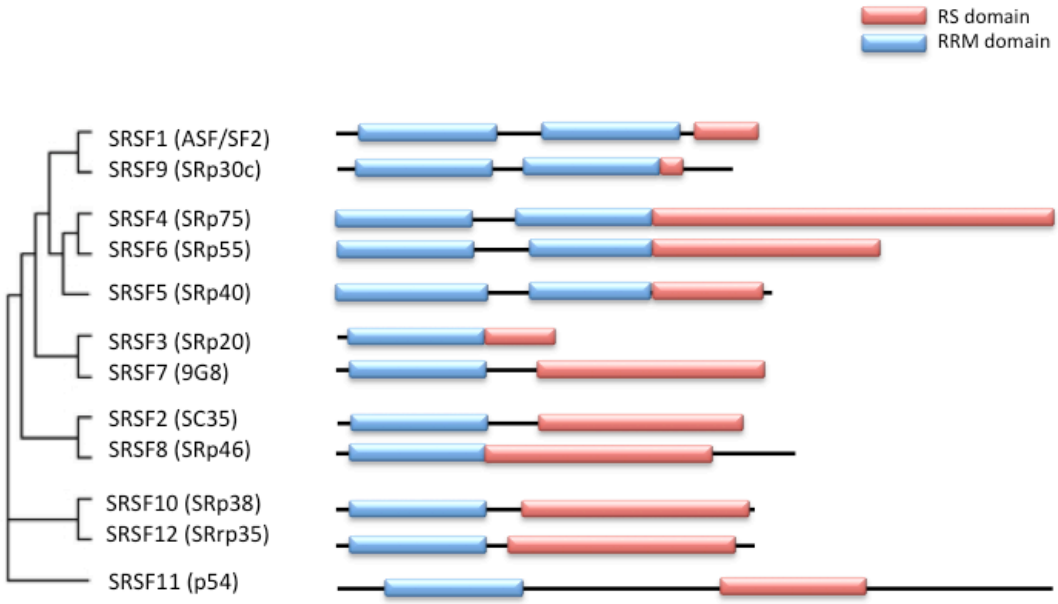

Figure 5. The SR protein family. Scheme representing the level of homology among human SR proteins (Manley and Krainer 2010), based on the result of a multiple sequence alignment using ClustalW2. Alternate names are in parentheses. Both RS and RRMs are modular domains, which means that RRMs can be exchanged between SR proteins, and may still bind to RNA in the absence of the RS domain. The RS domain can bind to a heterologous RNA-binding domain and be still functional.

However, a recent work has reported that the RS domains can also be involved in direct RNA contacts during splicing. A specific interaction between the RS domain and the branch point was described as promoting spliceosome formation (Shen and Green 2004). The sequence-specific binding to pre-mRNAs is crucial for the function of SR proteins in the earliest step of spliceosome assembly (Graveley 2000; Sanford, Ellis et al. 2005). The binding specificity of individual SR protein has been studied using the SELEX technique showing that the consensus

sequences recognized are highly degenerated (Liu, Zhang et al. 1998; Liu, Chew et al. 2000). Due to their involvement in splice site selection, specifically in promoting the selection of the proximal 5'SS (Mayeda and Krainer 1992; Caceres, Stamm et al. 1994) and 3'SS (Caceres, Stamm et al. 1994; Bai, Lee et al. 1999), SR proteins have been reported to be important players in regulating alternative splicing. They exert a role in promoting U2AF binding to weak 3'SS (Wu and Maniatis 1993; Zuo and Maniatis 1996) or antagonizing the activity of negative splicing factor such as hnRNP A1 (Caceres, Stamm et al. 1994) or other SR proteins (Gallego, Gattoni et al. 1997). SR proteins have been shown to promote exon inclusion when bound to a target site within exons (ESEs) (Figure 6A); however, in some cases they can act in a negative fashion. Much of initial understanding of ESEs derives from the regulation of inclusion of exon 4 in the *doublesex* (dsx) gene in Drosophila. The doublesex repeat element (dsxRE), in this exon, is one of the first best characterized ESE element consisting of six repeats of a 13-nucleotide consensus sequence and a purine-rich element located between repeat 5 and 6. A multisubunit complex, containing SR-related proteins, alternative splicing factor Transformer 2 (Tra2) and additional SR proteins assembles on *dsx* ESE element and once fully assembled, the *dsxRE* complex activates the recognition of a weak, sex specific 3' splice site, thereby promoting exon 4 inclusion and the female differentiation pathway ((Ryner and Baker 1991); (Tian and Maniatis 1992)). TRA2B protein, can also bind a target sequence recognized only by one SR protein and regulate splicing decision (Longman, Johnstone *et al*. 2000). TRA2B and other related SR proteins, contains RS domain but no direct RNA-binding domains. The archetype of this class of proteins is the *Drosophilla* female-specific TRA protein, which activates specific splicing events in *Doublesex* and *Fruitless* RNAs ((Ring and Lis 1994); (Lopez 1998)).

The negative effect on splicing can be mediated by the binding to an intronic sequence (ISS) (Ibrahim el, Schaal et al. 2005; Buratti, Stuani et al. 2007) or by the inhibitory complex interaction property (Barnard, Li et al. 2002). Protein-protein interaction screens have indicated, that through their RS domains, SR-family proteins, such as SC35 and ASF/SF2 can interact with each other, with U1-70K SR related protein, and with small U2AF35 subunit of the heterodimeric

U2AF35/65 auxiliary splicing factor, which contains a short RS domain (Fu 1995). These interaction studies led to the proposal that SR family and SR related proteins facilitate splicing by forming interactions across the exons and introns. However, it was proposed that, in naturally occurring enhancers, SR proteins apparently may bind as a component of a multiprotein complex, whom components are not yet identified but may include known splicing factors as the large RS domain proteins SRm160/300, Tra2, U1 snRNP and heterogeneous ribonucleoproteins, such as hnRNPs A1 and hnRNP H. SR protein activity is regulated through phosphorylation/dephosphorylation at multiple positions within the RS domain (Stamm 2008). This phosphorylation modulates protein-protein interaction, that serves as a bridge between the 5' and 3' splice sites across the introns and across the exons and/or between enhancers and adjacent splice site, within the spliceosome ((Tian and Maniatis 1992); (Black 2003); (Ram and Ast 2007)).

The RS domain phosphorylation is required for the translocation of the SR proteins from the cytoplasm to the nucleus and also for the recruitment of these factors from nuclear speckles ("splicing factor compartments") to the sites of pre-mRNA synthesis (Bourgeois, Lejeune et al. 2004).

The hnRNP proteins are large group of molecules identified by their association with pre-mRNA or hnRNAs (heterogeneous nuclear RNAs). These factors remain associated with pre-mRNA until its processing is completed and with mRNA during its export from nucleus to cytoplasm ((Hocine, Singer et al. 2010); (Kohler and Hurt 2007)). At least 20 hnRNPs have been identified, and are designated from hnRNP A1 to hnRNP U (Dreyfuss, Kim et al. 2002).

The structure of hnRNPs is modular, each of them are characterized by one or more RNA-binding domain of the RRM, KH (hnRNP K homology) domain, or RGG (arginine-glycine-glycine) boxes (Burd and Dreyfuss 1994), associated with an auxiliary domain often involved in protein-protein interactions (Dreyfuss, Matunis et al. 1993). For instance, the hnRNP A/B proteins contain two RNP domains at the N-terminus and a glycine-rich auxiliary domain at the carboxy end (Cartegni, Maconi et al. 1996). In a tethered function assay, the glycine-rich region is sufficient to induce exon skipping. The hnRNP proteins show general RNA-binding

specificity and individual proteins display preference for specific sequences that tend to coincide with sites of functional importance in pre-mRNA processing. However, hnRNP proteins generally do not bind specific sites exclusively but recognize different RNA sequences with a wide spectrum of affinities. This RNA binding ability is further modulated by cooperative protein-protein interactions (Dreyfuss, Matunis et al. 1993; Dreyfuss, Kim et al. 2002). hnRNP proteins participate in various nuclear events, such as transcriptional regulation ((Tomonaga and Levens 1995); (Michelotti, Michelotti et al. 1996); (Miau, Chang et al. 1998)), telomere length maintenance ((Eversole and Maizels 2000); (Fiset and Chabot 2001)), immunoglobulin gene recombination (Dempsey, Sun et al. 1999), splicing ((Ashiya and Grabowski 1997); (Chan and Black 1997); (Chou, Rooke et al. 1999); (Del Gatto-Konczak, Olive et al. 1999); Tange, Damgaard et al. 2001; Chen and Manley 2009), pre-ribosomal-RNA (Russell and Tollervey 1992), and 3' end processing (Kessler, Henry et al. 1997). These proteins are also important in nucleo-cytoplasmic transport of mRNA (Lee, Henry et al. 1996), in mRNA localization ((Hoek, Kidd et al. 1998); (Mouland, Xu et al. 2001)), translation (Habelhah, Shah et al. 2001) and stability (Xu, Chen et al. 2001). Although many of the hnRNPs localize in the nucleus, a subset of these proteins shuttle continuously between nucleus and cytoplasm. This indicates a role of these proteins in nuclear export and in other cytoplasmic processes (Pinol-Roma and Dreyfuss 1992; Martinez-Contreras, Cloutier et al. 2007). For many of the hnRNP proteins family multiple isoforms are produced by alternative splicing processes. This diversity is further increased by post-translational modifications of potential physiological significance, including phosphorylation, arginine methylation and sumoylation (Dreyfuss, Kim et al. 2002; Martinez-Contreras, Cloutier et al. 2007).

The hnRNP proteins frequently mediate splicing repression, particularly through binding to ESS elements or by sterical interference through protein interaction (Figure 6B) ((Cartegni, Chew et al. 2002); (Fisette, Toutant et al. 2010). Nevertheless, depending on the position of the splicing regulatory elements, hnRNPs can also associate with enhancer elements to help exon inclusion (Caputi and Zahler 2002) and a generic role for hnRNP A1 and F/H proteins in intron definition has been recently proposed (Martinez-Contreras, Fisette et al. 2006).

Many other cases of hnRNPs antagonizing SR proteins and promoting exon skipping have been reported over the last years ((Okunola and Krainer 2009); (Rooke, Markovtsov et al. 2003); (Guil, Gattoni et al. 2003); (Singh, Androphy et al. 2004); (Dreumont, Hardy et al. 2010)). Alternative mechanisms by which hnRNP proteins promote exon skipping consist in inhibiting intron or exon definition crosstalks ((Izquierdo, Majos et al. 2005); (Sharma 2008)), due to direct competition with U2AF65 for the binding to the $(Py)_n$ ((Lin and Patton 1995); (Matlin, Southby et al. 2007)) or looping of exons through contacts between hnRNPs flanking these exons ((Lamichhane, Daubner et al. 2010); (Oberstrass, Auweter et al. 2005)). hnRNP A1, the most studied, contains two RNA binding domains and a glycine rich auxiliary domain. HnRNP A1 has been shown to induce a shift toward the use of two competing 5'SS (Mayeda, Munroe et al. 1994) and also to affect the use of the 3' splice site, as in the case of K-SAM exon in FGFR2 receptor mRNA, resulting in skipping of this exon (Del Gatto, Gesnel et al. 1996). The application of the SELEX approach has identified UAGGGA/U as the highest "winner" sequence for hnRNP A1 (Burd and Dreyfuss 1994). hnRNP A1 can interact with itself and with other hnRNPs, as well as with U2 and U4 snRNPs ((Buvoli, Cobianchi et al. 1992); (Cartegni, Maconi et al. 1996)).

Other well-known hnRNPs that regulate splicing include the hnRNPs H and F, hnRNP G and hnRNP L. HnRNP proteins belonging to the H group (hnRNPs F, H, H' and 2H9) are encoded by different genes but share common binding site (GGGA) and similar structure. hnRNP H has been shown to act both as a activator and repressor of splicing. For example, hnRNP H acts as a powerful repressor in the rat β-tropomyosin gene by binding to the UGUGGG motif and causing exon 7 skipping in non muscle cells ((Chen, Kobayashi et al. 1999); (Chou, Rooke et al. 1999). It was also demonstrated that insertion of a UGUGGG motif in CFTR exon 9 results in lower inclusion of this exon (Pagani, Stuani et al. 2003; Buratti, Baralle et al. 2004). HnRNP G proteins, in humans, are encoded by two genes RBMY and RBMX located on chromosome Y and X respectively. The product of RBMX has been implicated in splicing regulation of two mutually exclusive exons in the α-tropomyosin gene, in particular hnRNP G was shown to promote skipping of the skeletal muscle specific exon (SK) and to enhance the inclusion of the non muscle

specific exon (NM) (Elliott, Oghene et al. 1998). Other hnRNP proteins, such as hnRNP L, K, E1 and E2, have traditionally been thought to regulate cytoplasmic export, stability and translation of specific mRNA ((Liu and Mertz 1995); (Makeyev, Eastmond et al. 2002); (Perrotti, Cesi et al. 2002)). However, each of these proteins was found also in the nucleus and may be involved in splicing reaction (Pinol-Roma et al. 1992). Rothrock et al. showed that hnRNP L and hnRNP E1 are the primary ESS binding proteins found in nuclear extracts from a T-derived cell line, and that a hnRNP L is the key regulatory protein responsible for ESS depending exon 4 silencing of the CD45 gene (Rothrock, House et al. 2005).

However, additional tissue-specific factors have been described as playing a role in regulating particular splicing events like Nova-1/2 (Jensen, Dredge et al. 2000), nPTB (Markovtsov, Nikolic et al. 2000) in brain, CELF proteins in striated muscle and brain (Ladd, Charlet et al. 2001) and ESRP proteins. A crude generalization of the splicing regulators is that proteins with RS domains are generally activators, while hnRNPs are repressors of splicing. However, there are many exceptions to this rule.

Activation by RS-domain proteins and repression by hnRNPs do not represent a rigid generalization. Interestingly, monosymptomatic forms of cystic fibrosis were found to correlate with the non-functional CFTR protein resulting from exon 9 skipping in the final CFTR transcript (Delaney, Rich et al. 1993). CFTR exon 9 is characterized to have a composite regulatory elements (so called CERES - composite exonic regulatory elements of splicing), a present context-dependent enhancing or silencing properties, which further affect exon 9 processing (Figure 6C) (Pagani, Stuani et al. 2003). However, proteins without RS domain can also activate directly. A nice example is provided by TIA1 splicing factor (T-cell-restricted intracellular antigen-1), which can activate an exon with suboptimal 5'SS through the binding of a pyrimidine-rich enhancer region (PCE, U-rich). The TIA1 interacts directly with U1C protein, thereby facilitating 5'SS recognition by assisting the recruitment of U1 snRNP to the adjacent 5'SS (Forch, Puig et al. 2002; Singh, Seo et al. 2011). In addition, an intronic splicing silencer (ISS) within intron 8-9 recruits SFRSF1 and SRSF5 downregulating exon 9 recognition. Although SR proteins generally promote exon recognition, in this splicing system SFRSF1 and

SRSF5 were found to favor exon 9 skipping (Pagani, Buratti et al. 2000; Buratti, Stuani et al. 2007) (Figure6). Finally, HnRNP proteins can frequently act as either repressor or activators of exon inclusion. In some cases, activation can be indirect, where two proteins have overlapping binding sites but only one act as a repressor. For instance, the repressive action of PTB can be antagonized in some cases by the competitive binding of CELF proteins to adjacent sites ((Gromak, Matlin et al. 2003). As mentioned previously, the SMN2 exon 7 alternative splicing has been extensively studied over the years leading to the identification of several *cis*- and *trans*- acting elements involved (Figure 6B). For instance, the +6C>T change creates a strong exonic splicing silencer (ESS) that recruits hnRNP A1 (Kashima, Rao et al. 2007), but also disrupts a pre-existing SF2/ASF binding site (Vezain, Saugier-Veber et al. 2010). At the 5'SS of the exon 7 there is another hnRNP A1 binding site (Kashima, Rao et al. 2007) and an additional ISS was also found in intron 7-8; both sequences further promote exon 7 skipping. This strong inhibition of exon 7 recognition is balanced by the presence of an ESE in the central region of SMN2 exon 7. This enhancer recruits several factors such as SRp30c, hnRNP G and hTra2β, which act as positive regulators of exon 7 inclusion (Hofmann, Lorson et al. 2000; Hofmann and Wirth 2002; Young, DiDonato et al. 2002; Bose, Wang et al. 2008; Clery, Jayne et al. 2011). Specifically, the integrity of an AG-rich sequence (AAAAAGAAGGAAGG) within the ESE was proved essential for the assembly of a mutimeric complex.

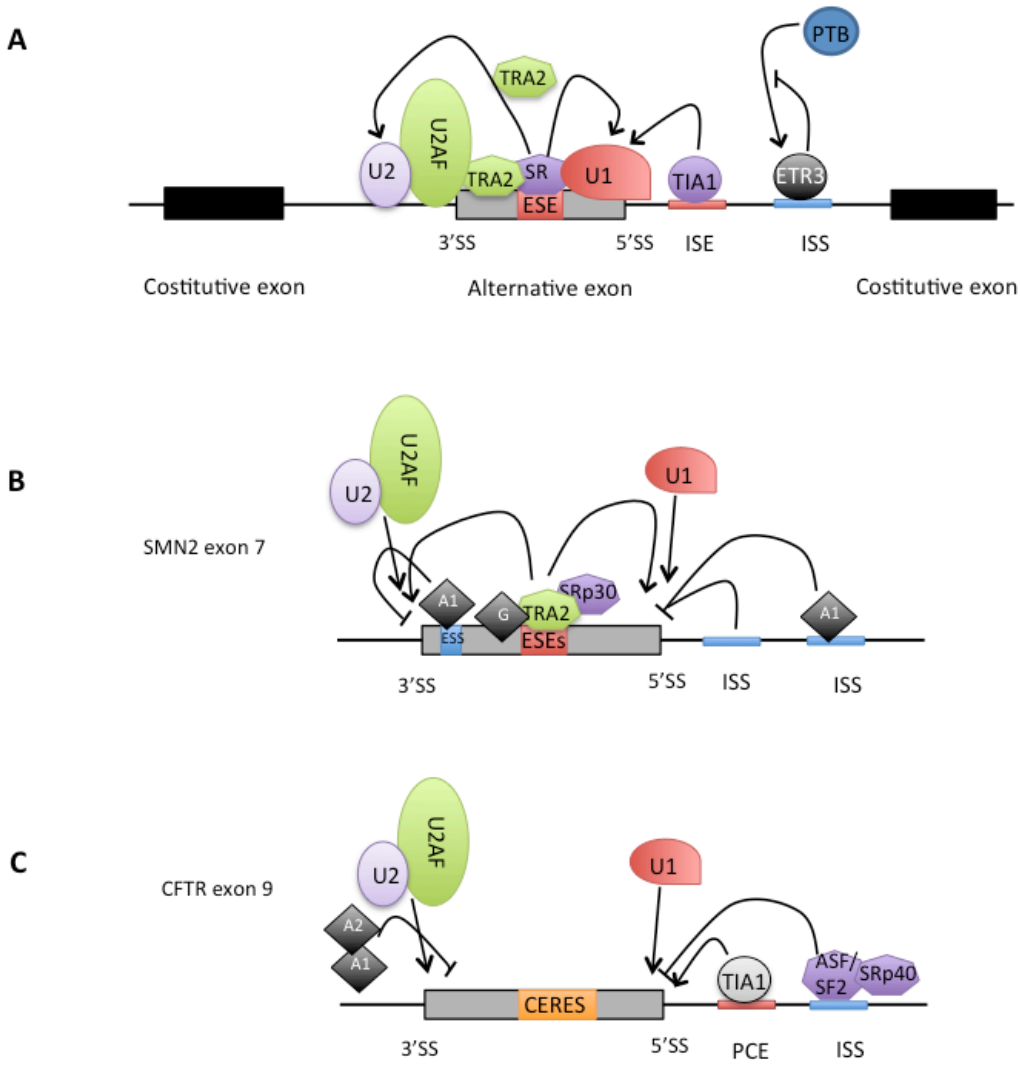

Figure 6. Mechanisms of alternative splicing by splice site selection. Schematic depicting mechanisms of splicing activation. *A,* SR (Ser–Arg) proteins bind to exonic splicing enhancers (ESEs) to stimulate the binding of U2AF to the upstream 3′ splice site (ss) or the binding of the U1 small nuclear ribonucleoprotein (snRNP) to the downstream 5′ ss. SR proteins function with other splicing co-activators, such as transformer 2 (TRA2). T cell-restricted intracellular antigen 1 (TIA1) binds to U-rich sequences (intronic splicing enhancers (ISEs)) immediately downstream of 5′ splice sites to facilitate U1 binding. CELF (CUGBP and ETR3-like factor) proteins, such as ETR3, bind to similar sequences as polypyrimidine- tract binding protein (PTB), thereby activating splicing by competing with PTB. *B,* Example in SM2 gene and *C*, CFTR exon 9 gene. *Cis*- and *trans*-acting elements involved.

Most splicing factors contain multiple RRM copies. It is known that RRMs joined by a single protein chain generally bind very similar sequences, albeit not in an identical manner. This could be the reason that *cis*-acting elements which regulate splicing often contain repetitive sequences (Chen and Manley 2009).

Intron/Exon architecture

Although the snRNPs are necessary for locating intron-exon junctions, this alone does not explain how authentic splice sites are recognized when sequences that match the consensus splice sites are likely to occur elsewhere in the pre-mRNA; and how the splicing machinery joins the exons in the correct order. Thus, in addition to splice site sequences, the exon/intron architecture in the pre-mRNA is important for efficient splice site recognition. Furthermore, the variable arrangement and size of exon and introns affect the splicing outcome; this referred to as intro and exon definition (Berget 1995).

The discrepancy between the length of human exons in comparison with that of introns (Hawkins 1988) led to the "exon definition" model of splicing in which exon is the unit recognized by the splicing machinery (figure 7), and the splice sites are first paired across exons, with subsequent spliceosome assembly proceeding through pairing of neighbour exon units. It was shown that the 5’ capping and the 5’ splice site are necessary to define the first exon (Izaurralde, Lewis et al. 1994). On the other hand, last exon is defined by 3' splice site and polyadenylation signal (Gunderson, Beyer et al. 1994). Moreover, it was shown that exon length might affect splicing. This indication is supported by the observation that a constitutively recognized internal exon was skipped by in vivo splicing machinery if its size was smaller than 50 nucleotides (Dominski and Kole 1991). This finding suggested that the exon is normally skipped because it is too short to allow the spliceosome to assemble at both ends simultaneously. On the other hand, the expansion of internal exons to length above 300 nucleotides led to activation of the cryptic splice site inside the exon or to exon skipping (Berget 1995) indicating that splicing efficiency is affected by length.

Moreover, the strength of splice sites can affect the splicing of both the introns flanking the exon and not only of the intron bearing the mutated splice

site, as predicted from the “intron definition model” and the resulting splicing phenotype was exon-skipping ((Talerico and Berget 1990); (Nakai and Sakamoto 1994)). However recent studies have shown that weak splice sites are more efficiently spliced when introns are small (Fox-Walsh and Hertel 2009); such findings support the concept that splice sites can be recognized across either the intron or the exon.

In the alternative "intron definition" model, splice sites are initially paired across introns rather than exons (figure 7). The intron definition model suggests that the intron is the unit recognized by the splicing machinery and proposes a scanning mechanism where the 5' and 3' splice signals (5’ss and 3’ss) are initially recognized and paired across the intron (Lang and Spritz 1983). Moreover, it is apparent that both exon definition and intron definition might occur in different parts of the pre-mRNA of the same gene and that other *cis*-elements exist to help direct the spliceosome to bone fide splice sites.

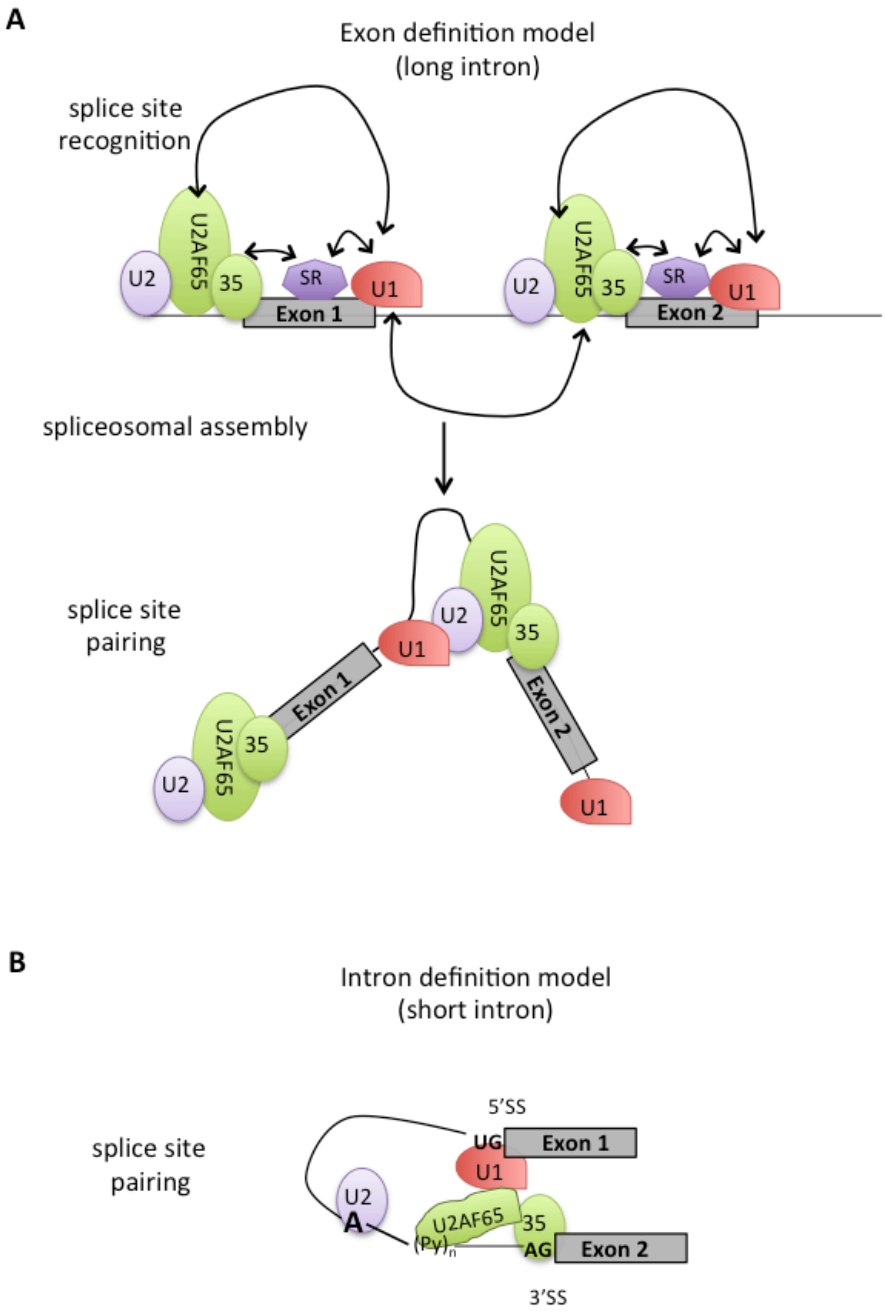

Figure 7. Exon definition versus intron definition models. *A,* Exon definition model: a gene consists of multiple short exons separated by considerably longer introns. In this model the exon is recognized as a unit during early spliceosome assembly. Multiple factors interact with exonic sequences in order to defining the 5' and the 3' borders of the exon. SR proteins can help this "cross exon" recognition through the binding exonic splicing enhancers (ESEs) and recruiting U1 snRNP to the 5'ss, U2AF65 and U2AF35 subunits to the PPT and to the 3'ss, respectively. *B,* Intron definition model: it has been proposed for the systems in which pre-mRNA has small introns. In this case the intron, rather than exon, is the recognized unit. Multiple factors favour the 5' and the 3' ss pairing at the intron ends. SR proteins function in a "cross intron" recognition complex by bridging together the U1 snRNP bound to the upstream 5'ss and the U2AF65 and U2AF35 subunits bound to the PPT and to the AG of the downstream 3'ss, respectively. Adapted from Ram and Ast (Ram and Ast 2007).

Alternative Splicing

The use of different pairs of splice sites generates distinct mRNA isoforms from a single gene, a phenomena known as alternative splicing. Although initially alternative splicing was thought to be only a minor RNA processing pathway (Sharp 1994) it has been recently estimated that about 95% of the human genes show alternative splicing, with about 80% of these events resulting in significant levels of different protein sequences ((Wang, Sandberg et al. 2008);(Pan, Shai et al. 2008)). Consequently alternative splicing generates protein isoforms with different biological functions, displaying distinct protein domains, subcellular localization or catalytic ability. This fact highlights the well-known relevance of alternative splicing in many cellular processes such as sex determination, cell differentiation, cell transformation or apoptosis ((Black 2003); (Tazi, Bakkour et al. 2009); (Smith and Valcarcel 2000); (Nilsen and Graveley 2010); (Pajares, Ezponda et al. 2007)). Therefore, alternative splicing is a key regulator of gene expression that also provides to proteome complexity. In fact, the enormous contribution of alternative splicing to the generation of proteomic diversity is believed to constitute a driving force in metazoan evolution ((Nilsen and Graveley 2010);(Keren, Lev-Maor et al. 2010); (Xing and Lee 2006); (Calarco, Xing et al. 2007)).

Every conceivable pattern of splicing can be found in nature (figure 8). A regulated exon can sometimes be included and sometimes excluded to produce a final transcript with an alternative coding sequence. In addition, introns that are normally excised can be retained in the mRNA or the position of either 5' or 3' ss can be shifted to make exons longer/shorter. A regulated exon that is sometimes included and sometimes excluded from the mRNA is usually referred to as a "cassette" exon. In some cases, multiple cassette exons are mutually exclusive producing mRNAs that always include one of few possible exon choices. In addition to these changes in splicing, alterations in transcriptional start site or polyadenylation site or the presence of N alternative cassette exons allow production of multiple mRNAs from a single gene. All these individual patterns can be combined in a single transcription unit to produce a complex array of splice isoforms ((Black 2003); (Smith and Valcarcel 2000)). Alternative inclusion or

skipping of cassette exons are the most common events in U2-type introns, while alternative 5' and 3' ss choices are the most observed alternative splicing events in U12-introns, due to the incompatibility of chimeric U12-U2 spliceosomes (Chang, Chen et al. 2008).

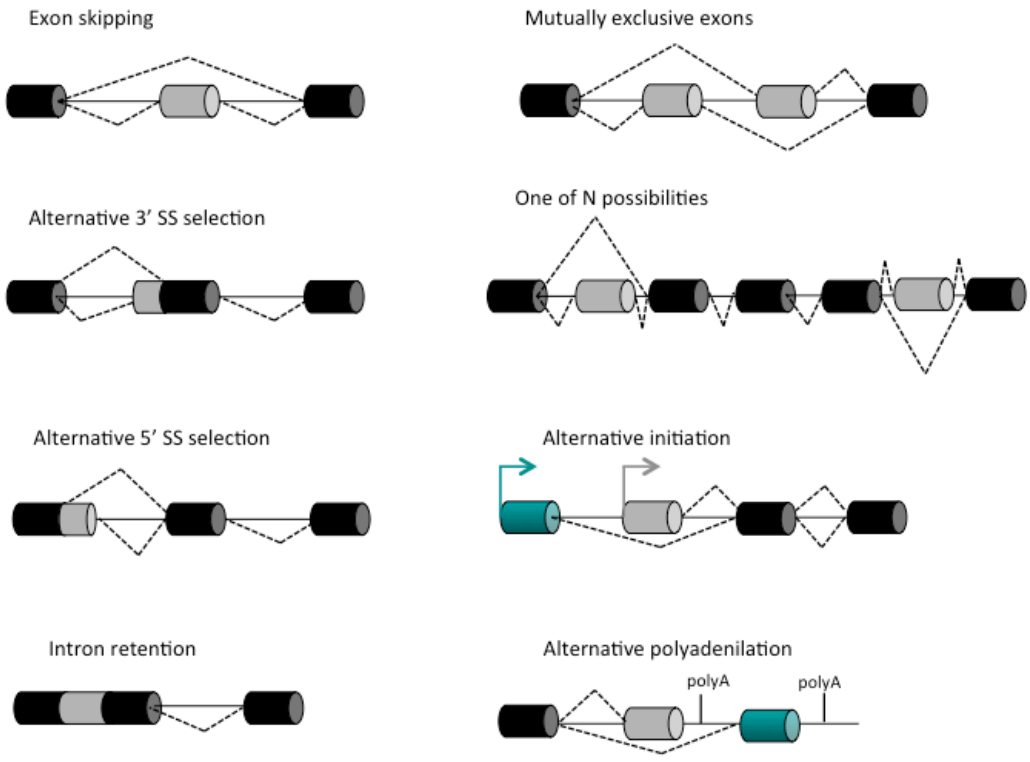

Figure 8. Patterns of alternative splicing. Alternative splicing generates different segments within mRNAs. Black boxes represent constitutive exons and coloured boxes indicate alternative exons.

The mechanisms that determine which splice sites are used and how this selection is regulated in different cell types or developmental stages have been heavily studied in recent years although it is clear that further studies will be required to fully understand these processes. Most alternatively spliced exons are thought to be controlled by multiple auxiliary *cis*-acting splicing sequences (see below), whose activity depends on their location relative to the canonical splice sites and the *trans*-acting factors that recognize them ((Black 2003); (Cartegni and Krainer 2002)). Indeed much effort has been made in identifying the

"combinatorial code" guiding alternative splicing choices, and recently a splicing code has been proposed, based on genome-wide data generated by splice-junction microarrays or RNA-seq studies ((Castle, Zhang et al. 2008); (Barash, Calarco et al. 2010)). Furthermore, the complexity of the spliceosome assembly onto the pre-mRNA and consequent catalysis reactions, together with the enormous number of factors involved, allows for fine regulation at every stage of the reaction ((Park, Parisky et al. 2004); (Pleiss, Whitworth et al. 2007); (Saltzman, Pan et al. 2011)).

In addition, alternative splicing decisions are tightly coupled to epigenetics factors such as RNA pol II elongation rate, nucleosome positioning and chromatin remodellers ((Kadener, Fededa et al. 2002); (Tilgner, Nikolaou et al. 2009); (Batsche, Yaniv et al. 2006)). All these events are coupled not only in time but also functionally as they influence each other and these interactions have an impact on exon definition and fate ((Das, Yu et al. 2007); (Cramer, Caceres et al. 1999); (Das, Dufu et al. 2006); (Luco and Misteli 2011)). Moreover, environmental signals such as external stimuli or DNA damage modulate alternative splicing either through post-translational modifications on *trans*-acting factors or alteration of epigenetic signals at the chromatin level ((Luco, Pan et al. 2010); (Blaustein, Pelisch et al. 2005)). In the last few years, a large number of studies have revealed the importance and ubiquity of this process in multicellular eukaryotes ((Graveley 2001); (Kim 2007)). A complete catalogue of the types of alternative splicing occurring in humans is now available ((Xing and Lee 2006); (Holste, Huo et al. 2006)). Estimations of the proportion of genes that are alternatively spliced in humans differ according to the methodology used, but they could reach 90% (Johnson, Castle et al. 2003) and around 86% with a minor isoforms frequency of at least 15% (Wang, Sandberg et al. 2008), suggesting that alternative splicing of human genes is the rule and not the exception. Other mammals exhibit a similar proportion of genes with splicing variants, but alternative isoforms are often lineage-specific, suggesting that alternative splicing is a dynamic process across evolutionary time ((Modrek and Lee 2003); (Modrek and Lee 2003); (Alekseyenko, Kim et al. 2007)). The obvious correspondence with gene duplication was made explicit by a study documenting differences in gene structure between human and

mouse orthologs (Modrek and Lee 2003). Modrek and Lee analyse a set of 9-434 orthologous genes in human and mouse. This work introduces an additionally distinction within alternative exons: “major form” if the exon appears in at least 50% of the transcripts and “minor form” otherwise. This minor form is free of selective constraint thus allowing it to accumulate changes more rapidly. The major-form of alternative exons are much more conserved between human and mouse. Modrek and Lee demonstrated that AS is likely to have facilitated many of the changes that have occurred in the structure of genes since the human/mouse divergence. This was illustrated by the finding that species-specific exons are 10 times more likely to be alternatively spliced than conserved exons. Notably, this facilitation is dependent on the low frequency incorporation of these species-specific exons into transcripts. Alternatively spliced exons specific to human or mouse are nearly eight times more likely to be spliced at low frequencies (i.e., as the minor form) than alternative exons conserved between these mammals (Modrek and Lee 2003). It is this low-frequency expression, by alternative splicing, of species-specific “internal paralogs” that is likely to protect newly formed exons from selection while ensuring that the gene’s ancestral function is not compromised.

Some other studies have tried to understand how alternative splicing originated in the course of evolutionary time, through the results of mutations in DNA sequences ((Sorek, Lev-Maor et al. 2004); (Koren, Lev-Maor et al. 2007)) or through the evolution of splicing regulatory factors (Izquierdo and Valcarcel 2006). Another approach focused on the evaluation of the evolutionary trajectory of alternatively spliced genes, trying, for instance, to compare selective pressure on alternative versus constitutive exons (Xing and Lee 2005), or trying to detect associations between alternative splicing and different types of evolutionary changes, such as exon creation/loss (Alekseyenko, Kim et al. 2007), exon duplication ((Koonin 2001); (Letunic, Copley et al. 2002)), or Alu element-mediated exonisation ((Sorek, Ast et al. 2002); (Zheng, Fu et al. 2005)). The emerging picture of alternative splicing events underscores its extreme richness and consolidates the view that its regulation is at the heart of gene expression and cell fate.

Intragenic Alternative Splicing Coordination

Alternative splicing (AS) is the process by which the exon sequences of primary transcripts are differentially included in mature mRNA, and it represents an important mechanism underlying the regulation and diversification of gene function ((Smith, Valcarcel 2000); (Gravelley 2001); (Matlin, Clark et al. 2005); (Blencowe 2005). AS functions to expand proteomic complexity and plays numerous important roles in gene regulation. The presence of multiple splice variants in the same gene, can increase the potential to generate various transcripts and adds an extra layer of complexity to gene regulation. This aspect is rarely considered in the analysis of splicing that normally take into account AS events one by one. Comparisons of data from transcript sequencing efforts, EST/cDNA sequences and microarray profiling experiments have provided evidence for AS coordination between multiple exons within a single gene ((Peng, Xue et al. 2008); (Xing, Resch et al. 2004); (Fededa, Petrillo et al. 2005); (Fagnani, Barash et al. 2007)). However, only few cases were verified experimentally (Fededa, Petrillo et al. 2005), and these studies did not address whether multiple exons in the same gene can be coregulated in a tissue-dependent manner, or the extent to which coordination between alternative exons occurs in tumors. Mouse Fibronectin gene (FN) and human Poly(rC)-binding protein 2 (PCBP2), are two cases in which different alternative exons belonging to the same gene appear to be coordinated (Fededa, Petrillo et al. 2005). Fededa et al. engineered a minigene carrying two alternative EDI regions in tandem of the FN gene that showed a polar effect across two splice sites. Mutations that change the alternative splicing of the upstream EDI deeply affect the splicing pattern of the downstream one and this effect was shown to be in part due to promoter architecture and PolII elongation rate (Xing, Resch et al. 2004; Fededa, Petrillo et al. 2005). Concerning the coordination detected in the mouse FN gene, Chauhan et al. 2004, did not found splicing coordination in several organs in mutant mice defective in regulated EDI splicing. Afterwards, newborn mice showed only in kidney a weak coordination and a strong coordination in embryo-derived fibroblast (Fededa, Petrillo et al. 2004). Thus, in general the coordination mechanism could be due to a “local-direct” effect of common splicing factors that act on the different splicing events

and/or to an indirect effect, that use the coupling of splicing with transcription to regulate distant events. These include the PolII elongation rate, loading of specific splicing factors on the PolII and specific chromatin signatures that can affect PolII processivity (Luco, Pan et al.). Interestingly, genotoxic stress inhibits PolII transcription elongation, which result in AS changes (Blencowe 2006; Munoz, Perez Santangelo et al. 2009).

The human calcium channel, voltage-dependent, T type, alpha 1G subunit (CACNA1G gene), is another example in which intragenic splicing coordination has been observed. Emerick et al. analyzed hundreds of full-length cDNA sequences in databases and found evidence for both pair-wise and high-order correlations between different alternative exons (Emerick, Parmigiani et al. 2007). They showed that splicing at one pair of loci in particular, exons 25C and 26, is highly linked, with insertion at one locus favoring deletion at the other. In addition, several loci in this gene, showed considerable pair-wise splicing linkage with multiple other sites. Studies based on EST data done by Peng et al. 2008 on two exons in an adjacent cassette exon pair (two exons which are both cassette exons and are adjacent in the final transcript), using a metric of correlation coefficients described the interaction between two adjacent cassette exons in human and mouse and again demonstrated that these pairs showed various correlation patterns. However, this work has a limitation due to poor amount of ESTs data analysed for this purpose. This work was mainly based on EST/cDNA sequences, which are usually relatively short fragments of gene transcripts, normally at the 3' end and usually do not cover distant cassette exons. Recently, Glauser et al. 2011, provides evidence for intragenic splicing coordination in the slo-1 gene in *C. Elegans* and identify putative specialized *cis*- regulatory elements that regulate the coordination of intragenic alternative splicing. A single mutation in this region alters these interdependent splicing events. No data are available regarding the intragenic AS coordination in cancer.

Alternative Splicing and Cancer

Alternative splicing is a widespread process used in higher eukaryotes to regulate gene expression; through alternative splicing multiple different transcripts can be generated from a single gene. Alternative splicing is highly relevant in molecular mechanism of gene regulation in physiological processes such as developmental programming as well as in disease ((Black 2003); (Garcia-Blanco, Baraniak et al. 2004)). In cancer, splicing is significantly altered. Tumors express a different collection of alternative splice forms than normal tissues. Many tumor-associated splice variants arise from genes with an established role in carcinogenesis or tumor progression, and their functions can be oncogenic, either by inactivating tumor suppressors or by gain of function of proteins promoting tumor development.

Thus, the identification of cancer-specific splice forms provides a novel source for the discovery of diagnostic or prognostic biomarkers and tumor antigens suitable as targets for therapeutic intervention (Kalnina, Zayakin et al. 2005). A large number of studies have been addressing aberrant and alternative splicing in cancer on a gene-by-gene basis. The investigation of individual genes has, however, revealed that the normal splicing process can be disrupted in cancer at various critical steps. The association between AS and cancer have been observed at different levels:

- *cis*-acting mutations in cancer associated genes can alter the pattern of splicing directly contribute to cancer function, such as *LKB1* (Liver kinase B1), or phosphatase and tensin homolog (PTEN) and adenomatosis polyposis colic (APC), or KIT (receptor of tyrosine kinase family) and BRCA1 (Breast cancer);
- cancer is associated to changes in the pattern of expression trans-acing regulatory splicing factors: i) SRproteins and HnRNPs; ii) TIA1 and TIAR and HUR proteins;
- transcription and several key gene involved in different pathways (apoptosis, EMT, proliferation), have been studied in detail.

Cis-acting mutations in cancer

Many examples of cancer-associated alterations in splicing are attributable to point mutations and single nucleotide polymorphisms that can interfere with normal splice site consensus sequences (figure 9), reducing binding affinity of spliceosomal proteins and splicing efficiency creating or disrupting splicing enhancers and silencers that may affect binding of regulatory splicing proteins. For example, this is the case of *LKB1* (Liver kinase B1), a tumor suppressor gene that encodes a serine/threonine protein kinase involved in the control of several cellular processes, including cell-cycle arrest, p53-mediated apoptosis, *Ras*-induced transformation, cell polarity. Mutations of *LKB1* leads to PJS (Peutz-Jeghers Syndrome), an autosomal dominant disorder associated with gastrointestinal polyposis and an increased cancer risk (Zhang, Sun et al. 2011). A group of PJS patients carry a mutation that affects the 5'splice site of intron 2, which is still used but not in conjunction with the normal 3'splice site. Instead, cryptic, non-canonical 3'splice sites adjacent to the normal one are used, which leads to frame shifting and consequently to the appearance of premature termination codons in the aberrantly spliced transcripts. The mutation thus affects the fidelity of splicing (Srebrow and Kornblihtt 2006). Other possible results of these changes include exon skipping, such as in the phosphatase and tensin homolog (PTEN) and adenomatosis polyposis colic (APC) splice variants that underlie familial cancer syndromes ((Agrawal, Pilarski et al. 2005); (Aretz, Uhlhaas et al. 2004)); intron retention; preferential use of a nearby cryptic splice site, such as in a Kruppel-like factor 6 splice variant associated with prostate cancer (Narla, Difeo et al. 2005). Furthermore, genomic sequence alterations can create new splice sites. An example involves the oncogene *KIT,* the receptor for tyrosine kynase family whose constitutive activation is due to a deletion of an intron-exon segment encompassing the 3'splice site of intron 10. *KIT* is associated with GIST (gastrointestinal stromal tumors) (Chen, Sabripour et al. 2005). These deletions create an intra-exonic 3'splice site within exon 11. The resulting polypeptides remain in-frame but lack an internal stretch that is crucial for auto-inhibition of the kinase. Also germline mutations in the *BRCA1* gene are well-known markers of predisposition to breast and ovarian cancers. The mutation in exon 18 disrupts an

ESE element and provokes exon 18 skipping. About 60% of BRCA1 ESEs are predicted to be affected by sequence variant as reported in the Breast Cancer Information Core (Pettigrew, Wayte et al. 2005).

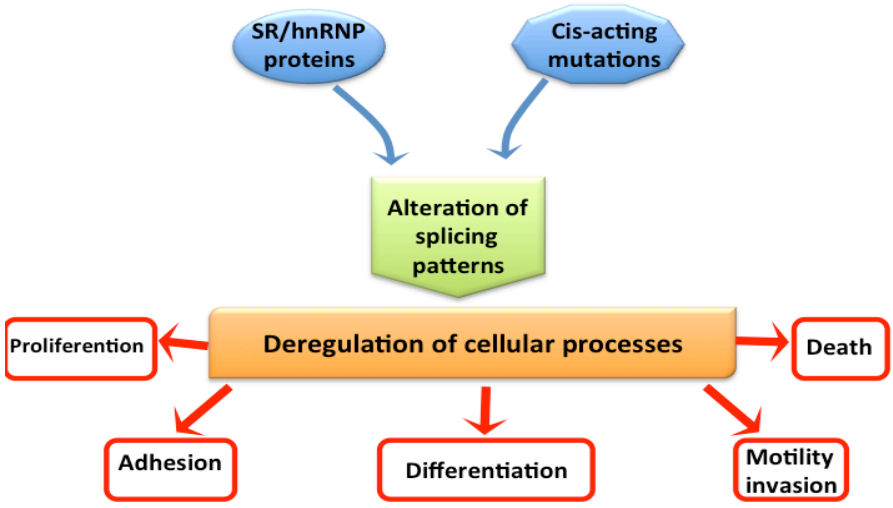

Figure 9. Causes and consequences of splicing pattern alterations. For simplicity, only SR and hnRNP proteins are shown. However, other factors not belonging to any of these families could also be targets of these signaling pathways. (Adapted from (Srebrow and Kornblihtt 2006).

HnRNP and SR proteins in cancer

Stimulation or inhibition by splicing factors is likely to contribute to splicing in cancer as well. The first proteins identified to regulate AS belong to the SR and hnRNP protein families ((Dreyfuss, Matunis et al. 1993); (Fu 1995); (Manley and Tacke 1996)). Several members of these two protein families have been shown recently to play important roles in proliferation and cancer.

Up-regulation of hnRNP A1/A2 proteins has a important functional consequences (figure 9). Consistent with an important role in tumors, siRNA-mediated knockdown of hnRNP A1/A2 in cancer cells, but not in normal cells, can result in apoptosis (Patry, Bouchard et al. 2003). In addition, human A1 has been implicated in lengthening and maintaining telomeres, a function that is conserved in *C. elegans* and possibly yeast ((Lin and Zakian 1994); (LaBranche, Dupuis et al. 1998); (Joeng, Song et al. 2004)). A1 binds to the single-stranded telomeric DNA

repeat sequence TAGGGT, where it is capable of stimulating telomerase activity ((Burd and Dreyfuss 1994); (Zhang, Qi et al. 2006)). hnRNP A1 shuttles between the nucleus and cytoplasm, and it also has a well-established role in regulating translation through its binding to internal ribosome entry sites (IRES), present in the 5' UTR of many mRNAs. Binding to such sites in the cyclin D1 and c-Myc mRNAs results in increased translation, making hnRNP A1 an important positive regulator of critical proto-oncogene expression (Jo, Martin et al. 2008). The fact that hnRNP A1 is transcriptionally up-regulated by c-Myc and is in turn able to promote the expression of c-Myc indicates that these two proteins may constitute a positive feedback loop in some circumstances.

André and collaborators in 2009, have reported the overexpression of 14 genes involved in splicing by comparing a large collection of malignant and benign breast lesions (Andre, Michiels et al. 2009). Furthermore, several SR-related proteins, including SRSF5, SRSF6 (formerly SRp40 and Srp55, respectively) and TRA2B have been shown to be overexpressed in breast cancer ((Andre, Michiels et al. 2009); (Pettigrew and Brown 2008); (Watermann, Tang et al. 2006)). However, as splicing factors are often involved in several steps of the gene expression process (from RNA processing to translation), it is not clear yet whether their alterations play a role in cancer through their involvement in splicing. In this context, Karni and collaborators have shown that the SR protein, SRSF1 (formerly ASF/SF2) that is overexpressed in various human tumors, is a potent oncogene and triggers malignant transformation ((Karni, Hippo et al. 2008); (Karni, de Stanchina et al. 2007); (Huang, Shen et al. 2007)). Importantly, the tumorigenic effects of SRSF1 overexpression may be explained by changes in alternative splicing of cancer-related genes as SRSF1 promotes the expression of an isoform of BIN1 that lacks tumor suppressor activity and the expression of an oncogenic isoform of the S6K1 kinase that leads to the activation of mTORC1.

SRSF1 has been implicated in a number of cancer-associated changes in AS events related to cell motility (Rac1 and Ron) and proliferation (Cyclin D1). Consistent with this, Krainer and colleagues (Karni, de Stanchina et al. 2007) demonstrated that the gene encoding SRSF1 could function as a proto-oncogene. Its expression was shown to be up-regulated frequently in cancer (figure 9). The

Ras/PI 3-kinase/AKT pathway leads to changes in activity of SR proteins, in particular SRSF1 and SRSF7. Consequently, it regulates alternative splicing of fibronectin (Fn) transcripts, an extracellular matrix protein involved in cell adhesion and migration, is expressed at low levels in adult tissues, and its inclusion has been shown to be a highly specific marker of liver metastasis (Rybak, Roesli et al. 2007).

Then, regulation of SR protein activity by phosphorylation has now been implicated in a cancer-associated AS event. Importantly, the EDA exon containing variant appears to promote cellular proliferation to a greater extent than the EDA-lacking variant, indicating a potential functional importance in cancer progression (Manabe, Oh-e et al. 1999). Interestingly, the regulation of variant exon inclusion is highly tissue- and tumor specific, and the splicing factors outlined above have been shown to preferentially control specific exons.

A number of RBPs such as TIA1/TIAR, RNA-binding motif 5 (RBM5) and HuR, that affect the splicing of apoptosis-related transcripts has been identified, highlighting the possibility that these proteins are regulators of apoptosis. Among them, TIA-1 and TIAR are highly conserved and widely expressed in mammals (Beck, Medley et al. 1996). The two proteins function in similar processes and often exhibit partial redundancy. Among the earliest functions attributed to TIA-1 and TIAR there was the ability to bind mRNAs and recruit them to cytoplasmic bodies (known as stress granules) in response to cellular stress such as heat shock (Kedersha, Gupta et al. 1999). Both proteins have also been found to bind AU-rich elements (AREs) and act as translational repressors ((Piecyk, Wax et al. 2000); (Kawai, Lal et al. 2006); (Kim, Kuwano et al. 2007)). TIA-1 and TIAR have been shown to be regulators of the inflammatory response that function by silencing translation of key mediators of inflammation, such as TNF-a and COX-2 ((Piecyk, Wax et al. 2000); (Lopez de Silanes, Galban et al. 2005)). Notable splicing substrates for TIA-1/ TIAR are Fas (discussed above) and the epithelial-specific exon IIIb in the fibroblast growth factor receptor 2 (FGFR2) pre-mRNA, which is frequently excluded during cancer progression (Del Gatto-Konczak, Bourgeois et al. 2000). Consistent with the fact that TIA-1/TIAR can promote production of the proapoptotic form of Fas, introduction of TIA-1/TIAR into cells promotes apoptosis

((Iseni, Garcin et al. 2002); (Tian, Streuli et al. 1991)). Given that TIA-1 and TIAR have functions associated with tumor suppressor genes (i.e., promoting apoptosis and inhibiting proliferation), alterations in the expression or regulation of these proteins might be expected to contribute to tumorigenesis in some contexts. However, there is currently little evidence for widespread down-regulation of TIA-1/TIAR in cancer.

Splicing and apoptosis

There are many examples of alternative splicing changes involved in apoptosis, or programmed cell death (Wu, Tang et al. 2003). Thus, because cancer cells display behavior that would normally elicit apoptosis, these cells must in some way suppress this process (Letai 2008). Given the apparent importance of particular splicing decisions in regulating apoptosis, it is not surprising that the levels of certain RNA Binding Proteins (RBPs) that control these events are a determinant of whether a cell undergoes apoptotic death.

One of the earliest examples of AS creating opposing isoforms in apoptosis is *Bcl-x*. *Bcl-X* is a member of the *BclII* family that has an important role in the breakdown of mitochondria during apoptosis, and it is alternatively spliced between a long antiapoptotic form (*BclxL*) and a short apoptosis-promoting form (*BclxS*), which is made by use of an upstream 5'splice site of exon 2 (figure 10). The downstream 5'splice site of *Bclx* can be blocked directly (but not degraded) by stable antisense oligonucleotides that divert splicing toward the proapoptotic upstream 5'splice site. This is a particularly powerful approach, because the more antiapoptotic isoform a cancer cell has, the more cytotoxic proapoptotic form can be made by switching splice site usage. No mutations have been observed in *cis-acting* splicing elements within these genes suggesting that the alterations could be due to changes in trans-acting splicing regulators.

Caspase-2 is a highly conserved cysteine protease first identified as a mammalian homolog of the CED-3 caspase in *Caenorhabditis elegans* (Wang, Miura et al. 1994). While it was first implicated in apoptosis on the basis of its similarity to CED-3, it has since been shown to act as a tumor suppressor that participates in a wide variety of cellular processes ((Ho, Wei et al. 2010); (Kumar,

Kumar et al. 2009)). Caspase-2 mRNA is alternatively processed to produce multiple isoforms (Figure 10). The predominant form in most tissues, caspase-2L, produces a full-length protein with proapoptotic properties (Wang, Miura et al. 1994). Inclusion of this exon 9, in caspase-2L, results in a frameshift leading to the introduction of a premature termination codon (PTC) in the mRNA, creating a short-lived non-sense-mediated decay (NMD) substrate (Solier, Logette et al. 2005). It is unclear under what circumstances caspase-2S mRNA might be stabilized, and conclusive evidence that it is translated is still lacking (Kitevska, Spencer et al. 2009). In any event, when expressed from cDNA, the truncated product of the caspase-2S mRNA was shown to protect against cell death in some contexts ((Wang, Miura et al. 1994); (Droin, Bichat et al. 2001)). Whether exon 9 inclusion in caspase-2 results in the production of an anti-apoptotic protein or simply results in reduction of caspase-2 mRNA levels through NMD, it is clear that production of the 2S isoform would favor survival of cancer cells, making its regulation of interest.

Alternative Splicing of the Fas receptor pre-mRNA provides a potentially important means by which tumors cells can escape elimination by the immune system (figure 10). The Fas protein (also known as CD95) is a widely expressed cell surface receptor that, when bound to Fas ligand (FasL) expressed on cytotoxic T cells, can initiate a cascade that eventually leads to cell death (Bouillet and O'Reilly 2009). Its most abundant isoform lacks the 63-nt exon 6 (E6), where the transmembrane domain is deleted (Cascino, Fiucci et al. 1995). The protein produced by the DE6 Fas isoform is soluble and capable of inhibiting Fas-mediated cell death, presumably by binding to FasL and preventing the interaction of FasL with membrane-bound Fas. Elevated production of soluble Fas (sFas) has been observed in a wide range of cancers, as determined by Fas serum concentrations, which show a strong correlation with tumor staging ((Sheen-Chen, Chen et al. 2003); (Kondera-Anasz, Mielczarek-Palacz et al. 2005)). In light of the potential for Fas AS to play a role in the suppression of the anti-tumor immune response, the regulation of Fas AS has been extensively investigated. Several RBPs have been shown to be involved in promoting the production of full-length Fas mRNA. TIA-1 and TIA-1-related protein (TIAR), two closely related RNA recognition motif

(RRM)- containing proteins involved in apoptosis (see below), bind to U-rich sequences downstream from Fas E6 and promote its inclusion in the mRNA (Izquierdo, Majos et al. 2005).

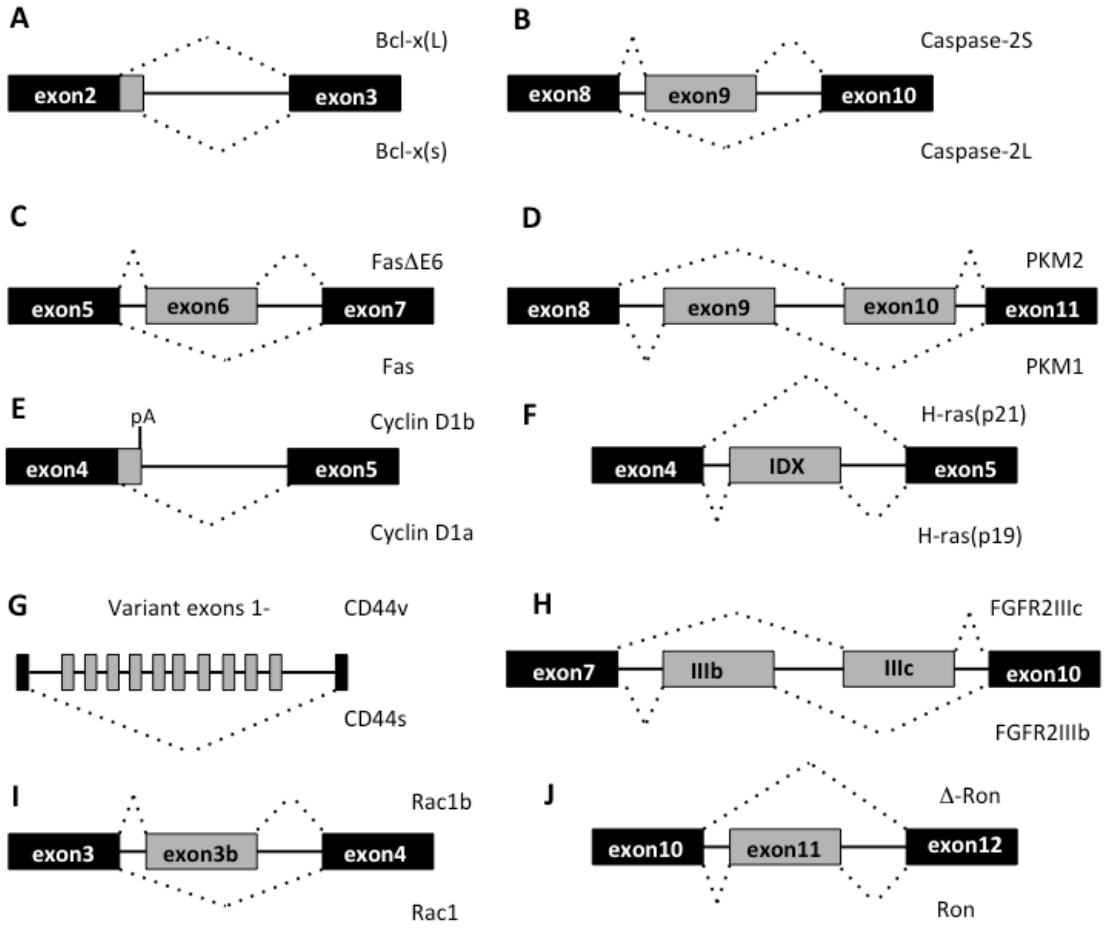

Figure 10. Schematic representation of the AS events discussed and implicated in cancer. In all cases examples of genes affected are indicated. *A-J,* alternative splicing patterns in cancer. All of the possible patterns of alternative splicing are found in cancer-specific transcripts. In each case, isoforms that are up-regulated in cancer or that are otherwise shown to have positive effects on growth, survival, or invasive behavior are shown at the top of each diagram. (Adapted from (Montuenga and Pio 2007).

Alternative Splicing cancer genes

Many tumor oncogenes are targets of AS regulation in cancers. While this often happens through mutations, it is now clear that changes in AS that are unconnected to mutations can profoundly affect the activity of some oncogenes.

An example of oncogene is Cyclin D1, but there are many others, equally or even more complex genes, such as BRCA1, FGFR2, TP63, and surviving (BIRC5). Cyclin D1 was first identified as a regulator of cell cycle progression through its association with cyclin-dependent kinase 4 or 6 (CDK4/6) (Braden, Lenihan et al. 2006). One role of the CDK4/6/cyclin D1 complex is to phosphorylate the transcription factor and tumor suppressor RB, thus relieving RB repression of E2F target genes and promoting cell cycle progression. In addition to its association with CDKs, cyclin D1 was later shown to have CDK-independent nuclear functions as a transcriptional regulator (Braden, Lenihan et al. 2006). It is now known that cyclin D1 is subject to AS/ polyadenylation that results in a more oncogenic protein. The two main isoforms are D1a, that is the more common full-length variant that contains five exons and shuttles between the nucleus and cytoplasm in a cell cycle-dependent manner, and cyclin D1b, that is polyadenylated at a site in intron 4 and is constitutively nuclear, likely due to loss of a glycogen synthase kinase 3b phosphorylation site present at the C terminus of D1a ((Lu, Gladden et al. 2003); (Solomon, Wang et al. 2003)). Cyclin D1b can be detected in noncancerous cells, but is up-regulated in some cancers such as breast and prostate ((Burd, Petre et al. 2006); (Wang, Dean et al. 2008)). The D1b isoform, like D1a, associates with CDK4 and appears to regulate CDK activity similarly to D1a (Lu, Gladden et al. 2003). Consistent with this, RBPs that influence the choice between D1a and D1b have also been identified.

Sam68, described above for its role in Bcl-x splicing, has been implicated in favoring the production of D1b (Paronetto, Cappellari et al. 2010). Binding sites for Sam68 were identified in intron 4, where it either inhibits E4 recognition or promotes polyadenylation in intron 4. A strong correlation between Sam68 expression levels and D1b production was also observed, underscoring the biological significance of these findings.

The SR protein SRSF1 has also been shown to bind preferentially to the

D1b transcript and promotes the production of D1b, and SRSF1 levels were also found to correlate with D1b production (Olshavsky, Comstock et al. 2010). Finally, it has also been reported that an oncogenic fusion between the multi- functional RBP EWS and the transcription factor FLI1, which is found in Ewing's sarcoma, can influence production of D1b. While EWS itself was shown to promote production of full-length D1a, the EWS-FLI1 fusion promoted production of D1b (Sanchez, Delattre et al. 2008).

The H-Ras gene appears to provide another example of an AS event that produces two proteins with entirely different activities with regard to proliferation. In the late 1980s, Levinson and colleagues (Cohen and Levinson 1988) identified an intronic mutation in H-Ras that essentially enhanced H-Ras expression, significantly in- creasing the transforming potential of the gene.

Alternative Splicing isoforms associated with metastasis and invasion

AS regulates several genes that play important roles in promoting invasive behavior. In addition, the epithelial-to-mesenchymal transition (EMT), a process that often plays a role in the acquisition of invasive behavior in cancer cells, is accompanied by a reprogramming of AS ((Thiery, Acloque et al. 2009); (Radisky, Levy et al. 2005); (Thiery and Sleeman 2006)). Down-regulation of a pair of epithelial-specific splicing factors may underlie many of the changes in splicing that occur during EMT.

The *CD44* gene is the most studied in AS in cancer and it is an excellent example to illustrate how aberrant splicing in cancers can be modulated by altered activity or translocation of splicing factors, and in response to extracellular and intracellular stimuli. It encodes a type 1 transmembrane glycoprotein involved in cell–cell and cell–matrix interactions. Some of these regulatory mechanisms might represent common pathways that allow cells to modify splicing patterns in response to extracellular stimuli or stress responses. The structural heterogeneity of the *CD44* gene products is caused primarily by AS of at least 10 out of the total 20 exons. The variant exons (v1–v10) are located right in the middle of the gene, clustered in-between 10 constitutive exons. Certain *CD44* variants have been implicated in tumorigenesis, tumor cell invasion, and metastasis (in particular the

v4–7 variant) in a broad range of human cancers (Herrlich, Morrison et al. 2000). For example, the v6 variant, found preferentially in head and neck cancers (Cheng and Sharp 2006) can form a stimulatory complex with hepatocyte growth factor (HGF) and its tyrosine kinase receptor MET, which is then able to activate the *RAS* signalling pathway. Activation of a pathway involving Ras, PI 3-kinase (PI 3- kinase) and *AKT* (the Ras/PI 3-kinase/AKT pathway) has been associated with multiple human cancers ((Mulder, Keijzer et al. 1989); (Scheid and Woodgett 2001); (Vivanco and Sawyers 2002)).

Like Rac1, AS of Ron transcripts (which encode the receptor of the macrophage-stimulating protein (MSP)) in cancer cells is closely tied to the invasive phenotype. It encodes the receptor and binding of its ligand triggers a signalling cascade that regulates a variety of cellular activities, such as cell growth, motility and invasion of extracellular matrices.

Ghigna et al. not only confirmed that *Ron* splicing is altered in breast and colon cancers but also shed light on the molecular mechanisms that regulates it (Ghigna, Giordano et al. 2005). *Ron* is a heterodimeric protein formed by α and β subunits, both derived from the proteolytic cleavage of a common precursor. Under normal conditions, binding of MSP to Ron results in tyrosine autophosphorylation of the receptor, leading to activation of signaling pathways that result in increased motility and invasive growth ((Ghigna, Giordano et al. 2005); (Wagh et al. 2008)).

An alternatively spliced isoform termed *DRon* was identified in human gastric carcinoma cells and induces an invasive phenotype in transfected cells (Collesi, Santoro et al. 1996). *ΔRon* mRNA originates by skipping of exon 11, which leads to the deletion of a 49 amino acid stretch in the b chain of the resulting polypeptide. This deletion abolishes the proteolytical cleavage and renders the protein constitutively active. Ghigna et al. identified two regulatory elements within exon 12 that control the level of inclusion of exon 11. The binding of the SR protein SRSF1 to one of these stimulates skipping of exon 11, increasing the level of the *ΔRon* isoform. Overexpression of SRSF1 lead to morphological and molecular changes characteristic of an EMT, but knockdown of SRSF1 by RNA interference (RNAi) reduces the levels of *Ron* and concomitantly decreases cell motility. Thus,

SRSF1 could regulate malignant transformation of certain epithelial tumors by inducing a *Ron*-dependent EMT.

Other examples of AS in cancers are attributable to the use of alternative individual splice sites, single alternative exons, and alternative introns. One type of alternative splicing involves the mutually exclusive use of alternative exons, and a mutually exclusive splicing of the cytoskeletal protein actinin-4 has been discovered recently to be associated with small cell lung cancer (Pio and Montuenga 2009). Various strategies are currently being used to exploit alternative splicing for the diagnosis and treatment of cancer.

Anoctamin/TMEM16 family members are Ca^{2+}-activated Cl^- channels

Ca^{2+} activated Cl^- currents (CaCCs) were first described in the early 1980's in *Xenopus* oocytes ((Miledi 1982); (Barish 1983)) and salamander photoreceptor inner segments (Bader, Bertrand et al. 1982), but until 4 years ago the proteins responsible for these channels were not yet identified. Prior to that, several other proteins were proposed as molecular candidates. These include ClC-3 (Huang, Liu et al. 2001), CLCAs (Loewen and Forsyth 2005), and bestrophins (Qu and Hartzell 2008). None of these proteins have properties that exactly fit those of classical CaCCs (Duran, Thompson et al. 2010). Thus, in 2008, the announcements that three labs had cloned genes that encoded classical CaCCs generated considerable excitement ((Caputo, Caci et al. 2008); (Schroeder, Cheng et al. 2008); (Yang, Cho et al. 2008)). The two genes that have been shown definitively to encode CaCCs are called *Tmem16A* and *Tmem16B.* These are two members of a family that consists of 10 genes in mammals (Milenkovic, Brockmann et al. 2010). Yang et al. 2008 proposed the new name "anoctamin" or Ano because these channels are ANion selective and have eight (OCT) transmembrane segments (anion+octa=8) and this name is now the official HUGO nomenclature and has replaced Tmem16 in Genbank. Tmem16A is now Ano1, Tmem16B is Ano2, and so-on. Although Tmem16 gene family was first identified by bioinformatic analysis in 2004, in 2008 Yang et al. used a bioinformatic approach to identify *TMEM16A* and then confirmed CaCC function by expression cloning in HEK293 cells and siRNA knockdown in mouse salivary glands (Yang, Cho et al. 2008). Caputo, Caci et al. 2008, used the observation that chronic Il-4 stimulation of airway epithelial cells resulted in increased CaCC activity to identify *TMEM16A* by microarray analysis, and demonstrated that TMEM16A also showed an ion channel activation, inhibition, and anion selectivity profile consistent with native airway CaCCs (Caputo, Caci et al. 2008). Lastly, Schroeder et al. used an elegant expression cloning approach to identify the Xenopus ortholog of TMEM16A (Schroeder, Cheng et al. 2008) and characterize its function and expression, i.e., in glands (mammary, salivary). Collectively, *TMEM16A* clearly demonstrates many if not all of the characteristics required of a candidate gene to produce airway epithelial CaCC.

It is now known that similar channels are expressed in many cell types. CaCCs play key roles in epithelial secretion (Kunzelmann, Milenkovic et al. 2007), membrane excitability in cardiac muscle and neurons ((Andre, Boukhaddaoui et al. 2003); (Guo, Young et al. 2008)), olfactory transduction (Matthews and Reisert 2003), regulation of vascular tone (Angermann, Sanguinetti et al. 2006) and photoreception (Lalonde, Kelly et al. 2008) (figure 12).

The molecular identity of these membrane proteins is still unclear. There are two possible mechanism for Ca^{2+} to activate CaCCs: some are activated directly by Ca^{2+} while others are activated indirectly via Ca^{2+}-dependent enzymes and phosphorylation, due to the relase of intracellular calcium (Arreola, Melvin et al. 1998). When the channel is activated leads to Cl^- secretion, which result in a depolarization of the plasma membrane. In some cells this depolarization increases the opening probability of voltage-gated Ca^{2+} channels, which result in additional Ca^{2+} influx and further depolarization. The opening of the channel can lead to hyperpolarizzation, therefore neuroexcitation and smooth-muscle contraction. They are activated by increases in Ca^{2+} concentration that occur upon fertilization, depolarize the membrane, and prevent additional sperm entry. In vertebrate photoreceptors, CaCCs are thought to play an important role in transmitter release (MacLeish and Nurse 2007).

Interestingly, anoctamin family has previously attracted the interest of both developmental and cancer biologists. Some members of this family are up-regulated in a number of tumors and its functional deficiency in others is linked to developmental defects.

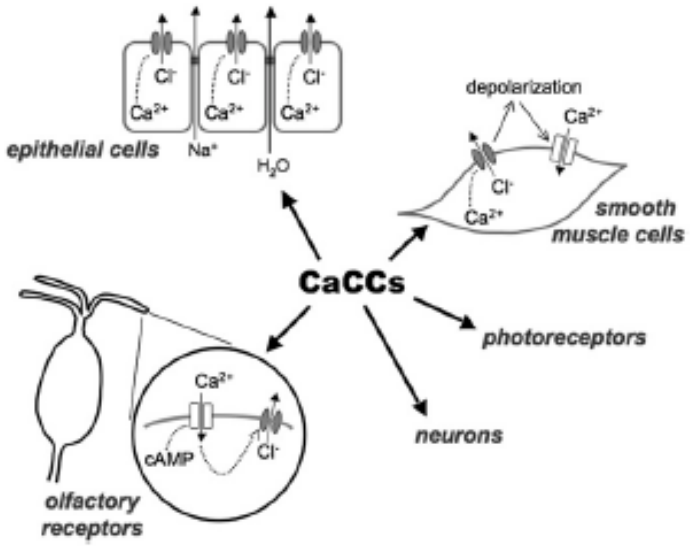

Figure 11. Physiological roles of CaCCs. In epithelial cells, activation of CaCCs by intracellular Ca^{2+} elevation leads to Cl^- secretion followed by transepithelial transport of Na^+ and water. In smooth muscle cells, activation of CaCCs is part of an amplification mechanism. Intracellular Ca^{2+} increase by extracellular stimuli activates CaCCs and Cl^- efflux. The resulting membrane depolarization opens voltage-dependent Ca^{2+} channels that cause a further intracellular Ca^{2+} increase, thus potentiating contraction. Another amplification mechanism occurs in olfactory receptors, where the initial Ca^{2+} increase is triggered by cAMP-gated channels. CaCC is also involved in phototransduction and regulation of neuronal excitability. (Taken from (Galietta 2009).

Members of the ANO family are found throughout the eukaryotes, including mammals, flies, worms, plants, protozoa and yeast. However, the ANOs seem best represented in the higher vertebrates. Mammals have 10 gene members whereas invertebrates and plants have distinctly fewer. *C. elegans,* for example, has only two ANO genes and *Drosophila* has six paralogues. Mammalian subfamilies 1 and 2 are closely related, as are 3 and 4, and 8 and 10. The ANO family is now the second largest of the five known Cl^- channel families. In mammals, ligand gated anion channels (e.g. GABA/glycine receptors) include hundreds of members, the CLCs have nine members, bestrophins have four, and CFTR is apparently a loner ((Jentsch, Stein et al. 2002); (Hartzell, Qu et al. 2008)).

This molecular diversity of the ANO family is reflected in the phenotypic variety of CaCC currents, in fact there is a considerable difference in the properties of the single channels. There appear to be at least four different classes

of CaCCs in different cell types and the channels may have multiple conductance states (Piper and Large 2003). Whether this will be explained by different ANO members or different heteromeric combinations of ANOs remains to be seen. Anoctamin is a secondary Cl^- channel airway. Airway epithelia that use ion transport mechanisms to control the level of airway surface liquid, which is important for mucous hydration and protection against infection. Airway epithelial cells coexpress CaCCs and cystic fibrosis transmembrane regulator (CFTR) in their apical membrane ((Boucher, Cheng et al. 1989; Kartner, Hanrahan et al. 1991)). Airway epithelial cells stimulated with ATP or UTP display a Ca^{2+}-dependent Cl^- secretion ((Knowles, Clarke et al. 1991; Tarran, Loewen et al. 2002)). UTP stimulates Gq-coupled P2Y purinergic receptors to increase IP3 production and subsequently Ca^{2+} release. This increases the short-circuit current and the airway surface liquid of murine tracheal epithelial cell line (Donaldson, Brown et al. 1989; Gabriel, Makhlina et al. 2000). The control of the airway mucous layer seems to be regulated by an interplay between CFTR and CaCCs (Tarran, Loewen et al. 2002). The basal level of the mucous layer is controlled by CFTR, whereas CaCCs act as an acute regulator of the liquid layer. The contribution of CaCCs to airway liquid layer homeostasis in murine airway epithelium probably explains the lack of a lung phenotype in mouse models of cystic fibrosis ((Boucher, Cheng et al. 1989); (Clarke, Grubb et al. 1994)). Given that CFTR and CaCCs are both apical Cl^- channels, it has been proposed that the activation of CaCCs could serve as a therapy for cystic fibrosis based on the idea that up-regulation or activation of CaCCs might compensate for loss of CFTR in airway fluid secretion (Knowles, Clarke et al. 1992). Two drugs that activate CaCCs by elevating intracellular Ca2+ are presently in clinical trials for treating cystic fibrosis ((Zeitlin, Boyle et al. 2004); (Storey and Wald 2008)).

Hydropathy plotting shows that all anoctamins have eight hydrophobic helices that are likely to be transmembrane domains with cytosolic N- and C-termini. This predicted topology has been confirmed experimentally for ANO7, whose topology has been determined using inserted HA epitope tag accessibility and endogenous N-glycosylation (Das, Hahn et al. 2008). Because of technical limitation and the fact that the topology of other ANOs has not been

experimentally determined, more investigation is required to establish the structure of these proteins. Anoctamin protein paralogs evolved from several gene duplication events followed by functional divergence of vertebrate anoctamins. Most of the amino acid replacements responsible for the functional divergence were fixed by adaptive evolution and this seem to be a common pattern in anoctamin gene family progression. Strong purifying selection and the loss of many gene duplication products indicate rigid structure-function relationships among anoctamins. In addition it has been identified a number of protein domains and amino acid residues which contribute to predicted functional divergence (Milenkovic, Brockmann et al. 2010).

TMEM16A

The last four years are characterized by a flurry of activity in the field of the CaCCs with the almost simultaneous publication of three papers reporting that TMEM16A is a bona fide CaCC ((Yang, Cho et al. 2008); (Caputo, Caci et al. 2008); (Schroeder, Cheng et al. 2008)). These publications have elicited much interest in the membrane biology field as it turns out that the functional expression of TMEM16A in heterologous systems yielded a conductance that for the first time showed the "classical" characteristics of the CaCCs.

TMEM16A (Anoctamin 1; ANO1) is an eight transmembrane protein that functions as a calcium-activated chloride channel and cytosolic N- and C-termini (Figure 13). Its pore is large and non-selective, allowing other negatively charged species to permeate. No atomic resolution structure of this channel has yet been obtained (Xiao, Yu et al. 2011). However, biochemical evidence suggests that the channel assembles as a dimer of two ANO1 polypeptide subunits ((Fallah, Romer et al. 2011); (Sheridan, Worthington et al. 2011)). Because this protein is thought to have 8 transmembrane domains and be anion-selective channels, the alternative name, Anoctamin (anion and octa=8), has been proposed. It has (~60%) primary sequence identity for TMEM16B, but decreases progressively with the other TMEM16 proteins.

ANO1 has a number of different names, the most common being TMEM16A, but others include TAOS2 (tumor amplified and overexpressed sequence) (Huang, Gollin et al. 2002), ORAOV2 (oral cancer overexpressed) (Mammalian Gene Collection Program Team, 2002) and DOG-1 (discovered on GIST-1) (West, Corless et al. 2004). As these names suggest, ANO1 is highly over-expressed in some cancers. ANO7 (also called D-TMPP and NGEP) is specifically expressed in prostate and is up-regulated in a number of prostate tumors (Kiessling, Weigle et al. 2005).

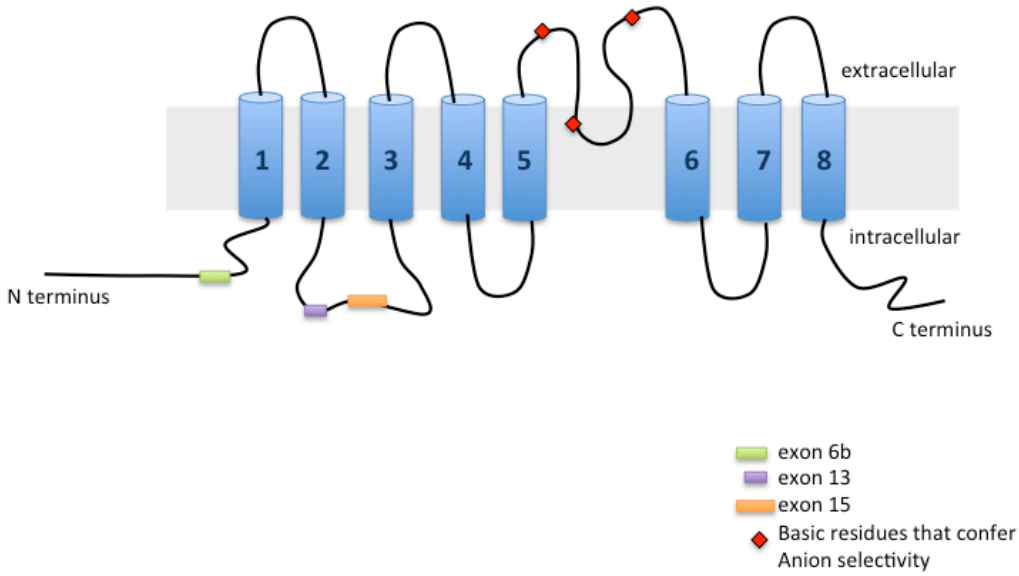

Figure 12. Structure of TMEM16A protein. The protein has eight putative transmembrane domains and intracellular amino and carboxy termini. Various isoforms are generated by inclusion or skipping of four alternative segments labelled exon 6b (22 residues), exon 13 (4 residues), and exon 15 (26 residues). The mechanism of calcium activation is unknown.

Another interesting characteristic of the TMEM16A protein is the presence of multiple isoforms that originate by alternative splicing (Caputo, Caci et al. 2008). ANO1 has at least four splice variants; it has 4 different alternatively spliced segments, *a, b, c,* and *d* corresponding, respectively, to an alternative initiation site, exon 6b, exon 13, and exon 15 (Ferrera, Caputo et al. 2009). Segments *a* is added at the N-terminus, thus extending the cytosolic portion of the protein. Segment *b* (exon 6b) is included before the first transmembrane domain. Segments *c* and *d* (exon 13 and exon 15, respectively) are located in the first intracellular loop. Figure 13 shows the sequence and topology of ANO1 containing all of the alternatively spliced exons, referred to as ANO1 (*abcd*) by Caputo, Caci et al. 2008. They found that the four main splice variants of ANO1 (*a, b, c* and *d)* has different electrophysiological properties. The most abundant TMEM16A isoforms are (*ac*), (*abc*), and (acd). However, there is also evidence of a protein lacking all alternative segments and therefore called TMEM16A(0). Recently it has been discovered that the TMEM16A(0) protein represents a basic version of the Ca^{2+}-activated Cl^- channel, having the pore and, at least, part of the Ca^{2+} sensors. The inclusion of additional domains, such as segment (*b*) and segment (*c*), may add other features like voltage- dependent control of channel gating and

modulation of ion selectivity/conductance. The regulation of TMEM16A expression by alternative splicing is fascinating because it could explain the variety of properties reported for CaCCs in different tissues and cell types ((Hartzell, Putzier et al. 2005); (Ferrera, Caputo et al. 2009, 2010)).

Analysis of ESTs in Genbank predicts that several of the other ANOs also have multiple splice variants. Some of these variants may not have channel functions because they are predicted to lack some or all of the transmembrane domains. The four splice variants of ANO1 exhibit different voltage-dependent and Ca^{2+}-dependent gating properties ((Ferrera, Caputo et al. 2009); (Xiao, Yu et al. 2011)). Thus, alternative splicing is likely to contribute to the heterogeneity of CaCC currents observed in native tissues. Recent studies indicate that alternative splicing may indeed have a functional meaning. For example, inclusion/skipping of segment *b* in the TMEM16A sequence seems to modulate the Ca^{2+} sensitivity of the corresponding Cl^- channels (Ferrera *et al.* 2009). The four amino acids (Glu-Ala- Val-Lys) of segment *c* are also important. Deletion of these amino acid residues (ΔEAVK-TMEM16A) generates CaCCs with altered biophysical properties. In a previous study, Ferrera et al. 2009 reported that this protein variant is largely devoid of activation by membrane depolarization (Ferrera *et al.* 2009). More recently, another study has shown that channels devoid of segment *c* have a significantly reduced Ca^{2+} sensitivity (Xiao *et al.* 2011). In particular, deletion of the first two amino acids of this segment did not alter the channel properties relative to (*abc*) variant. In contrast, deletion of the second two residues generated membrane currents similar to those associated with deletion of the whole four residue segment.

Ano1 is gated by both voltage and Ca^{2+} but examination of its sequence gives few clues about the sites that sense voltage or bind to Ca^{2+}. Unlike voltage-gated channels that have amphipathic transmembrane helices with charged amino acids that serve to sense voltage, Ano1 has no such sequences. Furthermore, there are no obvious E–F hands that might serve as Ca^{2+} binding sites or definitive IQ domains for CaM binding. The first intracellular loop, between TMD2 (TransMembrane Domain) and TMD3, has a large number of acidic amino acids including a stretch of 5 consecutive glutamates (444EEEEE448)

that have attracted attention as a possible Ca^{2+} sensor (Xiao, Yu et al. 2011). The last glutamate in this sequence is the first residue of a 4 amino acid alternatively spliced segment (448EAVK451). Neutralization of the glutamates has little effect on Ca^{2+} sensitivity, although deletion of the alternatively spliced segment (ΔEAVK) alters both voltage-dependent gating and Ca^{2+} sensitivity ((Ferrera, Caputo et al. 2009); (Xiao, Yu et al. 2011)). Thus, although the first intracellular loop plays an important role in coupling both voltage and Ca^{2+} binding to channel opening, it is unlikely to be the binding site for Ca^{2+}.

Mutational analysis of ANO1 suggests that the re-entrant membrane loop between TMD5 and TMD6 is important in ion selectivity. Yang *et al.* (2008) found that replacing few positively charged amino acids of the *'abcd'* variant with a negatively charged amino acid increased dramatically the cation permeability of the channel. Thus, the N- and C-termini and the first cytoplasmic loop of ANO1 have several regions rich in acidic amino acids that could possibly be involved in coordinating Ca^{2+}. However, at present there are no data about the Ca^{2+} binding site.

ANO1 is expressed in many of the tissues that are known to express CaCCs: bronchiolar epithelial cells, pancreatic acinar cells, proximal kidney tubule epithelium, retina, dorsal root ganglion sensory neurons, and sub- mandibular gland (Caputo et al. 2008; Yang et al. 2008; Schroeder et al. 2008). In addition to epithelia, Ano1 is robustly expressed in interstitial cells of Cajal, which are responsible for generating pacemaker activity in smooth muscle of the gut ((Huang, Rock et al. 2009); (Hwang, Blair et al. 2009); (Zhu, Kim et al. 2009)). Mice homozygous for a null allele of Ano1 fail to develop slow wave activity in gastrointestinal smooth muscles. The resulting loss of gastrointestinal motility may be an important contributor to the early death of ANO1 knockout mice (Huang, Rock et al. 2009) and decreased expression of Ano1 in interstitial cells of Cajal may contribute to gastroparesis common in diabetic patients (Mazzone, Bernard et al. 2011). Ano1 is also expressed robustly in various kinds of smooth muscle including vascular smooth muscle cells ((Huang, Rock et al. 2009); (Manoury, Tamuleviciute et al. 2010); (Davis, Forrest et al. 2010)). Treatment of rat pulmonary aortic smooth muscle cells with siRNA against Ano1 results in a

reduction of CaCCs (Manoury, Tamuleviciute et al. 2010). Ano1 is also strongly expressed in airway smooth muscle cells, suggesting the possibility that this channel may be involved in asthma. Asthma is characterized by disorders of smooth muscle Ca^{2+} signaling and remodeling of the airway smooth muscle (Mahn, Ojo et al. 2010). Considering that Ano1 is Ca^{2+} -regulated and implicated in tracheal development (Rock, Futtner et al. 2008), a role for Ano1 in asthma deserves attention. Ano1 is also expressed in small dorsal root ganglion neurons and is implicated in mediating nociceptive signals triggered by bradykinin (Liu, Linley et al. 2010). Bradykinin is a very potent inflammatory and pain-inducing substance that is released at sites of tissue damage or inflammation. Bradykinin acts on Gq-coupled B2 receptors to stimulate phospholipase-C, IP3 production, and release of Ca^{2+} from intracellular stores. The elevation of intracellular Ca^{2+} opens CaCCs apparently encoded by Ano1. CaCC current, along with KCNQ channel activation, depolarizes and increases action potential firing. Local injection of CaCC inhibitors attenuates the nociceptive effect of local injections of BK.

In 2009 Rock et al., reported a TMEM16A knockout mouse. All knockout homozygous mice died within one month of birth exhibiting severe tracheomalacia with gaps in the tracheal cartilage rings. They proposed that the cartilage ring defect observed in TMEM16A knockout animals was secondary to an improper stratification of the embryonic tracheal epithelium or the abnormal trachealis muscle. It is tempting to speculate that the absence of calcium-mediated chloride secretion in the trachea of mutant animals is the cause of the ensuing malformation.

Ano1 has been implicated in rotavirus induced diarrhea (Ousingsawat, Mirza et al. 2011).

As mentioned before for ANOs, even Ano1 is highly expressed in multiple tissues including airway epithelia, where it acts as an apical conduit for transepithelial Cl^- secretion and helps regulate lung liquid homeostasis and mucus clearance. Ano1 has attracted particular attention in the airways, because it has been suggested that activating this channel might be therapeutically beneficial for treating cystic fibro- sis (CF) patients (Rock, O'Neal et al. 2009). Recently, however

Namkung, Phuan et al. 2011, showed that novel Ano1 inhibitors were rather ineffective in inhibiting CaCCs in airway epithelial cells despite their efficacy in inhibiting heterologously expressed Ano1 as well as native CaCCs in salivary gland. This result is puzzling in light of the reports by several groups that Ano1 is expressed in airway epithelium and that knock- out of Ano1 decreases airway secretion ((Huang, Rock et al. 2009); (Ousingsawat, Martins et al. 2009); (Rock, O'Neal et al. 2009)). One possible explanation is that Ano1 in airway has a different splice variant or has other accessory proteins that alter its pharmacological profile. There is also evidence that TMEM16A gene is present in various cancers where it is upregulated, including gastrointestinal stromal tumors ((Espinosa, Lee et al. 2008); (Carles, Millon et al. 2006) see below).

The other TMEM16 proteins

TMEM16 gene family includes nine other members named as TMEM16B-K (Galindo and Vacquier 2005). The primary sequence identity is relatively high for TMEM16B (~60%) but decreases progressively with the other TMEM16 proteins, so that TMEM16F, G, H, J, and K are only 20–30% identical. All TMEM16 proteins have a similar putative topology, consisting of eight transmembrane segments and cytosolic N- and C-termini (Figure 13). Interestingly, the transmembrane segments are the regions of TMEM16 proteins showing maximal conservation. For example, the sequence of the putative sixth transmembrane domain of human TMEM16A (anoctamin-1 or ANO1) is 50% identical to that of TMEM16K (anoctamin-10, ANO10). ANO family members have a conserved C-terminal domain of unknown function.

The probable role of TMEM16A as an ion channel suggests that other TMEM16 proteins could be also involved in ion transport. Indeed, Schroeder et al. showed that heterologous expression of TMEM16B elicits the appearance of Ca^{2+-} activated Cl^- currents (Schroeder, Cheng et al. 2008). This finding was later confirmed by two other groups ((Stohr, Heisig et al. 2009); (Stephan, Shum et al. 2009)). In particular, TMEM16B (anoctamin-2, ANO2) is expressed in photoreceptors (Stohr, Heisig et al. 2009) and in the cilium of olfactory cells (Stephan, Shum et al. 2009), where it appears to play a special role in sensory

transduction.

Interestingly, TMEM16B shows some significant functional differences compared to TMEM16A. The channels associated with TMEM16B have a unitary conductance ~10-fold reduced relative to TMEM16A. Also, TMEM16B expression evokes Cl^- currents that have kinetics faster than those of TMEM16A. Differences in the properties of the currents associated with TMEM16A and TMEM16B may be very useful in understanding the structure-function relationship. Comparison of the primary structure of the two proteins, by demonstrating similarity or divergence, may lead to identification of the domains involved in Ca^{2+}-dependence, voltage sensitivity, and anion transport.

So far, much less is known for the other TMEM16 proteins. According to databases, TMEM16C is particularly expressed in the nervous system but there are no indications about its physiological role. TMEM16E (anoctamin-5, ANO5), also known as GDD1, is mutated in a human genetic disease called gnathodiaphyseal dysplasia, a possible calcification disorder of the bone (Tsutsumi, Kamata et al. 2004). TMEM16F and TMEM16K have ubiquitous expression, whereas TMEM16G seems specifically expressed in prostate. Among all TMEM16 proteins, TMEM16H is the one with the most intriguing structural characteristics. The region between the fifth and sixth transmembrane domains is rich in negative charges. In particular, it contains a stretch of 20 contiguous residues of glutamic and aspartic acid. The cytosolic C- terminus is instead extremely abundant in prolines (56 out of 282 total residues). It is not know at the moment whether the TMEM16 proteins, other than TMEM16A and TMEM16B, are also associated with Cl^- channels. It is possible that they represent different types of ion channels activated by other types of physiological stimuli.

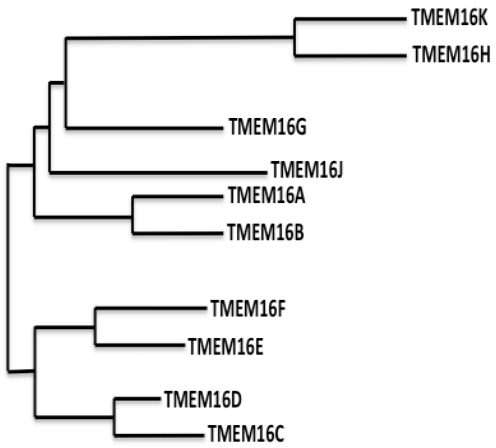

Figure 13. Phylogenetic tree depicting the TMEM16 protein family in human. Adapted from Scudieri, Sondo, Ferrera and Galietta 2011.

TMEM16A in cancer

The ANOs attracted the interest of cancer biologists for several years before their identification as ion channels because they are highly up-regulated in cancers (Galindo and Vacquier 2005). Because they are accessible cell surface proteins and are up-regulated in cancer, they are viewed as potential targets for therapeutic antibodies and as biomarkers for tumors ((Espinosa, Lee et al. 2008); (Das, Hahn et al. 2008)). The idea that ion channels may have functions in cancer is not new ((Shimizu, Hirose et al. 2008; Sontheimer 2008); (Shimizu, Lee et al. 2008); (Pardo and Stuhmer 2008)), but the addition of this well-studied channel family to the cancer proteome foreshadows new mechanistic insights.

ANO1 amplification and expression could be markers for distant metastasis in both oral and head and neck squamous cell carcinomas (HNSCC) and its locus is correlated with a poor outcome; moreover TMEM16A overexpression in 80% of head and neck squamous cell carcinoma (SCCHN), which correlated with decreased overall survival in patients with SCCHN ((Carles, Millon et al. 2006); (Huang, Godfrey et al. 2006)). ANO1 overexpression affects cell properties linked to metastasis. Inhibitors of CaCCs could be used to inhibit the tumourigenic properties of ANO1, whereas activators developed to increase CaCC activity could have adverse effects.

Gastrointestinal stromal tumor (GIST) is the most common kind of mesenchymal tumor found in the gastrointestinal tract. Most GISTs contain mutations in either KIT or PDGFRA receptor tyrosine kinases that result in their constitutive, ligand-independent activation. An inhibitor of KIT and PDGFRA is the primary therapy for metastatic or unresectable GIST. ANO1 is highly up-regulated in these tumors (Espinosa, Lee et al. 2008). Although ANOs are up-regulated in tumors, it does not seem that mutations in ANO1 are linked to carcinogenesis (Espinosa, Lee et al. 2008; Miwa, Nakajima et al. 2008). Rather, ANO1 may participate in cell proliferation and breast tumor progression (Duvvuri, Shiwarski et al. 2012). The activities of several anion channels correlate with the cell cycle ((Villaz, Cinniger et al. 1995); (Machaca and Haun 2002); (Klausen, Bergdahl et al. 2007)). Intriguingly, a dominant mutant of a *Drosophila* ANO, called *Axs* (aberrant x-segregation), is linked to chromosomal nondisjunction and progression of the meiotic cycle (Kramer and Hawley 2003).

ANO1 expression is significantly increased in patients with a propensity to develop metastasis ((Duvvuri, Shiwarski et al. 2012); (Kunzelmann 2005); ((West, Corless et al. 2004)). Given the role that Cl^- channels play in cell proliferation and migration, it is possible that Ano1 overexpression provides a growth or metastatic advantage to cancer cells (Kunzelmann 2005). Supporting the role of Ano1 in metastasis is that its overexpression stimulates cell movement (Ayoub, Wasylyk et al. 2010). Furthermore, recently it has been discovered that TMEM16A overexpression in breast cancer significantly promoted anchorage-independent growth in vitro, and loss of TMEM16A resulted in inhibition of tumor growth both in vitro and in vivo (Duvvuri, Shiwarski et al. 2012). Silencing of ANO1 decreases cell migration; treatment of cells with CaCC blockers has a similar effect, however a recent work demonstrated that TMEM16A-mediated CaCC is a negative regulator of cell proliferation. Their observations indicated that TMEM16A-mediated CaCC is an effective cell proliferation inhibitor by preventing cell cycle transition from the G0/G1 phase to the S phase via inhibition of cyclin D1 and cyclin E expression (Wang, Yang, Zheng et al. 2012). Thus, these results, seems to be contradictory to previous studies which reported that TMEM16A was

upregulated in several cancers, including oral cancer and gastrointestinal stromal tumors, before it was identified as CaCC. Although evidence suggests Ano1 may have a role in metastasis, it is still possible that the chromosomal region containing Ano1 (11q13) contains other genes involved in cancer progression. Notwithstanding the major role of AS in cancer, the function and the upregulation of the different TMEM16A AS isoforms in cancer are still unknown.

AIM OF THE THESIS

Alternative splicing in the TMEM16A gene has a significant implications for physiological function, including transepithelial fluid secretion, oocyte fertilization, olfactory and sensory signal transduction, smooth-muscle contraction, and neuronal and cardiac excitation, vascular tone, pain perception and GI tract motility.

In this thesis, the goal was to evaluate the regulation of three alternative splicing (AS) exons present in TMEM16A and explore if these events are independent or coordinated. Specific aims include: i) systematic analysis of exonic and intronic regulatory elements; ii) evaluation of intragenic splicing coordination of these AS events in normal adult human tissues and iii) whether changes in splicing isoform distribution are associated to cancer development.

RESULTS

Identification of Alternative Splicing events in *TMEM16A* and evaluation of the splicing pattern in normal adult human tissues

Bioinformatics analyses based on EST sequences from the Ensemble and UCSC Genome browsers databases revealed the presence of multiple mRNA isoforms with three conserved TMEM16A Alternative Splicing (AS) events and a possible not conserved alternative transcription start site. The AS events consist of three alternatively spliced exons in TMEM16A gene (Figure 14) at exon 6b, exon 13 and exon 15, of 66, 12 and 78 bp, respectively. The non conserved event occurs in the first exon and apparently is generated by the usage of an alternative promoter (Figure 14B). Bioinformatic prediction of the intrinsic strength of the splice sites using the "splice site prediction by neural network" website (available at http://www.fruitfly.org/seq_tools/splice.html), showed for exon 6b a weak 3'SS and an optimal 5'SS score (CV= 0.41 and 0.99) and for exon 15 a strong 3'SS (CV= 0.91) and a weak 5'SS splicing consensus sequence (CV=0.37). The scores of the short exon 13 were 0.81 and 0.68 for the 3' and 5'SS, respectively (Figure 16). To experimentally test whether the three highly conserved exons are actually alternatively spliced I evaluated the splicing pattern in human tissues. A pool of 20 RNAs derived from normal adult human tissues were tested by RT-PCR with primers targeting flanking exonic sequences (Figure 15A). The PCR products were analyzed by gel electrophoresis and the identities of PCR products with expected sizes for mRNAs including or excluding the test exon were confirmed by sequencing (Figure 15). On the contrary, attempts to amplify the non conserved (at DNA level) alternative promoter in TMEM16A in different human RNA tissues and cell lines were unsuccessful, suggesting a very restricted cell type-, developmental stage-, or signal-regulated expression.

The splicing products of the three evolutionary conserved exons showed different pattern of expression in normal adult human tissues. Exon 6b and exon 15 showed large tissue-dependent variability. Specifically, exon 6b is nearly

completely included in thyroid gland and liver, it represents more than 75% of the transcripts in placenta, prostate and trachea and is present in lower amounts in all the remaining human samples, as shown in figure 15B. On the contrary TMEM16A lacking exon 13 was observed only in brain and skeletal muscle, where they represent approximately 25% and 10% of total transcripts, respectively (Figure 15C). Exon 15 is virtually absent in liver, placenta and thyroid gland, present in low amounts (below 25%) in prostate, spleen, testis and trachea and significantly included (more than 70%) in ten samples, including adipose tissue, brain, cervix, colon, heart, kidney, lung, ovary, small intestine and thymus (Figure 15D).

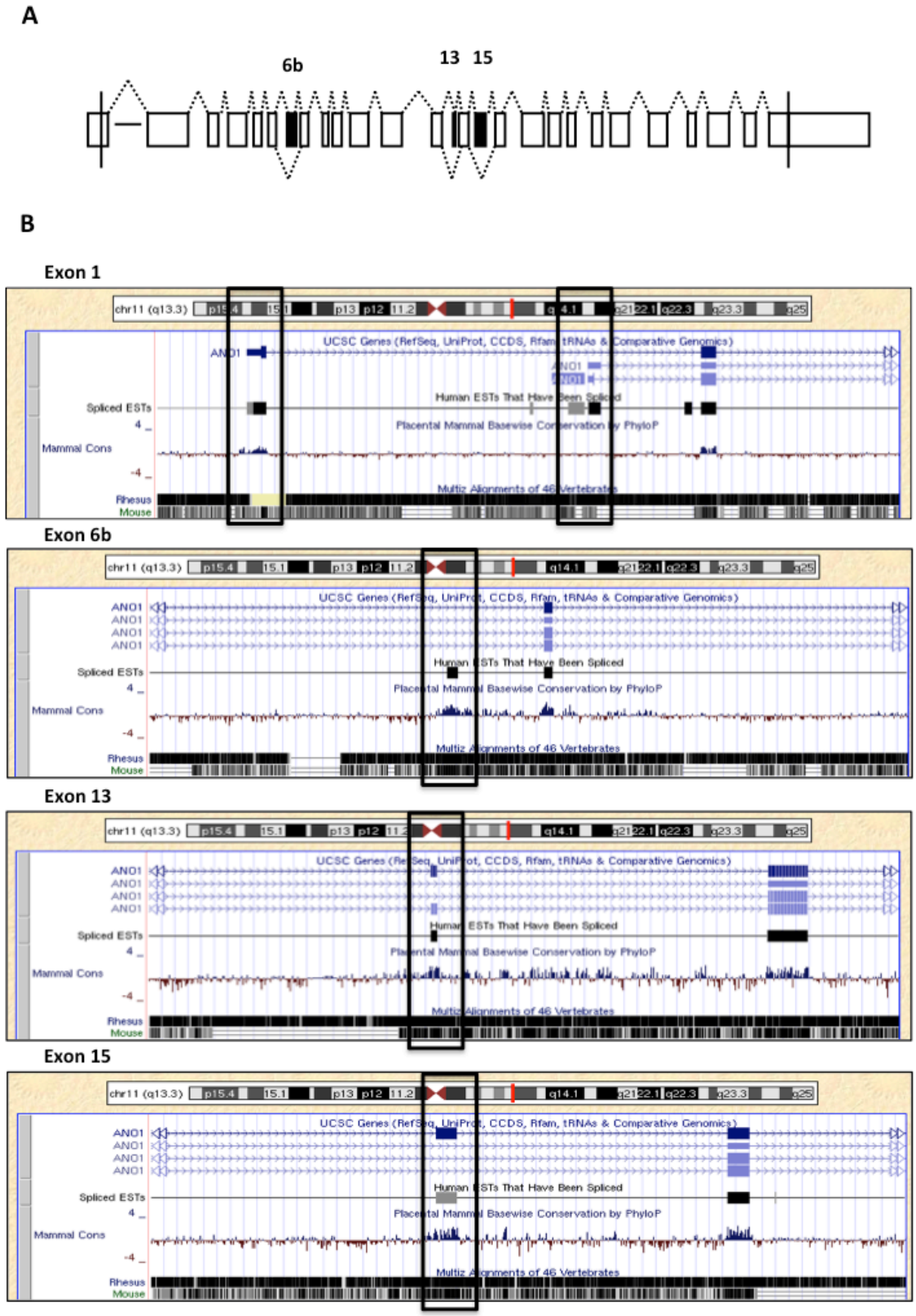

FIGURE 14. Computational identification of alternative spliced exons in TMEM16A. *A*, schematic representation of human TMEM16A coding sequence structure showing the constitutive and alternative spliced exons in white and black boxes, respectively. Exons 6b, 13, and 15 are 66 bp, 12 bp, and 78 bp, respectively. *B,* Pop-up window shows a schematic illustration of the bioinformatics analysis**,** derived from the UCSC Genome Browser using the Comparative Genomics track to examine alignments and evolutionary conservation, about individual AS exons of the human TMEM16A gene. Comparative genomic analysis with supporting EST information indicate they are found in mammal as distantly related as humans, mice rhesus and other species (data not shown).

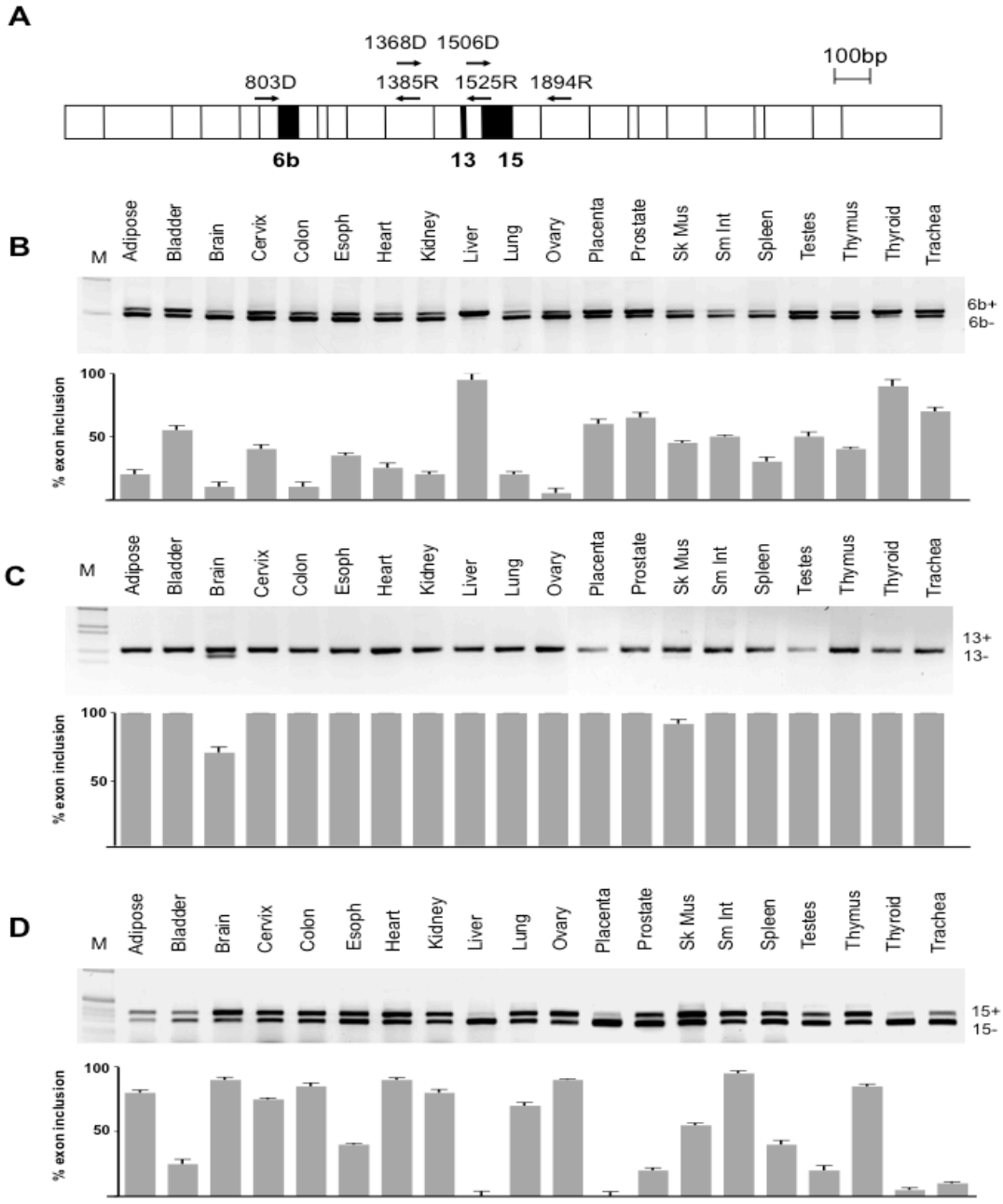

FIGURE 15. Alternative splicing pattern of *TMEM16A* in humans. *A*, schematic representation of TMEM16A coding sequence structure showing the constitutive and alternative spliced exons in white and black boxes, respectively. Exons 6b, 13, and 15 are 66 bp, 12 bp, and 78 bp, respectively. The small black superimposed arrows represent the positions of the primers used for the RT-PCR analysis. B–D, splicing pattern of exons 6b, 13, and 15, respectively. The upper part of each panel corresponds to the RT-PCR-amplified bands run on an agarose gel and stained with ethidium bromide; the lower graphs represent the percentage of exon inclusion for each tissue expressed as mean ±S.D. of three independent experiments done in duplicate. A panel of total human RNAs (20 different normal human tissues) was analyzed with the following primers: 803D and 1385R for exon 6b, 1368D and 1525R for exon 13, and 1506D and 1894R for exon 15. The identity of the transcripts was verified by direct sequencing, and the inclusion (ex+) or exclusion forms (ex-) are indicated. *M,* molecular 1-kb marker. Taken from Ferrera et.al. 2009

Analysis of TMEM16A exon 6b alternative splicing regulation

In order to investigate the regulation of the three AS exons identified in vivo in human tissues I used the well established hybrid minigene splicing assay. The minigenes I designed are a derivative of pTB, which is a modified version of the α-globin-fibronectin-EDB (Extra Domain B) minigene. The basic minigene (pTB) contains the exons 1, 2 and 3 of the α-globin and part of the fibronectin gene. Its transcription is under the control of a minimal α-globin promoter and the SV40 enhancer (Pagani, Stuani et al. 2003)). It has been previously used in other studies focused on normal and aberrant splicing and it reproduced the *in vivo* splicing pattern of several gene systems ((Muro, Caputi et al. 1999); (Pagani, Stuani et al. 2003); (Pagani, Stuani et al. 2003); (Baralle, Baralle et al. 2003)).

TMEM16A exons 6b, 13 and 15 along with part of their intronic flanking region (IVS 6 and IVS 7, IVS 12 and IVS 13 and IVS14 and IVS15, respectively) were cloned using a unique *Nde*I restriction site, which is located in the large fibronectin intron (Figure 16 and see Materials & Methods).

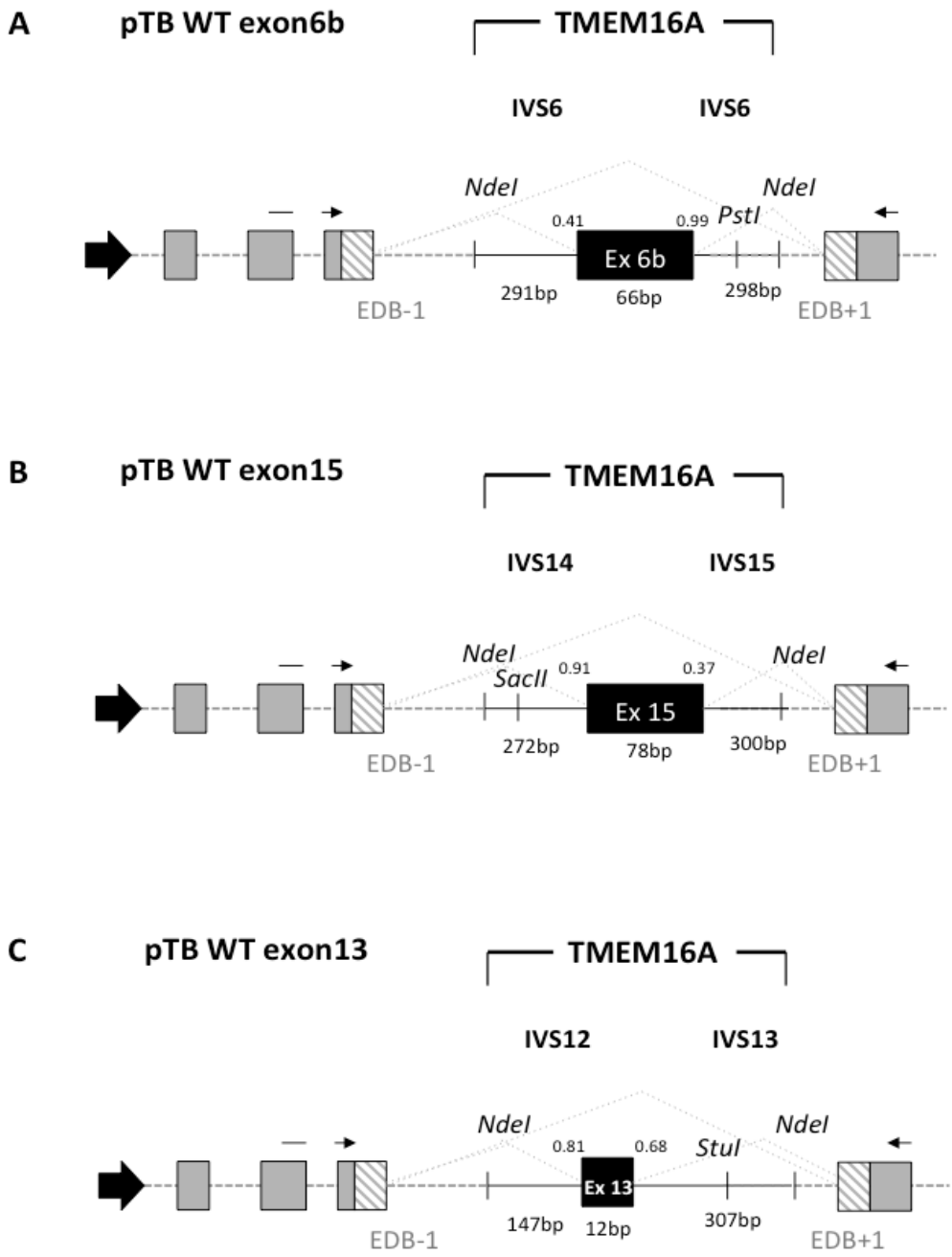

FIGURE 16. Schematic representation of the hybrid minigene system. *A,* schematic representation of the pTB hybrid minigene system. Dark grey, shaded and white boxes respectively represent α-globin, fibronectin EDB exons and human TMEM16A exon6b, with introns shown as thick lines. Exon6b and parts of its flanking introns (IVS) were cloned in the pTB plasmid using the restriction enzymes NdeI. The length of TMEM16A sequences is shown. Transcription is under the control of the minimal α-globin promoter and SV40 enhancer (big arrow at the 5'-end). The small black superimposed arrows represent the position of the primers used for the RT-PCR analysis after transient transfection of the minigene. The two alternative splicing possibilities, exon6b inclusion and exclusion, are indicated by grey dotted lines. The position of unique PstI restriction site used for subsequent cloning is shown. *B,* schematic representation of the pTB exon15 hybrid minigene system. *C,* schematic representation of the pTB exon13 hybrid minigene system.

Effect of splicing factors on TMEM16A exon 6b splicing

The first TMEM16A alternatively spliced exon I studied was exon 6b. Transient transfection of exon 6b construct (Figure 16A) was performed in HEK293 cells and the spliced mRNAs were analyzed through RT-PCR using alpha2,3 and bra2 oligonucleotides specific for the minigene sequence, therefore excluding the possibility of amplifying endogenous mRNA. The PCR products detected upon transfection of the WT exon 6b minigene showed the presence of two amplified bands: the upper one corresponds to exon 6b inclusion (583 bp) and the lower one to exon 6b exclusion (518 bp). The identity of the bands was verified by direct sequencing after elution of the bands from the gel. Quantitative analysis of band intensity showed ~ 65% of exon 6b inclusion (Figure 17, lane 1 and 7; Figure 18 lane 1, 7 and 11).

To identify the trans-acting protein involved in exon 6b regulation I performed cotransfection experiments of pTB WT ex6b minigene along with plasmids coding for a panel of 21 representative splicing factors. I select a panel of splicing factors that include two epithelial-specific splicing factors (ESRP1FF and ESRP2FF), ETR3, the CUG binding protein, a list of SR proteins (SRSF1, SRSF3, SRSF9, SRSF5, SRSF6, SRSF4, SRSF2 and TRA2B), the Py-rich binding proteins TIA1, PTB1, the general splicing factors U2AF35 and U2AF65, diverse hnRNPs (hnRNP A1, hnRNP A2 and hnRNP H) and two neuronal tissue specific splicing factors Nova2 and RbFOX1.

As shown in Figure 17 and 18, several splicing factors induced changes in the percentage of exon 6b inclusion. Co-transfection of ESRP1FF/2FF, ETR3 and CUG proteins, induced a splicing inhibition with a decrease of the percentage of exon inclusion (Figure 17, lane 3-6). These proteins decreased exon 6b inclusion from 65% to less then 40%. Overexpression of SR proteins (SRPs) differently regulates exon 6b splicing. Figure 17, showed that 4 out of 8 SRPs inhibited exon 6b, from 65% towards more or less 40-20% of inclusion (lanes 9, 11, 12 and 13), conversely, SRSF9 and TRA2B enhanced exon 6b inclusion to 88% and 85%, respectively (Figure 17, lanes 10 and 15). I also explored the effect of Py-rich binding proteins in exon 6b WT minigene, as shown in figure 18, PTB1 protein increased exon 6b inclusion, reaching 90% (lane 6) whereas TIA1, U2AF65 and

U2AF35 did not significantly affect splicing (Figure 18, lanes 3, 4 and 5). Similarly, co-transfection with hnRNPs expression vectors, hnRNP A1, hnRNP A2 and hnRNP H or with the neuronal protein $NOVA_2$, had no effect on exon 6b splicing. On the contrary, the tissue specific protein RbFOX1 exhibited a positive effect on exon 6b, rising exon inclusion level from 65% to 92% (Figure 18, lane 12).

Taken together, these results show that exon 6b is modulated by different splicing factors. It is positively regulated by 4 splicing factors SRSF9, TRA2B, PTB1 and RbFOX1 and negatively regulated by the UG-rich binding proteins (ESRP1FF/2FF, ETR3 and CUG) and by few SRPs (SRSF3, SRSF5, SRSF6, SRSF4).

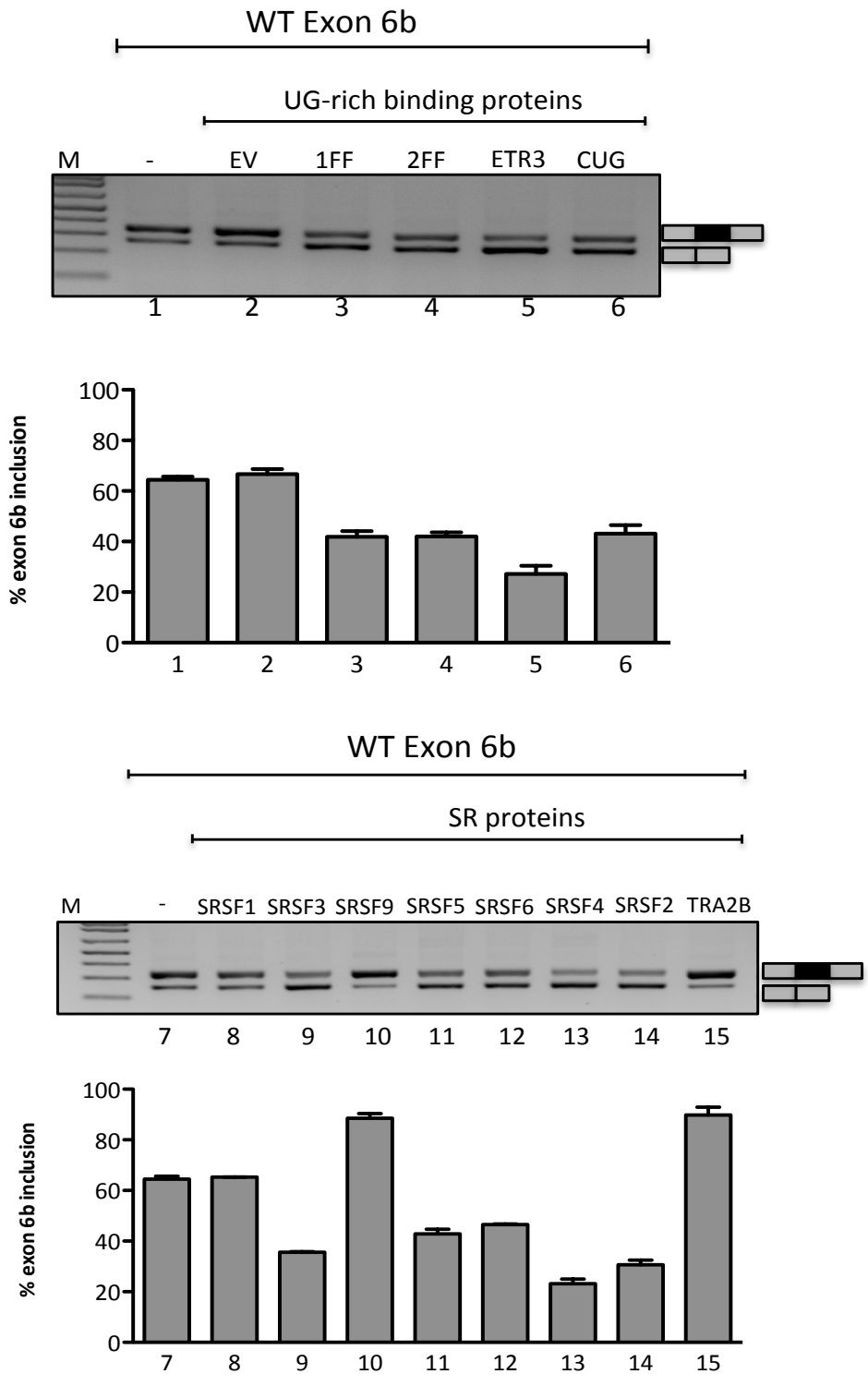

FIGURE 17. Splicing pattern of TMEM16A exon6b minigene co-transfected with splicing factors. Splicing pattern analysis of the RT-PCR products derived from RNA of transfected HEK293 cells, separated in electrophoresis on 2% agarose gel. TMEM16A exon6b minigene was transfected alone (0.5ug) or with splicing factors (0.5ug) and splicing pattern was evaluated by RT-PCR with alpha 2,3 and bra2 primers. The identity of the bands are indicated on the right side of the panel. M, molecular weight marker. (-) denotes WT position. EV is the Empty Vector. Quantification analysis of exon6b inclusion was estimated using ImageJ software and is expressed as ± SD, based on at least three independent experiments done in duplicate.

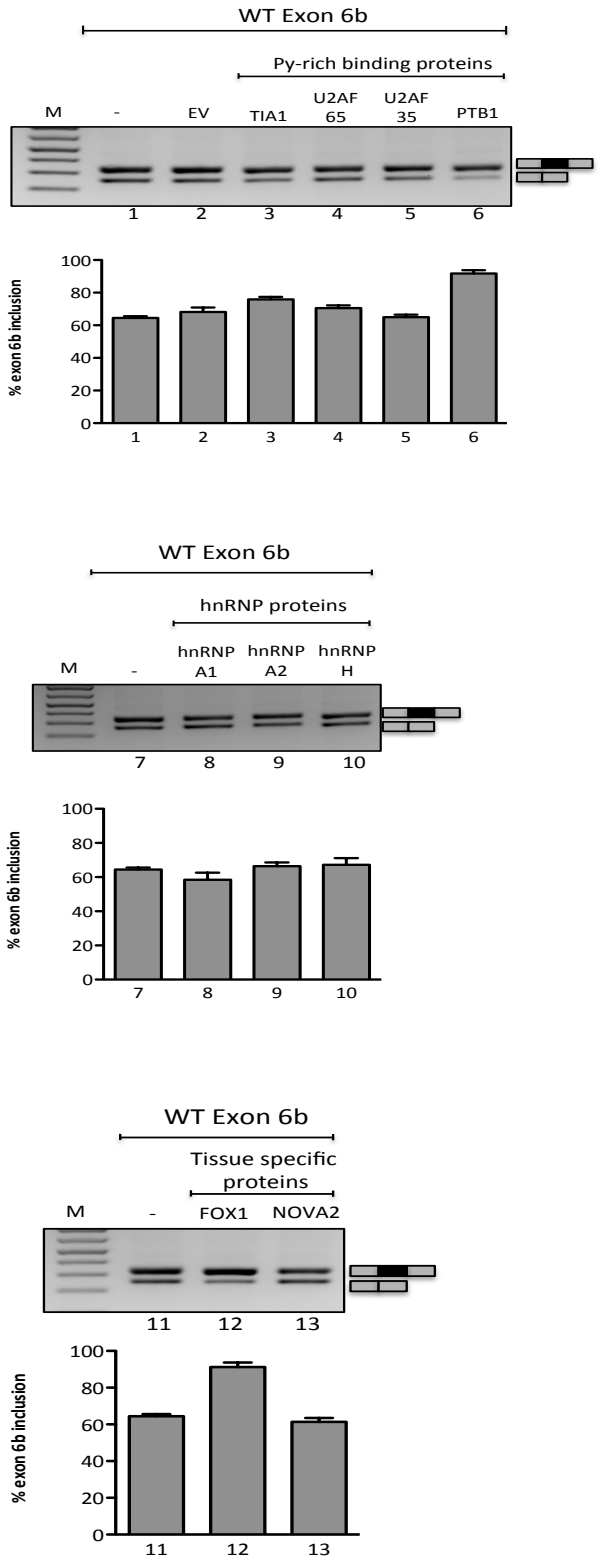

FIGURE 18. Splicing pattern of TMEM16A exon6b minigene co-transfected with splicing factors. Splicing pattern analysis of the RT-PCR products derived from RNA of transfected HEK293 cells, separated in electrophoresis on 2% agarose gel. TMEM16A exon6b minigene was transfected alone (0.5ug) or with splicing factors (0.5ug) and splicing pattern was evaluated by RT-PCR with alpha 2,3 and bra2 primers. The identity of the bands are indicated on the right side of the panel. M, molecular weight marker. (-) denotes WT position. EV is the Empty Vector. Quantification analysis of exon6b inclusion was estimated using ImageJ software and is expressed as ± SD, based on at least three independent experiments done in duplicate.

Identification of enhancers and silencers sequences that affect splicing of TMEM16A exon 6b

In order to identify putative exonic splicing regulatory elements (ESE and ESS), I analyzed, in first instance, exon 6b with several *in silico* programs and the results are shown in figure 19. Using three different web-based resource ESE-finder (http://rulai.cshl.edu/cgi-bin/tools/ESE3/esefinder.cgi), RESCUE-ESE (http://genes.mit.edu/burgelab/rescue-ese/) and PESXs (http://cubweb.biology.columbia.edu/pesx/) websites, I found several possible splicing regulatory elements. ESE-finder analysis (Figure 19A) indicated the location of potential binding sites for the splicing factors SRSF1 (ASF/SF2), SRSF2 (SC35) and SRSF6 (SRp55) concentrated in the central portion of the exon. RESCUE-ESE (Figure 19B), identified a long GAA-rich enhancer at the 5' end of the exon, and one enhancer at the end (drawn in yellow). PESXs program (Figure 19C) identified the same GAA-rich enhancer sequence at the 5' end of the exon. No putative ESSs were detected with this program.

To identify splicing regulatory elements within exon 6b sequence I engineered several mutant minigenes with a set of consecutive exonic deletions from base +6 to +63, as illustrated in figure 20. I introduced six consecutive deletions of approximately 10 bp each in the exon by PCR with specific primers on pTB WT as template: from position +6 to +10 (MUT1), from position +11 to +24 (MUT2), from position +25 to +33 (MUT3), from position +34 to +43 (MUT4), from position +44 to +54 (MUT5) and from position +55 to +63 (MUT6). These mutants were evaluated upon transfection into HEK293 cells and the percentage of exon 6b inclusion analyzed by RT-PCR and the splicing pattern evaluated on 2% agarose gel. In comparison to the WT exon 6b most of the mutants affected splicing. MUT1 did not change the splicing pattern whereas MUT2 induced complete exon skipping (Figure 20, lane 2 and 3, respectively). The other downstream deletion mutants (MUT4, MUT5, MUT6) increased exon 6b inclusion (Figure 20, lane 5, 6, 7). The higher molecular weight band present in MUT3 (Figure 20, lane 4) was a heterodimer created by the deletion mutant as determined by direct sequence analysis and sequencing after cloning of the upper band.

To further identify additional splicing regulatory elements I focused on the

downstream intronic sequences that contain Py-rich and UG rich elements. I engineered mutant minigenes with a set of consecutive intronic deletions as illustrated in figure 21A. I introduced four deletions: from position +13 to +32 (MUT7), from position +33 to +46 (MUT8), from position +47 to +68 (MUT9) and from position +69 till the end of the minigene (MUT10). These mutants were evaluated upon transfection into HEK293 cells and the percentage of exon 6b inclusion was analyzed by RT-PCR. In comparison to the WT TMEM16A exon 6b, MUT9 increased the percentage of exon inclusion from 65% to 100% (Figure 21B). MUT9 had a silenced effect on the splicing outcome indicating that the sequence TTCCAAATTGTATGTGTGTTTT deleted in MUT9 acts as an intronic splicing silencer (ISS). The MUT7 and partially MUT8 mutants slightly decreased exon 6b splicing pattern suggesting that the corresponding intronic sequences deleted are weak intronic splicing enhancers (ISEs).

Altogether these experiments indicate the AS of exon 6b is regulated by multiple of enhancers and silencers elements. I identify two enhancers, one in the exon (MUT2) that and one in the intron (MUT7) and three silencers (MUT4, MUT5 and MUT6 in the exon; MUT9 in the intron). In particular, the exonic GGGAAGAAAGAAGG sequence from position +11 to +24 behave like a strong ESE as its deletion in the MUT2 minigene leads to complete exclusion of exon 6b. Interestingly, this long GAA-rich region was predicted by the *in silico* tools. On the other hand, the downstream exonic sequences, behave as exonic splicing silencers (ESSs). I also identify an ISE and an ISS downstream of exon 6b.

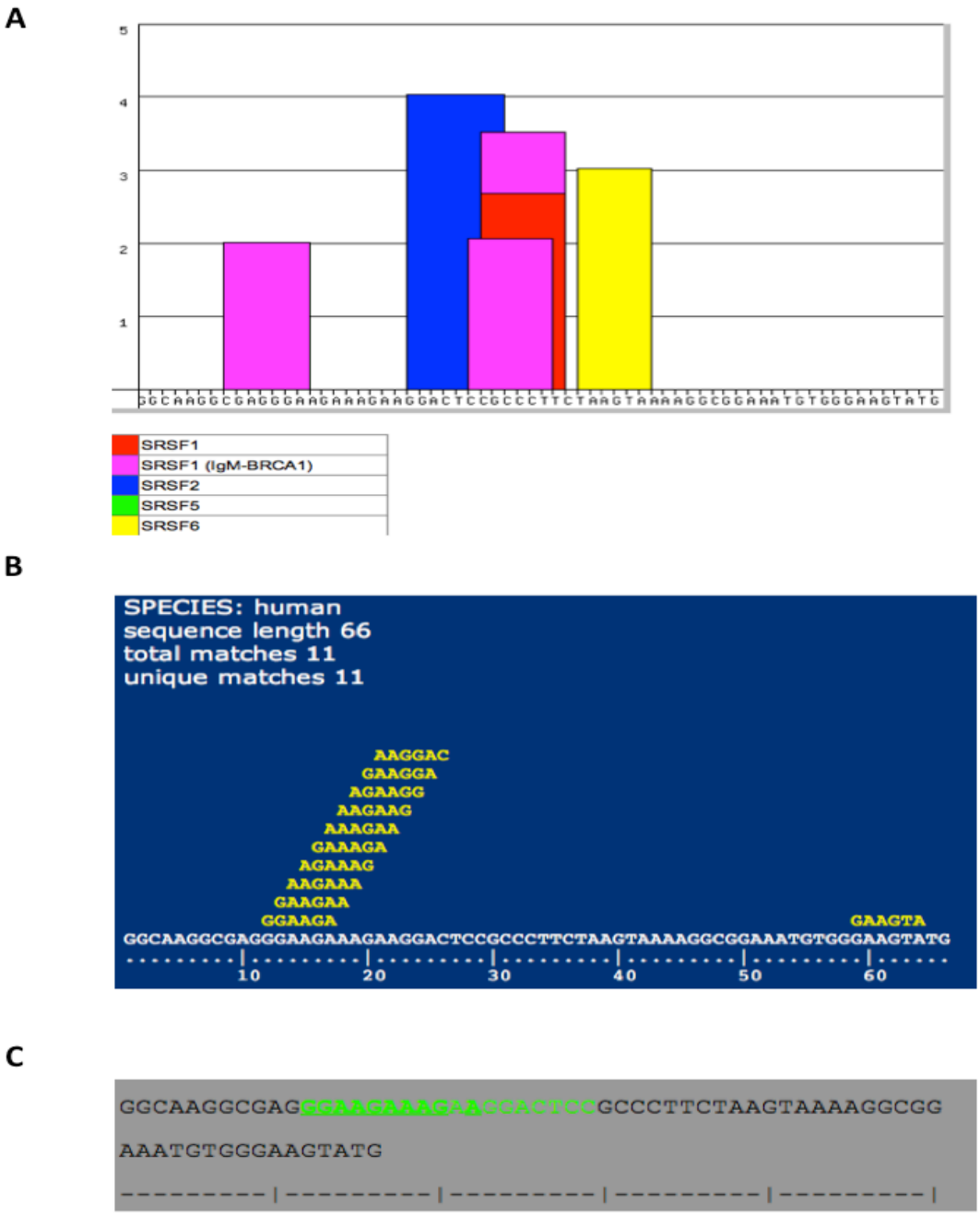

FIGURE 19. Predicted ESE sites within exon sequence from base +1 to +66. *A,* ESE-finder output for *TMEM16A* exon6b, using version 2.0 matrices and thresholds. Y-axis shows ESEfinder above-threshold scores for identified matches; X-axis corresponds to the exon6b sequence from base +1 to base +66. ESE finder analysis indicates the location of potential binding sites for the splicing factors SRSF1 (SF2/ASF, red magenta), SRSF2 (SC35, blue), SRSF5 (SRp40, green) and SRSF6 (SRp55, yellow). *B,* The RESCUE-ESE web server. The output displays the input sequence with the ESEs drawn above in yellow. *C,* The PESXs web server. The light grey sequence indicates the ESE candidates identified by the server.

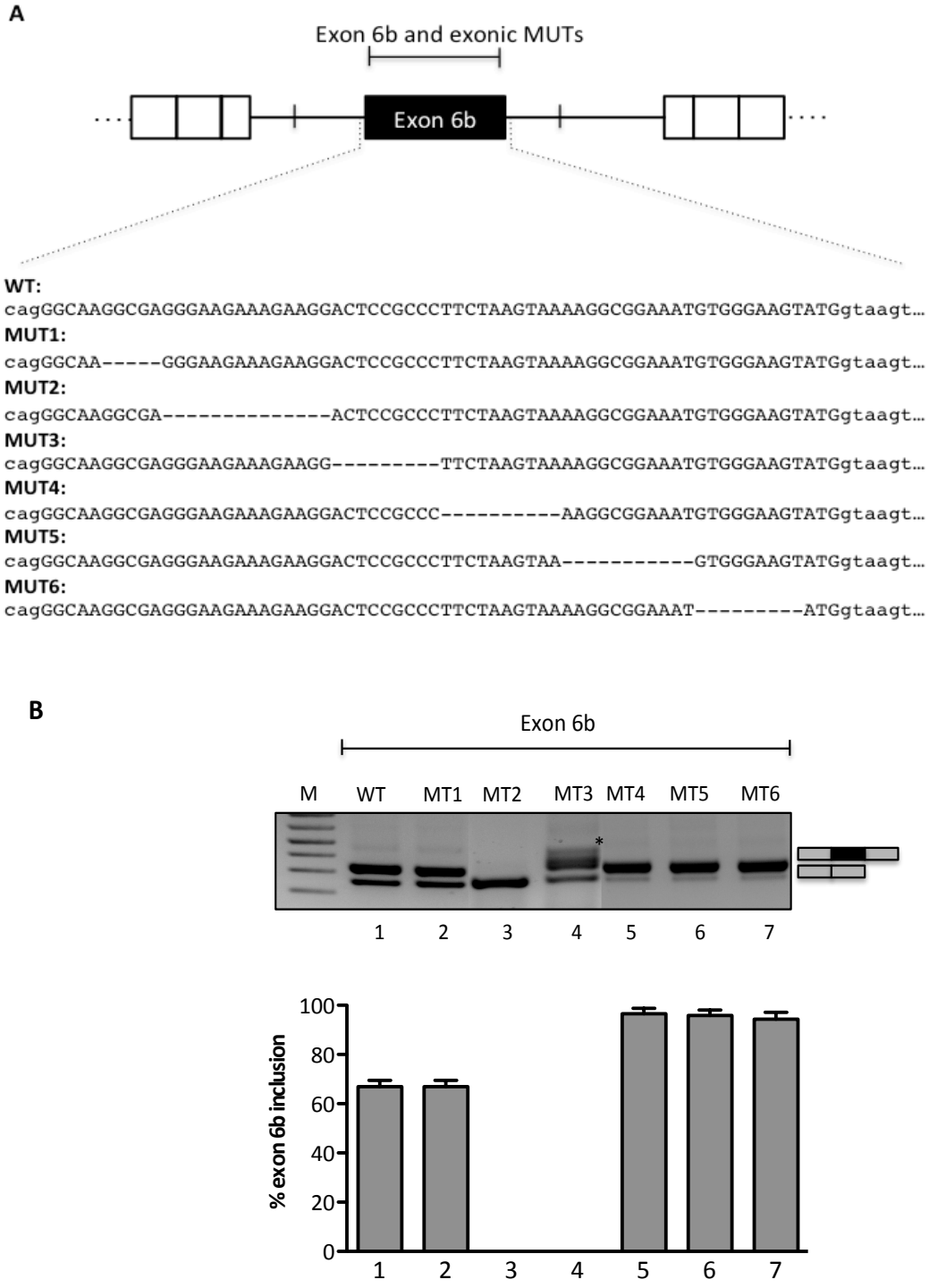

FIGURE 20. Exon deletion analysis of TMEM16A exon6b. *A,* Schematic representation of exon6b wt and exonic mutant minigenes. The mutants were created by overlap extension PCR, using specific oligonucleotide complementary to up- and downstream sequences of the deleted region. Sequence variations (below the wild-type sequence) are shown. Uppercase letters represent exonic sequence and lowercase letters intronic sequence. *B,* Splicing assay of the seven TMEM16A exon6b constructs (WT and MUTs) were transfected into HEK293 cells. Splicing pattern was evaluated by RT-PCR with alpha 2,3 and bra2 primers. Amplified products were separated in electrophoresis on 2% agarose gel. The identity of the bands are indicated on the right side of the panel. M, molecular weight marker. Quantification analysis of exon6b inclusion was estimated using ImageJ software and is expressed as ± SD, based on at least three independent experiments done in duplicate.

*, heterodimer.

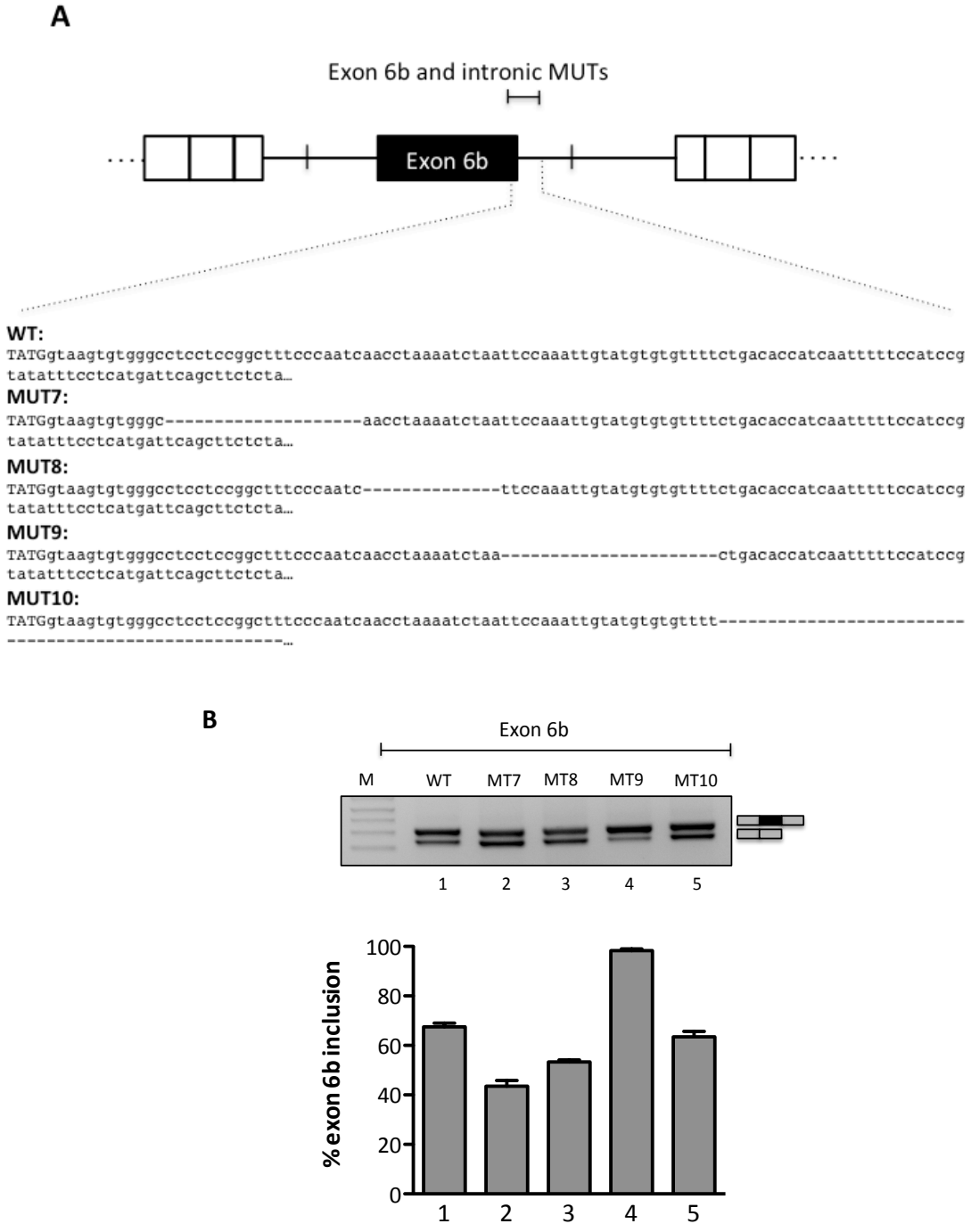

FIGURE 21. Intron deletion analysis of TMEM16A exon6b. *A,* Schematic representation of exon6b wt and intronic mutant minigenes. The mutants were created by overlap extension PCR, using specific oligonucleotide complementary to up- and downstream sequences of the deleted region. Sequence variations (below the wild-type sequence) are shown. Uppercase letters represent exonic sequence and lowercase letters intronic sequence. *B,* Splicing assay of the five TMEM16A exon6b constructs (WT and MUTs) were transfected into HEK293 cells. Splicing pattern was evaluated by RT-PCR with alpha 2,3 and bra2 primers. Amplified products were separated in electrophoresis on 2% agarose gel. The identity of the bands are indicated on the right side of the panel. M, molecular weight marker. Quantification analysis of exon6b inclusion was estimated using ImageJ software and is expressed as ± SD, based on at least three independent experiments done in duplicate.

Overexpression of splicing factors that induce exon 6b inclusion do not affect splicing in the absence of the 16bp long GAA-rich ESE

In order to understand the role of the two identified splicing enhancer elements and possible effect of *trans*-acting factors, I evaluated the effect of the four proteins that promoted exon 6b splicing: SRSF9, TRA2B, PTB1 and RbFOX1 (Figures 17 and 18) on the MUT2 and MUT7 minigenes. Deletion of the long GAA-rich ESE in MUT2 induced complete exon 6b skipping and overexpression of these splicing factors had no effect of splicing (Figure 22). On the contrary, co-transfection of SRSF9, TRA2B, PTB1 and RbFOX1 along with the MUT7 minigene was still able to induce exon inclusion (Figure 26). The absence of an enhancing effect by all the splicing factor on the MUT2 minigene deletion mutant indicates that the 16bp long GAA-rich ESE is a key element involved in exon 6b splicing regulation: its deletion completely abolish exon recognition and co-transfection of the splicing factor do not rescue splicing.

Most of the splicing inhibitory factors do not affect splicing in the ESSs deletion exon 6b minigenes

To test the relationship between the splicing inhibitory factors and the ESSs, I co-transfected the proteins with splicing inhibitory activity along with the MUT4, MUT5 and MUT6 exon 6b minigenes. Deletions of exonic sequences in these mutants induced nearly complete exon inclusion (Figure 20B) and co-transfection of the inhibitory splicing factors have a small effect on the percentage of exon inclusion. Only ETR3 and SRSF2 maintained a significant exon 6b splicing inhibition in all the exonic mutants. In fact co-transfection of these splicing factors along with MUT4, MUT5 and MUT6 minigenes, reduce the percentage of exon inclusion from 95% below 50-70% (Figure 23, 24 and Figure 25, respectively). On the other hand, overexpression of the other splicing factors, ESRP1FF/2FF, ETR3, CUGBP, SRSF3, SRSF5, SRSF6, SRSF4, hnRNPA1, hnRNPA2 and hnRNPH, showed a splicing pattern comparable with the single mutants. To test the role of the ISS, I co-transfected the most representative silencer SFs with the deletion mutant MUT9 (Figure 27). In this case, most of the proteins induce a significant decrease in the percentage of exon inclusion and again ETR3 showed

the strongest effect. In this case, co-transfection of ESRP1FF, CUGbp, SRSF2 and SRSF3 reduce the percentage of exon inclusion from 95% to 60% , co-transfection of ETR3 to 30% (Figure 27).

All together these results indicate the importance of the three ESSs and the ISS in determining the splicing outcome and suggest that the inhibitory splicing factors might regulate splicing through these regulatory elements.

In particular, the 3'end portion of the exon included in the MUT4, MUT5 and MUT6 deletions might affect splicing through the formation of a splicing inhibitory complex.

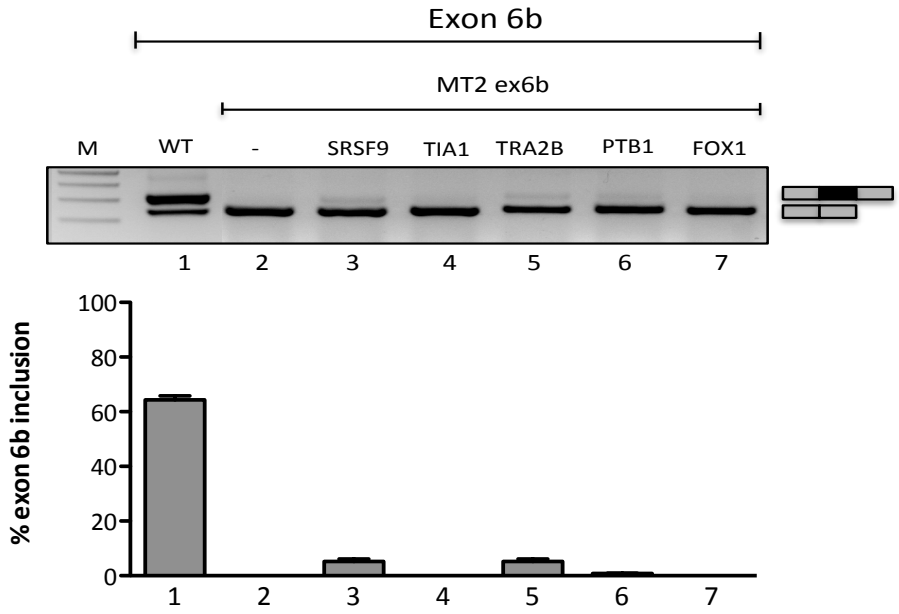

FIGURE 22. TMEM16A exon6b MUT2 minigene co-transfected with enhancing splicing factors. Splicing pattern analysis of the RT-PCR products derived from RNA of transfected HEK293 cells, separated on 2% agarose gel. GAA-rich MUT2 TMEM16A exon6b minigene was transfected alone (0.5ug) or with five splicing factors (0.5 ug) and the splicing pattern evaluated with alpha 2,3 and bra2 primers. None of the splicing factors are able to restore exon6b inclusion. The identity of the bands are indicated on the right side of the panel. M, molecular weight marker. (-) denotes the mutant position. Percentage of exon 6b inclusion was estimated using ImageJ software and is expressed as mean ± SD, based on at least three independent experiments done in duplicate.

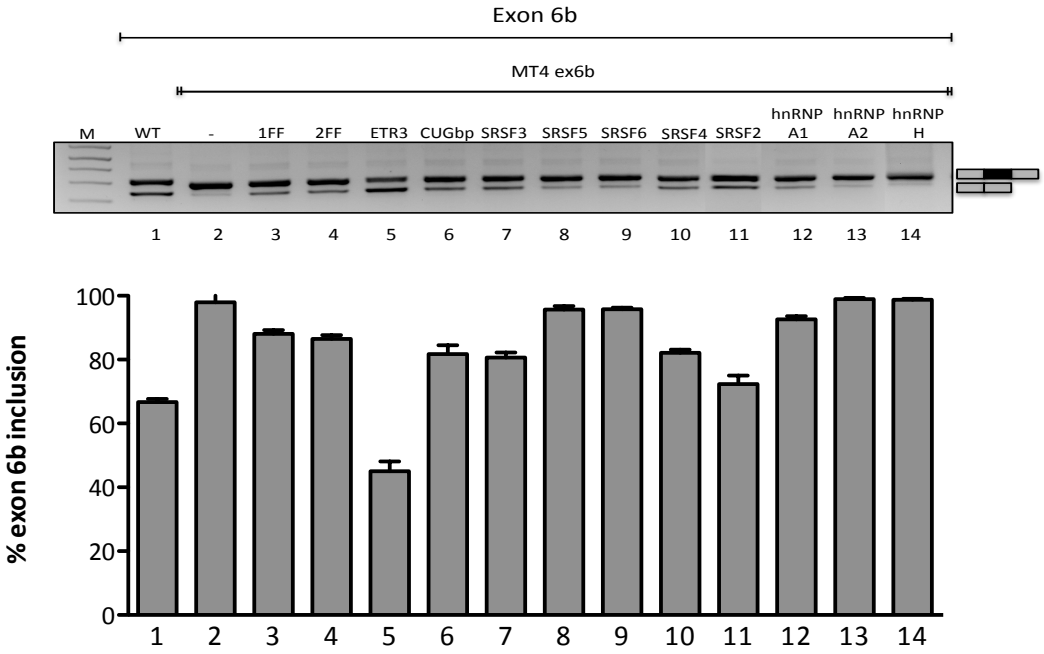

FIGURE 23. TMEM16A exon6b MUT4 minigene co-transfected with different splicing factors. Splicing pattern analysis of the RT-PCR products derived from RNA of transfected HEK293 cells, separated on 2% agarose gel. MUT4 TMEM16A exon6b minigene was transfected alone (0.5ug) or with eleven splicing factors (0.5 ug) and the splicing pattern evaluated with alpha 2,3 and bra2 primers. The identity of the bands are indicated on the right side of the panel. M, molecular weight marker. (-) denotes the mutant position. Percentage of exon 6b inclusion was estimated using ImageJ software and is expressed as mean ± SD, based on at least three independent experiments done in duplicate.

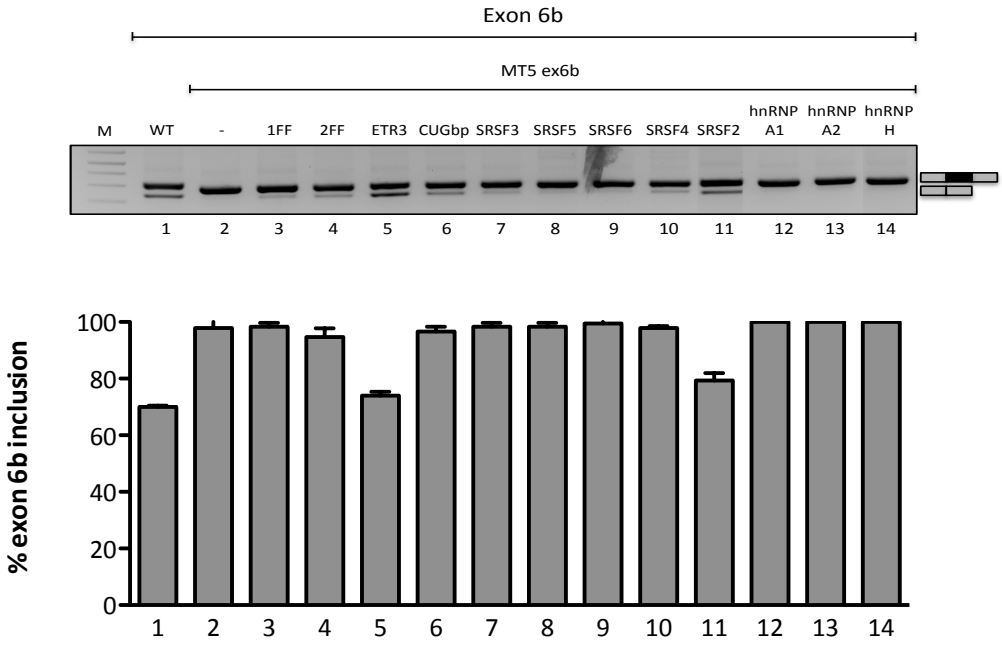

FIGURE 24. TMEM16A exon6b MUT5 minigene co-transfected with different splicing factors. Splicing pattern analysis of the RT-PCR products derived from RNA of transfected HEK293 cells, separated on 2% agarose gel. MUT5 TMEM16A exon6b minigene was transfected alone (0.5ug) or with twelve splicing factors (0.5 ug) and the splicing pattern evaluated with alpha 2,3 and bra2 primers. The identity of the bands are indicated on the right side of the panel. M, molecular weight marker. (-) denotes the mutant position. Percentage of exon 6b inclusion was estimated using ImageJ software and is expressed as mean ± SD, based on at least three independent experiments done in duplicate.

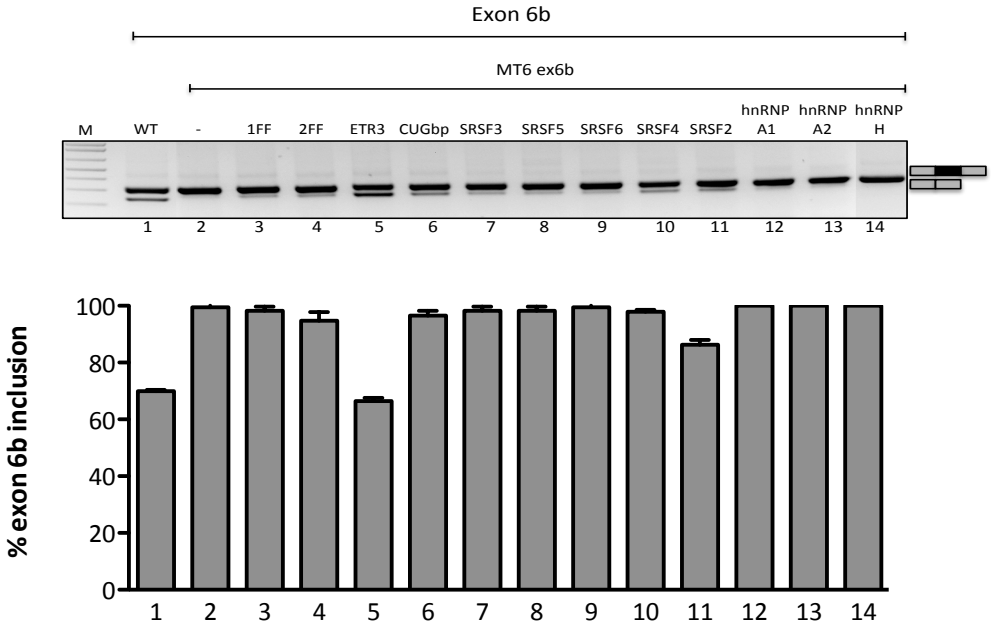

FIGURE 25. TMEM16A exon6b MUT6 minigene co-transfected with different splicing factors. Splicing pattern analysis of the RT-PCR products derived from RNA of transfected HEK293 cells, separated on 2% agarose gel. MUT6 TMEM16A exon6b minigene was transfected alone (0.5ug) or with twelve splicing factors (0.5 ug) and the splicing pattern evaluated with alpha 2,3 and bra2 primers. The identity of the bands are indicated on the right side of the panel. M, molecular weight marker. (-) denotes the mutant position. Percentage of exon 6b inclusion was estimated using ImageJ software and is expressed as mean ± SD, based on at least three independent experiments done in duplicate.

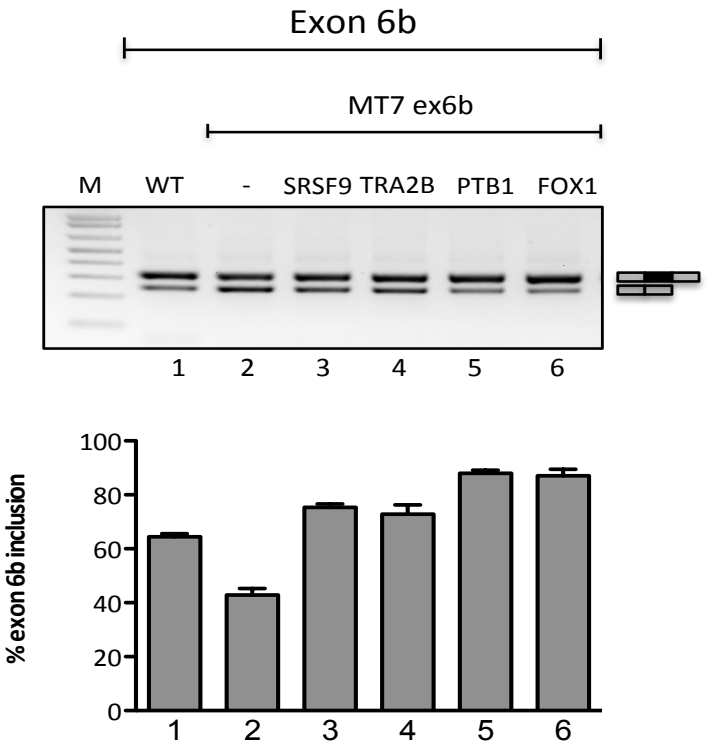

FIGURE 26. TMEM16A exon6b MUT7 minigene co-transfected with enhancing splicing factors. Splicing pattern analysis of the RT-PCR products derived from RNA of transfected HEK293 cells, separated on 2% agarose gel. Py-rich MUT7 TMEM16A exon6b minigenes were transfected alone (0.5ug) or with four splicing factors (0.5 ug) and the splicing pattern evaluated with alpha 2,3 and bra2 primers. None of the splicing factors did not change splicing pattern. The identity of the bands are indicated on the right side of the panel. M, molecular weight marker. (-) denotes the mutant position. Percentage of exon 6b inclusion was estimated using ImageJ software and is expressed as mean ± SD, based on at least three independent experiments done in duplicate.

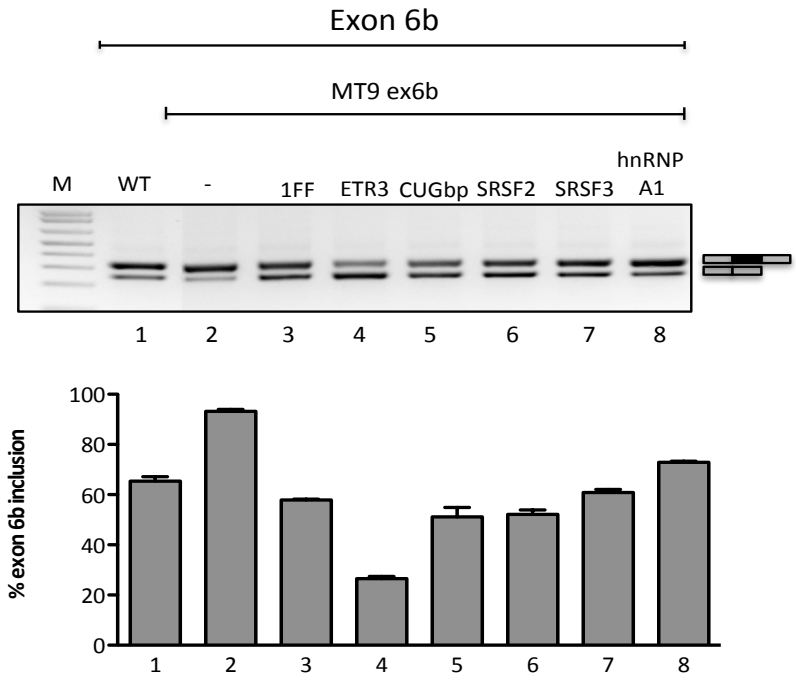

FIGURE 27. TMEM16A exon6b MUT9 minigene co-transfected with inhibitory splicing factors. Splicing pattern analysis of the RT-PCR products derived from RNA of transfected HEK293 cells, separated on 2% agarose gel. UG-rich MUT9 TMEM16A exon6b minigenes were transfected alone (0.5ug) or with six splicing factors (0.5 ug) and the splicing pattern evaluated with alpha 2,3 and bra2 primers. None of the splicing factors did not change splicing pattern. The identity of the bands are indicated on the right side of the panel. M, molecular weight marker. (-) denotes the mutant position. Percentage of exon 6b inclusion was estimated using ImageJ software and is expressed as mean ± SD, based on at least three independent experiments done in duplicate.

Role of the GAA-rich ESE in TMEM16A exon 6b

Mutation and deletion analysis of the exon 6b GAA-rich ESE

Due to the key role of the 16bp long GAA-rich ESE in the regulation of TMEM16A splicing I decided to investigate more in detail the properties of this element performing a series of point and deletion mutants (Figure 28). Sequence inspection identified two core adjacent AGAA elements that represent the optimal consensus binding site for TRA2B (Clery, Jayne et al. 2011), flanked by a AGGGA and GGA sequences (Figure 28). To evaluate the role of these four elements, I introduced nucleotide substitutions and deletions into the TMEM16A exon 6b minigene sequence. I engineered eleven mutant minigenes: six (MUT2A–F) affected the two core AGAA motifs and five (MUT2G–I) the two flanking sequences. In MUT2-A, the central AGAA motifs were substituted with a stretch of poly-A (from AGAAAGAA to AAAAAAAA), in MUT2-B and MUT2-C the upstream or downstream AGAA motifs were individually deleted whereas in MUT2D both were deleted, in MUT2-E and MUT2-F the central G of each AGAA motif was replaced with an A (from AGAAAGAA in AGAAAAAA and AAAAAGAA, respectively). MUT2-G, MUT2-H and MUT2-I affected the flanking AGGGA and GGA sequences introducing small deletions (MUT2-G has deletion in the first element, MUT2-H in the last and MUT2-I in both). Lastly, in MUT2-L and MUT2-M the flanking AGGGA and GGA elements, the Gs of the motifs were substituted with C (Figure 28).

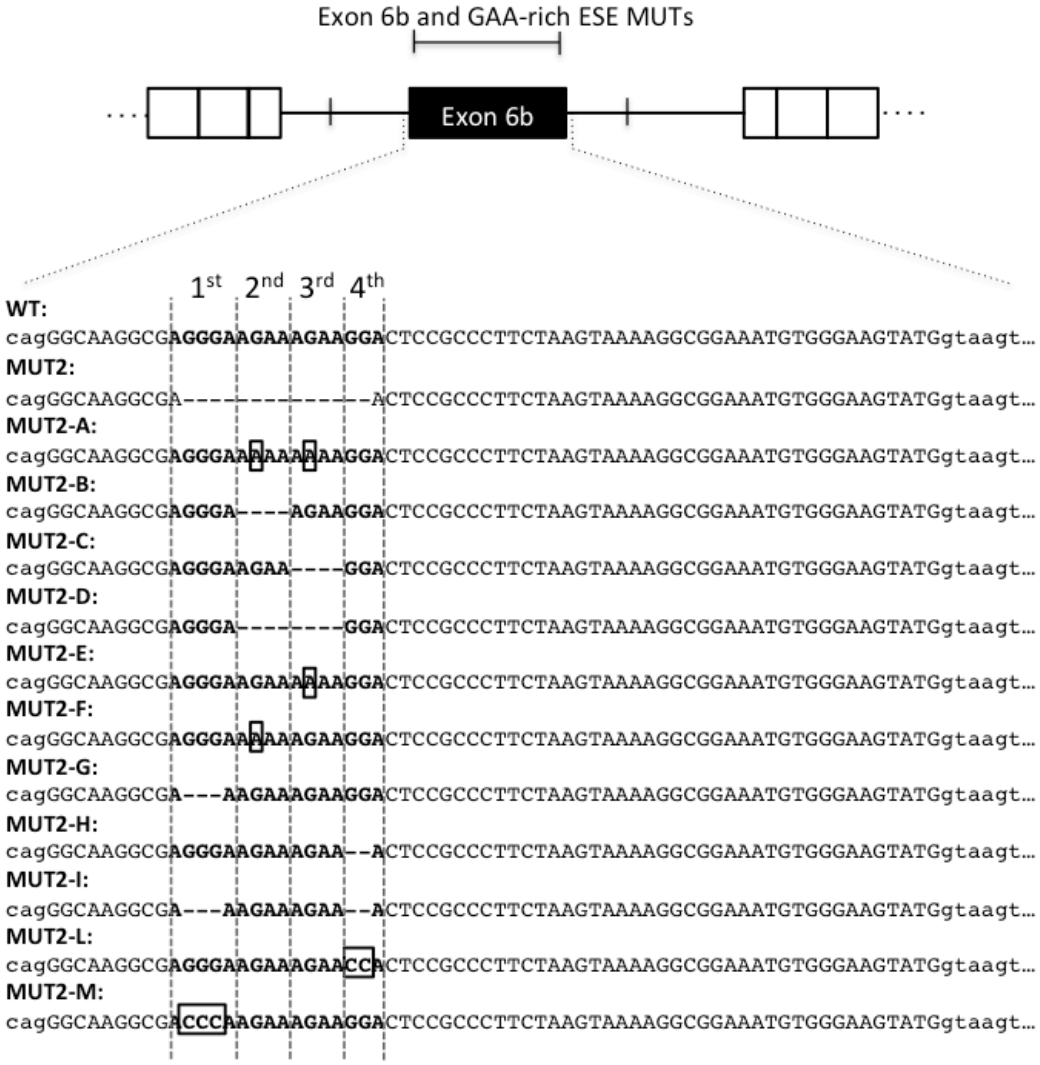

FIGURE 28. Mutagenesis of exon6b ESE element. Schematic representation of exon6b wt and GAA-rich ESE mutant minigenes. The mutants were created by overlap extension PCR into the GAA-rich ESE element, using specific oligonucleotide complementary to up- and downstream sequences of the mutated region. Sequence variations (below the wild-type sequence) are shown. Uppercase letters represent exonic sequence and lowercase letters intronic sequence.

The resulting minigenes were transiently transfected into HEK293 cells, and analyzed by RT-PCR. The splicing profile of each mutant was compared to the pattern of the pTB exon 6b WT plasmid. As shown in figure 29, most of the deletion or substitution across the four sequences that compose the GAA-rich ESE, have a dramatic effect on the splicing outcome, leading to almost complete exon 6b exclusion. The only exception is MUT2-M, which did not affect the splicing pattern: this could be due to the type of mutation introduced (substitution of three GGG of the first elements with three CCC). As the MUT2-G construct in which the first element is deleted showed nearly complete exon skipping, the substitution introduced in MUT2-M might create a new ESE element. On the other hand, some mutants maintained a small but significant percentage of exon 6b inclusion, MUT2-B, MUT2-C, MUT2-E and MUT2-G showed ~ 10-20% of exon inclusion (Figure 29) suggesting that some elements although necessary for the full ESE function, individually they have a lower enhancer activity. Overall, these results indicate that the entire 16bp GAA-rich ESE located at the 5' end of the exon 6b and distant 10 bp from the 3'ss, is a key regulatory element involved in splicing recognition and that a mutation that affect just one of the four discrete sequences that compose it is sufficient to induce exon 6b skipping.

A

	AGGGA	AGAA	AGAA	GGA	
WT	1	2	3	4	
MUT2	**X**	**X**	**X**	**X**	deletion
MUT2-A	1	**X**	**X**	4	substitution
MUT2-B	1	**X**	3	4	deletion
MUT2-C	1	2	**X**	4	deletion
MUT2-D	1	**X**	**X**	4	deletion
MUT2-E	1	2	**X**	4	substitution
MUT2-F	1	**X**	3	4	substitution
MUT2-G	**X**	2	3	4	deletion
MUT2-H	1	2	3	**X**	deletion
MUT2-I	**X**	2	3	**X**	deletion
MUT2-L	1	2	3	**X**	substitution
MUT2-M	**X**	2	3	4	substitution

B

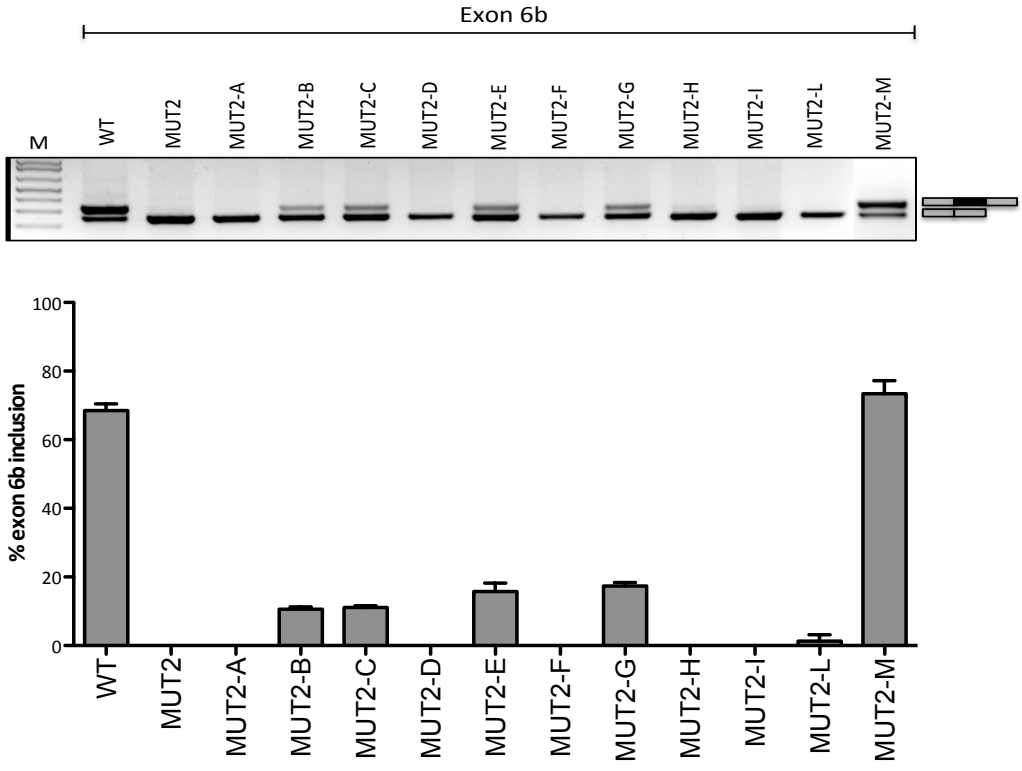

FIGURE 29. Splicing pattern analysis of GAA-rich ESE mutants in TMEM16A exon6b. *A,* Schematic representation of the site-direct mutagenesis of the 4 motifs of the 16bp long GAA-rich ESE element, (X) denotes the deletion or substitution positions. *B,* Exon6b wt and mutants minigenes were transfected into HEK293 cells and splicing pattern was then evaluated by RT-PCR with alpha 2,3 and bra2 primers. Amplified products were separated in electrophoresis on 2% agarose gel. The identity of the bands are indicated on the right side of the panel. M, molecular weight marker. Exon6b inclusion percentage was estimated using ImageJ software and is expressed as means ± SD, based on at least three independent experiments done in duplicate.

Effect of SRSF9, TRA2B, PTB1 and RbFOX1 overexpression on TMEM16A MUT2 exon 6b minigene

To get insight on the enhancer function of the 16bp long GAA-rich ESE I specifically focused on SRSF9 and TRA2B, that exhibited an enhancing effect on WT exon 6b recognition (Figure 17 and 18). TRA2B has an optimal AGAA consensus binding site (Clery, Jayne et al. 2011) that is duplicated in the TMEM16b ESE. In addition, SRSF9 and TRA2B have been described to regulate, through a similar GAA-rich ESE, alternative splicing of the SMN2 exon 7 (Clery, Jayne et al. 2011). In the SMN2 exon 7, two AGAA core sequences for TRA2B are flanked by one SRSF9 AGGA site and one hnRNPG motif ((Clery, Jayne et al. 2011); (Park, Han et al. 2006)). To understand the possible involvement of TRA2B and SRSF9 in TMEM16A exon 6b definition, the eleven GAA-rich ESE mutant minigenes shown in figure 28 and 29, were co-transfected with plasmids coding for these splicing factors in HEK293 cells. In parallel, I also tested the effect of the two other enhancing factors PTB1 and RbFOX1 .

In all of the minigenes, overexpression of the splicing factors did not induce exon 6b inclusion. In fact, the splicing factors did not induce exon inclusion in all the mutants that affect the 2 core AGAA motifs either individually (MUT2-B, MUT2-C, MUT2-F and MUT2-E) or in combination (MUT2-A and MUT2-D) (Figure 30). Similarly, overexpression of the proteins in mutants that affect the 1^{st} and 4^{th} motifs (MUT2-H, MUT2-I and MUT2-L) were not able to enhance exon 6b inclusion. Splicing of the MUT2-M, that is already completely included was not affected. Only in MUT2-G, unexpectedly co-transfection of RbFOX1 slightly increased the percentage of exon 6b inclusion.

Thus the enhancing splicing factors were not able to induce exon inclusion in all the mutants suggesting that the entire 16bp GAA-rich ESE is involved in splicing recognition.

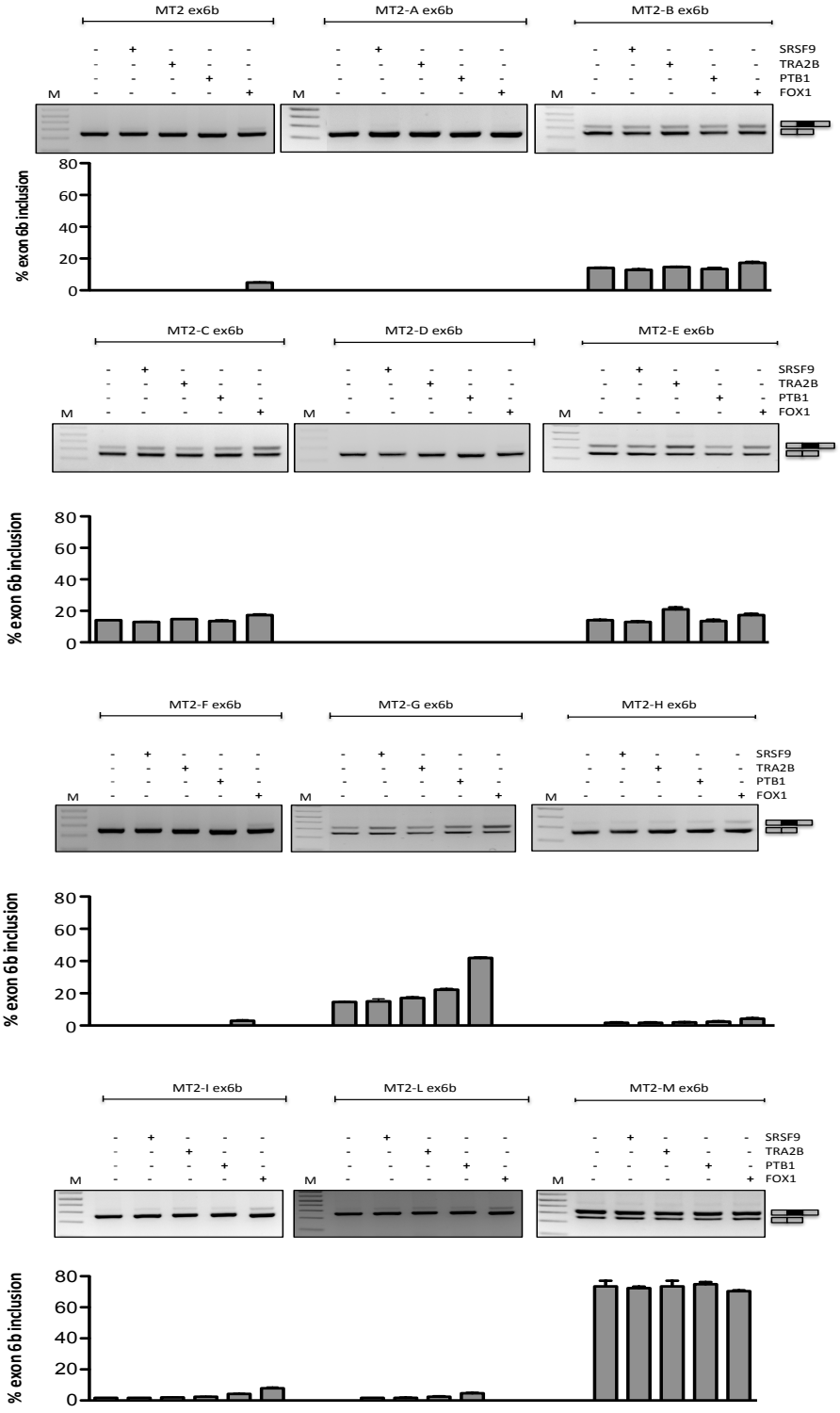

FIGURE 30. Effects of SRSF9, TRA2B, PTB1 and FOX1 splicing factors on exon6b GAA-rich ESE (wt and mutant) minigenes. Splicing assay in HEK293 cells of the thirteen exon6b ESE element constructs (WT and MUTs) reveals that, whereas SRSF9, TRA2B, PTB1 and FOX1 overexpression enhances WT exon6b inclusion, in most of the mutants the splicing pattern is unaffected by these regulatory proteins (N=3). Amplified products were resolved in 2% agarose gel. The identity of the bands are indicated on the right side of the panel. M, molecular weight marker. Splicing percentage was estimated using ImageJ software and is expressed as means ± SD, based on at least three independent experiments done in duplicate.

Analysis of TRA2B binding specificity against WT, MUT2-A, MUT2-E, MUT2-G, MUT2-H and MUT2-I mutants

To test directly the interaction between TRA2B and the 16bp long GAA-rich ESE element within exon 6b and evaluate the role of this splicing factors in the splicing regulation, I performed a pull down assay using as targets the six RNA sequences corresponding to the first part of exon 6b WT and mutants (Figure 31A). The target RNAs (42 nt-long) were T7-transcribed *in vitro*, treated with periodate in order to oxidize its 3' end making it able to bind the agarose beads. Next, incubation with nuclear extract was performed and proteins that remained bound to RNA were separated on a SDS-PAGE gel, transferred to PVDF filters and probed for the presence TRA2B with a specific antibody.

The results in figure 31B show that the WT sequence binds efficiently to TRA2B and that the disruption of the two core AGAA elements (2^{nd} and 3^{rd} motif of the ESE) in the MUT2-A, RNA completely abolish this binding, consistent with the functional effect of the entire enhancer observed in vivo in the minigene (Figure 29). Disruption of the 3^{rd} motif alone did not affect binding (MUT2-E), as well as the deletion of the fourth motifs in MUT2-H, suggesting that these sequences are not directly involved in TRA2B binding. Finally, deletion of the first motifs alone (MUT2-G) or along with the fourth motifs (MUT2-I), has no binding capability to TRA2B.

This data indicates that the first and second motifs are the major determinant for the TRA2B binding capacity to the GAA-rich ESE.

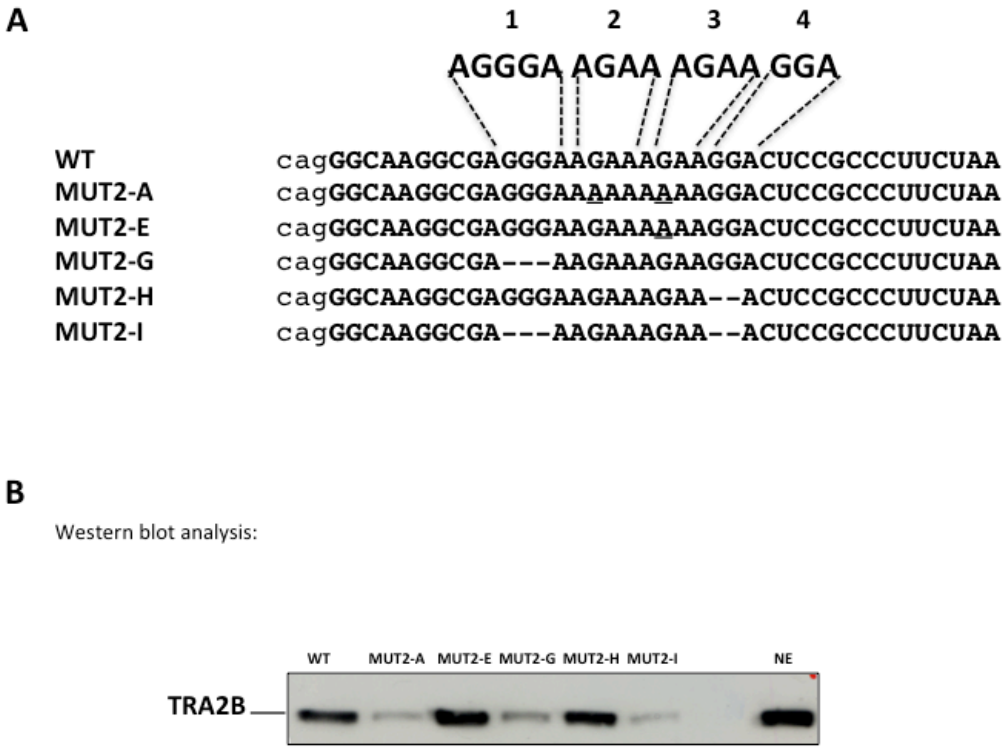

Figure 31. Western blot of pulldown analysis of TMEM16A exon6b WT and MUTs RNAs to determine the presence of TRA2B. *A,* Schematic representation of the RNA sequence transcribed *in vitro* (upper panel) that contains nucleotide changes and the target TMEM16A sequences. The mutagenized nucleotides are underlined. *B,* Binding analysis of TRA2B. The RNAs were *in vitro* transcribed, covalently linked to agarose beads and incubated with HeLa nuclear extract. The pulled down proteins were then analysed by western blotting with anti- TRA2B polyclonal antibody. Immunoblottings were detected using the ECL method. The nuclear extract sample (NE) corresponds to 1/20th of the amount used for the pulldown assay. The pulldown picture is representative of three independent experiments. As the picture shows, the WT, MUT2-E and MUT2-H RNA are able to pull down TRA2B. MUT2-A, MUT2-G and MUT2-I binds approximately only 10-15% of TRA2B protein, compared to the other RNAs. The percentage of binding was determined by the evaluation of the relative intensity of the bands.

Analysis of TMEM16A exon 15 in minigene splicing regulation

Effect of splicing factors families on TMEM16A exon 15 splicing

In order to detect splicing factors that may regulate TMEM16A exon 15 splicing, I transiently transfected exon 15 minigene (Figure 32) into HEK293 cells and the spliced mRNAs were analyzed through RT-PCR using alpha2,3 and bra2 oligonucleotides specific for the minigene sequence, therefore excluding the possibility of amplifying endogenous mRNA. The PCR products detected upon transfection of the WT exon 15 minigene showed the presence of two mRNA bands: the upper one correspond to exon 15 inclusion and the lower one to exon 15 exclusion (474bp and 396bp, respectively). The identity of the bands was verified by direct sequencing after elution of the bands from the gel. Quantitative analysis of band intensity showed nearly 23% of exon 15 inclusion (Figure 32, lane 1 and 7; figure 33, lane 1, 6 and 11). Further, I overexpressed different *trans*-acting elements that may regulate exon 15 splicing. Six main families of splicing factors have been transfected with pTB WT exon 15, in detail: UG-rich binding proteins; SR (serine/arginine) proteins; Py-rich binding proteins; hnRNP proteins and two neuronal tissue specific proteins. Total RNA was extracted and a RT-PCR was carried out with specific primer set and the amplified products were separated in 2% agarose gel. Overexpression by UG-rich binding proteins, SR proteins and hnRNP proteins, had no effect on exon 15 splicing (Figure 32, lane 3-15). Interestingly, only TIA1 and the brain specific isoform of RbFox-1 yielded in exon 15 inclusion. TIA1 from 23% to 55% (Figure 33, lane 2) and RbFox-1 from 23% to 75% of inclusion (Figure 33, lane 12).

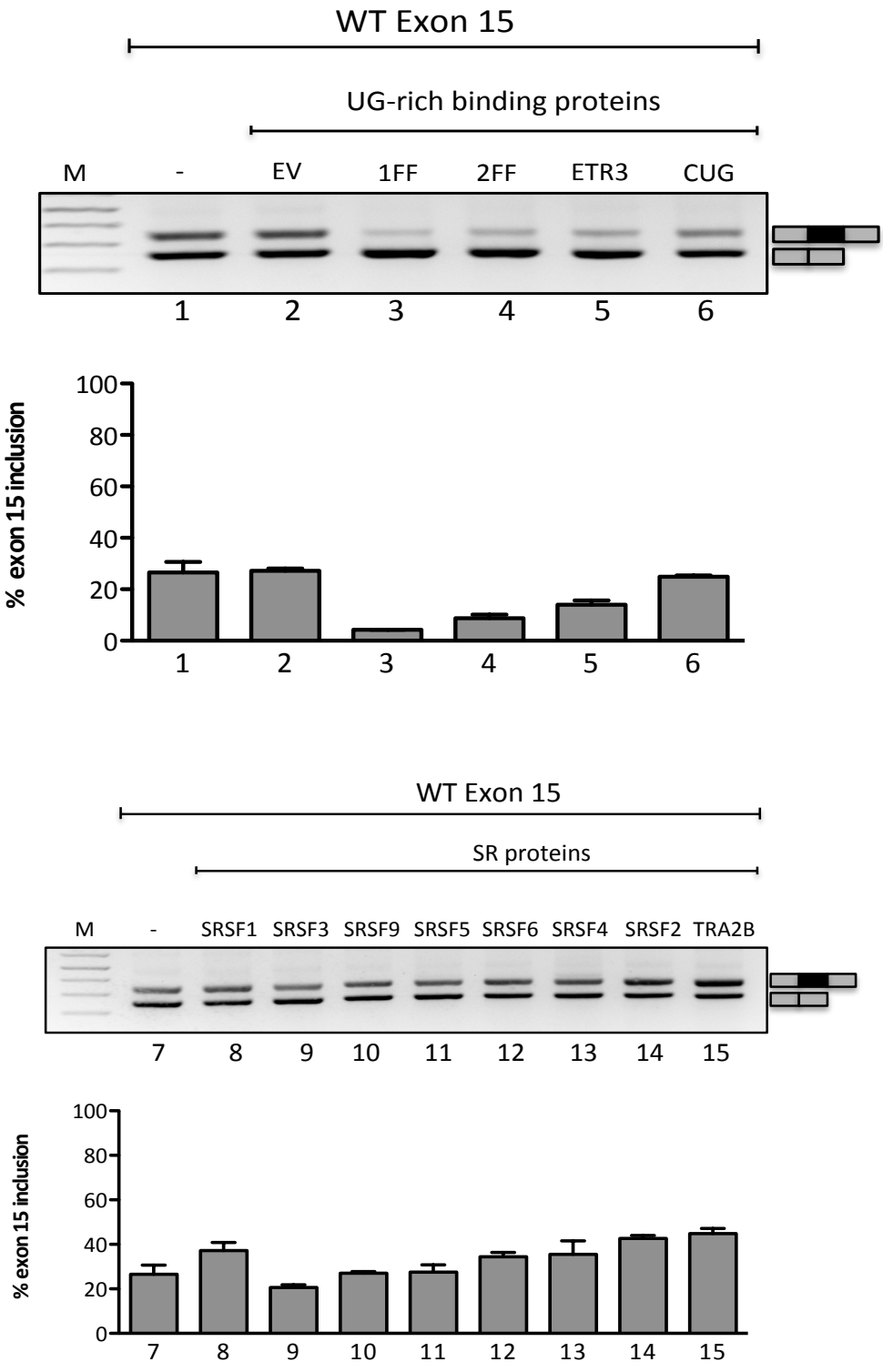

FIGURE 32. Splicing pattern of TMEM16A exon 15 minigene co-transfected with splicing factors.. Splicing pattern analysis of the RT-PCR products derived from RNA of transfected HEK293 cells, separated in electrophoresis on 2% agarose gel. TMEM16A exon15 minigene was transfected alone (0.5ug) or with splicing factors (0.5ug) and splicing pattern was evaluated by RT-PCR with alpha 2,3 and bra2 primers. The identity of the bands are indicated on the right side of the panel. M, molecular weight marker. (-) denotes the WT position. EV, Empty Vector. Quantification analysis of exon6b inclusion was estimated using ImageJ software and is expressed as ± SD, based on at least three independent experiments done in duplicate.

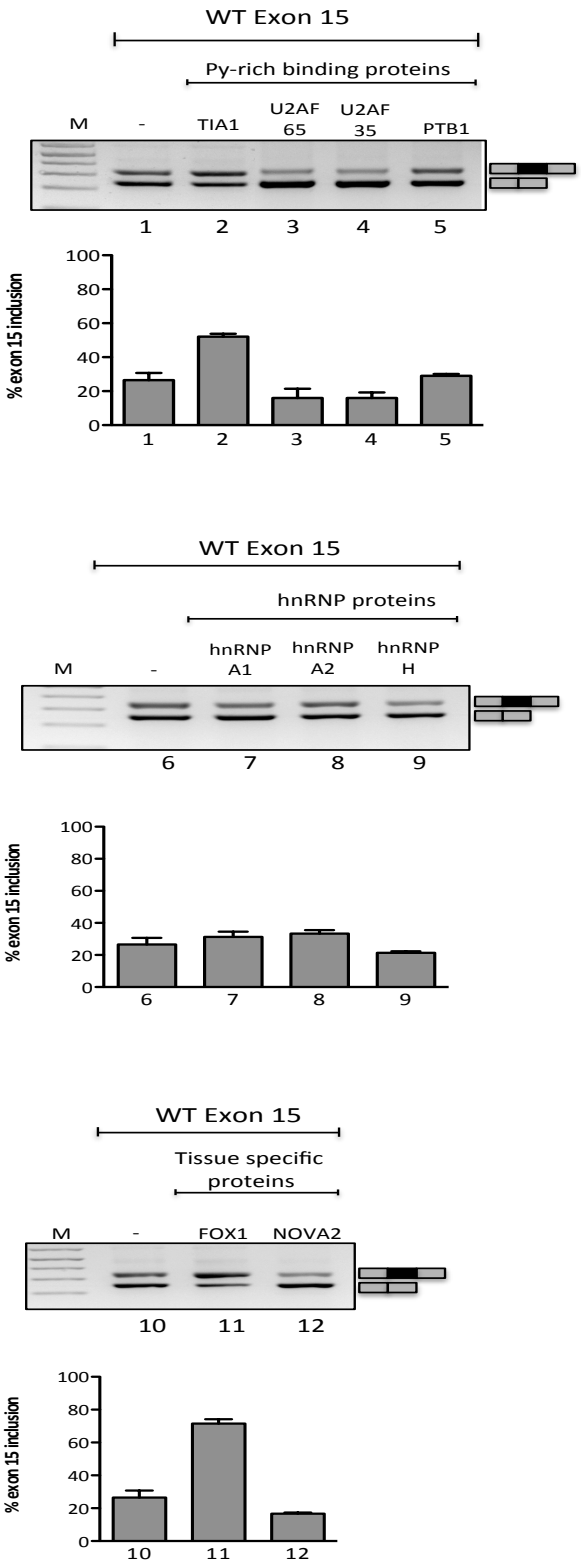

FIGURE 33. Splicing pattern of TMEM16A exon 15 minigene co-transfected with splicing factors. Splicing pattern analysis of the RT-PCR products derived from RNA of transfected HEK293 cells, separated in electrophoresis on 2% agarose gel. TMEM16A exon15 minigene was transfected alone (0.5ug) or with splicing factors (0.5ug) and splicing pattern was evaluated by RT-PCR with alpha 2,3 and bra2 primers. The identity of the bands are indicated on the right side of the panel. M, molecular weight marker. (-) denotes the WT position. EV, Empty Vector. Quantification analysis of exon6b inclusion was estimated using ImageJ software and is expressed as ± SD, based on at least three independent experiments done in duplicate.

Identification of enhancers and silencers sequences that affect splicing of TMEM16A exon 15

A number of web-based programs were used for bioinformatic analysis of potential splicing aberrations. Several programs have been designed to predict possible exonic or intronic splice enhancer (ESE/ISE) and exonic or intronic splice silencer (ESS/ISS) sites. It is important to note that these splice enhancer/silencer programs recognize multiple sequences that are potential binding sites of splicing factors, but cannot denote which sites are actually used under physiological conditions. Exonic variants of exon 15 were analyzed for possible splicing enhancer (ESE) with Exonic Splicing Enhancer (ESE)-finder (http://rulai.cshl.edu/cgi-bin/tools/ESE3/esefinder.cgi), with Relative Enhancer and Silencer Classification by Unanimous Enrichment (RESCUE)-ESE (http://genes.mit.edu/burgelab/rescue-ese). and using Putative Exonic Splicing Enhancer/Silencer (PESXs) (http://cubweb.biology.columbia.edu/pesx/) websites.

As shown in figure 34A, ESE-finder predicts that within exon 15 there are several putative ESEs dependent to the human SR proteins SRSF1 (SF2/ASF), SRSF5 (SRp40) and SRSF6 (SRp55) distributed through the entire exon. RESCUE-ESE (Figure 34B), identified 12 candidate ESE hexamers in exon 15. On the other hand, PESXs prediction (Figure 34C), showed no correlation with the two other tools, indeed PESXs identified two enhancer and one silencer sequences; the latter overlap with an ESE motif discovered with ESE-finder and RESCUE-ESE.

In order to identify putative splicing regulatory elements within TMEM16A exon 15, I engineered serial deletion mutants along the entire exon. The mutant minigenes are depicted in figure 35A. Hybrid minigenes carrying each deletion were transiently transfected into HEK293 cells and splicing was analyzed by RT-PCR and the splicing pattern evaluated on 2% agarose gel (Figure 35B). As control pTB WT exon 15 minigene was also included in the experiment. The results showed a decrease of exon 15 inclusion in the majority of the deletions, inducing complete skipping of exon 15. Only MUT9 behave differently it has a strong effect in promoting exon 15 inclusion (Figure 35B, lane 10). These results indicate that exon 15 has eight ESE elements (MUT1- MUT8) and one ESS (MUT9).

A

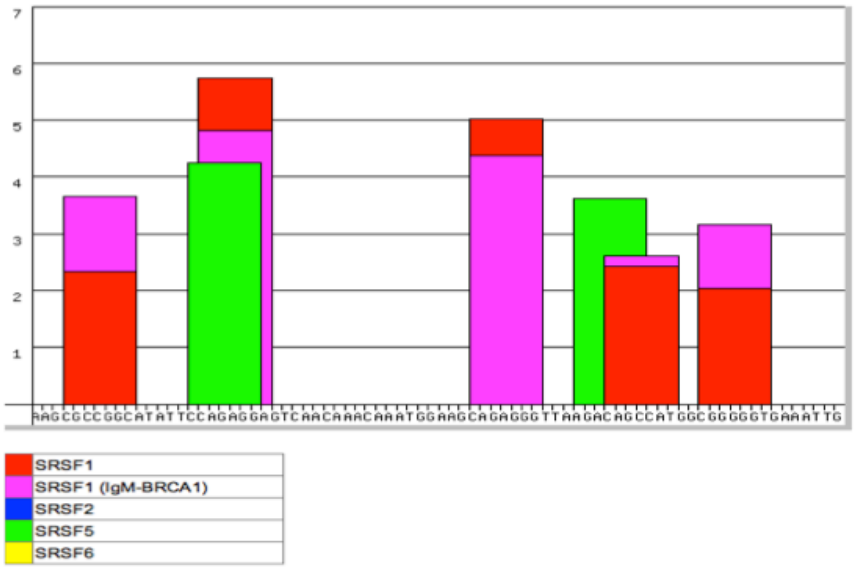

B

C

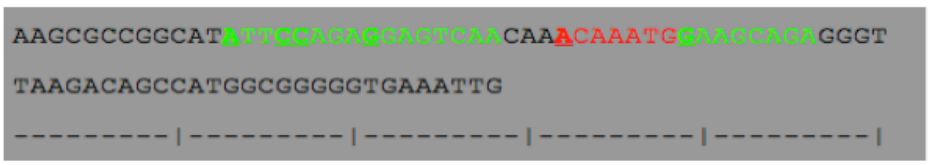

FIGURE 34. Predicted ESE and ESS sites within exon15 sequence from base +1 to +78. *A,* ESE-finder output for *TMEM16A* exon6b, using version 2.0 matrices and thresholds. Y-axis shows ESE-finder above-threshold scores for identified matches; X-axis corresponds to the exon6b sequence from base +1 to base +78. ESE finder analysis indicates the location of potential binding sites for the splicing factors SRSF1 (SF2/ASF, red magenta), SRSF2 (SC35, blue), SRSF5 (SRp40, green) and SRSF6 (SRp55, yellow). *B,* The RESCUE-ESE web server. The output displays the input sequence with the ESEs drawn above in yellow. *C,* The PESXs web server. The light green sequence indicates the ESE candidates identified by the server and the red sequence indicates the ESS candidates.

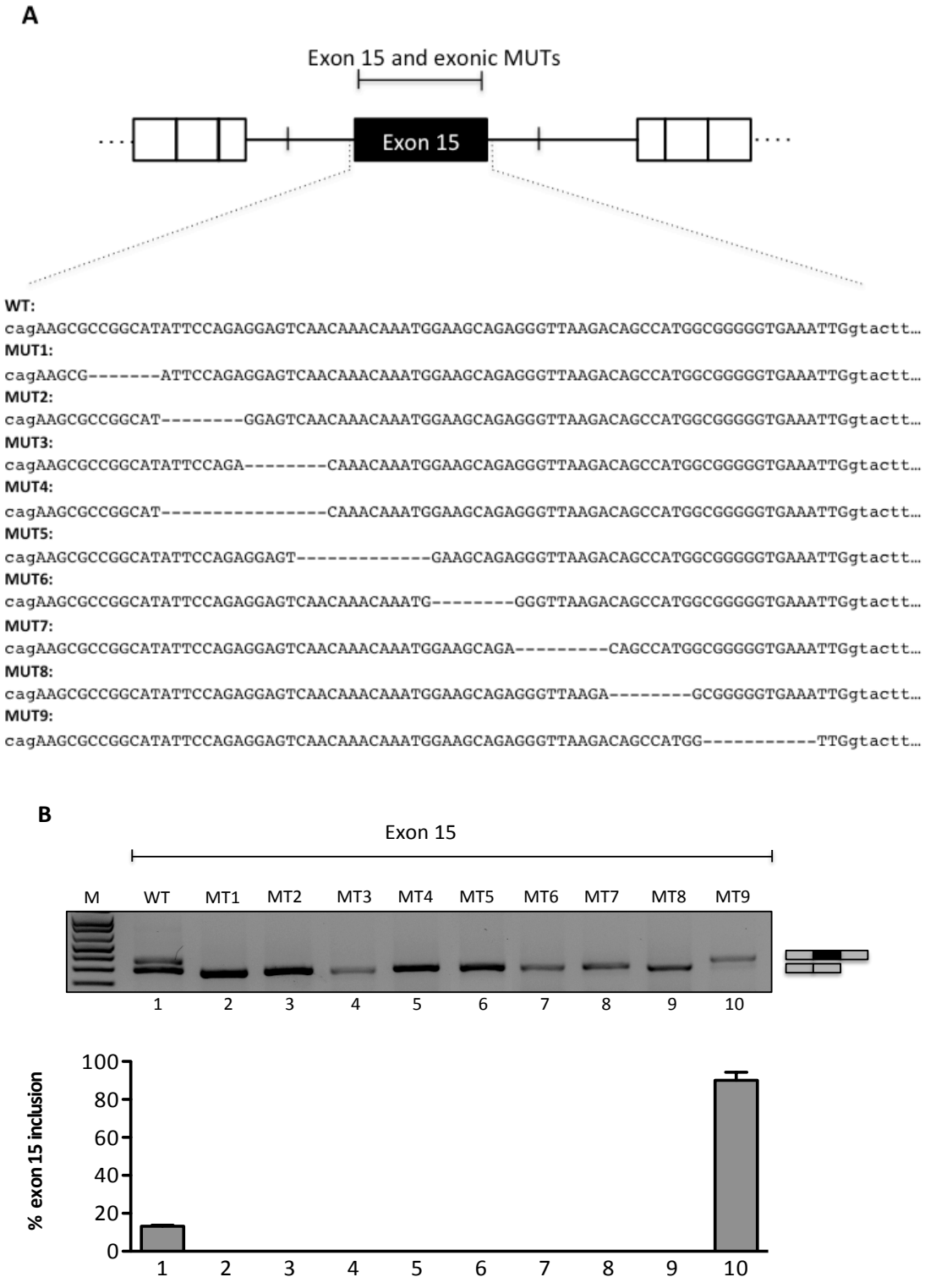

FIGURE 35. TMEM16A exon15 minigenes (WT and MUTs). *A,* Schematic representation of exon15 wt and exonic mutant minigenes. The mutants were created by overlap extension PCR, using specific oligonucleotide complementary to up- and downstream sequences of the deleted region. Sequence variations (below the wild-type sequence) are shown. Uppercase letters represent exonic sequence and lowercase letters intronic sequence. *B,* Splicing assay of the seven TMEM16A exon15 constructs (WT and MUTs) were transfected into HEK293 cells. Splicing pattern was evaluated by RT-PCR with alpha 2,3 and bra2 primers. Amplified products were separated in electrophoresis on 2% agarose gel. The identity of the bands are indicated on the right side of the panel. M, molecular weight marker. Quantification analysis of exon6b inclusion was estimated using ImageJ software and is expressed as ± SD, based on at least three independent experiments done in duplicate.

To further identify splicing regulatory elements I performed additional intronic deletions downstream exon 15 (Figure 36A) taking into consideration the presence in the intron of polyprimidine tracts and consensus binding sites for FOX1. Indeed, inspection of the intron showed three poly-pyrymidine-rich sequences and two consensus binding sites for RbFOX1 consisting of penta- and hexa-nucleotide (T)GCATG sequences. The MUT10 construct lacks the first Py-rich element, from position +7 to +15, MUT11 lacks the second Py-rich element, from position +59 to +69, whereas MUT12 lacks the third Py-rich element, from position +83 to +101. MUT13 has all the three Py-rich elements deleted. In addition, I created three mutant minigenes where I deleted the specific target sequence of RbFox family. MUT14 lacks the first penta-nucleotide sequence, while MUT15 lacks the second hexa-nucleotide and a third mutant, MUT16, both the RbFox target sequence were absent (Figure 36A). Mutation of each individual polyprimidine tract has no effect on the splicing pattern (MUT10, MUT11 and MUT12, respectively), whereas the larger intronic deletion in MUT13 that encompass the three sequences increased the percentage of exon inclusion. On the other hand deletion of the FOX1 binding sites , either alone (MUT14 and MUT15) or in combination (MUT16) induced exon skipping (Figure 36).

To understand the functional relationship splicing regulatory elements and the two enhancing factors, I performed, firstly co-transfection experiments of TIA1 and RbFOX1 along with the intronic deletion mutant minigenes.

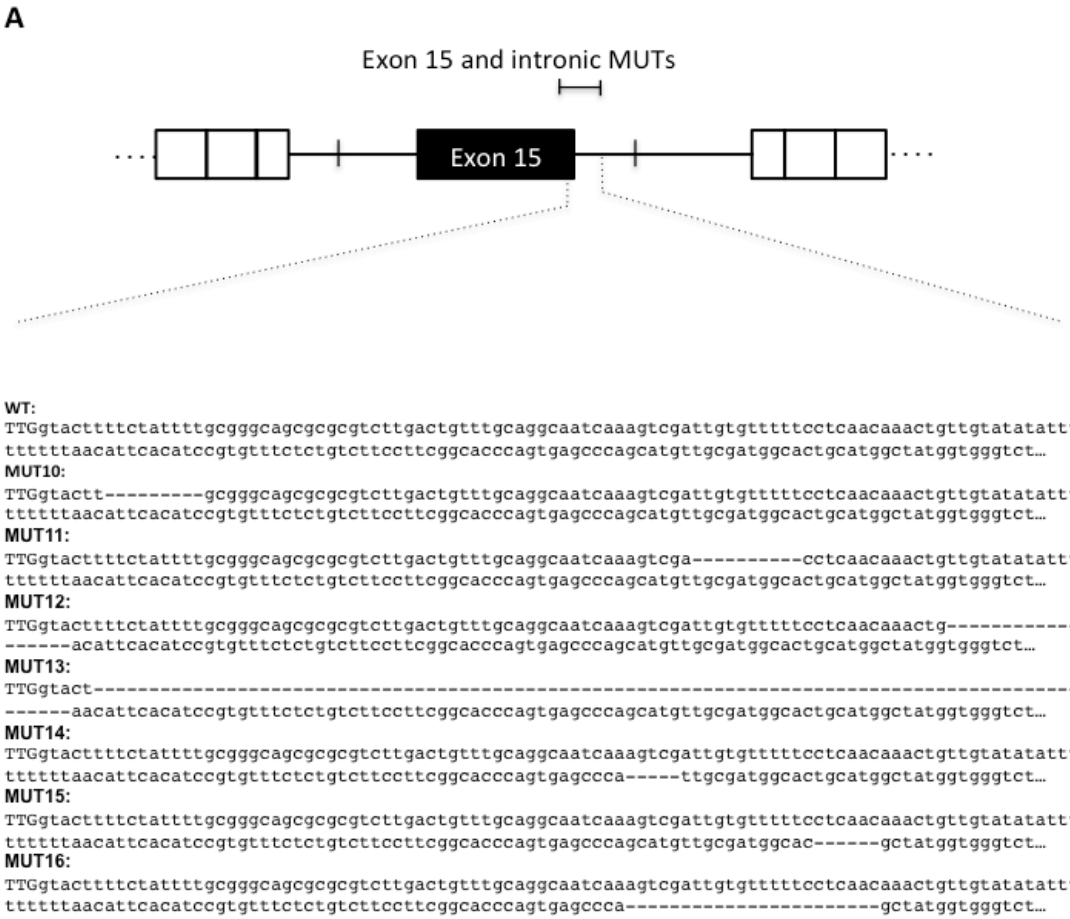

FIGURE 36. TMEM16A exon15 minigenes (WT and MUTs). *A,* Schematic representation of exon15 wt and intronic mutant minigenes. The mutants were created by overlap extension PCR, using specific oligonucleotide complementary to up- and downstream sequences of the deleted region. Sequence variations (below the wild-type sequence) are shown. Uppercase letters represent exonic sequence and lowercase letters intronic sequence. *B,* Splicing assay of the eigth TMEM16A exon15 constructs (WT and MUTs) were transfected into HEK293 cells. Splicing pattern was evaluated by RT-PCR with alpha 2,3 and bra2 primers. Amplified products were separated in electrophoresis on 2% agarose gel. The identity of the bands are indicated on the right side of the panel. M, molecular weight marker. Quantification analysis of exon6b inclusion was estimated using ImageJ software and is expressed as ± SD, based on at least three independent experiments done in duplicate.

In several gene system, these two splicing factors are known to interact with downstream intronic sequences (polypyrimide-rich and (T)GCATG consensus for TIA1 and RbFOX1, respectively) in order to induce exon inclusion (Del Gatto-Konczak, Bourgeois et al. 2000; Auweter, Fasan et al. 2006)

Interestingly, the MUT10 construct, with the deletion of the first polypyrimide tract did not respond to the TIA1-mediated splicing enhancement (Figure 37, lane 5) whereas the other minigenes with deletion of the second and third polypyrimide tract showed a significant increase in the percentage of exon inclusion similar to the WT construct (constructs MUT11 and MUT12 in Figure 37). MUT13 has a large intronic deletion and its nearly complete exon inclusion pattern was not affected by TIA1 (Figure 37, lanes 13 and 14). As expected, in these polypyrimide mutant minigenes the levels of exon 15 inclusion were not influenced by RbFOX1 protein overexpression, suggesting that RbFOX1 protein may act through different intronic sequences. Therefore, I tested RbFOX1 protein overexpression on the mutant minigenes in which the two specific consensus RbFOX1 binding sites were deleted. Deletion of the each individual consensus site did not afffect the RbFOX1-mediated splicing enhancement in MUT14 and MUT15. In this cases, the percentage of exon 15 inclusion increased to ~50% as is occurring in the WT minigene (Figure 38, lanes 4 and 6). On the contrary the deletion of both consensus sites only slightly responded to RbFOX1 overexpression. In fact, MUT16 minigene RbFOX1 induced only 10% of exon 15 inclusion (Figure 38, lane 8). The mild effect of RbFOX1 overexpression on exon 15 in the MUT16 minigene suggests that both the intronic penta- and hexa-nucleotide consensus sequences located downstream the weak 5'ss are important for RbFOX-mediated splicing regulation (Figure 38, lane 6 and 8).

Next I have evaluated the effect of the enhancing splicing factors on the minigenes with the exonic deletions. Overexpression of the two enhancing SFs in MUT1, MUT2, and MUT5 did not significantly change the percentage of exon inclusion (Figure 39). Splicing of MUT3 and MUT4 construct was slightly affected only by overexpression of RbFOX1 protein to 10% to 20% of inclusion (Figure 39, lane 12 and Figure 40 lane 3). RbFOX1 overexpression led to an increase of exon 15 inclusion from 10% to 40% in MUT6, MUT7 and MUT8 (Figure 40, lane 9 and

Figure 41, lane 3 and 6). These results suggest that the large exonic sequences ~40bp-long and deleted in MUT1-MUT5 are also important for TIA1 or RbFOX1 splicing enhancement.

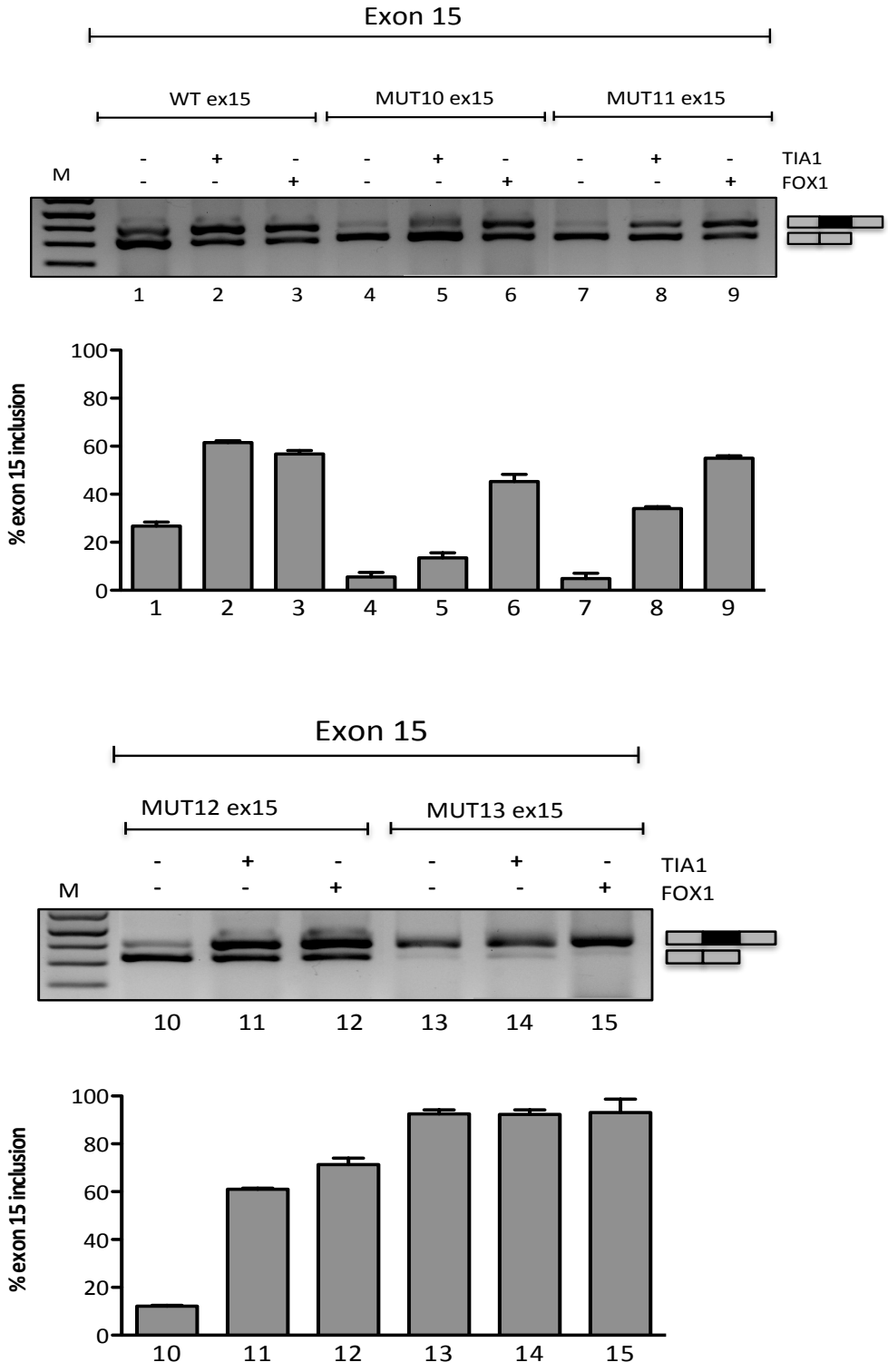

FIGURE 37. Effects of TIA1 and brain RbFOX1 splicing factors on exon15 Py-rich mutant minigenes. Splicing assay in HEK293 cells of the five exon15 constructs (WT and MUTs) reveals that, whereas TIA1 overexpression enhances wt exon15 inclusion, in the first PY-rich mutant splicing pattern is affected by TIA1. RbFOX1 overexpression in the mutants contest, did not change exon15 splicing pattern (N=3). Amplified products were resolved in 2% agarose gel. The identity of the bands are indicated on the right side of the panel. M, molecular weight marker. Splicing percentage was estimated using ImageJ software and is expressed as means ± SD, based on at least three independent experiments done in duplicate.

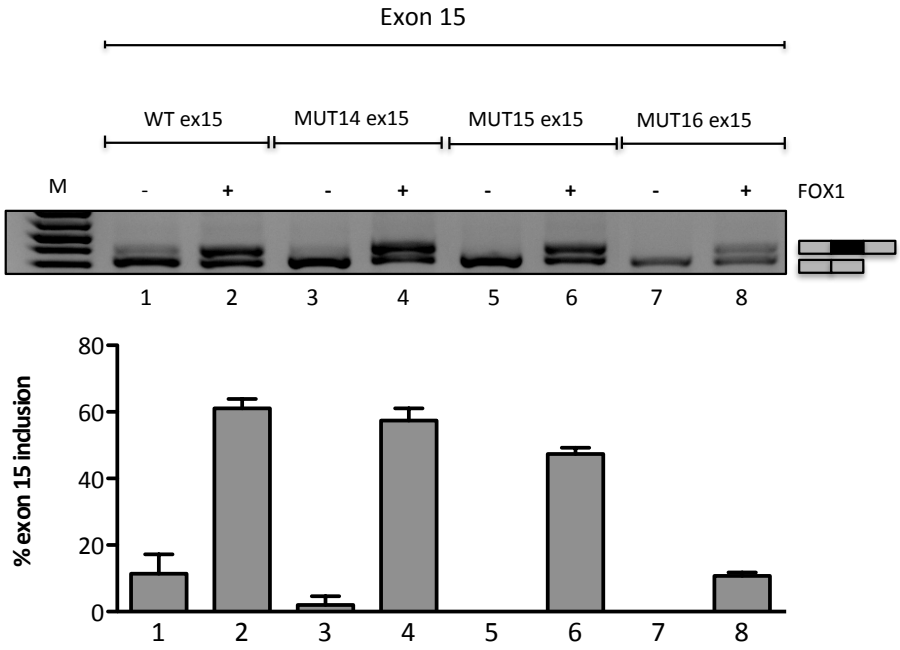

FIGURE 38. Effects of RbFOX1 splicing factor on exon15 mutant minigenes. Splicing assay in HEK293 cells of the four exon15 constructs (WT and MUTs) reveals that, whereas FOX protein overexpression enhances wt exon15 inclusion, whereas in mutant15 and mutant16 the splicing pattern is affected by FOX1 (N=3). Amplified products were resolved in 2% agarose gel. The identity of the bands are indicated on the right side of the panel. M, molecular weight marker. Splicing percentage was estimated using ImageJ software and is expressed as means ± SD, based on at least three independent experiments done in duplicate.

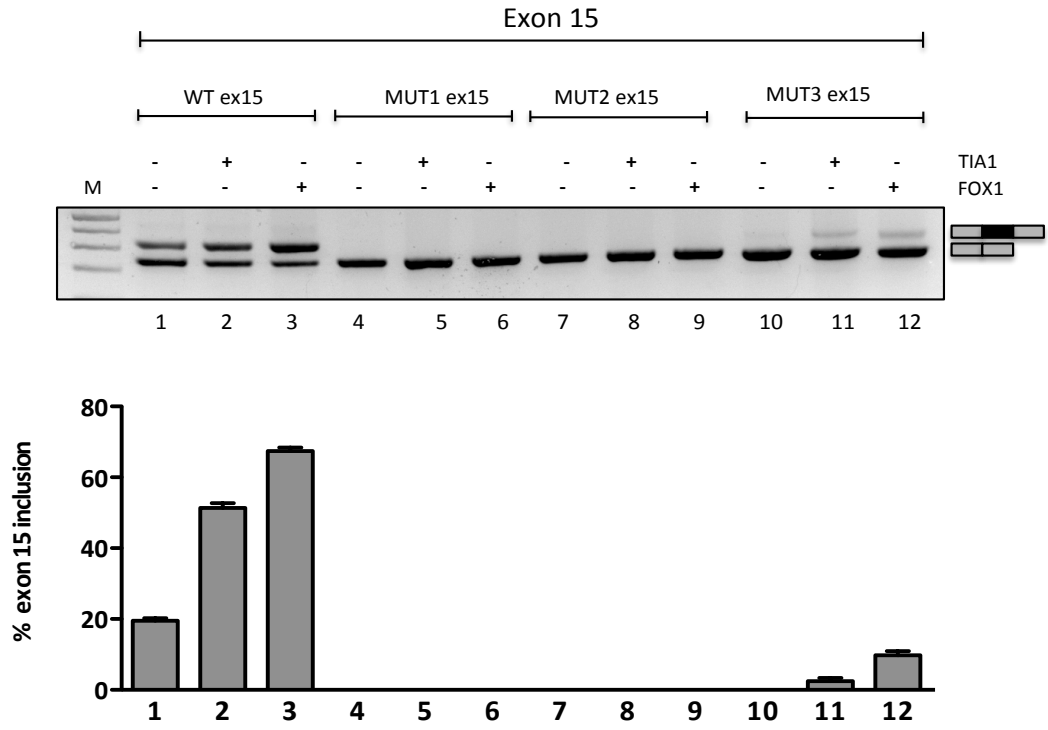

FIGURE 39. TMEM16A exon15 exonic mutant minigenes co-transfected with with TIA1 and FOX1 splicing factors. Splicing pattern analysis of the RT-PCR products derived from RNA of transfected HEK293 cells, separated on 2% agarose gel. WT and mutant minigenes were transfected alone (0.5 μg) or with splicing factors (0.5 μg) and the splicing pattern evaluated with alpha 2,3 and bra2 primers. The identity of the bands are indicated on the right side of the panne. M, molecular weight marker. Splicing percentage was estimated using ImageJ software and is expressed as means ± SD, based on at least three independent experiments done in duplicate.

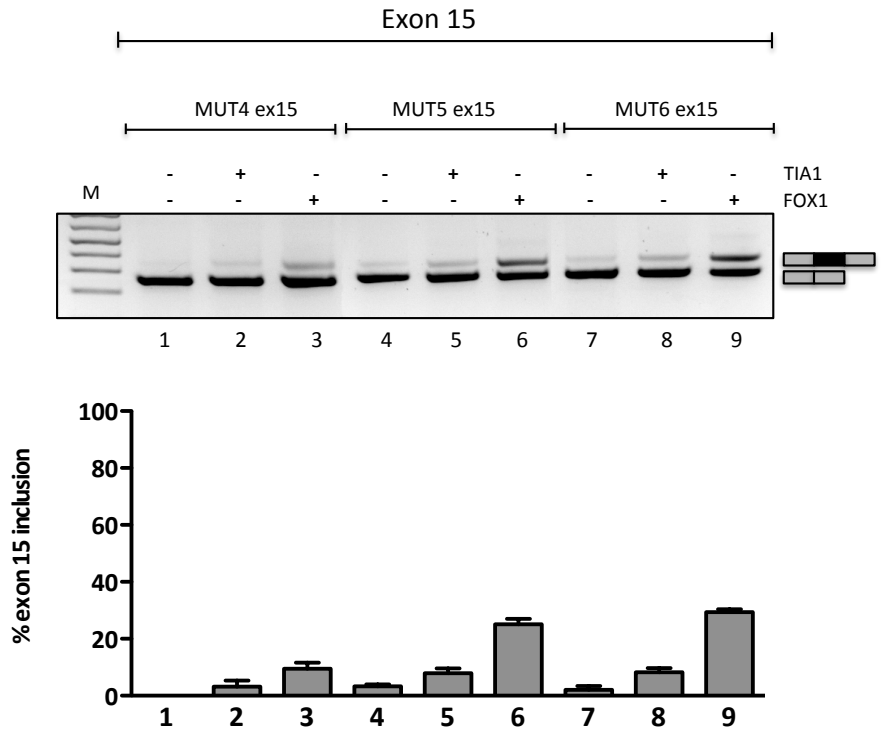

FIGURE 40. TMEM16A exon15 exonic mutant minigenes co-transfected with TIA1 and FOX1 splicing factors. Splicing pattern analysis of the RT-PCR products derived from RNA of transfected HEK293 cells, separated on 2% agarose gel. WT and mutant minigenes were transfected alone (0.5 μg) or with splicing factors (0.5 μg) and the splicing pattern evaluated with alpha 2,3 and bra2 primers. The identity of the bands are indicated on the right side of the panne. M, molecular weight marker. Splicing percentage was estimated using ImageJ software and is expressed as means ± SD, based on at least three independent experiments done in duplicate.

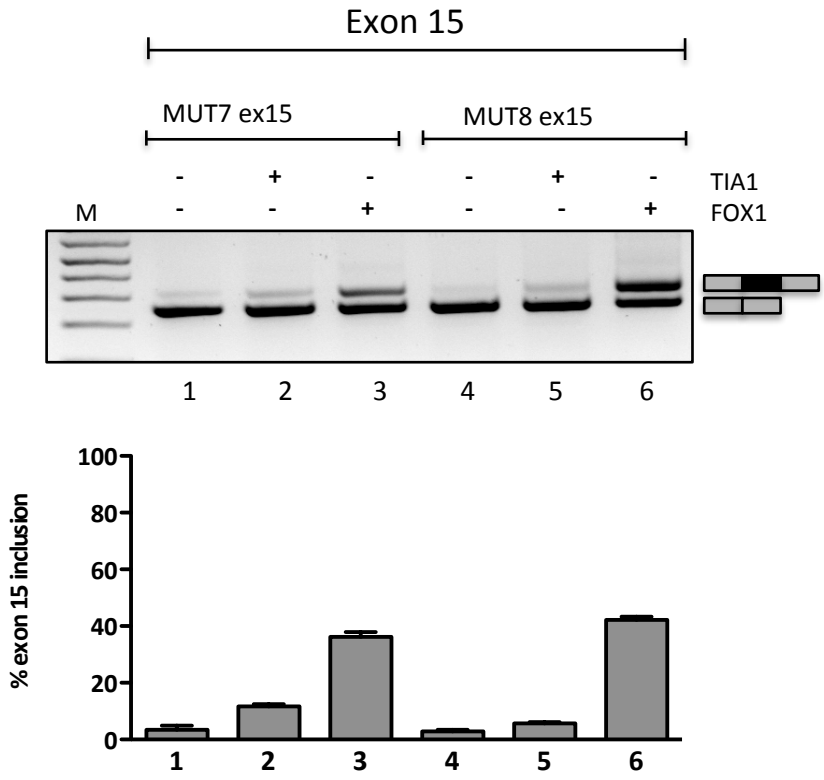

FIGURE 41. TMEM16A exon15 exonic mutant minigenes co-transfected with several splicing factors. Splicing pattern analysis of the RT-PCR products derived from RNA of transfected HEK293 cells, separated on 2% agarose gel. WT and mutant minigenes were transfected alone (0.5 μg) or with splicing factors (0.5 μg) and the splicing pattern evaluated with alpha 2,3 and bra2 primers. The identity of the bands are indicated on the right side of the panne. M, molecular weight marker. Splicing percentage was estimated using ImageJ software and is expressed as means ± SD, based on at least three independent experiments done in duplicate.

Analysis of TMEM16A exon 13 in minigene splicing regulation

Transfection of TMEM16A exon 13 in HEK293 cells showed approximately 10% of exon inclusion (Figure 42). To identify the splicing factors that are involved in its regulation I performed co-transfection experiments. Among the different splicing factors evaluated, only RbFOX1 and U2 auxiliary factor 65, had an effects on exon 13 splicing, promoting its inclusion from 10% to more or less 65%. The other proteins such as UG-rich binding proteins, SR proteins and hnRNP proteins, had no effect on exon 13 splicing regulation (Figure 42 and 43). The RbFox-1 protein enhancer activity was previously reported to be dependent on the presence of (T)GCATG sequences located in downstream intronic sequences (cit). In TMEM16A, downstream exon 13, the sequence from position +67 to +70 contains the TGCA core sequence for RbFOX1. To test if this element is involved in the RbFOX1 mediated splicing enhancement, I deleted this sequence to generate the MUT1 ex13 minigenes (Figure 44A). WT and MUT1 exon 13 minigenes were co-transfected along with brain specific RbFOX1 and U2AF65 protein into HEK293 cells. The overexpression of the two proteins induced in both cases increase in exon inclusion. However, in comparison to the WT minigene, both RbFOX1 and U2AF65 had on MUT1 a lower enhancing effect. In the WT context, co-transfection of RbFOX1 results in 60% of exon inclusion whereas in the MUT1 minigene it induces only 40% (Figure 44B). Similarly but less evident, in the WT context, co-transfection of U2AF65 results in 50% of exon inclusion whereas in the MUT1 minigene it induces 40%. This result suggest that the intronic TGCA consensus binding is partially involved in the splicing enhancement mediated by RbFOX1 and U2AF65.

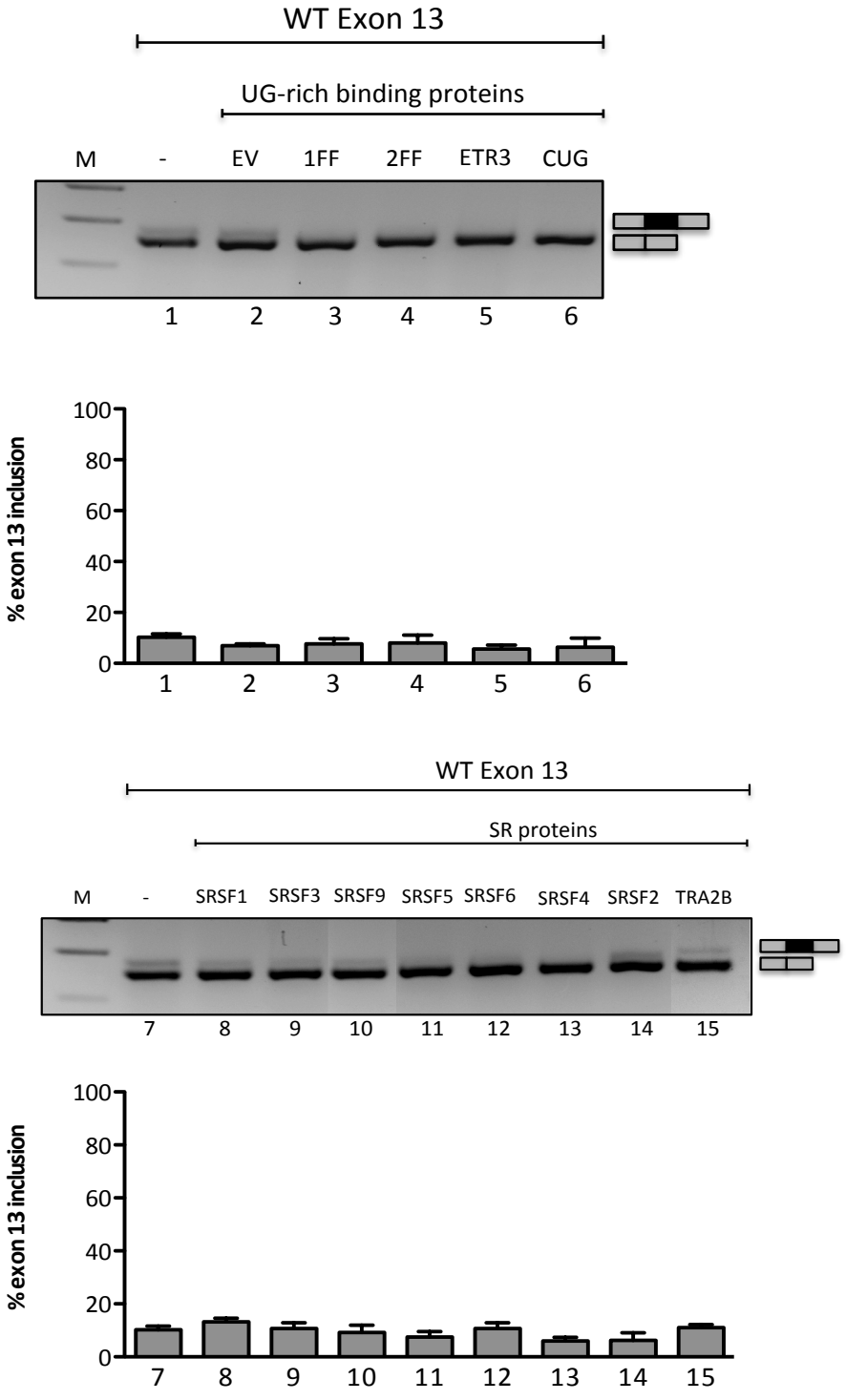

FIGURE 42. Splicing pattern of TMEM16A exon 13 minigene co-transfected with splicing factors. Splicing pattern analysis of the RT-PCR products derived from RNA of transfected HEK293 cells, separated in electrophoresis on 2% agarose gel. TMEM16A exon13 minigene was transfected alone (0.5ug) or with splicing factors (0.5ug) and splicing pattern was evaluated by RT-PCR with alpha 2,3 and bra2 primers. The identity of the bands are indicated on the right side of the panel. M, molecular weight marker. (-) denotes WT position. EV, Empty Vector. Quantification analysis of exon6b inclusion was estimated using ImageJ software and is expressed as ± SD, based on at least three independent experiments done in duplicate.

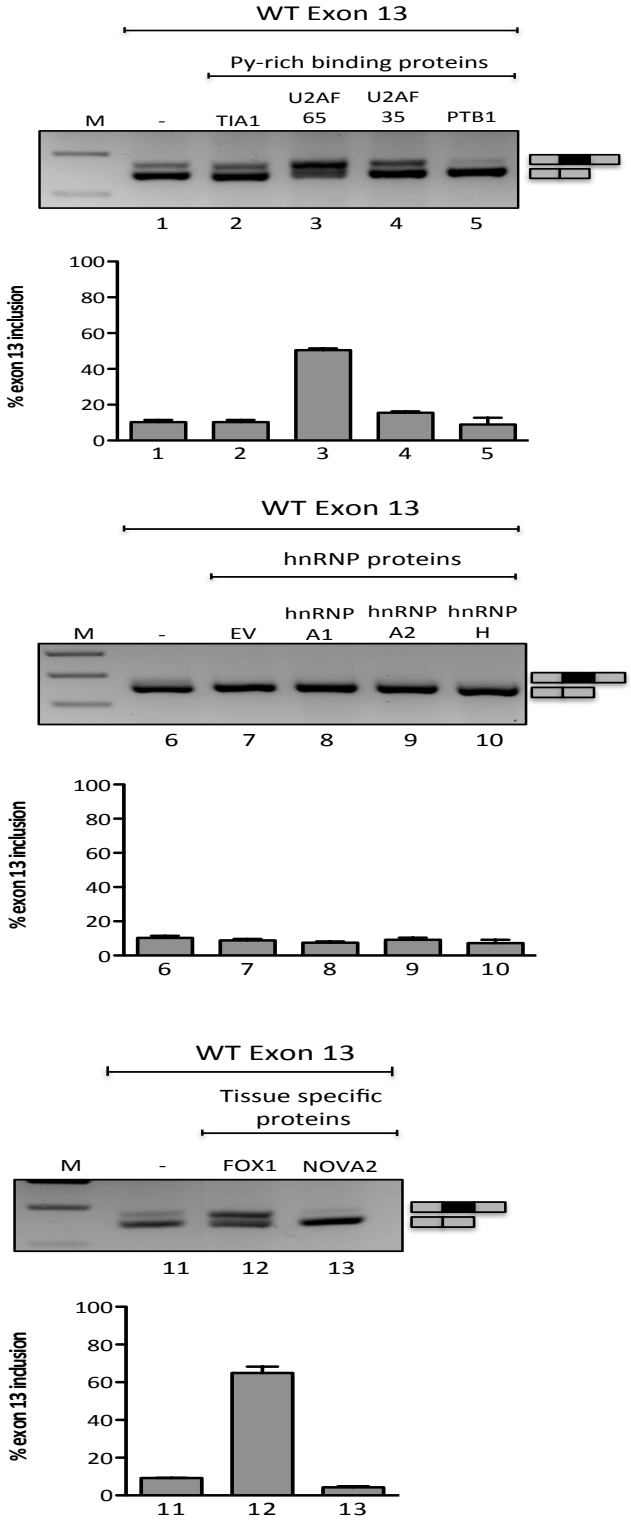

FIGURE 43 Splicing pattern of TMEM16A exon 13 minigene co-transfected with splicing factors. Splicing pattern analysis of the RT-PCR products derived from RNA of transfected HEK293 cells, separated in electrophoresis on 2% agarose gel. TMEM16A exon13 minigene was transfected alone (0.5ug) or with splicing factors (0.5ug) and splicing pattern was evaluated by RT-PCR with alpha 2,3 and bra2 primers. The identity of the bands are indicated on the right side of the panel. M, molecular weight marker. (-) denotes WT position. EV, Empty Vector. Quantification analysis of exon6b inclusion was estimated using ImageJ software and is expressed as ± SD, based on at least three independent experiments done in duplicate.

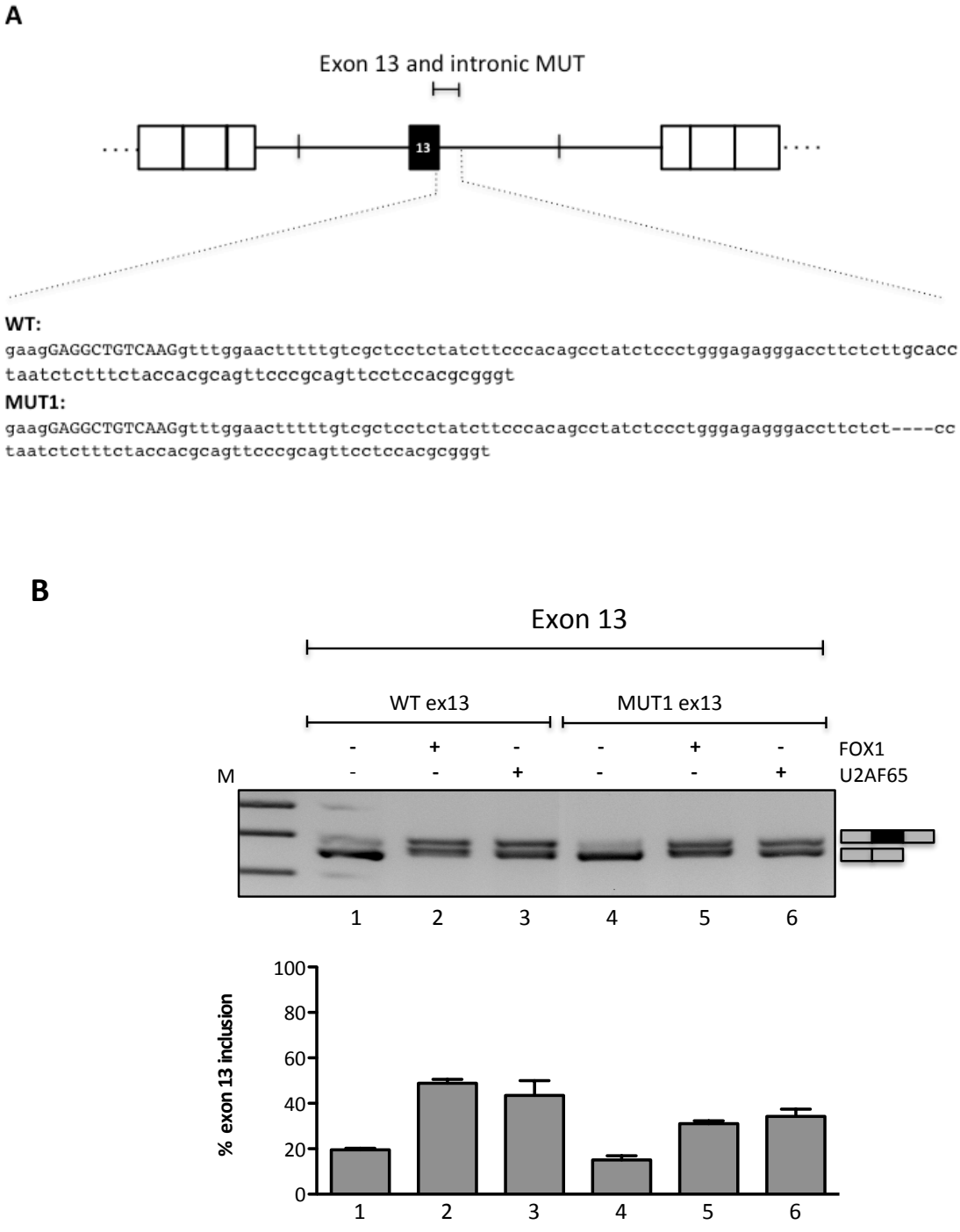

FIGURE 44. TMEM16A exon13 minigenes (WT and MUT). *A,* Schematic representation of exon13 wt and intronic mutant minigenes. The mutant was created by overlap extension PCR, using specific oligonucleotide complementary to up- and down-stream sequences of the deleted region. Sequence variations (below the wild-type sequence) are shown. Uppercase letters represent exonic sequence and lowercase letters intronic sequence. *B,* Effects of RbFOX1 and U2AF65 splicing factors on exon13 mutant minigenes. Splicing assay in HEK293 cells of the two exon13 constructs (WT and MUT) reveals that, none of the splicing factors overexpressed are able to change exon13 splicing pattern compare to the wt (N=2). Amplified products were resolved in 2% agarose gel. The identity of the bands are indicated on the right side of the panel. M, molecular weight marker. Splicing percentage was estimated using ImageJ software and is expressed as means ± SD, based on at least three independent experiments done in duplicate.

Analysis of TMEM16A mRNA isoforms in human tissues

The data shown in figure 15, obtained through RT-PCR and agarose gels analysis indicated that several normal adult human tissues that predominantly include exon 6b tend also to exclude exon 15 from the mature transcript and vice-versa suggesting a possible relationship between these two AS events. For example, exon 6b is nearly completely included in liver and thyroid gland tissues, whereas exon 15 is virtually absent in these tissues. Thus, in order to assess the relative abundance of the TMEM16A isoforms present in the different tissues, I set up a denaturing capillary electrophoresis of fluorescent-5' end labeled RT-PCR (Figure 45A). In this assay, the relatively long-range PCR amplifies TMEM16A transcripts that include the three AS events. As shown in figure 45B, eight mRNA isoforms of different molecular size are expected to originate from the long range PCR due to the possible combination of the three alternatively spliced exons 6b, 13 and 15. I detected, in the majority of tissues four splice variants of 725bp, 791bp, 803bp and 869bp, which correspond to 6b-13+15-, 6b+13+15-, 6b-13+15+ and 6b+13+15+ isoforms, respectively (isoforms 2, 4, 6 and 8 in figure 45B). Figure 45C illustrates a typical electropherogram of three tissues that contains these four isoforms. As expected, in only two tissues, namely brain and skeletal muscle, I observed the appearance of additional bands of 779bp and 713bp (figure 45D), which originate from exon 13 skipping and correspond to 6b+13-15- and 6b-13-15- isoforms, respectively (isoforms 1 and 3).

The assignment of peak to specific splice variants was based upon predicted and measured molecular weights using the standard MW markers and direct sequencing of the most abundant bands eluted from the agarose gels. In addition, as the isoforms 4 and 5 could not be clearly distinguished by size I assumed, for quantitative purposes, that, the band of 791bp corresponds to band 4 in the samples where exon 13 is completely included, which represent the majority of tissues. The percentage of each isoform is calculated considering the area under the peaks, and the value is assigned to its appropriate peak in figure 45C (726 or 791 or 804 or 869bp). The percentage of each bar of the histogram,

was calculated by subtracting the sum of all the different isoform percentages from 100.

To verify the reliability of the semi-quantitative analysis, I compared the percentage of exon inclusion calculated either with the long range PCR or with amplification of each exon. RNA samples derived from the normal human tissues were amplified as indicated in figure 46A with FAM primers either with the long range PCR or the short PCRs, loaded on a capillary electrophoresis followed by the calculation of the percentage of exon 6b and 15 inclusion. As can be see in figure 46B, I observed a very good correlation in the percentage of exon 6b and 15 inclusion between the two methods, indicating that the amplification with long range PCR did not significantly affect the semi-quantitative analysis of each splicing isoform.

The long range PCR analysis in the 20 normal adult human tissues shows a different pattern of expression of the four isoforms accordingly to the tissues; for example in liver and thyroid tissues the isoform 6b+ 15- is prevalent, representing approximately 95 and 80% respectively, of the total transcripts (Figure 47).

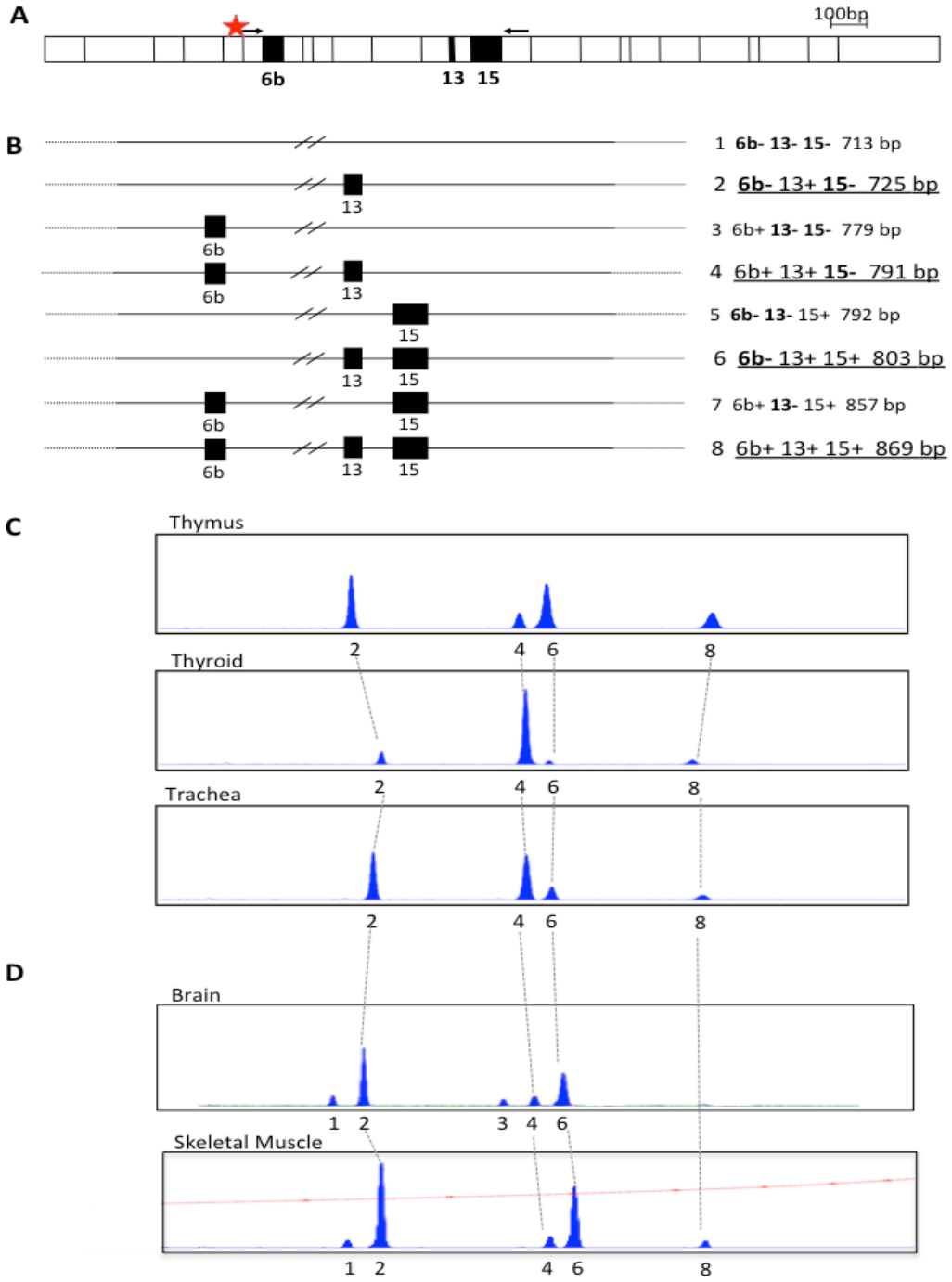

FIGURE 45. Analysis of *TMEM16A* specific isoforms in normal adult human tissues through capillary electrophoresis. *A,* general strategy used to amplify TMEM16A specific isoforms. Forward primer, 803D^{FAM} was fluorescently labeled. RT-PCR product obtained with 803D^{FAM} and 1894R primers spans TMEM16A from exon6 to exon16, a region encompassing the three alternative exons (black boxes). *B,* cartoon indicating eight possible TMEM16A transcript variants as a result of combination of exon 6b, 13 and 15 inclusion and/or exclusion. The four isoforms underlined are the most common, with exon13 included. The expected sizes of RT-PCR products are indicated on the right. *C,* typical electrophoregram of the RT-PCR products, evaluated by capillary electrophoresis of tissues that express isoforms with exon13. Each peak correspond to the isoforms indicated in B. Peak 2 is a transcript of 725bp (exon6b and exon15 are skipped from the transcript, while exon13 is included), peak 4 is a transcript of 791bp (exon6b and exon13 are included in the transcript, exon15 is excluded), peak 6 is a transcript of 803bp, it is 12bp longer than peak 4 due to the absent of exon6b and the presence of exon15. Peak 8, is a transcript of 869bp (all three alternative exons are included). *D,* typical electrophoregram of the RT-PCR products of tissues that express the isoforms without exon13.

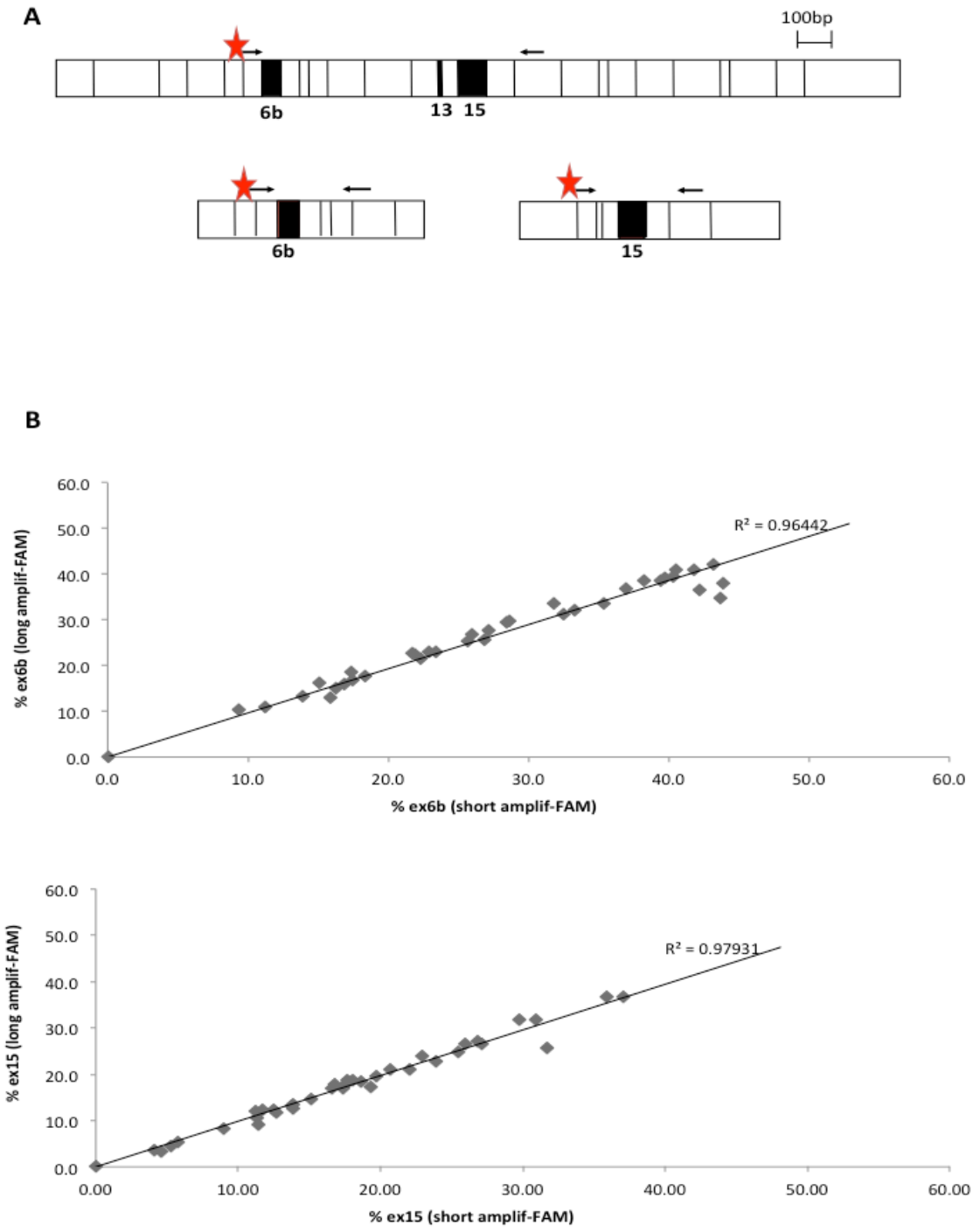

FIGURE 46. Correlation analysis between the long RT-PCR and the short FAM amplification in normal adult human tissues. *A,* Illustration of the system used for IASC of TMEM16A gene. *B,* (Top) Correlation between the long FAM-amplification and the short FAM-amplification on exon6b of TMEM16A gene. (Bottom) Correlation between the long FAM-amplification and the short FAM-amplification on exon15 of TMEM16A gene. Linear regression lines were fitted to the data points obatined from the two amplification systems. Experimental conditions were as described under Material and Methods.

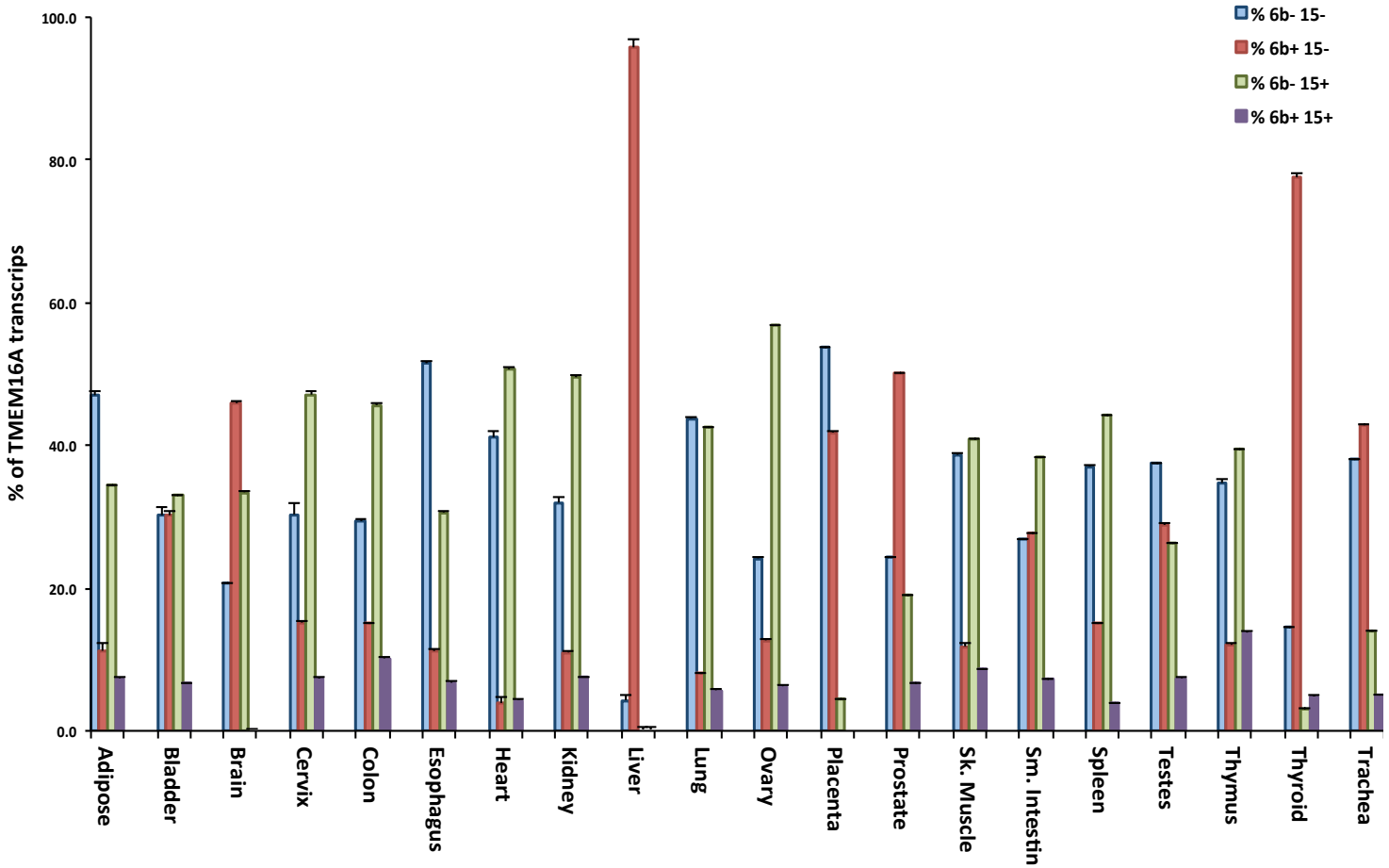

FIGURE 47. Quantification chart of *TMEM16A* specific isoforms in normal adult human tissues through capillary electrophoresis. Isoforms pattern analysis of 20 different normal adult human tissues after separation on a denaturing capillary system of fluorescently labeled RT-PCR. The corresponding outcomes are depicted. The percentages of the bars were determined from the total area of each peak. The error bars are included to display the high level of reproducibility obtained with three separate reverse transcriptions and amplifications done in duplicate.

To evaluate the relationship between the two major AS events on the same transcript and the presence of a possible splicing coordination, I compared the percentage of exon 6b inclusion in transcripts that include exon 15 to transcripts that exclude it. Significant differences in these percentages were considered as indicative of the presence of TMEM16A isoforms in which the two AS events are coordinated. The principle of the analysis along with a graphic representation of the distribution of the different isoforms and of two representative tissues, Cervix and Adipose (a positive and a negative case of coordination, respectively) are shown in figure 48. In these two examples, the overall percentage of exon 6b inclusion is similar in Cervix (20%) and in the Adipose tissue (23%) (lane 1, in figure 48 and B). However, the distribution of the exon 6b abundance in 15+ and 15- transcripts is different between the two tissues. In fact when the exon 15 is included (lane 2), the inclusion of exon 6b is reduced to 13% in Cervix but not in Adipose tissues. Similarly, in transcripts without exon 15 (lane 3) the inclusion of exon 6b increased to 34% in Cervix but did not change in Adipose tissues. Thus, even if the total percentage of exon 6b is similar in the two tissues, only one tissue (i.e. Cervix) show some degree of splicing coordination. The analysis showed that in this tissue exon 6b has preferential association with transcripts in which exon 15 is skipped and vice versa. Analysis of 20 normal adult human tissues indicate that in 14 of them the two AS exons 6b and 15 are coordinated. I observed coordination in Bladder, Brain, Cervix, Colon, Kidney, Liver, Ovary, Placenta, Prostate, Small Intestine, Spleen, Testes, Thyroid and Trachea tissues, although Adipose, Esophagus, Heart, Lung, Skeletal Muscle and Thymus tissues were not coordinated (Figure 48C). The same analysis was also performed considering, the distribution of exon 15 inclusion associated to exon 6b isoforms and the results are shown in figure 49. This analysis gave comparable results. For example, in Cervix tissue, when the upstream exon 6b is included in the mature transcripts, inclusion of the downstream exon 15 falls from 55% in the total amount in the four different isoforms to 32%. Consequently, skipping of the exon 6b, is associated to an increase in the inclusion of the exon 15 from 32% to 61%. Whereas, in Adipose tissue, exon 15 inclusion remains nearly equal in all the three conditions.

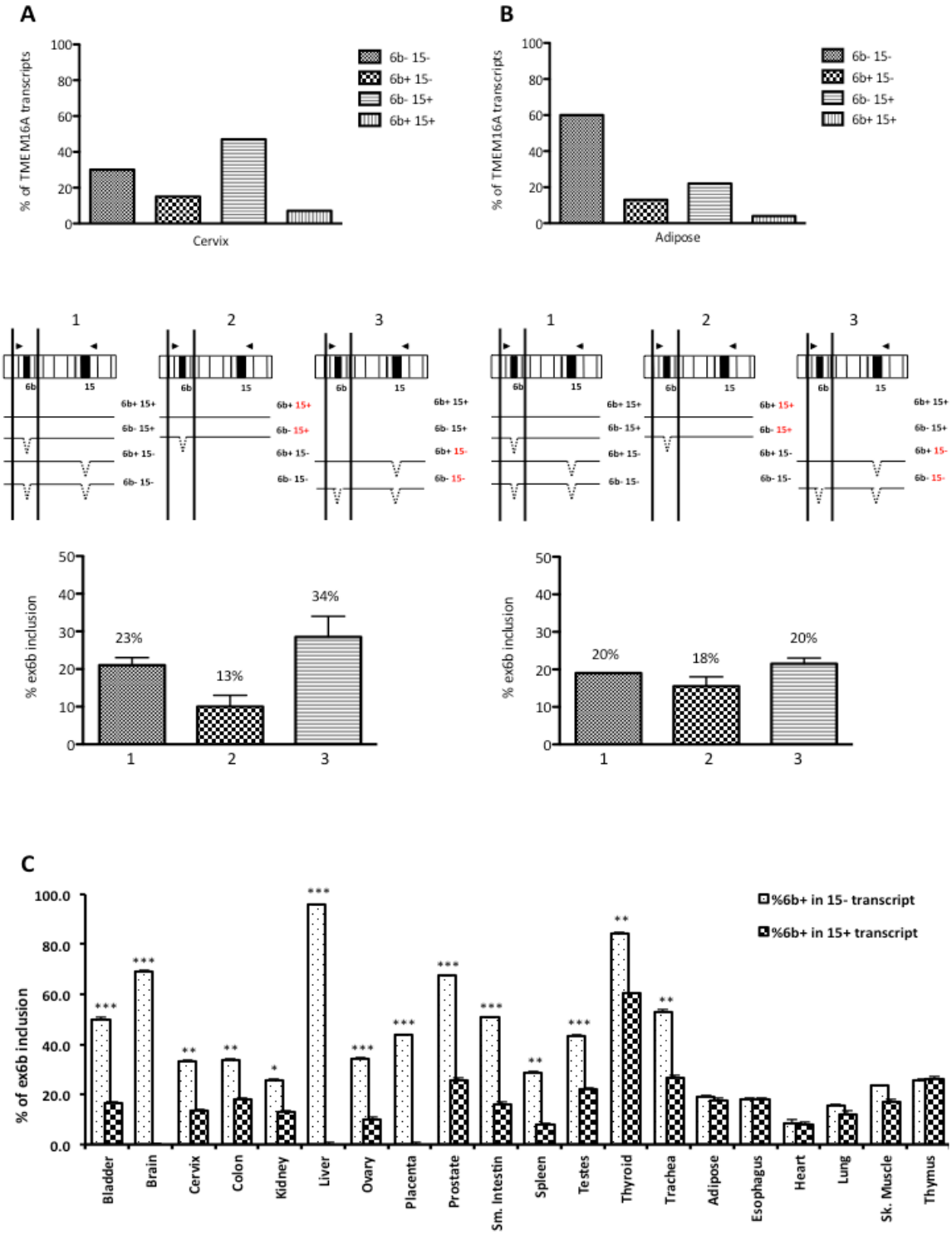

FIGURE 48. Coordination of TMEM16A mRNA isoforms in normal adult human tissues. *A and B,* an example of a positive and negative case of ISC, in cervix and adipose tissues respectively. The top scheme represents the quantification of the four different isoforms in the two human tissues. On the middle panel of the figure, bioinformatic evidence of coordination of the two alternative splicing region, exon6b and exon15. The tables indicate the inclusion of the upstream alternative exon (exon6b) associated to the downstream alternative exon (exon15) isoforms. 1,2,3, indicates the three different conditions: condition 1 denoted the total amount of the upstream exons in the four different isoforms, condition 2 represented exon6b inclusion when exon15 is present in the mature transcript, whereas condition 3 depicted the percentage of inclusion of the upstream exon6b when the mRNA lacks the downstream exon. Statistically analysis was performed using paired Student's t-test. *C,* Quantification of exon6b inclusion associated to exon15 inclusion or exclusion in 20 different normal adult human tissues.

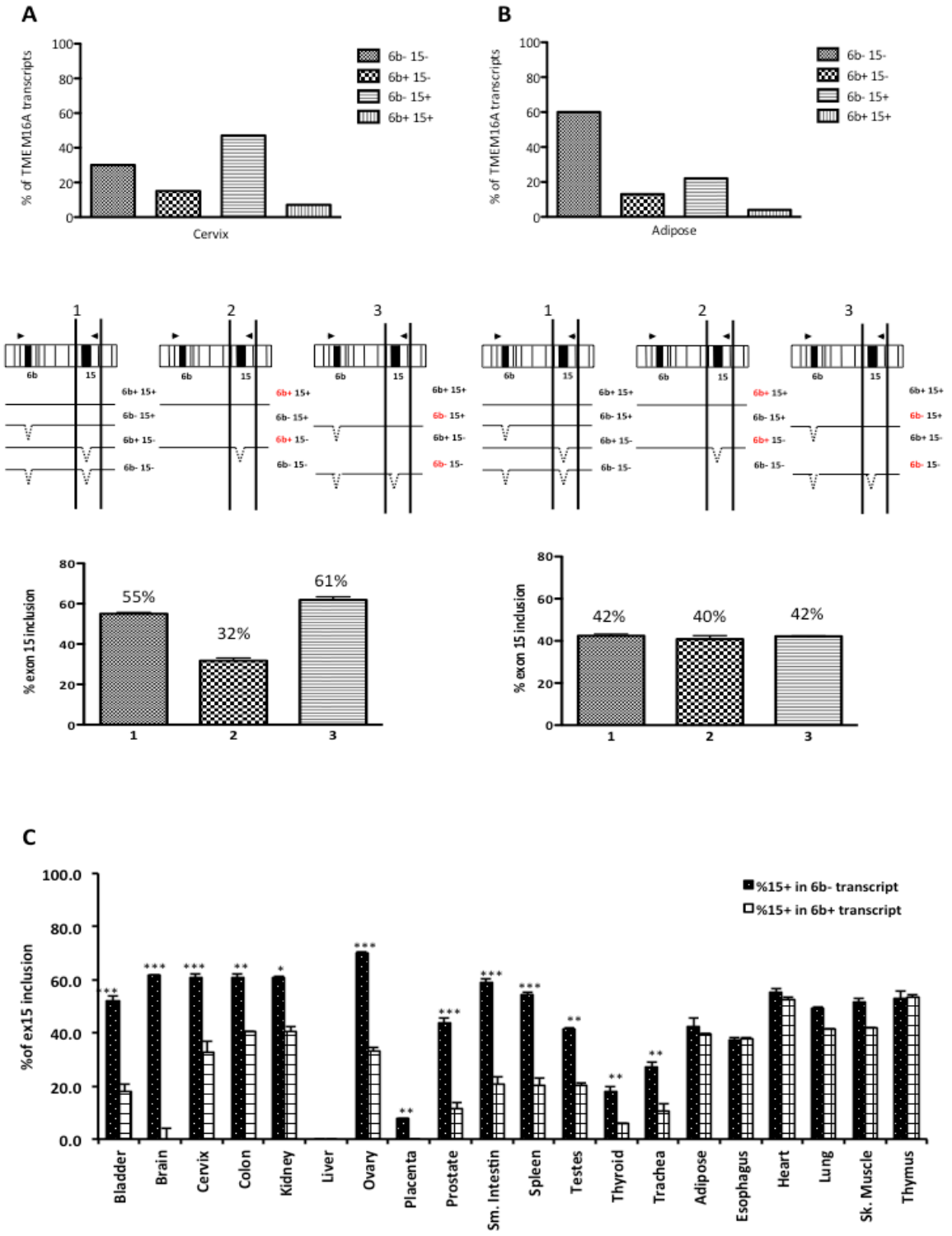

FIGURE 49. Coordination of TMEM16A mRNA isoforms in normal adult human tissues. *A and B,* an example of a positive and negative case of ISC, in cervix and adipose tissues respectively. The top scheme represents the quantification of the four different isoforms in the two human tissues. On the middle panel of the figure, bioinformatic evidence of coordination of the two alternative splicing region, exon6b and exon15. The tables indicate the inclusion of the downstream alternative exon (exon15) associated to the upstream alternative exon (exon6b) isoforms. 1,2,3, indicates the three different conditions: condition 1 denoted the total amount of the downstream exons in the four different isoforms, condition 2 represented exon15 inclusion when exon6b is present in the mature transcript, whereas condition 3 depicted the percentage of inclusion of the downstream exon15 when the mRNA lacks the upstream exon. Statistically analysis was performed using paired Student's t-test. *C,* Quantification of exon15 inclusion associated to exon6b inclusion or exclusion in 20 different normal adult human tissues.

Analysis of TMEM16A mRNA isoforms in mouse tissues

To evaluate the TMEM16A isoform distribution in mouse tissues, and thus the evolutionary conservation of the AS events, I studied in first instance the splicing pattern of exon 13 followed by a long range amplification with fluorescent primers that includes the three alternatively spliced exons (Figure 50). Amplification of exon 13 alone was necessary for a correct identification of the isoforms in the subsequent long-rang PCR.

RT-PCR analysis obtained using primers targeting flanking exon 13 sequences, showed two mRNA bands: the upper corresponds to exon 13 inclusion (282 bp) and the lower one to exon 13 exclusion (270 bp). The identity of the bands was verified by direct sequencing after elution of the bands from the gel. A number of tissues showed skipping of exon 13 (Figure 51A). In particular, tissues derived from mouse brain (Medulla, Cerebral cortex, Brain and Olfactory bulb), embryonic tissues (Embrio 10.5 and Embrio 14.5), Small Intestine, Stomach, Spleen, Testes, Foreskin gland and Thymus showed variable degree of exon 13 skipping (Figure 51A; Figure 51B). The other tissues analyzed did not show any band originating from skipping of exon 13.

Long range-PCR with oligonucleotides complementary to exon 6 and 16 of the TMEM16A cDNA is shown in Figure 50A and a typical pattern obtained from mouse tissues that include or exclude exon 13 is reported in Figure 50C and 50D, respectively. Eight mRNA isoforms of different length can originate from the possible combination of alternative usage of exon 6b, exon 13 and exon 15 (Figure 50B) and through capillary electrophoresis six of them were identified (Figure 50 C and D), Tissues that include exon 13 showed three major TMEM16A isoforms that correspond to 6b-13+15- (isoform 2 of 778bp), 6b+13+15- (isoform 4 of 843bp) and 6b-13+15+ (isoform 6 of 856bp). On the other hand, tissues with exon 13 skipping, presented two additional bands that correspond to 6b-13-15- (isoform 1 of 766bp) and 6b+13-15- (isoform 3 of 831bp).

The long range PCR analysis in the 9 mouse tissues that include exon 13 showed a very similar pattern of expression of the four isoforms. In particular, the most expressed isoform corresponds to isoform 2 in which the two exons 6b and

15 are skipped (6b-15-13+) followed by the isoform 4 (6b+15-13+). Unexpectedly, the isoforms in which exon 15 is included were absent or present at very low amount (Figure 52).

Comparison of the expression of the TMEM16A isoforms between the nine human and mouse tissues that completely include exon 13 showed a very different pattern (Figure 53). The most evident change is regards the isoforms that include exon 15, which are almost absent in the mouse tissues. For example, the 6b+15- isoform is predominant in human lung or ovary but nearly absent in the corresponding mouse tissues. In addition, in liver the most abundant variant present in human is 6b+15- (~90%) while in mouse is 6b-15- (~80%). These result indicate that TMEM16A pattern of splicing and isoforms expression is not conserved between human and mouse. In addition, as exon 15 is largely excluded in most of the mouse tissues it seems that there is no an evident TMEM16A splicing coordination in this animal.

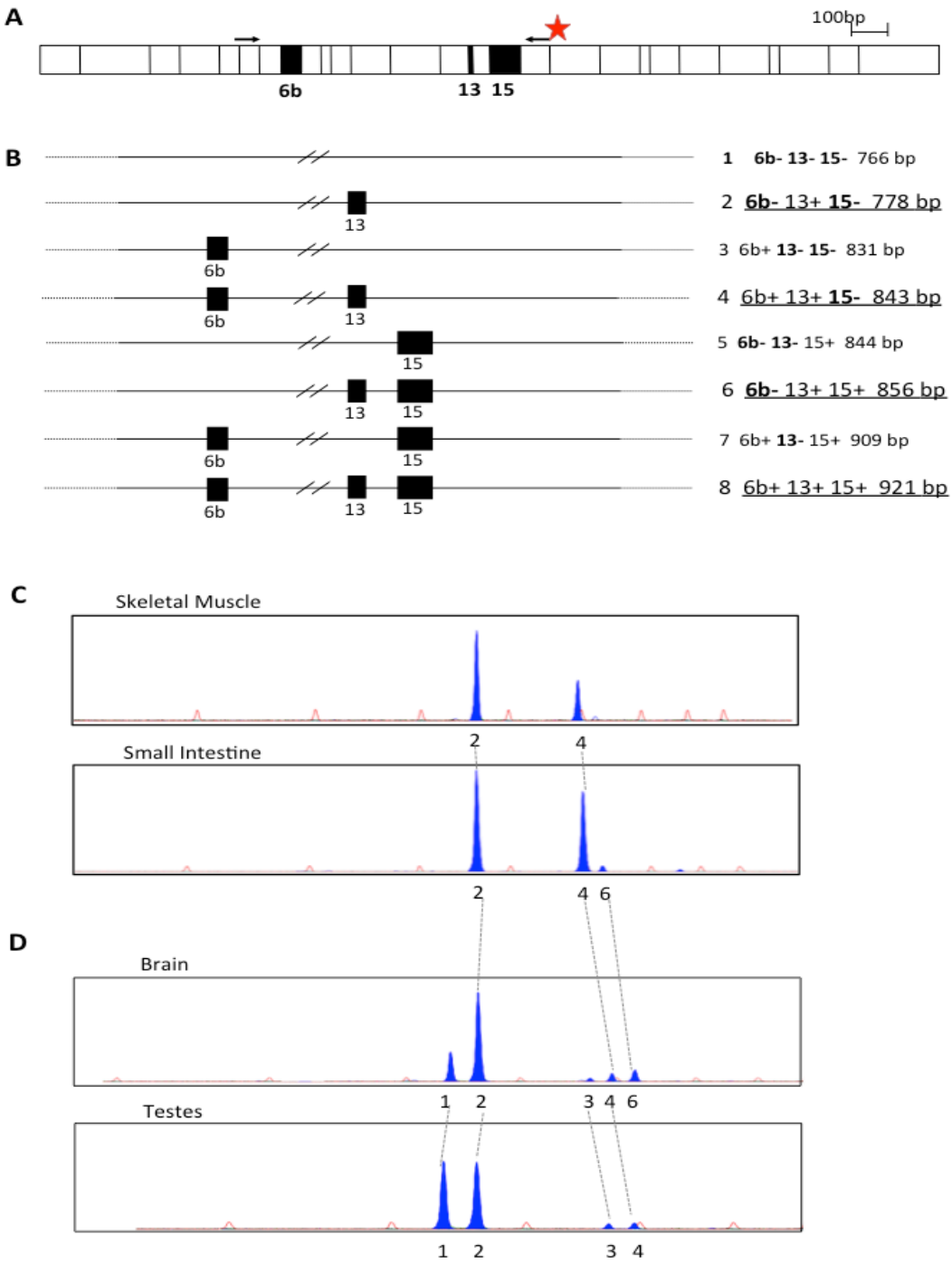

FIGURE 50. Analysis of *TMEM16A* specific isoforms in mouse tissues through capillary electrophoresis. *A,* general strategy used to amplify TMEM16A specific isoforms. Forward primer, 1602R^{FAM} was fluorescently labeled, RT-PCR product obtained with 681D and 1602R^{FAM} primers spans TMEM16A from exon6 to exon16, a region encompassing the three alternative exons (black boxes). *B,* cartoon indicating eight possible TMEM16A transcript variants as a result of combination of exon 6b, 13 and 15 inclusion and/or exclusion. The four isoforms underlined are the most common, with exon13 included. The expected sizes of RT-PCR products are indicated on the right. *C,* typical electrophoregram of the RT-PCR products, evaluated by capillary electrophoresis of tissues that express isoforms with exon13. Each peak correspond to the isoforms indicated in B. Peak 2 is a transcript of 778bp (exon6b and exon15 are skipped from the transcript, while exon13 is included), peak 4 is a transcript of 843bp (exon6b and exon13 are included in the transcript, exon15 is excluded), peak 6 is a transcript of 856bp, it is 12bp longer than peak 4 due to the absent of exon6b and the presence of exon15. Peak 8, is a transcript of 921bp (all three alternative exons are included). *D,* typical electrophoregram of the RT-PCR products of tissues that express the isoforms without exon13.

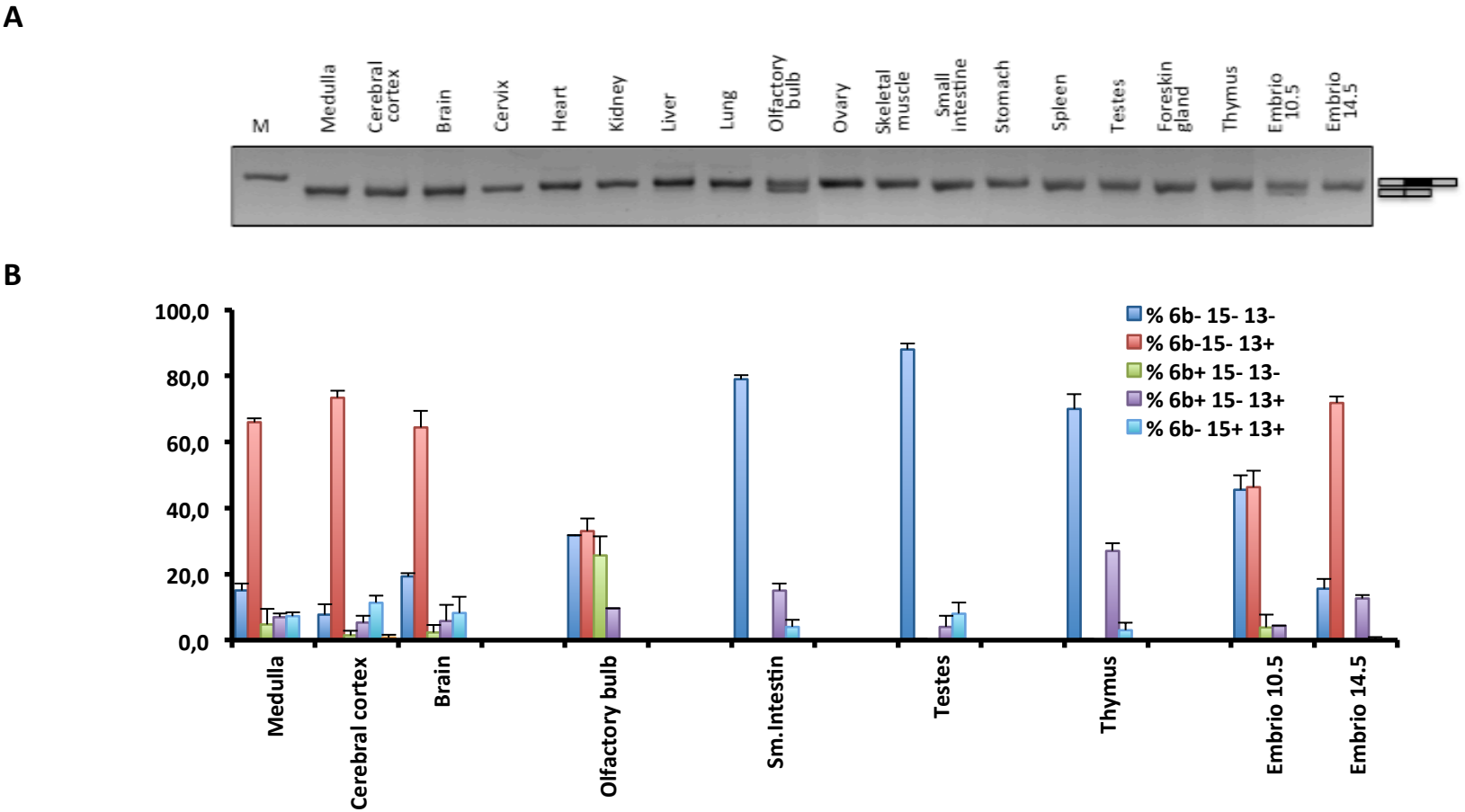

FIGURE 51. Quantification chart of *TMEM16A* specific isoforms in mouse tissues that have showed exon 13 skipping through capillary electrophoresis. *A,* Splicing pattern of exon 13. RT-PCR products run on an agarose gel and stained with ethidium bromide. The identity of the bands are indicated on the right side of the panel. M, molecular weight marker. *B,* Six isoforms pattern analysis of 21 different mouse tissues after separation on a denaturing capillary system of fluorescently labeled RT-PCR. The corresponding outcomes are depicted. The percentages of the bars were determined from the total area of each peak. The error bars are included to display the high level of reproducibility obtained with three separate reverse transcriptions and amplifications done in duplicate.

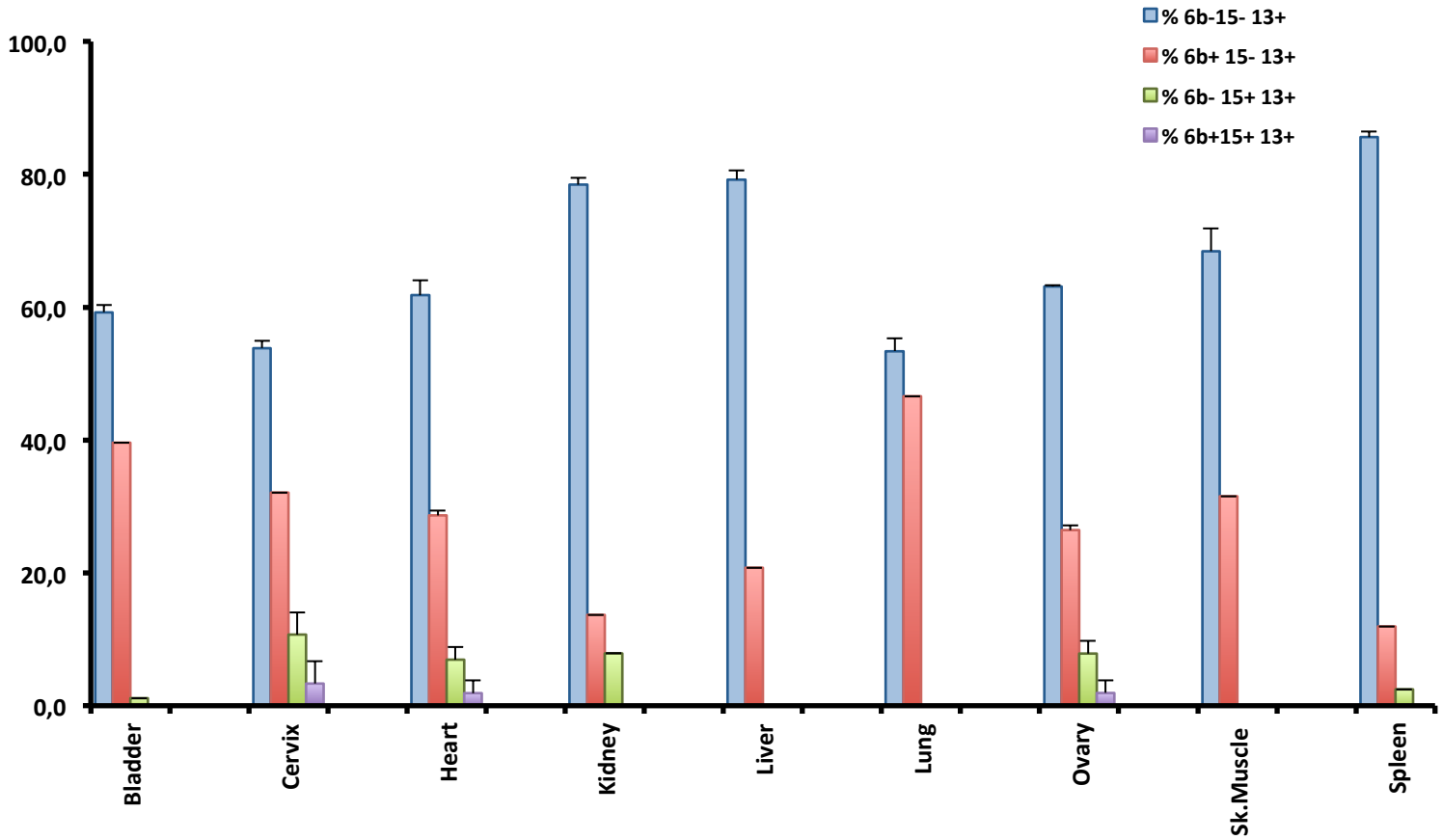

FIGURE 52. Quantification chart of *TMEM16A* specific isoforms in mouse tissues that showed exon 13 inclusion through capillary electrophoresis. Four isoforms pattern analysis of 9 different mouse tissues after separation on a denaturing capillary system of fluorescently labeled RT-PCR. The corresponding outcomes are depicted. The percentages of the bars were determined from the total area of each peak. The error bars are included to display the high level of reproducibility obtained with three separate reverse transcriptions and amplifications done in duplicate.

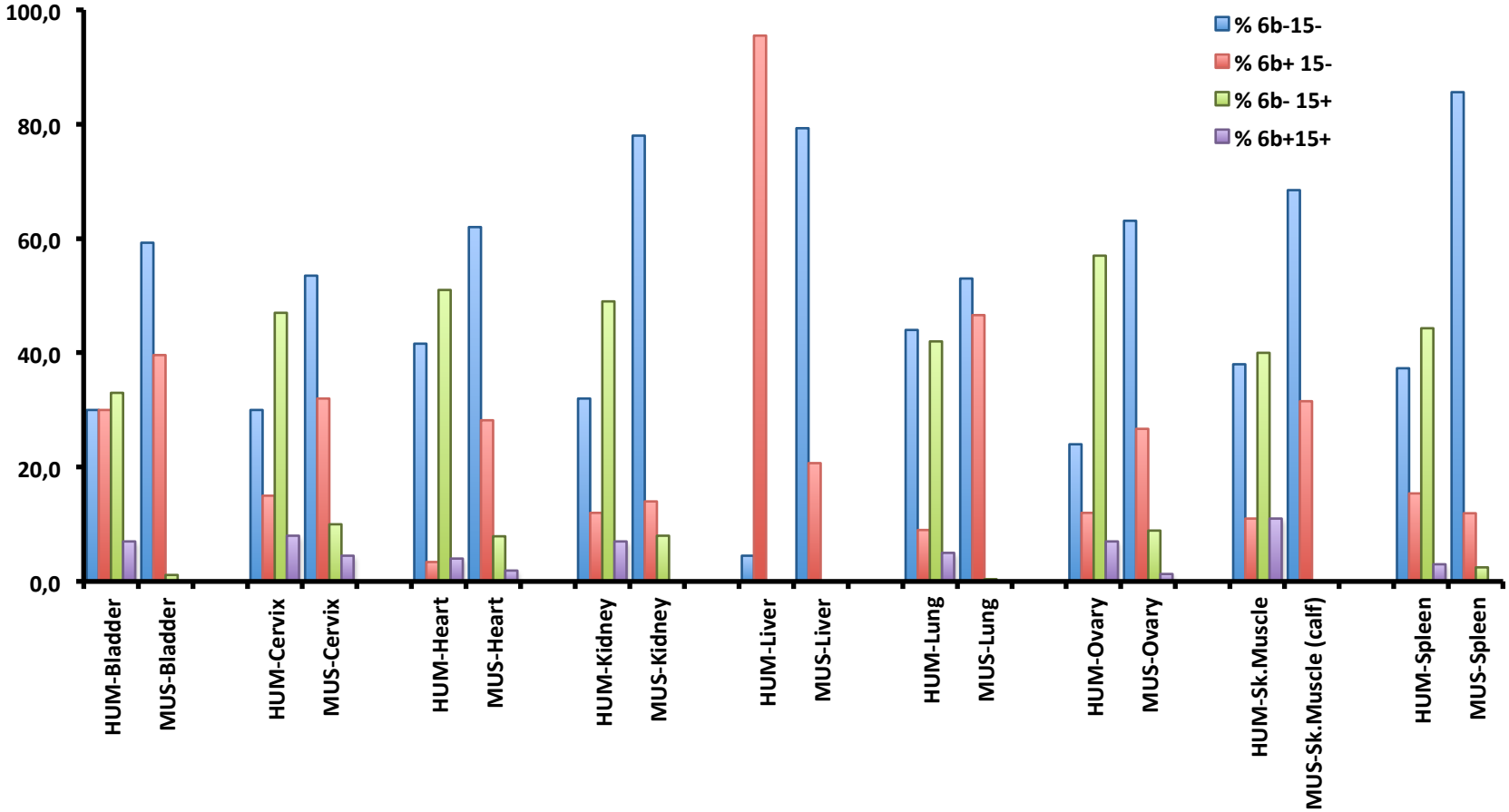

FIGURE 53. Comparative quantification chart between human and mouse tissues of *TMEM16A* specific isoforms through capillary electrophoresis. Four isoforms pattern analysis of 13 different human and mouse tissues after separation on a denaturing capillary system of fluorescently labeled RT-PCR. The corresponding outcomes are depicted. The percentages of the bars were determined from the total area of each peak. The error bars are included to display the high level of reproducibility obtained with three separate reverse transcriptions and amplifications done in duplicate.

Alternative splicing of TMEM16A in human breast cancer tissues

TMEM16A has been associated to several types of tumors including breast cancer (Duvvuri, Shiwarski, Xiao, et al. 2012). To better understand the role of TMEM16A in cancer, I examined the pattern of AS in 18 breast cancers and the corresponding 18 normal mammalian breast tissues obtained from the same surgical specimen, listed in Table 1. Samples were manually collected by the pathologist at the Gorizia Hospital, Italy within 15 minutes after surgical resection and immediately stored in RNA Later solution. Corresponding samples were analyzed in routine diagnostic procedure by histology and immunohistochemistry analysis. The absence of tumor cells in the normal breast tissues was confirmed by histological analysis.

In Table 1, samples are classified in virtue of their histological evaluation (second column), D defined as ductal breast or L defined as lobular breast samples; grading (third column), necrosis (forth column) and receptors (fifth, sixth, seventh and eighth column). ER, estrogen receptor; PgR, progesterone receptor; Ki67, nuclear proliferation marker and HER2, human epidermal growth factor receptor 2. The histological evaluation showed 14 ductal and 3 lobular tumors and 1 ductal-bifasic. The majority of tumors are positive for the estrogen and progesterone receptor markers (15 and 13 tissues, respectively). The nuclear proliferation marker Kit67 was low (+1 grading) in most tumors (n=12) and high (grading +2 and +3) in 6 tumors. The HER2 marker was detected in 5 breast cancers.

SAMPLES	HISTOLOGY	GRADING	NECROSIS	E.R.	Pg.R.	Ki67	HER2
3118N	D	G1	-	3+	2+	1+	-
3118T	D	G1	-	3+	2+	1+	-
3237N	D	G1	-	3+	3+	1+	-
3237T	D	G1	-	3+	3+	1+	-
3659N	D	G1	-	3+	3+	1+	-
3659T	D	G1	-	3+	3+	1+	-
4962N	D	G1	-	3+	3+	1+	-
4962T	D	G1	-	3+	3+	1+	-
5212N	D-bifasic	G1/G3	-	3+	2+	3+	-
5212T	D-bifasic	G1/G3	-	3+	2+	3+	-
2701N	L	G2	-	1+	1+	1+	+
2701T	L	G2	-	1+	1+	1+	+
3581N	D	G2	-	3+	3+	1+	-
3581T	D	G2	-	3+	3+	1+	-
3884N	D	G2	-	3+	3+	1+	-
3884T	D	G2	-	3+	3+	1+	-
4392N	L	G2	-	3+	3+	1+	-
4392T	L	G2	-	3+	3+	1+	-
2695N	L	G3	-	3+	3+	1+	-
2695T	L	G3	-	3+	3+	1+	-
3122N	D	G3	-	2+	3+	3+	+
3122T	D	G3	-	2+	3+	3+	+
3577N	D	G3	FOCAL	3+	0	1+	-
3577T	D	G3	FOCAL	3+	0	1+	-
3979N	D	G3	-	3+	0	1+	-
3979T	D	G3	-	3+	0	1+	-
4309N	D	G3	+	0	0	3+	-
4309T	D	G3	+	0	0	3+	-
4503N	D	G3	+	0	0	3+	+
4503T	D	G3	+	0	0	3+	+
5056N	D	G3	FOCAL	3+	1+	2+	+
5056T	D	G3	FOCAL	3+	1+	2+	+
5295N	D	G3	-	0	0	2+	+
5295T	D	G3	-	0	0	2+	+
5566N	D	G3	FOCAL	3+	3+	1+	-
5566T	D	G3	FOCAL	3+	3+	1+	-

TABLE 1. Clinicopathological variables in normal and human breast cancer samples. 36 breast samples obtained by surgical excision where divided in their normal (N) and tumor (T) portions. Samples are classified in virtue of their histological evaluation (second column), D defined as ductal breast or L defined as lobular breast samples; grading (third column), necrosis (forth column) and receptors (fifth, sixth, seventh and eighth column). ER, estrogen receptor; PgR, progesterone receptor; Ki67, nuclear proliferation marker and HER2, human epidermal growth factor receptor 2.

TMEM16A isoforms expression in the 36 paired tumor-normal breast tissues were evaluated by denaturing capillary electrophoresis of fluorescent-5' end labeled RT-PCR that amplifies transcripts across the AS events as done for the normal human tissue (Figure 45). I detected, in all the samples only four spliced variants of 725bp, 791bp, 803bp and 869bp, which correspond to 6b-13+15-, 6b+13+15-, 6b-13+15+ and 6b+13+15+ isoforms, respectively (isoforms 2, 4, 6 and 8 in figure 45B). No band with skipping of exon 13 was detected. The data were analyzed either considering the percentage of inclusion of each exon on the total transcript or evaluating individually the different TMEM16A isoforms. In the normal breast, exon 6b and 15 are present in approximately 40% and 10% of the TMEM16A transcripts, respectively and these percentages did not change significantly in the tumors (Figure 54A). Exon 13 was completely included in all the samples analyzed (Figure 54A).

On the other hand, the analysis of the distribution of the four mRNA isoforms showed that in the normal breast tissue about 50% of the transcripts are without exon 6b and 15, 40% include exon 6b and exclude exon 15, 8% include exon 15 and exclude exon 6b whereas only approximately 3% of the transcripts have both exons. In comparison to the normal breast, the tumor tissues did not show any significant difference in the isoform distribution (figure 54B). The scatter of the standard deviation (SD) in tumor samples is increased in comparison to normal breast tissues, suggesting a higher variability of the four isoforms distribution in cancer.

Next, to evaluate the relationship between the two major AS events on the same transcript I compared, in normal and tumor samples, the percentage of exon 6b inclusion in transcripts that include exon 15 to transcripts and that exclude it. Significant differences in these percentages were considered as indicative of splicing coordination between the two AS events. This analysis revealed that in 9 out of 18 normal breast tissues (50%) the two AS events were coordinated. Interestingly, 15 breast cancers, showed evidence of coordination (84%). This increase in the number of samples with splicing coordination is due to the fact that 6 normal breasts that were not coordinated turn to be coordinated in the corresponding cancer tissues. The coordination between exon 6b inclusion

associated to exon 15 isoforms is shown in Figure 55A and the same results were observed considering exon 15 inclusion associated to exon 6b isoforms (Figure 56). By this measure, as the pie graphs summarize in Figure 57, in TMEM16A transcripts derived from normal breast the exon 6b and 15 showed evidence of splicing coordination in 50% of the samples and this percentage increase to 84% in tumors.

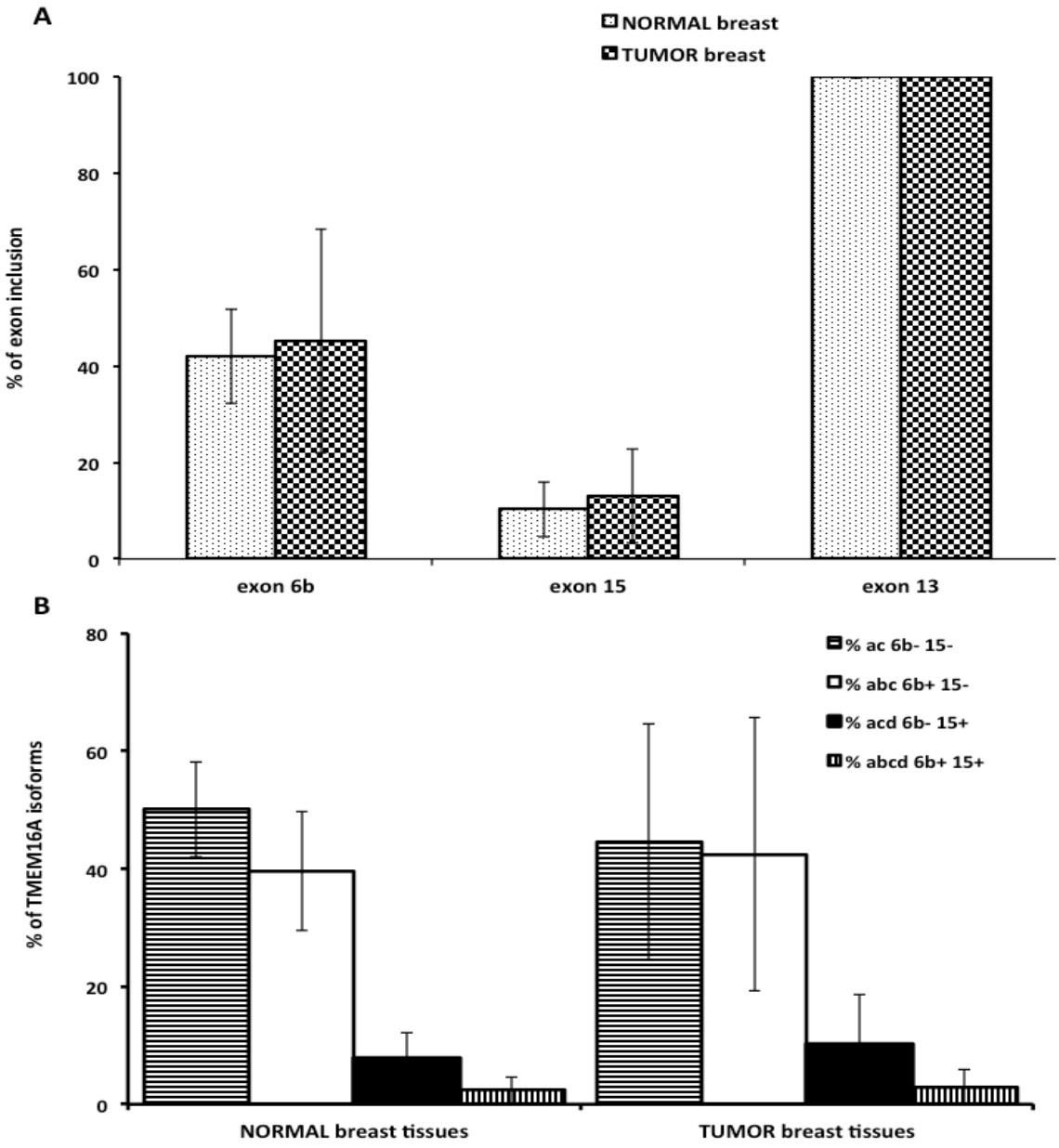

FIGURE 54. Analysis of the Alternative spliced exons of TMEM16A in human normal breast and breast cancer tissues. *A,* mean of the two alternatively spliced exons6b and 15, in normal and tumor breast tissues. The percentage is expressed as means ± SD, based on at least three independent capillary electrophoresis analyses. *B,* Mean of TMEM16A isoforms profiles in normal and tumor breast tissues, percentage is expressed as means ± SD, based on at least three independent capillary electrophoresis analyses.

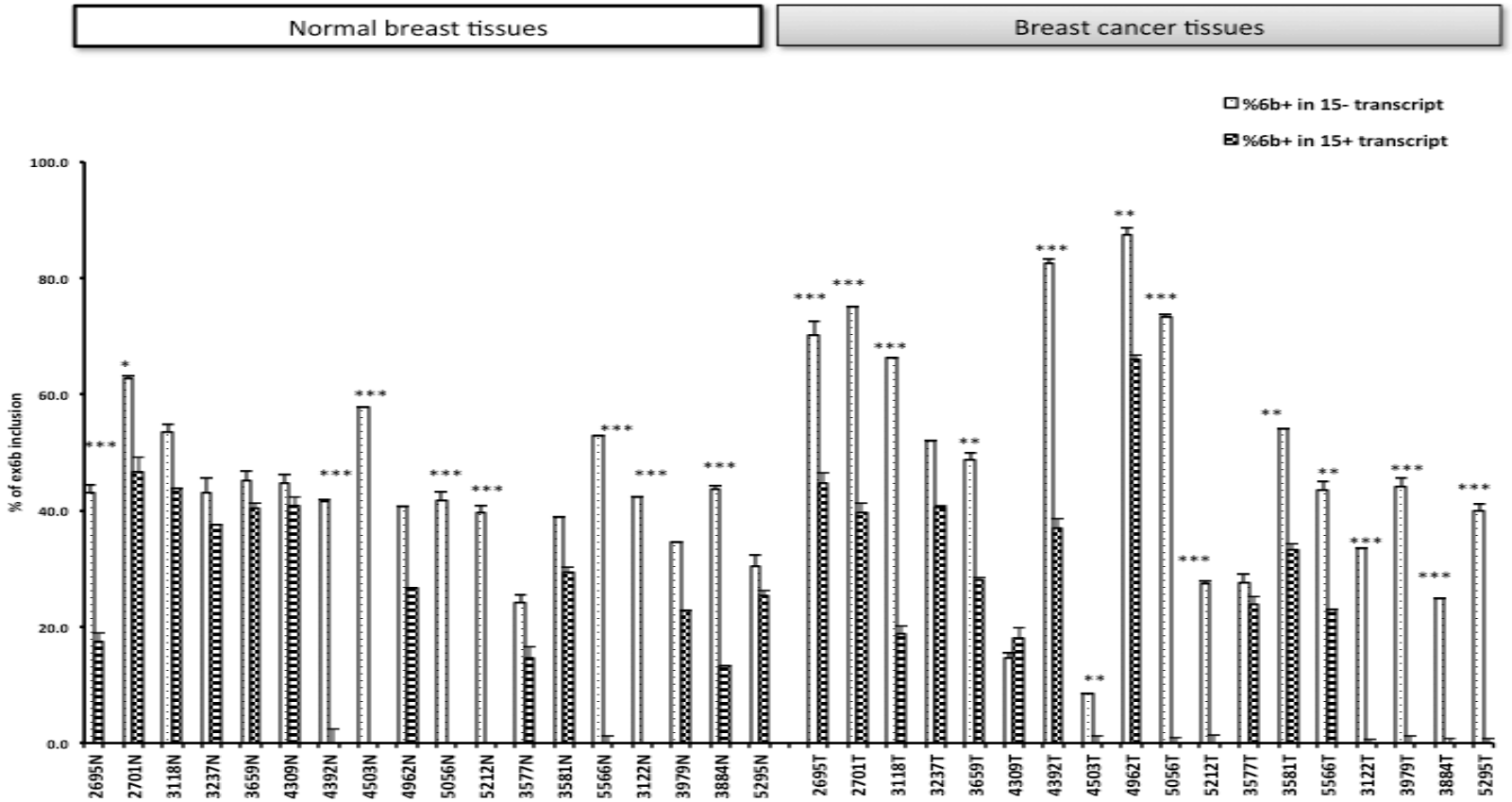

FIGURE 55. Comparative analysis of TMEM16A mRNA isoforms coordination between normal and breast cancer tissues. Quantification of exon6b inclusion associated to exon15 inclusion or exclusion between normal and breast cancer tissues. The former 18 samples are Normal breast tissues, the latter are the corresponding breast cancer tissues.

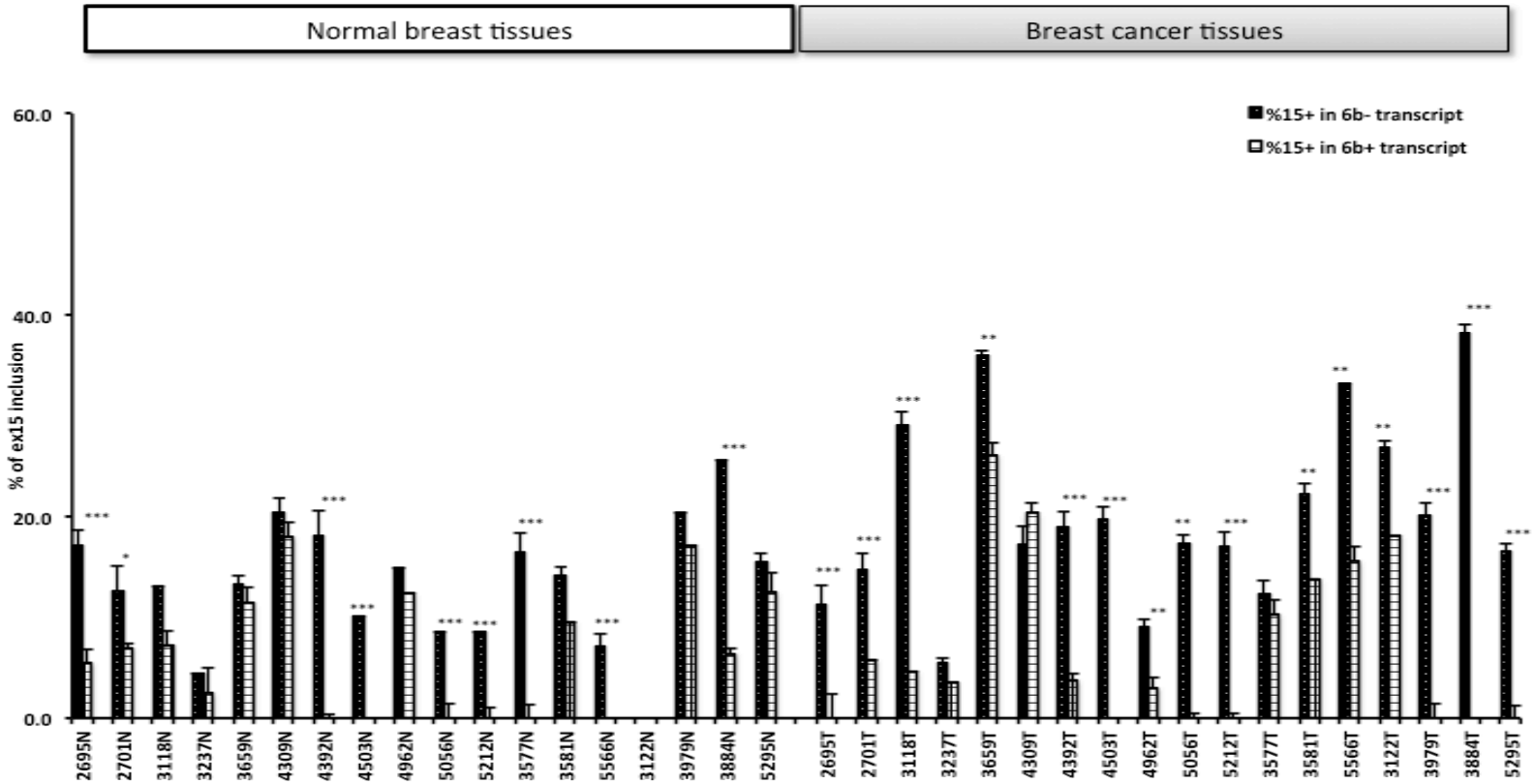

FIGURE 56. Comparative analysis of TMEM16A mRNA isoforms coordination between normal and breast cancer tissues. Quantification of exon15 inclusion associated to exon6b inclusion or exclusion between normal and breast cancer tissues. The former 18 samples are Normal breast tissues, the latter are the corresponding breast cancer tissues.

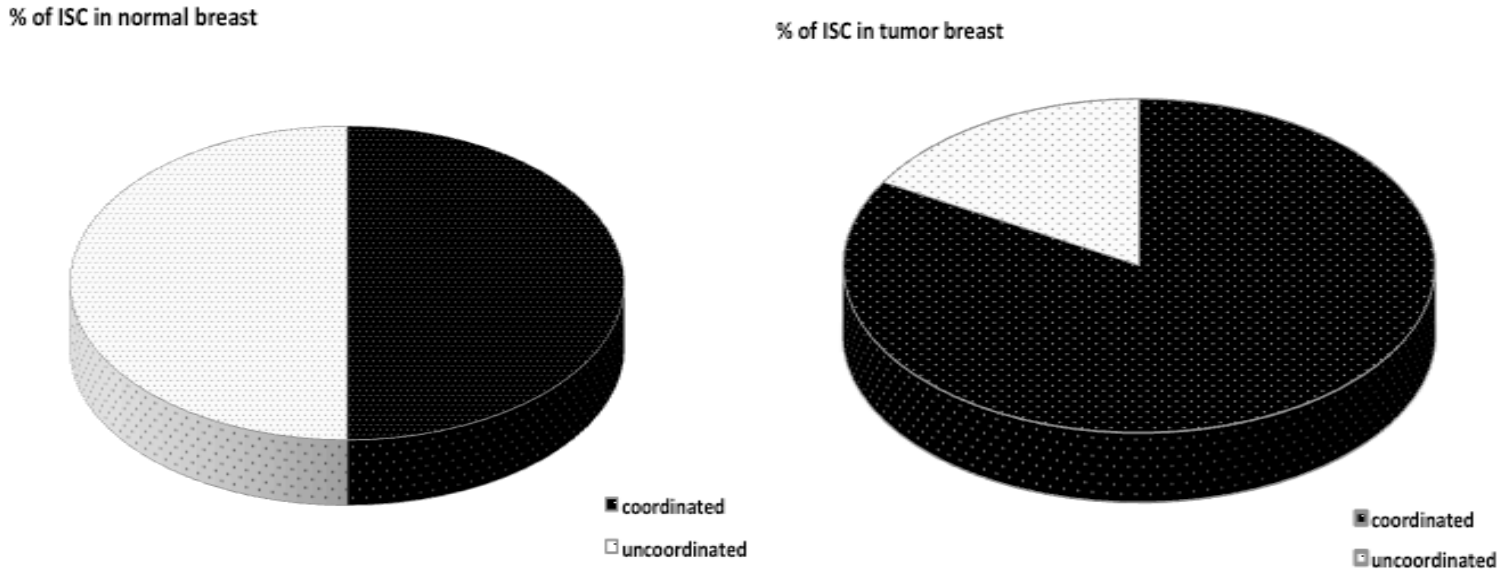

FIGURE 57. Comparative analysis of TMEM16A mRNA isoforms coordination between normal and breast cancer tissues. The left pie-chart shows the amount of coordination in normal breast tissues, the right pie-chart depicts the amount of ISC in breast cancer tissues. The percentage is expressed as means ± SD, based on at least three independent capillary electrophoresis analyses.

DISCUSSION

In this study, I have investigated the AS regulation of three AS exons of TMEM16A and the possible interdependence between them in normal and cancer tissues. I have evaluated the effect of different families of splicing factors on the pattern of splicing and the role of enhancers and silencers sequences. As shown in the results section, this has been mostly performed *in vitro* using several artificial experimental systems through minigene-based techniques in order to identify *cis*-elements, demonstrating regulation of few splicing events by specific RNA binding proteins.

This study identify some *cis*- and *trans*-acting elements involved in the regulation of the three TMEM16A AS exons and provides evidence for intragenic splicing coordination in the TMEM16A gene in more tissues. The observed changes in breast tumors might be important in cancer development.

Identification of TMEM16A splice variants and expression in normal adult human tissues

From the original observation that identify the TMEM16A protein as a Ca^{2+}-dependent Cl^- channel (Yang, Cho et al. 2008; Caputo, Caci et al. 2008; Schroeder, Cheng et al. 2008) it was clear that alternative splicing can potentially generate several isoforms (Ferrera, Caputo et al. 2009). In particular, Ferrera et al. using available EST sequences identified four possible AS events (*a, b, c* and *d)*. Functional analysis of a limited numbers of the possible resulting protein isoforms showed significant changes in their electrophysiological parameters, indicating that TMEM16A alternative splicing is an important way of controlling the channel function. The four splice variants of TMEM16A exhibited different voltage-dependent and Ca^{2+}-dependent gating properties ((Ferrera, Caputo et al. 2009); (Xiao, Yu et al. 2011)). For example, inclusion/skipping of segment *b* (exon 6b) in the TMEM16A sequence seems to modulate the Ca^{2+} sensitivity of the corresponding Cl^- channels (Ferrera et al. 2009). The four amino acids (Glu-Ala-

Val-Lys) of segment *c* (exon 13) are also important. Deletion of these amino acid residues (DEAVK-TMEM16A) generates CaCCs with altered biophysical properties (Xiao et al. 2011). In particular, deletion of the first two amino acids of this segment did not alter the channel properties relative to (*abc*) variant. In contrast, deletion of the second two residues generated membrane currents similar to those associated with deletion of the whole four residue segments.

To extend this original observation and determine the TMEM16A splicing pattern in vivo in the first part of my thesis I performed bioinformatic and RT-PCR analysis on the possible AS events. Three alternative exons 6b, 13 and 15 have a high degree of sequence conservation between related species and the resulting transcripts were easily amplified from human RNAs showing a characteristic tissue specific splicing pattern (Figure 14). I found various levels of inclusion/skipping of exons 6b and 15 depending on the tissue. As shown in figure 15, the five tissues that predominantly include exon 6b (liver, placenta, prostate, thyroid, and trachea) tend also to exclude exon 15 from the mature transcript. In contrast to these exons, the unusually short exon 13a is partially skipped only in brain and skeletal muscle (Figure 15) suggesting a specific function of the resulting isoform in these tissues. In contrast to previous observation (Ferrera, Caputo, Ubby et al. 2009) I was not able to amplify any transcript originating from the usage of this alternative promoter. The corresponding genomic sequences are not evolutionary conserved suggesting a human specific expression. It is possible that the resulting isoform, which was reported to be functionally inactive (Ferrera, Caputo, Ubby et al. 2009) has a very restricted cell-type expression. This splicing variants was recently described to be reduced in human diabetic gastroparesis (Mazzone, Bernard et al. 2011). Mazzone et al. identified by quantitative RT-PCR that nondiabetic patients always includes segment *a,* whereas patients with diabetic gastroparesis, has more transcripts lacking this segment. They found that the expression of segment *a* in patients with diabetic gastroparesis is associated with the type of diabetes as it was increased in patients with type 2 diabetes, compared with type 1. Thus, the exact identity and role of segment *a* is unclear. In Ferrera et al. 2009, it has been hypothesized, that its expression could be restricted to a particular cell type or developmental stage.

Regulation of TMEM16A exon 6b Alternative Splicing

To understand the regulation of the three alternatively spliced exons I have used a well established minigene system on which I have evaluated the effect of a representative panel of splicing factors. This first approach, used to identify for each case positive and /or negative splicing regulators, was followed by mapping of enhancer and silencer splicing regulatory sequences through deletion analysis. Lastly, the functional relationship between splicing regulatory sequences and splicing factors was evaluated through cotransfection experiments on deletion mutants and in the most interesting case tested through direct binding on naked RNA.

The experiments described in the result section, showed that TMEM16A exon 6b is regulated by several splicing factors and contains multiple enhancer and silencer sequences. In cotransfection experiments, four proteins were able to positively regulate exon 6b splicing: SRSF9 (SRp30), TRA2B, PTB1 and RbFOX1 (Figure 17, lane 8 and 15; Figure 18, lane 6 and 12), whereas several others factors ESRP1FF/2FF, ETR3, CUGbp and a number of SR proteins (SRSF3, SRSF5, SRSF6, SRSF4 and SRSF2) induced exon skipping (Figure 17). On the other hand, deletion analysis showed two enhancers and four silencers regulatory sequences. The enhancers include a strong GAA-rich ESE located at the 5' portion of the exon, where its deletion induce complete exon skipping (MUT2 of Figure 20) and a less efficient downstream ISE (MUT7 of Figure 21). The four silencers encompass the last part of the exon (MUT4, MUT5 and MUT6) or are located in the intron (MUT9) (See Figure 20 and 21).

A strong GAA-rich enhancer mediates the exon 6b recognition through four enhancing splicing factors (SRSF9, TRA2B, PTB1 and Fox1)

Overexpression of the four enhancing splicing factors (SRSF9, TRA2B, PTB1 and Fox1) on the two enhancer mutants, showed no effect when the long GAA-rich ESE is deleted (MUT2) whereas their enhancing effect is maintained on the MUT7 ISE (Figure 26). The absence of any effect of all the four enhancing splicing factors on the MUT2 minigene indicates that this GAA-rich ESE is an essential

element involved in exon 6b splicing recognition.

Interestingly, the strong enhancer element found within TMEM16A exon 6b is very similar to the ESE sequence identified in the central region of SMN2 exon 7 (Figure 58), which is known to be a typical binding site for TRA2B and also it is positively regulated by other factors such as SRSF9 (Clèry et al. 2011). In the SMN2 exon 7, the ESE contains two adjacent consensus binding sites for TRA2B, namely AGAA and GGAA. Clèry et al. recently demonstrated that the repetition of this AGAA motif, increases the efficiency of TRA2B recruitment. Interestingly Clèry et al. 2011 and Grellscheid, Dalgliesh et al. 2011 demostrated that loss of even a single motif sequence resulted in complete loss of exon activation which could not be rescued by elevating levels of TRA2B. Furthermore they showed that the number of Tra2B binding sites required within an exon to establish a splicing response is likely to depend on splice site strength and other splicing signals. For example, the inclusion of another Tra2B-responsive exon such as SMN2 exon 7, which has a two TRA2B binding site, additionally depends on binding of hnRNPG and SRp30c. Thus, they suggest that the presence of more consecutive motifs, which is seen in most of the TRA2B-dependent ESEs (Grellscheid, Dalgliesh et al. 2011), increases the efficiency of TRA2B recruitment on the nascent RNA. These might occur either by allowing multiple binding registers for TRA2B or by preventing the formation of secondary structures. In addition, the presence of flanking purine residues was suggested to prevent binding of other protein competitors that otherwise interacts with different sequences (Clèry, Jayne et al. 2011)

In the exon 6b, all the four contiguous motifs that consist of two core adjacent AGAA consensus TRA2B sites flanked by two purine-rich elements, namely AGGGA and GGA, are directly involved in exon recognition (Figure 28). Each motif mediates the exon recognition as their deletion or mutagenesis induce significant exon skipping (Figure 29). However, while the deletion of the two central core AGAA motifs was completely deleterious for splicing, deletion of the other elements maintained some splicing efficiency (~10-20% of exon inclusion) (MUT2-B, MUT2-C, MUT2-E and MUT2-G of Figure 29). Interestingly, the deletion of each motif prevented the enhancing effect mediated by SRSF9, TRA2B, PTB1

and RbFOX1 (Figure 30), suggesting that these splicing factors require the whole GAA-rich ESE for splicing enhancement. However, while SRSF9 and TRA2B can directly interact with this ESE, (and indeed pull down assay demonstrated direct binding of TRA2B, see below) it is very unlikely that PTB1 and RbFOX1 interact directly with the long enhancer as it does not contain any obvious consensus binding sites. PTB1 is an important splicing regulator (Wagner and Garcia-Blanco 2001) that interacting with polypyrimidine tracts with a preferred UCUU binding site (Perez, Lin et al. 1997) is mainly involved in splicing repression (Garcia-Blanco, Jamison et al. 1989); (Valcarcel and Gebauer 1997), even if recently CLIP analysis showed that, depending on the context and on the position of the binding sites, it can also induce exon inclusion (Llorian, Schwartz et al. 2010). PTB effect on splicing may result from competition with U2AF65 at the polypirimidine tract of the 3'ss or with a looping mechanism between flanking introns that exclude the exon from the mature mRNA ((Lin and Patton 1995); (Singh, Valcarcel et al. 1995)). On the other hand, FOX1 proteins bind mainly to intronic (U)GCAUG elements and their splicing effect depends on their binding position on the nascent RNA. In general, its binding to downstream intronic region induces exon inclusion, whereas binding to the upstream intron results in exon skipping ((Kuroyanagi 2009); (Fogel, Wexler et al. 2012); (Licatalosi, Mele et al. 2008); (Yeo, Coufal et al. 2009). The mechanism of FOX1-dependent splicing regulation is not known.

In exon 6b, it is possible that PTB and FOX1 are part of an enhancing complex that is assembled on the GAA-rich ESE. In common with the model for SMN (Clèry et al. 2011), it is possible that TRA2B interaction with the core AGAA sequences will recruit these two additional splicing factors PTB and FOX1, to activate the inclusion of exon 6b. Alternatively, their effect might be due to an interaction with other none obvious consensus sequences on the nascent RNA.

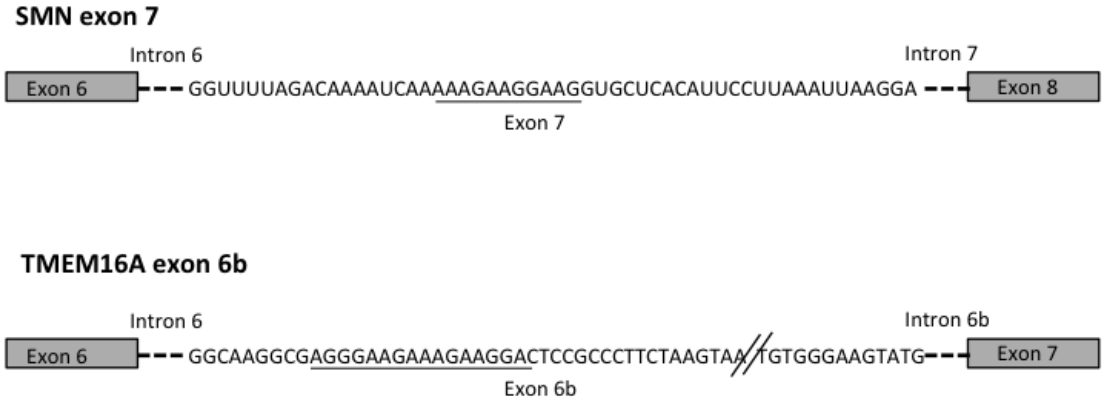

Figure 58. GAA-rich ESE sequence of *SMN2* exon 7 and TMEM16A exon 6b splicing. Schematic representation of the SMN2 and TMEM16A minigenes. The exon 7 and exon 6b sequences are shown and the previously reported Tra2B interacting sequence are underlined. Adapted from Clery, Stamm et al. 2011.

On the other hand, in pull down assay, TRA2B directly binds to the entire GAA-rich enhancer (Figure 31). In addition, the analysis of several mutants RNAs showed that the first two motifs of the 16bp long ESE are the major determinants for its binding (Figure 31). However, as all the mutants tested are associated to significant exon skipping in splicing assay it is clear that additional splicing factors are possibly involved. These factors, like PTB and FOX1 might assist or facilitate TRA2B to form a functional enhancing complex on the GAA-rich enhancer.

Role of splicing inhibitory factors and silencer sequences in exon 6b alternative splicing regulation

The positive effect of the GAA-rich ESE in TMEM16A exon 6b is balanced by the presence of a series of exonic and intronic silencers (Figures 20 and 21) and by a list of different splicing factors that preferentially bind to UG-rich sequences ESRP1FF/2FF, ETR3, CUGbp or belong to the SR protein family (SRSF1, SRSF3, SRSF9, SRSF5, SRSF6, SRSF4, SRSF2 and TRA2B).

Several data based on CLIP and SELEX experiments indicate that ESRP1FF/2FF, ETR3 and CUGbp preferentially binds to UG-rich sequences ((Warzecha, Shen et al. 2009); (Takahashi, Sasagawa et al. 2000); (Lu, Timchenko et al. 1999); (Dujardin, Buratti et al. 2010); (Faustino and Cooper 2005). In the context of the exon 6b, we observed UG-rich sequences only in the downstream intron and indeed their deletion induced exon inclusion (MUT9, Figure 21) thus identifying them as ISSs. However, overexpression of the UG-binding proteins still induce exon skipping in MUT9 (Figure 27), suggesting that these proteins might not directly interact with the ISS. In addition, the splicing silencing effect of most of the inhibitory factors is not evident when some ESS are deleted and in particular in the MUT5 and MUT6 minigenes (Figures 24 an 25, respectively), suggesting that these two flanking exonic sequences significantly contribute to the inhibitory outcome. Additional splicing factors may be possibly involved. Only ETR3 and SRSF2 maintain some small inhibitory effect in these two ESE deletion mutants (Figures 24 and 25).

Interestingly, whereas two canonical SR proteins are clearly involved in promoting exon 6b inclusion (TRA2B and SRSF9), several other SR proteins negatively regulate exon 6b splicing (Figure 17, lane 8-15). In general, SR proteins are splicing activators that interacting with ESE facilitating recognition of weak splice sites, and this is probably the mechanism of TRA2B and SRSF9 in exon 6b. However, there are well studied examples in which the SR proteins can repress splicing ((Buratti, Stuani et al. 2007)); (Kanopka, Muhlemann et al. 1996)). In the cystic fibrosis transmembrane conductance regulator (CFTR) gene SRSF1 and SRSF5 (ASF/SF2 and SRp40, respectively) repress exon 9 splicing through their binding to an intronic splicing silencer (Buratti, Stuani et al. 2007) located downstream the

exon. Similarly, SRSF1 represses adenovirus IIIa splicing through a repressor element but activates splicing through this element in a heterologous setting (Kanopka, Muhlemann et al. 1996). In splicing of the caspase-2 gene, SRSF1 and SRSF2 cause skipping of the 61bp exon 9, and hnRNP A1, a well studied splicing repressor, activates exon inclusion (Jiang, Zhang et al. 1998). These examples highlight the context-dependent nature of splicing regulatory elements. In the TMEM16A exon 6b it is possible that the inhibitory SR proteins might act through an uncharacterized intronic splicing regulatory element upstream exon 6b or indirectly through interaction with other splicing factors to form inhibitory complexes.

Regulation of TMEM16A exon 15 Alternative Splicing

TIA1 and RbFOX1 enhances TMEM16A exon 15 inclusion

In contrast to TMEM16A exon 6b, only two splicing factors, TIA1 and RbFOX1 promoted exon 15 inclusion (Figure 33, lane 2 and 12). These splicing factors are known to act mainly through interaction with downstream intronic sequences. In fact, TIA1 binding to uridine-rich sequences downstream the donor sites of alternative spliced exons facilitate U1 snRNP binding to weak 5'SS (Forch, Puig et al. 2000); ((Aznarez, Barash et al. 2008)). Similarly, FOX1 proteins binding to downstream intronic (T)GCATG elements induces exon inclusion, ((Kuroyanagi 2009); (Fogel, Wexler et al. 2012); (Licatalosi, Mele et al. 2008); (Yeo, Coufal et al. 2009). As these splicing factors are known to act through interaction with downstream intronic sequences I have specifically looked for regulatory elements in the corresponding sequences of TMEM16A exon 6b. Contransfection experiment showed that one polypyrimidine tract near the 5'SS in involved in TIA1-mediated enhancement and two consensus binding sites for RbFOX1, a penta- and an hexa-nucleotide (T)GCATG sequences are involved RbFOX1 regulation (Figures 37 and 38). These results are consistent with the presence of a weak exon 15 5'SS that significantly deviates from the consensus and therefore subjective to the influence of downstream *cis*-acting splicing regulatory elements. In addition, deletion and cotransfection analysis showed that also a large part of the exonic sequences are also important for exon 15 splicing regulation. As also some exonic deletion mutants do not respond to TIA1 and RbFOX1 overexpresssion (Figures 39-41), it is possible that the deletion of these ESEs has a dominant effect over the intronic splicing regulation. The deletion of these ESEs induce a severe exon skipping that cannot be rescued by TIA1 or RbFOX1 interaction at the downstream intronic elements. Further studies will be required to identify the enhancing splicing factors involved and establish the specificity of the RNA-splicing factors interactions involved.

Regulation of TMEM16A exon 13 Alternative Splicing

U2AF65 and RbFOX1 enhances TMEM16A exon 13 inclusion

Data from in vitro analysis showed that the extremely short TMEM16A exon 13 is regulated by two splicing factors that promote its inclusion: U2 auxiliary factor 65 (U2AF65) and RbFOX1 (Figure 42 and Figure 43). FOX1 strongly activate inclusion of exon 13, presumably by interacting with a downstream tetra-sequence (T)GCA. Deletion of this region resulted in a minor rescue of TMEM16A exon 13 inclusion upon co-transfection of the two enhancing proteins U2AF65 and RbFOX1 (Figure 44B). The short exon 13 has a restricted alternative expression in brain and skeletal muscle, thus suggesting that its skipping is regulated by tissue-specific regulatory factors. Because of steric interference between splicing complexes that assemble on the donor and acceptor sites, very few exons have a short length, and their regulation seems to be dependent on intronic splicing regulatory sequences (Simpson, Thow, Clark, et al. 2002). In mammals, several splicing factors are tissues-specific or are involved in brain- and/or muscle-specific splicing, such as Fox- 1/2 (Jin, Suzuki et al. 2003), PTBP1/2 (PTB/nPTB) ((Markovtsov, Nikolic et al. 2000), CUGBP1/2, NOVA ((Jensen, Dredge et al. 2000)) and SR proteins ((Hsu, Chen et al. 2011); (Calarco, Superina et al. 2009)).

Model for regulated splicing of TMEM16A exon 6b, 15 and 13

The analysis of its three alternatively spliced exons identify some important *cis*- and *trans*-acting factors involved in their regulation, which in general are not shared by them. Exon 6b inclusion is regulated by a series of exonic and intronic splicing enhancers and silencers and several splicing factors but the key element involved is represented by a strong 16bp long GAA-rich ESE element that interact with the splicing enhancer factor TRA2B. This element was not identified in the other exon. Exon 15 identification relies on ESEs distributed along the entire exon and is regulated by intronic regulatory elements recognized by TIA1 and RbFOX1. Lastly, the peculiar short exon 13 is regulated by RbFOX1 and U2 auxiliary factor 65 (U2AF65).

Based on our analysis we propose a model for WT exon 6b, 15 and 13 splicing regulation (Figure 59). TMEM16A exon 6b WT contain a strong GAA-rich ESE region localized within the exon (Figure 59A). The 16bp long enhancer regulatory element is required for the definition of the TMEM16A WT exon6b, as either its entire, short deletions or when deleted in combination, they induced complete exon skipping (Figure 20B, lane 3 and Figure 29B). The first two enhancer motifs mediates the effect through binding to TRA2B.

Although still at the initial stages, I have been able to determine that TIA1 and FOX1 proteins are important for exon 15 splicing. Indeed, overexpression of FOX1 and TIA1 protein, together with the TMEM16A WT minigene resulted in inclusion of TMEM16A exon 15 in the mature transcript, this was associated with the presence of a Poly-pyrimidine- (Py-) rich and two (T)GCATG motifs downstream of the exon (Figure 59B). In this case even upon overexpression of the FOX1 protein, the inclusion of TMEM16A exon 15 was strongly inhibited when both the two adjacent (T)GCATG motifs where deleted together and also when TIA1 was overexpressed in the mutant where the first and the second Py-rich element were deleted.

TMEM16A exon 13 contains a short weak downstream intronic region, namely (T)GCA, that seems to be indispensable for exon 13 recognition by FOX1 (Figure 59C). Further experiments are needed in order to refine the area of the *cis*-acting elements in exon 13 and 15 as well as the *trans*-acting factors involved. All the direct and circumstantial evidence support the tentative model for the regulation of the three AS exons of TMEM16A presented in figure 60 that takes into account all the experimental evidence collected in this thesis.

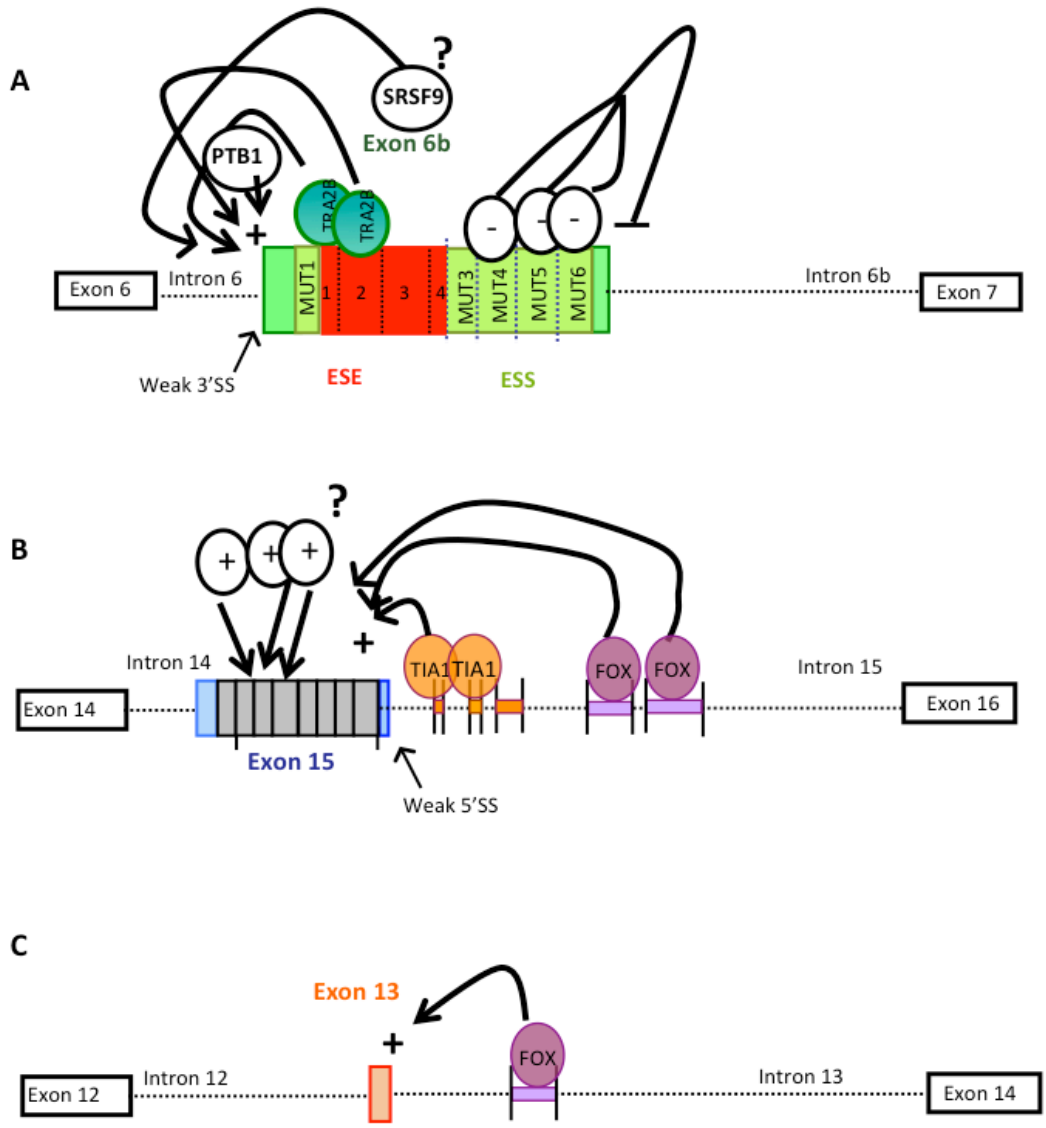

Figure 59. Model for regulated splicing of TMEM16A exon 6b, 13 and 15. *A,* Schematic representation of the *cis*- and *trans*- acting factors identified controlling the inclusion or exclusion of TMEM16A exon 6b. A 16bp long GAA-rich ESE element (red boxes) within the exon and the trans acting factors through which these protein function. *B,* Schematic representation of the *cis*- and *trans*- acting factors identified controlling the inclusion of TMEM16A exon 15. The Two Poly-pyrimidine-rich sequences (orange boxes) located in the intron of exon 15 stimulates TMEM16A exon 15 splicing by the action of TIA1. The increased definition of the TMEM16A exon 15 is also provided by the presence of Fox1 protein binding to the two (T)GCATG motifs (purple boxes). *C,* Schematic representation of *cis*- and *trans*- acting factors identified controlling the inclusion of TMEM16A exon 13 splicing. Exon 13 is regulated by RbFOX1 through the (T)GCA motif downstream the exon (purple boxes).

Evidence that the alternatively spliced exon 6b and 15 of TMEM16A are coordinated: tissue-dependent pattern and changes in breast tumors

Approximately 25% of human genes have more than one alternative spliced region with the possibility to enormously expand the protein diversity through the generation of functionally different isoforms. The presence of multiple splice variants in the same gene, can increase the potential to generate various transcripts and adds an extra layer of complexity to gene regulation. This aspect is rarely considered in the analysis of splicing that normally take into account AS events one by one. Previous bioinformatic studies of EST/cDNA sequences, provide significant evidence for coordination between regions within a single gene ((Peng, Xue et al. 2008); (Xing, Resch et al. 2004); (Fededa, Petrillo et al. 2005)). However, only few cases were verified experimentally (Fededa, Petrillo et al. 2005), and these studies did not address whether multiple exons in the same gene can be coregulated in a tissue-dependent manner, or the extent to which coordination between alternative exons occurs in tumors. In this thesis, I have investigated using a semiquantitative long-range PCR the TMEM16A isoform distribution in normal human and mouse tissues and in breast tumors. In several normal human tissues I observed a non random distribution on TMEM16A mRNA isoforms at the two alternative spliced exons 6b and 15 suggesting a splicing coordination between these two AS events. This analysis showed that exon 6b has a preferential association with transcripts in which exon 15 is skipped and vice versa: 14 out of 20 human adult normal tissues showed splicing coordination (Figure 48 and Figure 49). To understand if the AS coordination is evolutionary conserved I have also evaluated mouse tissues. Unexpectedly, I observed that both the TMEM16A pattern of splicing and isoform expression are not conserved between human and mouse (Figure 53). In addition, as exon 15 is largely excluded in most mouse tissues, it seems that splicing coordination is not occurring in this animal. A previous study did not observed splicing coordination in genetically engineered mice defective in regulated EDA1 splicing of the Fibronectin gene (FN) (Chauhan, Iaconcig et al. 2004) in the majority of tissues. Later, reevaluation of

these mice showed only in kidney a weak coordination and a strong coordination in embryo-derived fibroblasts (Fededa, Petrillo et al. 2005). Unfortunately, data in human normal tissues regarding FN coordination are not available. As TMEM16A splicing coordination seems to be present in human-derived RNA but not mouse tissues, it is possible that specie-specific events are involved. In addition, some differences in the splicing coordination might be a consequence of cell-type or developmental specificities, as previously suggested (Fededa, Petrillo et al. 2005). The mechanisms underlying splicing coordination are largely unknown. Polar effects across two splice sites have been reported before for FN, whereby exon skipping at a site proximal to a gene promoter affects exon skipping at a more distal site ((Fededa, Petrillo et al. 2005); (Fagnani, Barash et al. 2007)). A possible mechanisms underlying the splicing coordination could be induced by PolII elongation, recruitment of specific splicing factors on the PolII and specific chromatin signatures that can affect PolII processitivity (Luco, Pan et al. 2010).

Based on current literature, as reported in the introduction, TMEM16A is associated to several types of tumors, including breast cancer (Duvvuri, Shiwarski et al. 2012). TMEM16A has been associated with increased proliferation ((Kunzelmann 2005); (Ayoub, Wasylyk et al. 2010)). Here, I have investigated both the changes TMEM16A alternative splicing pattern in breast cancer as well as the changes in its splicing coordination. I could not detect any significant difference in the pattern of splicing of individual TMEM16A exons, indicating that breast tumors are not associated with a consistent change in the splicing pattern of this gene (Figure 54). However and unexpectedly, I observed an increase of splicing coordination between exon 6b and exon 15 in breast tumor samples (Figures 55, 56 and 57). Considering the complexity of the basic mechanism proposed to be involved in regulation of splicing coordination (PolII elongation, promoter occupancy and chromatin configuration) (Fededa, Petrillo et al. 2005), I would have expected in tumors a relaxation of this apparently fine-tuned mechanism. What could be the advantage of a tumor cell to maintain an intragenic splicing coordination? It is possible that there is no any specific advantage by the tumor cell to produce a peculiar TMEM16A isoform, but it is possible that during the tumor expansion the cell would maintain active the mechanism involved in

intragenic splicing coordination. This might be not specifically significant for the TMEM16A expression but for splicing of other genes more deeply involved in proliferation or apoptosis of tumor cells. In this context, the maintenance of splicing coordination might be required for preventing a massive transcript alteration that will lead to cell death.

However, in common with the other studies that evaluate coordination ((Fededa, Petrillo et al. 2005); (Johnson, Glauser et al. 2011); (Fagnani, Barash et al. 2007); (Peng, Xue et al. 2008)) a possible limitation in our analysis is represented by the heterogeneity of cell types. This aspect, which is also present in the majority of studies that use total RNA extracted from human samples, might influence the final evaluation of the extend of coordination and would be very difficult to solve experimentally. Even if the advent of massive sequencing technologies (like RNA-SEQ) has allowed rapid the identification and quantification of AS events on a large basis, the study of how the individual AS event in a gene are assembled to generate the possible final transcript isoforms are largely unexplored and available only for very few cases (FN gene, slo-1 gene, Exo70 gene, (Fededa, Petrillo et al. 2005); (Johnson, Glauser et al. 2011); (Fagnani, Barash et al. 2007), respectively). In this context, we cannot exclude that the presence of different cells types expressing diverse TMEM16A isoforms might be responsible of the observed splicing coordination in one half of normal breast tissues. The histological evaluation did not show the presence of tumor cells in these normal samples; however, a variable relative abundance of different cell types (like epithelial, stromal and adypocytes) cannot be excluded. In addition, variable proportion of these cell types are present among normal individuals and largely influenced by the hormonal status. On the other hand, even if a confounding effect of the cellular heterogeneity on splicing coordination might be present, the fact that the expression of the two AS exons 6b and 15 is coordinated in the majority of TMEM16A transcripts derived from tumors (84%) suggest that the cancer progression (or the related clonal expansion) is not associated with a relaxation of this phenomenon. This suggests unexpectedly that the breast tumor cells maintain the ability to coordinate two distant AS events in TMEM16A.

CONCLUSION AND FUTURE DIRECTIONS

The molecular mechanisms behind the AS of TMEM16A exons 6b, 13 and 15 have been investigated and my analysis is consistent with the model depicted in Figure 59 A, B and C. The data collected in this thesis suggest that the TMEM16A exon 6b splicing is regulated primarily by the presence of two proteins SRSF9, TRA2B that function through a unique 16bp long GAA-rich *cis*-acting element. This ESE element was identified mainly by large deletion analysis and further by binding experiments that confirmed the presence of TRA2B factor in this exonic region. In addition, it would be important to explore the potential role of intronic regions, which, might contribute to the splicing regulation. The TMEM16A exon 15 is regulated by TIA1 and FOX1 proteins that function through two distinct intronic splicing enhancers (ISEs) mapped downstream the exon. It will be necessary to better characterize their specific contribution in the regulation of TMEM16A exon 15 splicing. Further experiments will characterize, in more detail the nucleotide composition and the binding properties of these ISE sequences. Furthermore, this study brings some insights into the regulation of the small exon 13, which is specifically regulated by FOX1 and U2AF65. It would be important to study more in detail exon 13 regulation and to explore the potential role of the two proteins that contribute to the splicing regulation acting on an upstream and a downstream region of the exon.

Besides, this study has improved our understanding of TMEM16A splicing coordination with the identification and characterization of a non random distribution of the mRNA isoforms in normal adult human breast tissues and tumor.

Determining the localization of different TMEM16A isoforms within tissues and tumors has important implications with regard to the function of TMEM16A. The functional consequence of TMEM16A channel isoform diversity remains to be determined. We can speculate however, that TMEM16A variants would create channels with altered biophysical properties, such as that reported for exon 6b, 13 and 15 in TMEM16A ((Ferrera, Caputo, Ubby et al. 2009); (Mazzone, Bernard et al.

2011)). TMEM16A channels have been shown to form homodimers ((Fallah, Romer et al. 2011); (Sheridan, Worthington et al. 2011)), therefore, it is likely that TMEM16A variants may interact with each other to form channels with different functional properties. Another possibility is that alternatively spliced isoforms may differently associate with accessory proteins. All these aspects add further complexity to the physiological and pathological role of this important CaCC channel and future studies will be required to better understand the fine regulation of TMEM16A Alternative Splicing.

MATERIALS AND METHODS

Chemical reagents

General chemicals were purchased from Sigma Chemical Co., Merck, Gibco BRL, Boehringer Mannheim, Carlo Erba and Serva.

Standard solutions

All solutions are identified in the text except for the following:

a) TE: 10 mM Tris-HCl (pH 7.4), 1 mM EDTA (pH 7.4)

b) PBS 1X: 137 mM NaCl, 2.7 mM KCl, 10 mM Na2HPO4, 1.8 mM KH2PO4, pH 7.4

c) 10X TBE: 108 g/l Tris, 55 g/l Boric acid, 9.5 g/l EDTA

d) 6X DNA sample buffer: 0.25 % w/v bromophenol blue, 0.25 % w/v xylene cyanol FF, 30 % v/v glycerol in H2O.

e) 5X Running Buffer: 30 g Tris-HCl, 144 g glycine, 5 g SDS in 1L

f) 1X Blotting buffer: 3.03 g Tris-HCl, 14.4 g glycine, 20% methanol in 1L

g) 10X Protein sample buffer: 20 % w/v SDS, 1 M DTT, 0.63 M Tris-HCl (pH 7), 0.2 % w/v bromophenol blue, 20 % v/v glycerol, 10 mM EDTA (pH 7).

h) PBS 1X: 137 mM NaCl, 2.7 mM KCl, 10 mM Na2HPO4, 1.8 mM KH2PO4, pH7.4

DNA preparation

Small scale preparation of plasmid DNA from bacterial cultures.

Single bacterial colony was selected and transferred into 3 ml of LB medium containing the ampicillin in a loosely capped 15-ml tube. The culture was incubated overnight at 37°C with vigorous shaking. Rapid purification of small amounts of recombinant plasmid DNA was performed using the method based on alkaline lysis of recombinant bacteria previously described by Sambrook (Sambrook 1989). Briefly, the bacterial pellet was resuspend in 100 µl of solution I (10 mM EDTA pH 8.0, 25 mM Tris-HCl pH 8.0, 50 mM glucose). Then 200 µl of solution II for lysis (0.2 M NaOH, 1% SDS) was added and the contents mixed by inversion. Lysis was then stopped with 150 µl of solution III for neutralization (60 ml of 5M potassium acetate, 11.5 ml of glacial acetic acid, 28.5 ml H20) and the

content was mixed by inversion. The bacterial lysate was then centrifuged in an Eppendorf microcentrifuge at maximum speed for 5 minutes and the supernatant transferred to a new tube. An equal volume of 1:1 v/v phenol: chloroform solution was added to the supernatant. The tube was then vortexed and centrifuged as above. The step was repeated with aqueous phase and the equal volume of chloroform. The aqueus phase containing DNA was then recovered and the DNA was precipitated by adding 2 volumes of ethanol. The final pellet was resuspended in 47 µl of dH20 with 3 µl of RNase A (Sigma Chemicals Ltd.) from a stock of 20 mg/ml prepared in sterile water and boiled for 10 minutes to destroy trace amounts of DNase activity. The DNA sample was then digested at 37°C for 1 hour in order to eliminate all the RNA from the sample. Routinely, 2-3 µl of such DNA preparation were taken for restriction enzyme digestion and sequence analysis.

Large scale preparation of plasmid DNA from bacterial cultures

Large-scale and pure preparations of plasmid DNA were necessary in order to perform different kind of experiments like transfection, in vitro transcription and vectors/inserts preparation. JetStar purification kit (Genomed) was used according to the manufacturer's instructions. In order to get a good amount of plasmid, we used an overnight bacterial culture of 50 ml in LB medium.

Genomic DNA preparation

Peripheral blood (5 ml) was treated with 20 ml of Lysis Buffer (Sucrose 0.32 M, Tris-HCl 10 mM pH 7.5, MgCl2 5 mM, Triton X-100 1%) and incubated on ice for 15 min. The mix was centrifuged 10 min at 1000 g at 4 °C. The pellet was washed three times with Fisio Buffer (NaCl 0.075 M, EDTA 0.025 M pH 8) and resuspended in 1 ml of Resuspension Buffer (Tris-HCl 10 mM pH 7.5-8, NaCl 0.4 M, EDTA 2 mM). 200 µl of SDS 10% were added and the mixture was incubated at 37 °C overnight to facilitate the extraction. The following day 600 µl of NaCl saturated water solution was added and the samples were mixed for 15 seconds to allow the protein precipitation. The mix was centrifuged 15 min at 1500g to pellet the proteins. The supernatant was recovered and the centrifugation

repeated a second time. Finally, 1 volume of isopropanol was added to the supernatant to precipitate the DNA. Precipitated DNA was removed with a Pasteur, washed in 1 ml of 70% ethanol and resuspended in 500 µl of water. The DNA was then checked by electrophoresis on a 0.8% w/v agarose gel, quantified by spectrophotometer and stored at -20°C until used for PCRs.

RNA preparation from cultured cells

Cultured cells were washed two times with 1X PBS and then RNA TRI reagent, purchased from Ambion, was added according to the manufacturer's instructions. Chloroform extraction was performed and supernatant precipitation was obtained by adding isopropanol. Then we rinsed the pellet in 70% ethanol. The final pellet was resuspended in H20 and stored at -80°C. The RNA quality was checked by electrophoresis on a 1% agarose gel. If it was the case half of the resuspended RNA could be treated with DNase RNase-free (Roche Diagnostic) in 1X DNase buffer. The digest was incubated at 37°C for 30 minutes, and then the RNA was purified by acid phenol extraction and precipitated by adding 2 volumes of ethanol and 1/10 volume of 3M NaOAc pH 5.2. The final pellet was resuspended in H2O and frozen at –80 °C. The RNA quality was checked again by electrophoresis on 1% agarose gels.

Estimation of nucleic acid concentration

The concentration of a DNA or RNA sample can be checked by the use of UV spectrophotometry. Both RNA and DNA absorb UV light very efficiently making it possible to detect and quantify either at low concentrations. The nitrogenous bases in nucleotides have an absorption maximum at about 260 nm. An optical density of 1.0 at 260 nm is usually taken to be equivalent to a concentration of 50 µg/ml for double stranded DNA, 40 µg/ml for single stranded DNA and RNA, and approximately 20 µg/ml for single-stranded oligonucleotide sample. The ratio of the absorbance at 260 nm/ absorbance at 280 nm is a measure of the purity of a sample; it should be 1.8 for pure sample of DNA and 2 for RNA. These values are reduced by protein contamination (Sambrook 1989).

Enzymatic modification of DNA

Restriction enzymes

Restriction enzymes were from New England Biolabs, Inc (USA) or Pharmacia Biotech (Sweden). All buffers were also supplied by the same company and were used according with the manufacturer's instructions. For many analytical digests we also used 0.5X, 1X or 2X concentration of 10x OPA buffer (100 mM Tris-acetate (pH 7.5), 100 mM magnesium acetate and 500 mM potassium acetate). For analytical digests 100-500 ng DNA were digested in a volume of 20 µl containing the appropriate U of the restriction enzyme per µg DNA. The digest was incubated for 2-4 hours at the optimal temperature required by the enzyme used. Preparative digestions of vectors and inserts were made of 5-10 µg DNA using the appropriate condition needed by the restriction enzyme in 100-200 µl reaction volume. Enzymatic activity was then removed either by heat inactivation or by phenol-chloroform extraction.

DNA Polymerase I, Large (Klenow) fragment

Klenow enzyme was used to treat PCR products for blunt-end creation by 3' overhang removal and 3' recessed end fill-in. Briefly the DNA was dissolved in any 1X restriction enzyme NEBuffer or 1X EcoPol Reaction Buffer and supplemented with 33 µM each dNTP if "fill-in" was required (DNA fragments with protruding 3'ends). Then, 1U of Klenow per µg DNA was added and the mixture was incubated 15 minutes at RT. The reaction was inactivated by by heating at 75°C for 20 minutes.

T4 Polynucleotide Kinase

T4 polynucleotide kinase (New England Biolabs Inc) catalyzes the transfer and exchange of phosphate from ATP to the 5´ -hydroxyl terminus of double-and single-stranded DNA and RNA to allow subsequent ligation or end-label for probes production. The proper units of T4 polynucleotide kinase, 1X of its reaction buffer (70 mM Tris-HCl pH 7.6, 10 mM MgCl2, 5 mM dithiothreitol) and ATP were added to the DNA and incubated at 37°C for 30 minutes. The enzyme was inactivated by incubation at 65°C for 20 min.

Calf intestal phosphatase (CIP)

Calf intestal phosphatase (CIP), provided from New England Biolabs Inc, catalyzes the removal of 5´ phosphate groups from DNA and RNA. Since CIP-treated fragments lack the 5´ phosphoryl termini required by ligases, they cannot self-ligate. This property was used to decrease the vector background in cloning strategies. The standard reaction was carried out in a final volume of 50-100 µl using 1U of enzyme per 0.5 µg DNA at 37°C for 1 hour.

T4 DNA ligase

T4 DNA ligase catalyzes the formation of phosphodiester bonds between neighbouring 3´-hydroxyl- and 5´-phosphate ends in double-stranded DNA, requiring ATP as a cofactor in this reaction. This enzyme was purchased from Roche Diagnostic and was used to join double stranded DNA fragments with compatible sticky or blunt ends. A standard reaction comprises 20 ng of linearised vector and 5-10 fold molar excess of insert in a total volume of 20 µl containing 1X ligase buffer and 1U of enzyme. Reactions were carried out at room temperature for at least 2-4 hours. In some ligations synthetic oligonucleotides were used as inserts for the reactions. In these cases, amounts added to each reaction to obtain ligation of the oligonucleotides in the resulting plasmids were about 50-100 fold molar excess over the DNA vector.

Agarose gel electrophoresis of nucleic acid

DNA samples were size fractionated by electrophoresis in agarose gels ranging in concentrations from 0.8 % w/v (large fragments) to 2 % w/v (small fragments). The gels contained ethidium bromide (0.5 µg /ml) and 1X TBE solution. Horizontal gels were used for fast analysis of DNA restriction enzyme digests, estimation of DNA concentration, or DNA fragment separation prior to elution from the gel. A fast analysis of RNA samples was obtained by using a 1% agarose gel. The gels were electrophoresed at 50-80 mA in 1X TBE running buffer for a time depending on the fragment length expected and gel concentration. DNA was visualized by UV transillumination and the result recorded by digital photography.

Elution and purification of DNA fragments from agarose gels

This protocol was used to purify both vectors and inserts of DNA for cloning purpose. The DNA samples were electrophoresed onto an agarose gel as described previously. The DNA was visualized with UV light and the required DNA fragment band was excised from the gel. This slab was cut into pieces, and the QIAquick Gel Extraction Kit was used according to the manufacturer's instructions. Briefly, 3 volumes of Buffer QX1 were added to 1 volume of gel for DNA fragments and then incubated at 50 ˚C for 10 min, vortexing every 5 min. After the gel slice was dissolved completely 1 gel volume of isopropanol was added to the sample. The mixture was loaded into a prepared column and centrifuged at maximum speed for 1 min. The flowthrough was discarded. One washing step was performed using 750 µl of PE buffer. The bound DNA was eluted with 30-50 µl of sterile water. The amount of the recovered DNA was approximately calculated by UV fluorescence of intercalated ethidium bromide in agarose gel electrophoresis.

Amplification of selected DNA fragments

The polymerase chain reaction was performed using both genomic or plasmid DNA as templates and following the basic protocols of Roche Diagnostic Taq DNA polymerase. The volume of the reaction was 50 µl and comprised: 1x Taq buffer, dNTP mix (100 µM each), oligonucleotide primers (100 nM each), Taq DNA polymerase 2.5-5 U and 100 ng of genomic DNA or 0.1 ng of plasmid. All the synthetic DNA oligonucleotides used for PCR amplification were purchased from Sigma Aldrich (http://orders.sigma-genosys.eu.com) or IDT-TEMA (http://eu.idtdna.com/order/order.aspx). The standard amplification conditions were the following: 94°C for 3 min for the initial denaturation, 94°C for 45 s, 54°C for 45 s, 72°C for 45 s for 30 cycles and 72°C for 10 min for the final extension. PCRs were optimized to be in the exponential phase of amplification and products were routinely fractionated in 2% (w/v) agarose gels.When different PCR conditions were used; they are described in each particular case. The amplifications were performed on Cetus DNA Thermal Cycler (Perkin Elmer) or on a Gene Amp PCR System (Applied Biosystem).

Sequence analysis for cloning purpose

Sequence analysis of plasmid DNA was performed using CEQ 2000 sequencer (Beckman Coulter).The plasmid DNA of interest (approximately 500 ng) was purified through a MicroSpin S-400 HR Column (Amersham Pharmacia Biotech). The DNA was then amplified by asymmetric PCR (only one primer) using fluorescent labeled dideoxy nucleotide terminations according to the manufacturers' instructions. The samples were analyzed by loading them into the automatic sequencer.

Bacterial culture

The E.coli DH5α strain was used for ligation transformation, plasmid amplification and growth. The E.coli BL12 DE3 (Novagen) bacteria were used for protein production. Both bacteria strains were maintained in short term as single colonies on agar plates at 4°C and for long term storage on glycerol stocks (sterile glycerol to a final 30 % v/v concentration to liquid bacterial cultures) stored at -80°C. When necessary, from glycerol stocks the bacteria were plated and amplified by an overnight incubation in Luria-Bertani medium (per liter: 10 g Difco Bactotryptone, 5 g Oxid yeast extract, 10 g NaCl, pH 7.5). Bacterial growth media were sterilized before use by autoclaving. Ampicillin (Sigma-Aldrich) was added to media to a final concentration of 100 μg/ml.

Cell culture

The cell line used for transfection and co-transfection experiments of hybrid minigenes were HEK293 cells, human embryonic kidney.

Preparation of bacterial competent cells

Bacterial competent cells of both strains were prepared following the method described by Chung (Chung, Niemela et al. 1989). E.coli strains were grown overnight in 10 ml of LB at 37°C. The following day, 200 ml of fresh LB were added and the cells were grown at room temperature for 2-3 h until the OD600 was 0.3 – 0.4. Then the cells were put in ice and centrifuged at 4°C and 1000 g for 15 minutes. The pellet was resuspended in 1/10 volume of cold 1X TSS solution

(10% v/v PEG, 5% v/v DMSO, 35 mM MgCl2, pH 6.5 in LB medium). The cells were divided into aliquot, rapidly frozen in liquid nitrogen and stored at -80°C. Competent cells efficiency was tested using 0.1 ng of pUC19 control DNA plasmid. Transformation efficiency should be greater than 1 x 106 transformants/µg pUC19 DNA. So the competence was deemed satisfactory if this procedure resulted in more than 100 colonies.

Transformation of bacteria

Transformations of ligation reactions were performed using half of the initial reaction volume. Transformation of positive clones was carried out using 1ng of the DNA plasmid. Briefly the transformation protocol consisted in 30 min of incubation on ice of DNA with 50 µl of competent cells followed by a heat shock at 42°C for 2 minutes. The cells were placed again on ice for 2 minutes and then spread onto agarose plates containing the appropriate antibiotic concentration (100 µg/ml of ampicillin). The plates were incubated for 12-15 hours at 37°C in order to allow the colonies formation. When the DNA inserts were cloned into β-galactosidase-based virgin plasmid (pUC19, Bluscript KS), 30 µl of IPTG 100 mM and 30 µl of X-gal (4% v/v in dimethylformamide) were prepared onto the surface of the agarose before plating to facilitate the screening of positive clones (white colonies) through identification of β-galactosidase activity (blue colonies).

Construction of minigene system

Reporter minigenes used

Transient transfection of minigenes is a commonly used in vivo technique to identify the different features of exon regulation during splicing process. It is a good method to study specific cis-acting elements that control constitutive and alternative exons, the cell-specific splicing pattern and also to identify trans-acting factors that recognize these elements and regulate splicing (Cooper 2005).

A minigene, as its name indicates, is a simplified version of a gene.

In this study, the splicing pattern of the three AS exons of tMEM16A gene has been investigated by using a reporter minigene/splicing-constructs: pTB. The splicing-construct pTB is composed by the alpha-globin exons 1, 2 and 3, and

fibronectin exon 3 under the control of the SV40 promoter within the pBluescript vector backbone (Pagani, Stuani et al. 2003) (Figure 5).

The intronic region between the two fibronectin exons contains a unique NdeI site which facilitates subcloning of an exon with flanking intronic regions.This system allows to insert WT or mutant exons, and study their impact on splicing outcome. In the presence of a WT exon, the splicing pattern of the minigene should be equivalent to that of the endogenous exon in the specific tissue or organ. On the other hand, the presence of mutations may affect pre-mRNA processing, causing aberrant splicing pattern due to exon skipping, intron retention, nonsense-mediated decay (NMD) or activation of cryptic sites. If in presence of a mutation the splicing pattern is not altered, it can be considered as neutral.

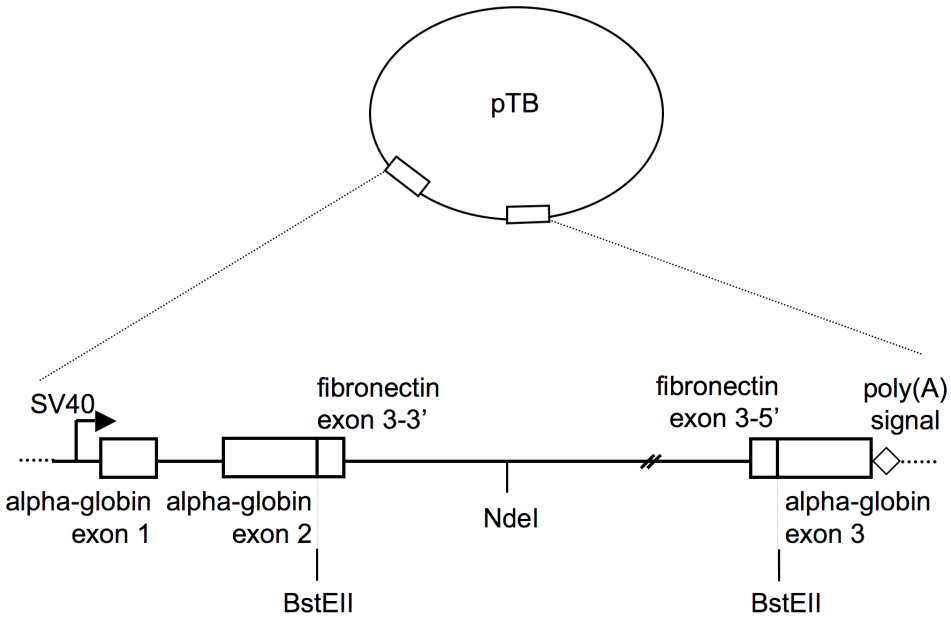

Figure 57. Schematic representation of the reporter minigenes used in this study. pTB reporter minigene. The exons defining the minigenes and the cloning restriction sites are indicated.

Constructs TMEM16A exon 6b, 13 and 15 wild type and mutant in the pTB reporter minigene

The TMEM16A genomic region encompassing exon 6b and adjacent intronic sequences (291 bp of intron 6, full length exon 6b and 298 bp of intron 6) was amplified with ANO1Nde2482Dir and ANO1Nde3117Rev primers carrying the NdeI enzymes restriction sites at their extremities (oligo sequences are reported in appendix in Table 2) and blunt ligated in the SmaI site of pBluscript KS to generate pBS TMEMex6b. Similarly, the last 147 bp of intron 12 along with 307 bp of intron 13 and the full length exon 13 were amplified with ANO1ex13_2595NdeDir and ANO1ex13_3060NdeRev primers carrying the NdeI enzymes restriction sites at their extremities (oligo sequences are reported in appendix in Table 2) and blunt ligated in SmaI site of pBluscript KS to generate pBS TMEMex13. Using the same cloning strategy described above, the TMEM16A genomic region containing full length exon 15, 272 bp of intron 14 and 300 bp of intron 15, was amplified from normal DNA using ANO1ex15_2585NdeDir and ANO1ex15_3197NdeRev primers carrying the NdeI enzymes restriction sites at their extremities (oligo sequences are reported in appendix in Table 2) and blunt ligated in the SmaI site of pBluscript KS to generate TMEMex15. Following sequencing in order to check the nucleotide sequence to be correct, the subcloning in the pTB minigene was performed using the unique enzyme restriction site NdeI; the final minigenes named pTBTMEMex6b, pTBTMEMex13 and pTBTMEMex15 (figure 13). The α-globin, the fibronectin exons and TMEM16A exon 6b, exon 13 and exon 15 are in frame. All the nucleotide substitutions were produced using as PCR template pTB-WT hybrid minigenes (exon 6b, exon 13 and exon 15). The TMEM16A exon 6b, exon 13 and exon 15 intronic deletion mutant minigenes were created by overlapping PCR using suitable primers on pTB ex6b, ex13 and ex15 WT as templates, accordingly. The first round of PCRs was performed using two sets of primers, combining an external primer with an internal one. The external oligonucleotides for exon 6b were ANO1Nde2482Dir and ANO1Nde3117Rev, for exon 13 ANO1ex13_2595NdeDir and ANO1ex13_3060NdeRev and for exon 15 ANO1ex15_2585NdeDir and ANO1ex15_3197NdeRev (Table 2). The internal oligonucleotides carried the

deletions (listed in table 2) and annealed downstream the 5' SS. The second round of PCR was carried out using the external primers and the two amplified products as template, obtained from the previous two separated PCRs. Finally the mutant amplicons were cloned into pTB vector using the *NdeI* restriction site. The identity of all minigene constructs was ultimately confirmed through sequencing analysis.
All pTB exon 6b and exon 15 constructs carrying exonic deletions were synthesized by Genescript Inc. (Piscataway, NJ, USA). They consists of a fragment of approximately 650 bp lacking part of the exon relative to the deletion mutant, cloned into a pUC57 backbone, cloning site: *EcoRV*, using *NdeI* restriction sites. *TMEM16A* exon 6b and 15 mutant *Nde*I-*Nde*I cassettes were taken from pUC57 and subcloned into pTB exon 6b and exon 15. Thus, six exon 6b and nine exon 15 pTB TMEM16A constructs were created: pTB exon 6b MUT1, pTB exon 6b MUT2, pTB exon 6b MUT3, pTB exon 6b MUT4, pTB exon 6b MUT5, pTB exon 6b MUT6 and pTB exon 15 MUT1, pTB exon 15 MUT2, pTB exon 15 MUT3, pTB exon 15 MUT4, pTB exon 15 MUT5, pTB exon 15 MUT6, pTB exon 15 MUT7, pTB exon 15 MUT8 and pTB exon 15 MUT9. Whereas, all pTB exon 6b GAA-rich constructs carrying point, double or complex mutations were generated by site-directed mutagenesis using standard PCR conditions. The DNA fragments containing the exon 6b GAA-rich element modified were generated by PCR reaction using the pTB WT exon 6b minigene reporter as template. In example, for the MUT2-A construct two distinct PCR have been performed, one using the oligos ANO1Nde2482Dir and MUT-A_ex6bmt2E_1aRev and another one using the oligos MUT-A_ex6bmt2E_1aDIR and ANO1Nde3117Rev. Corresponding oligos were used for the other constructs (oligos used for PCR reactions: MUT2-B, MUT2-C, MUT2-D, MUT2-E, MUT2-F, MUT2-G, MUT2-H, MUT2-I, MUT2-L and MUT2-M-Dir and Rev and the external oligos ANO1Nde2482Dir and ANO1Nde3117Rev; oligo sequences are reported in appendix in Table 2).

Maintenance and analysis of cells in culture

HEK293 cells were grown in Dulbecco's Modiefied Eagle Medium (with glutamine, sodium pyruvate, pyriodoxine and 4.5 g/l glucose) supplemented with 10% fetal calf serum (Euro Clone) and antibiotic Antimycotic (Sigma) according to

the manufacturer's instruction. A standard 100mm dish containing a confluent monolayer of cells was washed with 1XPBS solution, treated with 1-2 ml Trypsin (PBS containing 0.045 mM EDTA and 0.1% trypsin) and incubated at 37°C for 2 minutes or until cells were dislodged. After adding 5 ml of media, cells were precipitated by centrifugation and resuspended in pre-warmed medium. 1-2 mL of this cell suspension was added to 10 mL medium in a fresh plate and was gently mixed before incubation.

***In vitro* splicing assay in cell culture**

A total of $3X10^5$ HEK293 cells were seeded in 35mm Petri dishes and grown in DMEM-GlutaMAX-I media (GIBCO) supplemented with 10% fetal bovine serum (EuroClone). After 24 hours, the 80% confluent plates were transfected with 0.5µg of plasmidic DNA using the effectene transfection reagent (Qiagen) according to the manufacturer's protocols. The DNA used for transfections was prepared with JetStar purification kit (Genomed) as previously described. Briefly, 0.5 µg of each *TMEM16A* exon 6b, 13 or 15 minigenes were mixed with 4 µL of Enhancer for each transfection and the mixture was incubated at room temperature for 5 minutes to allow the condensation of the DNA. Then, 5 µL of Effectene were added to the mixture and incubated for 10 minutes. After the addition of 500 µL of complete culture medium the mixture was added to the cells in 1,5 mL of the same medium and incubated at 37°C. Finally, total RNAs were collected after 24 hours using the TRIReagent (Ambion Inc) according to manufacturer's instructions. The RNA quantity was detected using the Nanodrop spectrophotometer instrument (Thermo Scientific) and equal amounts were used for cDNAs synthesis (see "cDNA synthesis and analysis" later in the text). Co-transfections of pTB ex6b, ex13 or ex15 minigenes with plasmid carrying cDNA coding for different proteins were carried out using a 1:1 ratio (i.e., 0.5 µg pTB ex6b WT and 0.5 µg of a protein).

cDNA synthesis and analysis

All the RNAs extracted from the cells were retro-transcribed into cDNAs and subsequently PCR-amplified. The 12µl-volume reaction mixtures composed of 200ng of random primers (Pharmacia), 1mM dNTPs mix (Promega) and 2µg of RNA were denaturated at 94°C for 2 minutes and then chilled on ice. Afterwards specific solutions (Invitrogen) were added to the reaction mix: 10mM DTT, 1X first strand buffer (10mM Tris-HCl ph8.4, 50mM KCL, 2.5mM MgCl2), 200U of MML-V reverse transcriptase enzyme (moloney murine leukemia virus). The final mixture was then incubated at 37°C for 1 hour and 3µl of the retro-transcribed cDNAs were used as PCR template. To amplify only the messengers derived from the pTB plasmid, the primers alpha 2,3-Dir and bra2-Rev were used because specific for the junction between the alfa-globin exons 2-3 and the EDB +1 exon respectively, Table 2. Briefly, the amplification conditions were the following: 94°C for 3 min for the initial denaturation, 94°C for 45 s, 56°C for 45 s, 72°C for 45 s for 30 cycles and 72°C for 10 min for the final extension. Finally the PCR products representing the splicing products were separated on 2% agarose gels and ethidium bromide-stained. Quantification of band intensities in the acquired pictures was performed using the ImageJ64 software (available at http://rsb.info.nih.gov/ij).

Human RNA (First Choice Human Total RNA Survey Panel, Ambion, Inc.) was retrotranscribed in standard conditions and amplified with 803D and 1385R for exon 6b, 1368D and 1525R for exon 13, and 1506D and 1894R for exon 15 primers. In the case of the Intragenic Alternative Splicing Coordination (ISC), the standard PCR was modified. DNA samples were amplified using $803D^{FAM}$ fluorescently labeled and 1894R primers. Briefly, the number of cycles was increased up to 35 using these conditions: 94°C for 3 min for the initial denaturation, 94°C for 45 s, 56°C for 45 s, 72°C for 1 min and 72°C for 10 min for the final extension.

Finally the PCR products representing the splicing products were separated on 2% agarose gels and ethidium bromide-stained. The identity of the resulting splicing products was verified by Capillary electrophoresis analysis (CE).

Capillary electrophoresis analysis

Quantitative analyses of the TMEM16A splicing variants were performed by Capillary electrophoresis (CE) provided by BMR genomics (http://www.bmr-genomics.it/). Quantitation of each mRNA isoforms was based on the principle of RNA-PCR. The relative amount of each mRNA form was calculated based on the corrected integrated area of each peak separated by CE. The use of CE to accurately quantitate PCR products has been normalized by an internal standard. DNA samples were amplified using forward HEX fluorescently labeled primer. RT-PCR product obtained with ANO1_23358Dir ^{HEX} and ANO1_2923Rev primers spans TMEM16A from exon 22 to exon 26, a region encompassing four constitutive exons, following separation by CE, comparing its integrated area with those of the AS exons.

RNA extracted from human adult normal tissues, normal and tumor breast tissues were first amplified using a labelled fluorescent 803Dir primer (FAM) and 1894Rev and then amplified with a labelled fluorescent ANO1_23358Dir primer (HEX) and ANO1_2923Rev. Thus, 1 µL of the PCR product was dehydrated at the temperature of 60°C for 20 min and sent for the CE analysis (oligo sequences are reported in appendix in Table 2).

Human normal and tumor tissue selection

Ductal and Lobular epithelial breast tumors and normal breast samples were kindly provided by Dr. B. Thomann, Clinical Director of General Surgery, "Presidio Ospedaliero di Gorizia, Italy. Normal breast samples were obtained either from mammary reductions of healthy individuals or through mastectomy from patients with matched tumor samples Tumor and normal tissues were obtained from similar age group patients. The ages ranged from 50 to 65 y for both normal and breast cancer tissues. Breast tissue and breast tumors from the same individuals were separated at the time of excision, embedded immediately, and or frozen at -85°C or conserved in RNA Later (Ambion Inc) at – 20°C until use. RNA extraction, RNA quality control, RT-PCR, and capillary electrophoresis were done as previously described for normal adult human tissues, except for the tumor breast RNA samples that had an additional cleaning step (RNeasy; Qiagen).

The RNA quantity was detected using the Nanodrop spectrophotometer instrument (Thermo Scientific) and equal amounts were used for cDNAs synthesis.

Breast tissue and breast tumors were classified according to current histological evaluation (second column), D defined as ductal breast or L defined as lobular breast samples; grading (third column), necrosis (forth column) and receptors (fifth, sixth, seventh and eighth column). ER, estrogen receptor; PgR, progesterone receptor; Ki67, nuclear proliferation marker and HER2, human epidermal growth factor receptor 2 reported in table1). All tissues were collected in accordance with human subjects approval.

Mouse tissues samples collection

All mice were C57BL kindly supplied by Dr. L.J. Gallietta (Head of the Functional Genomic Unit of the laboratory of Molecular Genetics of Gaslini Institute in Genoa, Italy). Total RNA extraction from various murine tissues was accomplished using TRIReagent (Ambion Inc) according to manufacturer's instructions and included an on-column RNA-clean up-DNase treatment step. RNA quality was measured using a Nanodrop spectrophotometer and reverse-transcribed with with 681D and $1602R^{FAM}$ fluorescently labeled primers, that spans TMEM16A from exon6 to exon16, a region encompassing the three alternative exons (oligos are listed in appendix table 2). All samples were stored at −20°C prior to PCR amplification.

***In silico* analysis and predictions**

The bioinformatic analysis, thus the comparative genomic alignments for TMEM16A gene and the identification of the different alternative spliced transcripts were detected using the "Ensembl" website and the "UCSC Genome Browser", (available at http://www.ensembl.org/Homo_sapiens/Info/Index and at http://genome.ucsc.edu/cgi-bin/hgGateway respectively).

The 5'SS consensus values (CVs) were calculated according to the "splice site prediction by neural network" website. (available at http://www.fruitfly.org/seq_tools/splice.html).

In silico analysis of the ESE and ISE sequences were performed using the “ESE-finder”, “RESCUE-ESE” and “PESxs” websites (available at http://rulai.cshl.edu/cgi-bin/tools/ESE3/esefinder.cgi?process=home, http://genes.mit.edu/burgelab/rescue-ese/ and http://cubweb.biology.columbia.edu/pesx/ respectively).

Statistical Analysis

A statistical analysis was performed on the investigated groups of data using the Student's t-test (also known as two-sample t-test) and the Fisher’s exact test, the most common statistical data analysis procedure for hypothesis testing. Specifically, Student's t-test the tested hypothesis was the “null hypothesis” (the hypothesis of “no difference” between two measured phenomena/groups of data) versus and the “alternative hypothesis” (the hypothesis of significant difference between two measured phenomena). For example, in this work for each alternative exons hypothesis tested has been whether there was a significant (not due to chance) difference in the percentage of inclusion of the upstream exon between the presence (i.e. group A) or absence (i.e. group B) of the downstream exon and vice-versa. The p value (probability value) represents the estimated probability of rejecting the null hypothesis and accepting alternative hypothesis. Therefore, if the p value is lower than the chosen significance level, the null hypothesis is rejected and the analyzed data are considered “statistically significant”. Enrichment statistical significance of the two AS exons in TMEM16A gene was evaluated by Fisher's exact test. It is a statistical test used to determine if there are nonrandom associations (contingency) between two categorical variables. Although the choice of significance level is arbitrary, in this case the conventional 5%, 1% and 0.1% levels were used ($p<0.05$ *; $p<0.01$ **; $p<0.001$ ***). In order to perform this test, all the experiments were repeated at least three times since the Student's t-test investigates the null hypothesis of no difference between the means of two normally distributed groups of data.

RNA binding protein analysis

In vitro transcription for pull down analysis

Oligos for *in vitro* transcription were generated by annealing the sense and antisense oligos purchased from IDT (Tema Ricerca), for both WT and MUT2-A, MUT2-E, MUT2-G, MUT2-I mutants exon 6b sequences (listed in table 2). Oligos were then *in vitro* transcribed with T7 RNA Polymerase (Promega) according to standard procedures. Briefly, 2-5 µg of DNA were transcribed using 40 U of T7 RNA polymerase, in the presence of 1X transcription buffer, and 10 mM DTT, both supplied from Promega, 50 U of RNAsi inhibitor and 5 mM each of the four NTPs to a final volume of 100 µl. Following incubation for 2 h at 37°C, the RNA was purified using NICK columns (Amersham Bioscences), precipitated and resuspended in RNAse-free water. Approximately 10 µg of target TMEM16A RNA oligos were placed in 400 µl of reaction mixture (100 mM NaOAC, pH 5.0 and 5mM sodium m-periodate), incubated for 1 h in the dark at room temperature, ethanol-precipitated and finally resuspended in 100 µl of 100 mM NaOAC (pH 5.0). Approx. 400 µl of adipic acid dehydrazide agarose beads 50% slurry (Sigma) previously equilibrated with 100 mM NaOAC (pH 5.2) were added to each periodate-treated RNA and the mix was incubated for 12 h at 4°C on a rotator. The beads with the bound RNA were then washed two times with 1 ml of 2 M NaCl, and equilibrated in 1X washing buffer (5.2 mM HEPES at pH 7.5, 1 mM MgCl2, 0.8 mM MgAcetate). Then the beads were incubated, in a final volume of 500 µl, with 0.5 mg of HeLa cell nuclear extract (C4, Biotech), 1X binding buffer (5.2 mM HEPES, pH 7.9, 1 mM MgCl2, 0.8 mM MgAcetate, 0.52 mM DTT, 3.8% glycerol, 0.75 mM ATP, 1mM GTP) and Heparin (final concentration 2.5-5 µg/µl), for 30 min on a rotator, at room temperature. The beads were then washed four times with 1.5 ml of washing buffer before addition of SDS sample buffer and loading on SDS-10% polyacrylamide gels. Conventional gel SDS PAGE was performed in vertical gels with the required percentage of polyacrylamide (37.5:1 acrylamide:bis-acrylamide, ProtoGel, National Diagnostics), depending on each case. The gels were run at 40 mA in 1X SDS-PAGE running buffer. After running, gels were either stained with coomassie Blue R250 in methanol-water-acetic acid 45:45:10 (v/v/v) for proteins visualizzation or electroblotted onto PVDF

membrane (Amersham Biosciences) for Western Blot analysis. SDS-PAGE gels were then blotted on standard nitrocellulose membrane and incubated in blocking solution (PBS1X, 0.2% Tween, 2% milk) over night. Primary antibodies were incubated with the membrane in the same buffer for 2 hours. Afterwards, the membrane was then washed three times in washing solution (PBS1X, 2%Tween), incubated with the proper HRP-secondary antibodies (anti-mouse/rabbit, Dako) for 1 hour, washed twice and stained with chemiluminescence kit (ECL, Pierce Biotechnology). The primary antibodies that were applied in western blotting analysis are: anti-TRA2B monoclonal antibody (Zymed, 1:3000) and anti-SRproteins monoclonal antibody (Zymed 1:1000).

REFERENCES

Aebi, M., H. Hornig, et al. (1987). "5' cleavage site in eukaryotic pre-mRNA splicing is determined by the overall 5' splice region, not by the conserved 5' GU." Cell **50**(2): 237-246.

Agrawal, S., R. Pilarski, et al. (2005). "Different splicing defects lead to differential effects downstream of the lipid and protein phosphatase activities of PTEN." Human molecular genetics **14**(16): 2459-2468.

Alekseyenko, A. V., N. Kim, et al. (2007). "Global analysis of exon creation versus loss and the role of alternative splicing in 17 vertebrate genomes." RNA **13**(5): 661-670.

Andre, F., S. Michiels, et al. (2009). "Exonic expression profiling of breast cancer and benign lesions: a retrospective analysis." The lancet oncology **10**(4): 381-390.

Andre, S., H. Boukhaddaoui, et al. (2003). "Axotomy-induced expression of calcium-activated chloride current in subpopulations of mouse dorsal root ganglion neurons." Journal of neurophysiology **90**(6): 3764-3773.

Angermann, J. E., A. R. Sanguinetti, et al. (2006). "Mechanism of the inhibition of Ca2+-activated Cl- currents by phosphorylation in pulmonary arterial smooth muscle cells." The Journal of general physiology **128**(1): 73-87.

Aretz, S., S. Uhlhaas, et al. (2004). "Familial adenomatous polyposis: aberrant splicing due to missense or silent mutations in the APC gene." Human mutation **24**(5): 370-380.

Arreola, J., J. E. Melvin, et al. (1998). "Differences in regulation of Ca(2+)-activated Cl- channels in colonic and parotid secretory cells." The American journal of physiology **274**(1 Pt 1): C161-166.

Ashiya, M. and P. J. Grabowski (1997). "A neuron-specific splicing switch mediated by an array of pre-mRNA repressor sites: evidence of a regulatory role for the polypyrimidine tract binding protein and a brain-specific PTB counterpart." RNA **3**(9): 996-1015.

Ayoub, C., C. Wasylyk, et al. (2010). "ANO1 amplification and expression in HNSCC with a high propensity for future distant metastasis and its functions in HNSCC cell lines." British journal of cancer **103**(5): 715-726.

Aznarez, I., Y. Barash, et al. (2008). "A systematic analysis of intronic sequences downstream of 5' splice sites reveals a widespread role for U-rich motifs and TIA1/TIAL1 proteins in alternative splicing regulation." Genome research **18**(8): 1247-1258.

Bader, C. R., D. Bertrand, et al. (1982). "Voltage-activated and calcium-activated currents studied in solitary rod inner segments from the salamander retina." The Journal of physiology **331**: 253-284.

Bai, Y., D. Lee, et al. (1999). "Control of 3' splice site choice in vivo by ASF/SF2 and hnRNP A1." Nucleic Acids Res **27**(4): 1126-1134.

Baralle, M., D. Baralle, et al. (2003). "Identification of a mutation that perturbs NF1 agene splicing using genomic DNA samples and a minigene assay." Journal of medical genetics **40**(3): 220-222.

Barash, Y., J. A. Calarco, et al. (2010). "Deciphering the splicing code." Nature **465**(7294): 53-59.

Barberan-Soler, S., P. Medina, et al. (2011). "Co-regulation of alternative splicing by diverse splicing factors in Caenorhabditis elegans." Nucleic acids research **39**(2): 666-674.

Barish, M. E. (1983). "A transient calcium-dependent chloride current in the immature Xenopus oocyte." The Journal of physiology **342**: 309-325.

Barnard, D. C., J. Li, et al. (2002). "Regulation of alternative splicing by SRrp86 through coactivation and repression of specific SR proteins." Rna **8**(4): 526-533.

Barreau, C., L. Paillard, et al. (2006). "Mammalian CELF/Bruno-like RNA-binding proteins: molecular characteristics and biological functions." Biochimie **88**(5): 515-525.

Batsche, E., M. Yaniv, et al. (2006). "The human SWI/SNF subunit Brm is a regulator of alternative splicing." Nature structural & molecular biology **13**(1): 22-29.

Beck, A. R., Q. G. Medley, et al. (1996). "Structure, tissue distribution and genomic organization of the murine RRM-type RNA binding proteins TIA-1 and TIAR." Nucleic acids research **24**(19): 3829-3835.

Berget, S. M. (1995). "Exon recognition in vertebrate splicing." The Journal of biological chemistry **270**(6): 2411-2414.

Berget, S. M. and P. A. Sharp (1977). "A spliced sequence at the 5'-terminus of adenovirus late mRNA." Brookhaven symposia in biology(29): 332-344.

Berglund, J. A., K. Chua, et al. (1997). "The splicing factor BBP interacts specifically with the pre-mRNA branchpoint sequence UACUAAC." Cell **89**(5): 781-787.

Birney, E., S. Kumar, et al. (1993). "Analysis of the RNA-recognition motif and RS and RGG domains: conservation in metazoan pre-mRNA splicing factors." Nucleic Acids Res **21**(25): 5803-5816.

Black, D. L. (2003). "Mechanisms of alternative pre-messenger RNA splicing." Annual review of biochemistry **72**: 291-336.

Blaustein, M., F. Pelisch, et al. (2005). "Concerted regulation of nuclear and cytoplasmic activities of SR proteins by AKT." Nature structural & molecular biology **12**(12): 1037-1044.

Blencowe, B. J. (2000). "Exonic splicing enhancers: mechanism of action, diversity and role in human genetic diseases." Trends in biochemical sciences **25**(3): 106-110.

Blencowe, B. J. (2006). "Alternative splicing: new insights from global analyses." Cell **126**(1): 37-47.

Bose, J. K., I. F. Wang, et al. (2008). "TDP-43 overexpression enhances exon 7 inclusion during the survival of motor neuron pre-mRNA splicing." J Biol Chem **283**(43): 28852-28859.

Boucher, L., C. A. Ouzounis, et al. (2001). "A genome-wide survey of RS domain proteins." Rna **7**(12): 1693-1701.

Boucher, R. C., E. H. Cheng, et al. (1989). "Chloride secretory response of cystic fibrosis human airway epithelia. Preservation of calcium but not protein kinase C- and A-dependent mechanisms." J Clin Invest **84**(5): 1424-1431.

Boucher, R. C., E. H. Cheng, et al. (1989). "Chloride secretory response of cystic fibrosis human airway epithelia. Preservation of calcium but not protein kinase C- and A-dependent mechanisms." The Journal of clinical investigation **84**(5): 1424-1431.

Bouillet, P. and L. A. O'Reilly (2009). "CD95, BIM and T cell homeostasis." Nature reviews. Immunology **9**(7): 514-519.

Bourgeois, C. F., F. Lejeune, et al. (2004). "Broad specificity of SR (serine/arginine) proteins in the regulation of alternative splicing of pre-messenger RNA." Prog Nucleic Acid Res Mol Biol **78**: 37-88.

Braden, W. A., J. M. Lenihan, et al. (2006). "Distinct action of the retinoblastoma pathway on the DNA replication machinery defines specific roles for cyclin-dependent kinase complexes in prereplication complex assembly and S-phase progression." Molecular and cellular biology **26**(20): 7667-7681.

Buratti, E., C. Stuani, et al. (2007). "SR protein-mediated inhibition of CFTR exon 9 inclusion: molecular characterization of the intronic splicing silencer." Nucleic Acids Res **35**(13): 4359-4368.

Burd, C. G. and G. Dreyfuss (1994). "RNA binding specificity of hnRNP A1: significance of hnRNP A1 high-affinity binding sites in pre-mRNA splicing." The EMBO journal **13**(5): 1197-1204.

Burd, C. J., C. E. Petre, et al. (2006). "Cyclin D1b variant influences prostate cancer growth through aberrant androgen receptor regulation." Proceedings of the National Academy of Sciences of the United States of America **103**(7): 2190-2195.

Buvoli, M., F. Cobianchi, et al. (1992). "Interaction of hnRNP A1 with snRNPs and pre-mRNAs: evidence for a possible role of A1 RNA annealing activity in the first steps of spliceosome assembly." Nucleic acids research **20**(19): 5017-5025.

Caceres, J. F., S. Stamm, et al. (1994). "Regulation of alternative splicing in vivo by overexpression of antagonistic splicing factors." Science **265**(5179): 1706-1709.

Calarco, J. A., Y. Xing, et al. (2007). "Global analysis of alternative splicing differences between humans and chimpanzees." Genes & development **21**(22): 2963-2975.

Calarco, J. A., S. Superina, et al. (2009). "Regulation of vertebrate nervous system alternative splicing and development by an SR-related protein." Cell **138**(5): 898-910.

Caputi, M. and A. M. Zahler (2002). "SR proteins and hnRNP H regulate the splicing of the HIV-1 tev-specific exon 6D." Embo J **21**(4): 845-855.

Caputo, A., E. Caci, et al. (2008). "TMEM16A, a membrane protein associated with calcium-dependent chloride channel activity." Science **322**(5901): 590-594.

Carles, A., R. Millon, et al. (2006). "Head and neck squamous cell carcinoma transcriptome analysis by comprehensive validated differential display." Oncogene **25**(12): 1821-1831.

Cartegni, L., S. L. Chew, et al. (2002). "Listening to silence and understanding nonsense: exonic mutations that affect splicing." Nat Rev Genet **3**(4): 285-298.

Cartegni, L. and A. R. Krainer (2002). "Disruption of an SF2/ASF-dependent exonic splicing enhancer in SMN2 causes spinal muscular atrophy in the absence of SMN1." Nature genetics **30**(4): 377-384.

Cartegni, L., M. Maconi, et al. (1996). "hnRNP A1 selectively interacts through its Gly-rich domain with different RNA-binding proteins." Journal of molecular biology **259**(3): 337-348.

Cascino, I., G. Fiucci, et al. (1995). "Three functional soluble forms of the human apoptosis-inducing Fas molecule are produced by alternative splicing." Journal of immunology **154**(6): 2706-2713.

Castle, J. C., C. Zhang, et al. (2008). "Expression of 24,426 human alternative splicing events and predicted cis regulation in 48 tissues and cell lines." Nature genetics **40**(12): 1416-1425.

Celotto, A. M. and B. R. Graveley (2001). "Alternative splicing of the Drosophila Dscam pre-mRNA is both temporally and spatially regulated." Genetics **159**(2): 599-608.

Chan, R. C. and D. L. Black (1997). "Conserved intron elements repress splicing of a neuron-specific c-src exon in vitro." Molecular and cellular biology **17**(5): 2970.

Chang, W. C., H. H. Chen, et al. (2008). "Alternative splicing of U12-type introns." Frontiers in bioscience : a journal and virtual library **13**: 1681-1690.

Charlet, B. N., P. Logan, et al. (2002). "Dynamic antagonism between ETR-3 and PTB regulates cell type-specific alternative splicing." Molecular cell **9**(3): 649-658.

Chasin, L. A. (2007). "Searching for splicing motifs." Advances in experimental medicine and biology **623**: 85-106.

Chauhan, A. K., A. Iaconcig, et al. (2004). "Alternative splicing of fibronectin: a mouse model demonstrates the identity of in vitro and in vivo systems and the processing autonomy of regulated exons in adult mice." Gene **324**: 55-63.

Chen, C. D., R. Kobayashi, et al. (1999). "Binding of hnRNP H to an exonic splicing silencer is involved in the regulation of alternative splicing of the rat beta-tropomyosin gene." Genes & development **13**(5): 593-606.

Chen, L. L., M. Sabripour, et al. (2005). "A mutation-created novel intra-exonic pre-mRNA splice site causes constitutive activation of KIT in human gastrointestinal stromal tumors." Oncogene **24**(26): 4271-4280.

Chen, M. and J. L. Manley (2009). "Mechanisms of alternative splicing regulation: insights from molecular and genomics approaches." Nature reviews. Molecular cell biology **10**(11): 741-754.

Cheng, C. and P. A. Sharp (2006). "Regulation of CD44 alternative splicing by SRm160 and its potential role in tumor cell invasion." Molecular and cellular biology **26**(1): 362-370.

Chou, M. Y., N. Rooke, et al. (1999). "hnRNP H is a component of a splicing enhancer complex that activates a c-src alternative exon in neuronal cells." Molecular and cellular biology **19**(1): 69-77.

Chung, C. T., S. L. Niemela, et al. (1989). "One-step preparation of competent Escherichia coli: transformation and storage of bacterial cells in the same solution." Proc Natl Acad Sci U S A **86**(7): 2172-2175.

Clarke, L. L., B. R. Grubb, et al. (1994). "Relationship of a non-cystic fibrosis transmembrane conductance regulator-mediated chloride conductance to organ-level disease in Cftr(-/-) mice." Proc Natl Acad Sci U S A **91**(2): 479-483.

Clery, A., S. Jayne, et al. (2011). "Molecular basis of purine-rich RNA recognition by the human SR-like protein Tra2-beta1." Nature structural & molecular biology **18**(4): 443-450.

Cohen, J. B. and A. D. Levinson (1988). "A point mutation in the last intron responsible for increased expression and transforming activity of the c-Ha-ras oncogene." Nature **334**(6178): 119-124.

Collesi, C., M. M. Santoro, et al. (1996). "A splicing variant of the RON transcript induces constitutive tyrosine kinase activity and an invasive phenotype." Molecular and cellular biology **16**(10): 5518-5526.

Cooper, T. A. (2005). "Use of minigene systems to dissect alternative splicing elements." Methods **37**(4): 331-340.

Cramer, P., J. F. Caceres, et al. (1999). "Coupling of transcription with alternative splicing: RNA pol II promoters modulate SF2/ASF and 9G8 effects on an exonic splicing enhancer." Molecular cell **4**(2): 251-258.

Das, R., K. Dufu, et al. (2006). "Functional coupling of RNAP II transcription to spliceosome assembly." Genes & development **20**(9): 1100-1109.

Das, R., J. Yu, et al. (2007). "SR proteins function in coupling RNAP II transcription to pre-mRNA splicing." Molecular cell **26**(6): 867-881.

Das, S., Y. Hahn, et al. (2008). "Topology of NGEP, a prostate-specific cell:cell junction protein widely expressed in many cancers of different grade level." Cancer research **68**(15): 6306-6312.

David, C. J. and J. L. Manley (2008). "The search for alternative splicing regulators: new approaches offer a path to a splicing code." Genes Dev **22**(3): 279-285.

Davis, A. J., A. S. Forrest, et al. (2010). "Expression profile and protein translation of TMEM16A in murine smooth muscle." American journal of physiology. Cell physiology **299**(5): C948-959.

Del Gatto, F., M. C. Gesnel, et al. (1996). "The exon sequence TAGG can inhibit splicing." Nucleic acids research **24**(11): 2017-2021.

Del Gatto-Konczak, F., C. F. Bourgeois, et al. (2000). "The RNA-binding protein TIA-1 is a novel mammalian splicing regulator acting through intron sequences adjacent to a 5' splice site." Molecular and cellular biology **20**(17): 6287-6299.

Delaney, S. J., D. P. Rich, et al. (1993). "Cystic fibrosis transmembrane conductance regulator splice variants are not conserved and fail to produce chloride channels." Nat Genet **4**(4): 426-431.

Dempsey, L. A., H. Sun, et al. (1999). "G4 DNA binding by LR1 and its subunits, nucleolin and hnRNP D, A role for G-G pairing in immunoglobulin switch recombination." The Journal of biological chemistry **274**(2): 1066-1071.

Dominski, Z. and R. Kole (1991). "Selection of splice sites in pre-mRNAs with short internal exons." Mol Cell Biol **11**(12): 6075-6083.

Donaldson, J., A. M. Brown, et al. (1989). "Temporal changes in the calcium-dependence of the histamine H1-receptor-stimulation of cyclic AMP accumulation in guinea-pig cerebral cortex." Br J Pharmacol **98**(4): 1365-1375.

Dreumont, N., S. Hardy, et al. (2010). "Antagonistic factors control the unproductive splicing of SC35 terminal intron." Nucleic acids research **38**(4): 1353-1366.

Dreyfuss, G., V. N. Kim, et al. (2002). "Messenger-RNA-binding proteins and the messages they carry." Nat Rev Mol Cell Biol **3**(3): 195-205.

Dreyfuss, G., M. J. Matunis, et al. (1993). "hnRNP proteins and the biogenesis of mRNA." Annu Rev Biochem **62**: 289-321.

Dreyfuss, G., M. J. Matunis, et al. (1993). "hnRNP proteins and the biogenesis of mRNA." Annual review of biochemistry **62**: 289-321.

Droin, N., F. Bichat, et al. (2001). "Involvement of caspase-2 long isoform in Fas-mediated cell death of human leukemic cells." Blood **97**(6): 1835-1844.

Duran, C., C. H. Thompson, et al. (2010). "Chloride channels: often enigmatic, rarely predictable." Annual review of physiology **72**: 95-121.

Dujardin, G., E. Buratti, et al. (2010). "CELF proteins regulate CFTR pre-mRNA splicing: essential role of the divergent domain of ETR-3." Nucleic acids research **38**(20): 7273-7285.

Duvvuri, U., D. J. Shiwarski, et al. (2012). "TMEM16A Induces MAPK and Contributes Directly to Tumorigenesis and Cancer Progression." Cancer research.

Elliott, D. J., K. Oghene, et al. (1998). "Dynamic changes in the subnuclear organisation of pre-mRNA splicing proteins and RBM during human germ cell development." Journal of cell science **111 (Pt 9)**: 1255-1265.

Espinosa, I., C. H. Lee, et al. (2008). "A novel monoclonal antibody against DOG1 is a sensitive and specific marker for gastrointestinal stromal tumors." The American journal of surgical pathology **32**(2): 210-218.

Esperante, S. A., C. M. Rivolta, et al. (2008). "Identification and characterization of new variants of three associated SNPs and a microsatellite in the TSH receptor gene which are useful for genetic studies." Molecular and cellular probes **22**(5-6): 281-286.

Eversole, A. and N. Maizels (2000). "In vitro properties of the conserved mammalian protein hnRNP D suggest a role in telomere maintenance." Molecular and cellular biology **20**(15): 5425-5432.

Fagnani, M., Y. Barash, et al. (2007). "Functional coordination of alternative splicing in the mammalian central nervous system." Genome biology **8**(6): R108.

Fallah, G., T. Romer, et al. (2011). "TMEM16A(a)/anoctamin-1 shares a homodimeric architecture with CLC chloride channels." Molecular & cellular proteomics : MCP **10**(2): M110 004697.

Faustino, N. A. and T. A. Cooper (2005). "Identification of putative new splicing targets for ETR-3 using sequences identified by systematic evolution of ligands by exponential enrichment." Molecular and cellular biology **25**(3): 879-887.

Fededa, J. P., E. Petrillo, et al. (2005). "A polar mechanism coordinates different regions of alternative splicing within a single gene." Mol Cell **19**(3): 393-404.

Feeney, R. J. and G. W. Zieve (1990). "Nuclear exchange of the U1 and U2 snRNP-specific proteins." The Journal of cell biology **110**(4): 871-881.

Ferrera, L., A. Caputo, et al. (2009). "Regulation of TMEM16A chloride channel properties by alternative splicing." The Journal of biological chemistry **284**(48): 33360-33368.

Fiset, S. and B. Chabot (2001). "hnRNP A1 may interact simultaneously with telomeric DNA and the human telomerase RNA in vitro." Nucleic acids research **29**(11): 2268-2275.

Fisette, J. F., J. Toutant, et al. (2010). "hnRNP A1 and hnRNP H can collaborate to modulate 5' splice site selection." RNA **16**(1): 228-238.

Fogel, B. L., E. Wexler, et al. (2012). "RBFOX1 regulates both splicing and transcriptional networks in human neuronal development." Human molecular genetics.

Forch, P., O. Puig, et al. (2000). "The apoptosis-promoting factor TIA-1 is a regulator of alternative pre- mRNA splicing." Mol Cell **6**(5): 1089-1098.

Forch, P., O. Puig, et al. (2002). "The splicing regulator TIA-1 interacts with U1-C to promote U1 snRNP recruitment to 5' splice sites." The EMBO journal **21**(24): 6882-6892.

Fox-Walsh, K. L. and K. J. Hertel (2009). "Splice-site pairing is an intrinsically high fidelity process." Proceedings of the National Academy of Sciences of the United States of America **106**(6): 1766-1771.

Fu, X. D. (1995). "The superfamily of arginine/serine-rich splicing factors." RNA **1**(7): 663-680.

Gabriel, S. E., M. Makhlina, et al. (2000). "Permeabilization via the P2X7 purinoreceptor reveals the presence of a Ca2+-activated Cl- conductance in the apical membrane of murine tracheal epithelial cells." J Biol Chem **275**(45): 35028-35033.

Galietta, L. J. (2009). "The TMEM16 protein family: a new class of chloride channels?" Biophysical journal **97**(12): 3047-3053.

Galindo, B. E. and V. D. Vacquier (2005). "Phylogeny of the TMEM16 protein family: some members are overexpressed in cancer." International journal of molecular medicine **16**(5): 919-924.

Gallego, M. E., R. Gattoni, et al. (1997). "The SR splicing factors ASF/SF2 and SC35 have antagonistic effects on intronic enhancer-dependent splicing of the beta-tropomyosin alternative exon 6A." Embo J **16**(7): 1772-1784.

Gallo, J. M. and C. Spickett (2010). "The role of CELF proteins in neurological disorders." RNA biology **7**(4): 474-479.

Garcia-Blanco, M. A., S. F. Jamison, et al. (1989). "Identification and purification of a 62,000-dalton protein that binds specifically to the polypyrimidine tract of introns." Genes & development **3**(12A): 1874-1886.

Garcia-Blanco, M. A., A. P. Baraniak, et al. (2004). "Alternative splicing in disease and therapy." Nature biotechnology **22**(5): 535-546.

Ghigna, C., S. Giordano, et al. (2005). "Cell motility is controlled by SF2/ASF through alternative splicing of the Ron protooncogene." Molecular cell **20**(6): 881-890.

Gooding, C., F. Clark, et al. (2006). "A class of human exons with predicted distant branch points revealed by analysis of AG dinucleotide exclusion zones." Genome biology **7**(1): R1.

Graveley, B. R. (2000). "Sorting out the complexity of SR protein functions." RNA **6**(9): 1197-1211.

Graveley, B. R. (2001). "Alternative splicing: increasing diversity in the proteomic world." Trends in genetics : TIG **17**(2): 100-107.

Gromak, N., A. J. Matlin, et al. (2003). "Antagonistic regulation of alpha-actinin alternative splicing by CELF proteins and polypyrimidine tract binding protein." RNA **9**(4): 443-456.

Guil, S., R. Gattoni, et al. (2003). "Roles of hnRNP A1, SR proteins, and p68 helicase in c-H-ras alternative splicing regulation." Molecular and cellular biology **23**(8): 2927-2941.

Gunderson, S. I., K. Beyer, et al. (1994). "The human U1A snRNP protein regulates polyadenylation via a direct interaction with poly(A) polymerase." Cell **76**(3): 531-541.

Guo, D., L. Young, et al. (2008). "Calcium-activated chloride current contributes to action potential alternations in left ventricular hypertrophy rabbit." American journal of physiology. Heart and circulatory physiology **295**(1): H97-H104.

Habelhah, H., K. Shah, et al. (2001). "ERK phosphorylation drives cytoplasmic accumulation of hnRNP-K and inhibition of mRNA translation." Nature cell biology **3**(3): 325-330.

Han, K., G. Yeo, et al. (2005). "A combinatorial code for splicing silencing: UAGG and GGGG motifs." PLoS Biol **3**(5): e158.

Hartzell, C., I. Putzier, et al. (2005). "Calcium-activated chloride channels." Annual review of physiology **67**: 719-758.

Hartzell, H. C., Z. Qu, et al. (2008). "Molecular physiology of bestrophins: multifunctional membrane proteins linked to best disease and other retinopathies." Physiological reviews **88**(2): 639-672.

Hawkins, J. D. (1988). "A survey on intron and exon lengths." Nucleic Acids Res **16**(21): 9893-9908.

Herrlich, P., H. Morrison, et al. (2000). "CD44 acts both as a growth- and invasiveness-promoting molecule and as a tumor-suppressing cofactor." Annals of the New York Academy of Sciences **910**: 106-118; discussion 118-120.

Hertel, K. J. (2008). "Combinatorial control of exon recognition." The Journal of biological chemistry **283**(3): 1211-1215.

Hiller, M., K. Huse, et al. (2005). "Creation and disruption of protein features by alternative splicing -- a novel mechanism to modulate function." Genome biology **6**(7): R58.

Ho, L. L., X. Wei, et al. (2010). "Mob as tumor suppressor is activated at the cell membrane to control tissue growth and organ size in Drosophila." Developmental biology **337**(2): 274-283.

Ho, T. H., B. N. Charlet, et al. (2004). "Muscleblind proteins regulate alternative splicing." The EMBO journal **23**(15): 3103-3112.

Hocine, S., R. H. Singer, et al. (2010). "RNA processing and export." Cold Spring Harbor perspectives in biology **2**(12): a000752.

Hoek, K. S., G. J. Kidd, et al. (1998). "hnRNP A2 selectively binds the cytoplasmic transport sequence of myelin basic protein mRNA." Biochemistry **37**(19): 7021-7029.

Hofmann, Y., C. L. Lorson, et al. (2000). "Htra2-beta 1 stimulates an exonic splicing enhancer and can restore full-length SMN expression to survival motor neuron 2 (SMN2)." Proc Natl Acad Sci U S A **97**(17): 9618-9623.

Hofmann, Y. and B. Wirth (2002). "hnRNP-G promotes exon 7 inclusion of survival motor neuron (SMN) via direct interaction with Htra2-beta1." Hum Mol Genet **11**(17): 2037-2049.

Holste, D., G. Huo, et al. (2006). "HOLLYWOOD: a comparative relational database of alternative splicing." Nucleic acids research **34**(Database issue): D56-62.

House, A. E. and K. W. Lynch (2008). "Regulation of alternative splicing: more than just the ABCs." The Journal of biological chemistry **283**(3): 1217-1221.

Hsu, S. Y., Y. J. Chen, et al. (2011). “Pnn and SR family proteins are differentially expressed in mouse central nervous system.” Histochem Cell Biology **135**(4):361-73.

Huang, C. S., C. Y. Shen, et al. (2007). "Increased expression of SRp40 affecting CD44 splicing is associated with the clinical outcome of lymph node metastasis in human breast cancer." Clinica chimica acta; international journal of clinical chemistry **384**(1-2): 69-74.

Huang, F., J. R. Rock, et al. (2009). "Studies on expression and function of the TMEM16A calcium-activated chloride channel." Proceedings of the National Academy of Sciences of the United States of America **106**(50): 21413-21418.

Huang, P., J. Liu, et al. (2001). "Regulation of human CLC-3 channels by multifunctional Ca2+/calmodulin-dependent protein kinase." The Journal of biological chemistry **276**(23): 20093-20100.

Huang, X., T. E. Godfrey, et al. (2006). "Comprehensive genome and transcriptome analysis of the 11q13 amplicon in human oral cancer and synteny to the 7F5 amplicon in murine oral carcinoma." Genes, chromosomes & cancer **45**(11): 1058-1069.

Huang, X., S. M. Gollin, et al. (2002). "High-resolution mapping of the 11q13 amplicon and identification of a gene, TAOS1, that is amplified and

overexpressed in oral cancer cells." Proceedings of the National Academy of Sciences of the United States of America **99**(17): 11369-11374.

Hui, J., L. H. Hung, et al. (2005). "Intronic CA-repeat and CA-rich elements: a new class of regulators of mammalian alternative splicing." The EMBO journal **24**(11): 1988-1998.

Hung, L. H., M. Heiner, et al. (2008). "Diverse roles of hnRNP L in mammalian mRNA processing: a combined microarray and RNAi analysis." RNA **14**(2): 284-296.

Hwang, S. J., P. J. Blair, et al. (2009). "Expression of anoctamin 1/TMEM16A by interstitial cells of Cajal is fundamental for slow wave activity in gastrointestinal muscles." The Journal of physiology **587**(Pt 20): 4887-4904.

Ibrahim el, C., T. D. Schaal, et al. (2005). "Serine/arginine-rich protein-dependent suppression of exon skipping by exonic splicing enhancers." Proc Natl Acad Sci U S A **102**(14): 5002-5007.

Irimia, M., D. Penny, et al. (2007). "Coevolution of genomic intron number and splice sites." Trends in genetics : TIG **23**(7): 321-325.

Iseni, F., D. Garcin, et al. (2002). "Sendai virus trailer RNA binds TIAR, a cellular protein involved in virus-induced apoptosis." The EMBO journal **21**(19): 5141-5150.

Izaurralde, E., J. Lewis, et al. (1994). "A nuclear cap binding protein complex involved in pre-mRNA splicing." Cell **78**(4): 657-668.

Izquierdo, J. M., N. Majos, et al. (2005). "Regulation of Fas alternative splicing by antagonistic effects of TIA-1 and PTB on exon definition." Molecular cell **19**(4): 475-484.

Izquierdo, J. M. and J. Valcarcel (2006). "A simple principle to explain the evolution of pre-mRNA splicing." Genes & development **20**(13): 1679-1684.

Jantsch, M. F. and J. G. Gall (1992). "Assembly and localization of the U1-specific snRNP C protein in the amphibian oocyte." The Journal of cell biology **119**(5): 1037-1046.

Jensen, K. B., B. K. Dredge, et al. (2000). "Nova-1 regulates neuron-specific alternative splicing and is essential for neuronal viability." Neuron **25**(2): 359-371.

Jentsch, T. J., V. Stein, et al. (2002). "Molecular structure and physiological function of chloride channels." Physiological reviews **82**(2): 503-568.

Jiang, Z. H., W. J. Zhang, et al. (1998). "Regulation of Ich-1 pre-mRNA alternative splicing and apoptosis by mammalian splicing factors." Proceedings of the National Academy of Sciences of the United States of America **95**(16): 9155-9160.

Jin, Y., H. Suzuki, et al. (2003). "A vertebrate RNA-binding protein Fox-1 regulates tissue-specific splicing via the pentanucleotide GCAUG." The EMBO journal **22**(4): 905-912.

Jo, O. D., J. Martin, et al. (2008). "Heterogeneous nuclear ribonucleoprotein A1 regulates cyclin D1 and c-myc internal ribosome entry site function through Akt signaling." The Journal of biological chemistry **283**(34): 23274-23287.

Joeng, K. S., E. J. Song, et al. (2004). "Long lifespan in worms with long telomeric DNA." Nature genetics **36**(6): 607-611.

Johnson, B. E., D. A. Glauser, et al. (2011). "Alternatively spliced domains interact to regulate BK potassium channel gating." Proceedings of the National Academy of Sciences of the United States of America **108**(51): 20784-20789.

Johnson, J. M., J. Castle, et al. (2003). "Genome-wide survey of human alternative pre-mRNA splicing with exon junction microarrays." Science **302**(5653): 2141-2144.

Kadener, S., J. P. Fededa, et al. (2002). "Regulation of alternative splicing by a transcriptional enhancer through RNA pol II elongation." Proceedings of the National Academy of Sciences of the United States of America **99**(12): 8185-8190.

Kalnina, Z., P. Zayakin, et al. (2005). "Alterations of pre-mRNA splicing in cancer." Genes, chromosomes & cancer **42**(4): 342-357.

Kambach, C. and I. W. Mattaj (1994). "Nuclear transport of the U2 snRNP-specific U2B'' protein is mediated by both direct and indirect signalling mechanisms." Journal of cell science **107 (Pt 7)**: 1807-1816.

Kanopka, A., O. Muhlemann, et al. (1996). "Inhibition by SR proteins of splicing of a regulated adenovirus pre-mRNA." Nature **381**(6582): 535-538.

Karni, R., E. de Stanchina, et al. (2007). "The gene encoding the splicing factor SF2/ASF is a proto-oncogene." Nature structural & molecular biology **14**(3): 185-193.

Karni, R., Y. Hippo, et al. (2008). "The splicing-factor oncoprotein SF2/ASF activates mTORC1." Proceedings of the National Academy of Sciences of the United States of America **105**(40): 15323-15327.

Kartner, N., J. W. Hanrahan, et al. (1991). "Expression of the cystic fibrosis gene in non-epithelial invertebrate cells produces a regulated anion conductance." Cell **64**(4): 681-691.

Kashima, T., N. Rao, et al. (2007). "hnRNP A1 functions with specificity in repression of SMN2 exon 7 splicing." Hum Mol Genet **16**(24): 3149-3159.

Kashima, T., N. Rao, et al. (2007). "hnRNP A1 functions with specificity in repression of SMN2 exon 7 splicing." Human molecular genetics **16**(24): 3149-3159.

Kashima, T., N. Rao, et al. (2007). "An intronic element contributes to splicing repression in spinal muscular atrophy." Proc Natl Acad Sci U S A **104**(9): 3426-3431.

Kawai, T., A. Lal, et al. (2006). "Translational control of cytochrome c by RNA-binding proteins TIA-1 and HuR." Molecular and cellular biology **26**(8): 3295-3307.

Kedersha, N. L., M. Gupta, et al. (1999). "RNA-binding proteins TIA-1 and TIAR link the phosphorylation of eIF-2 alpha to the assembly of mammalian stress granules." The Journal of cell biology **147**(7): 1431-1442.

Keren, H., G. Lev-Maor, et al. (2010). "Alternative splicing and evolution: diversification, exon definition and function." Nature reviews. Genetics **11**(5): 345-355.

Kessler, M. M., M. F. Henry, et al. (1997). "Hrp1, a sequence-specific RNA-binding protein that shuttles between the nucleus and the cytoplasm, is required for mRNA 3'-end formation in yeast." Genes & development **11**(19): 2545-2556.

Kiessling, A., B. Weigle, et al. (2005). "D-TMPP: a novel androgen-regulated gene preferentially expressed in prostate and prostate cancer that is the first characterized member of an eukaryotic gene family." The Prostate **64**(4): 387-400.

Kim, H. S., Y. Kuwano, et al. (2007). "Elucidation of a C-rich signature motif in target mRNAs of RNA-binding protein TIAR." Molecular and cellular biology **27**(19): 6806-6817.

Kitevska, T., D. M. Spencer, et al. (2009). "Caspase-2: controversial killer or checkpoint controller?" Apoptosis : an international journal on programmed cell death **14**(7): 829-848.

Klausen, T. K., A. Bergdahl, et al. (2007). "Cell cycle-dependent activity of the volume- and Ca2+-activated anion currents in Ehrlich lettre ascites cells." Journal of cellular physiology **210**(3): 831-842.

Knowles, M. R., L. L. Clarke, et al. (1991). "Activation by extracellular nucleotides of chloride secretion in the airway epithelia of patients with cystic fibrosis." N Engl J Med **325**(8): 533-538.

Knowles, M. R., L. L. Clarke, et al. (1992). "Extracellular ATP and UTP induce chloride secretion in nasal epithelia of cystic fibrosis patients and normal subjects in vivo." Chest **101**(3 Suppl): 60S-63S.

Kohler, A. and E. Hurt (2007). "Exporting RNA from the nucleus to the cytoplasm." Nature reviews. Molecular cell biology **8**(10): 761-773.

Konarska, M. M., J. Vilardell, et al. (2006). "Repositioning of the reaction intermediate within the catalytic center of the spliceosome." Molecular cell **21**(4): 543-553.

Kondera-Anasz, Z., A. Mielczarek-Palacz, et al. (2005). "Soluble Fas receptor and soluble Fas ligand in the serum of women with uterine tumors." Apoptosis : an international journal on programmed cell death **10**(5): 1143-1149.

Koonin, E. V. (2001). "Computational genomics." Current biology : CB **11**(5): R155-158.

Koren, E., G. Lev-Maor, et al. (2007). "The emergence of alternative 3' and 5' splice site exons from constitutive exons." PLoS computational biology **3**(5): e95.

Kuroyanagi, H. (2009). "Fox-1 family of RNA-binding proteins." Cellular and molecular life sciences : CMLS **66**(24): 3895-3907.

Kramer, A. (1996). "The structure and function of proteins involved in mammalian pre-mRNA splicing." Annu Rev Biochem **65**: 367-409.

Kramer, J. and R. S. Hawley (2003). "The spindle-associated transmembrane protein Axs identifies a membranous structure ensheathing the meiotic spindle." Nature cell biology **5**(3): 261-263.

Kumar, A., M. Kumar, et al. (2009). "Molecular mechanisms of ginsenoside Rp1-mediated growth arrest and apoptosis." International journal of molecular medicine **24**(3): 381-386.

Kunzelmann, K. (2005). "Ion channels and cancer." The Journal of membrane biology **205**(3): 159-173.

Kunzelmann, K., V. M. Milenkovic, et al. (2007). "Calcium-dependent chloride conductance in epithelia: is there a contribution by Bestrophin?" Pflugers Archiv : European journal of physiology **454**(6): 879-889.

LaBranche, H., S. Dupuis, et al. (1998). "Telomere elongation by hnRNP A1 and a derivative that interacts with telomeric repeats and telomerase." Nature genetics **19**(2): 199-202.

Ladd, A. N., N. Charlet, et al. (2001). "The CELF family of RNA binding proteins is implicated in cell-specific and developmentally regulated alternative splicing." Mol Cell Biol **21**(4): 1285-1296.

Lalonde, M. R., M. E. Kelly, et al. (2008). "Calcium-activated chloride channels in the retina." Channels **2**(4): 252-260.

Lam, B. J. and K. J. Hertel (2002). "A general role for splicing enhancers in exon definition." RNA **8**(10): 1233-1241.

Lamichhane, R., G. M. Daubner, et al. (2010). "RNA looping by PTB: Evidence using FRET and NMR spectroscopy for a role in splicing repression." Proceedings of the National Academy of Sciences of the United States of America **107**(9): 4105-4110.

Lamond, A. I. and D. L. Spector (2003). "Nuclear speckles: a model for nuclear organelles." Nature reviews. Molecular cell biology **4**(8): 605-612.

Lang, K. M. and R. A. Spritz (1983). "RNA splice site selection: evidence for a 5' leads to 3' scanning model." Science **220**(4604): 1351-1355.

Lee, M. S., M. Henry, et al. (1996). "A protein that shuttles between the nucleus and the cytoplasm is an important mediator of RNA export." Genes & development **10**(10): 1233-1246.

Letai, A. G. (2008). "Diagnosing and exploiting cancer's addiction to blocks in apoptosis." Nature reviews. Cancer **8**(2): 121-132.

Letunic, I., R. R. Copley, et al. (2002). "Common exon duplication in animals and its role in alternative splicing." Human molecular genetics **11**(13): 1561-1567.

Licatalosi, D. D., A. Mele, et al. (2008). "HITS-CLIP yields genome-wide insights into brain alternative RNA processing." Nature **456**(7221): 464-469.

Lim, L. P. and C. B. Burge (2001). "A computational analysis of sequence features involved in recognition of short introns." Proceedings of the National Academy of Sciences of the United States of America **98**(20): 11193-11198.

Lin, C. H. and J. G. Patton (1995). "Regulation of alternative 3' splice site selection by constitutive splicing factors." RNA **1**(3): 234-245.

Lin, J. J. and V. A. Zakian (1994). "Isolation and characterization of two Saccharomyces cerevisiae genes that encode proteins that bind to (TG1-3)n single strand telomeric DNA in vitro." Nucleic acids research **22**(23): 4906-4913.

Liu, B., J. E. Linley, et al. (2010). "The acute nociceptive signals induced by bradykinin in rat sensory neurons are mediated by inhibition of M-type K+ channels and activation of Ca2+-activated Cl- channels." The Journal of clinical investigation **120**(4): 1240-1252.

Liu, H. X., S. L. Chew, et al. (2000). "Exonic splicing enhancer motif recognized by human SC35 under splicing conditions." Mol Cell Biol **20**(3): 1063-1071.

Liu, H. X., M. Zhang, et al. (1998). "Identification of functional exonic splicing enhancer motifs recognized by individual SR proteins." Genes Dev **12**(13): 1998-2012.

Liu, X. and J. E. Mertz (1995). "HnRNP L binds a cis-acting RNA sequence element that enables intron-dependent gene expression." Genes & development **9**(14): 1766-1780.

Llorian, M., S. Schwartz, et al. (2010). "Position-dependent alternative splicing activity revealed by global profiling of alternative splicing events regulated by PTB." Nature structural & molecular biology **17**(9): 1114-1123.

Loewen, M. E. and G. W. Forsyth (2005). "Structure and function of CLCA proteins." Physiological reviews **85**(3): 1061-1092.

Lopez, A. J. (1998). "Alternative splicing of pre-mRNA: developmental consequences and mechanisms of regulation." Annual review of genetics **32**: 279-305.

Lopez de Silanes, I., S. Galban, et al. (2005). "Identification and functional outcome of mRNAs associated with RNA-binding protein TIA-1." Molecular and cellular biology **25**(21): 9520-9531.

Lu, F., A. B. Gladden, et al. (2003). "An alternatively spliced cyclin D1 isoform, cyclin D1b, is a nuclear oncogene." Cancer research **63**(21): 7056-7061.

Lu, X., N. A. Timchenko, et al. (1999). "Cardiac elav-type RNA-binding protein (ETR-3) binds to RNA CUG repeats expanded in myotonic dystrophy." Human molecular genetics **8**(1): 53-60.

Luco, R. F. and T. Misteli (2011). "More than a splicing code: integrating the role of RNA, chromatin and non-coding RNA in alternative splicing regulation." Current opinion in genetics & development **21**(4): 366-372.

Luco, R. F., Q. Pan, et al. "Regulation of alternative splicing by histone modifications." Science **327**(5968): 996-1000.

Luco, R. F., Q. Pan, et al. (2010). "Regulation of alternative splicing by histone modifications." Science **327**(5968): 996-1000.

Machaca, K. and S. Haun (2002). "Induction of maturation-promoting factor during Xenopus oocyte maturation uncouples Ca(2+) store depletion from store-operated Ca(2+) entry." The Journal of cell biology **156**(1): 75-85.

MacLeish, P. R. and C. A. Nurse (2007). "Ion channel compartments in photoreceptors: evidence from salamander rods with intact and ablated terminals." Journal of neurophysiology **98**(1): 86-95.

Mahn, K., O. O. Ojo, et al. (2010). "Ca(2+) homeostasis and structural and functional remodelling of airway smooth muscle in asthma." Thorax **65**(6): 547-552.

Makeyev, A. V., D. L. Eastmond, et al. (2002). "Targeting a KH-domain protein with RNA decoys." RNA **8**(9): 1160-1173.

Manabe, R., N. Oh-e, et al. (1999). "Alternatively spliced EDA segment regulates fibronectin-dependent cell cycle progression and mitogenic signal transduction." The Journal of biological chemistry **274**(9): 5919-5924.

Manley, J. L. and A. R. Krainer (2010). "A rational nomenclature for serine/arginine-rich protein splicing factors (SR proteins)." Genes & development **24**(11): 1073-1074.

Manley, J. L. and R. Tacke (1996). "SR proteins and splicing control." Genes & development **10**(13): 1569-1579.

Manoury, B., A. Tamuleviciute, et al. (2010). "TMEM16A/anoctamin 1 protein mediates calcium-activated chloride currents in pulmonary arterial smooth muscle cells." The Journal of physiology **588**(Pt 13): 2305-2314.

Mardon, H. J., G. Sebastio, et al. (1987). "A role for exon sequences in alternative splicing of the human fibronectin gene." Nucleic acids research **15**(19): 7725-7733.

Markovtsov, V., J. M. Nikolic, et al. (2000). "Cooperative assembly of an hnRNP complex induced by a tissue-specific homolog of polypyrimidine tract binding protein." Mol Cell Biol **20**(20): 7463-7479.

Martinez-Contreras, R., P. Cloutier, et al. (2007). "hnRNP proteins and splicing control." Adv Exp Med Biol **623**: 123-147.

Martinez-Contreras, R., J. F. Fisette, et al. (2006). "Intronic binding sites for hnRNP A/B and hnRNP F/H proteins stimulate pre-mRNA splicing." PLoS Biol **4**(2): e21.

Matlin, A. J., J. Southby, et al. (2007). "Repression of alpha-actinin SM exon splicing by assisted binding of PTB to the polypyrimidine tract." RNA **13**(8): 1214-1223.

Matthews, H. R. and J. Reisert (2003). "Calcium, the two-faced messenger of olfactory transduction and adaptation." Current opinion in neurobiology **13**(4): 469-475.

Mayeda, A. and A. R. Krainer (1992). "Regulation of alternative pre-mRNA splicing by hnRNP A1 and splicing factor SF2." Cell **68**(2): 365-375.

Mayeda, A., S. H. Munroe, et al. (1994). "Function of conserved domains of hnRNP A1 and other hnRNP A/B proteins." The EMBO journal **13**(22): 5483-5495.

Mayeda, A., G. R. Screaton, et al. (1999). "Substrate specificities of SR proteins in constitutive splicing are determined by their RNA recognition motifs and composite pre-mRNA exonic elements." Molecular and cellular biology **19**(3): 1853-1863.

Mazzone, A., C. E. Bernard, et al. (2011). "Altered expression of Ano1 variants in human diabetic gastroparesis." The Journal of biological chemistry **286**(15): 13393-13403.

McCullough, A. J. and S. M. Berget (1997). "G triplets located throughout a class of small vertebrate introns enforce intron borders and regulate splice site selection." Molecular and cellular biology **17**(8): 4562-4571.

Miau, L. H., C. J. Chang, et al. (1998). "Identification of heterogeneous nuclear ribonucleoprotein K (hnRNP K) as a repressor of C/EBPbeta-mediated gene activation." The Journal of biological chemistry **273**(17): 10784-10791.

Michelotti, G. A., E. F. Michelotti, et al. (1996). "Multiple single-stranded cis elements are associated with activated chromatin of the human c-myc gene in vivo." Molecular and cellular biology **16**(6): 2656-2669.

Miledi, R. (1982). "A calcium-dependent transient outward current in Xenopus laevis oocytes." Proceedings of the Royal Society of London. Series B, Containing papers of a Biological character. Royal Society **215**(1201): 491-497.

Milenkovic, V. M., M. Brockmann, et al. (2010). "Evolution and functional divergence of the anoctamin family of membrane proteins." BMC evolutionary biology **10**: 319.

Minovitsky, S., S. L. Gee, et al. (2005). "The splicing regulatory element, UGCAUG, is phylogenetically and spatially conserved in introns that flank tissue-specific alternative exons." Nucleic acids research **33**(2): 714-724.

Miwa, S., T. Nakajima, et al. (2008). "Mutation assay of the novel gene DOG1 in gastrointestinal stromal tumors (GISTs)." Journal of gastroenterology **43**(7): 531-537.

Modrek, B. and C. J. Lee (2003). "Alternative splicing in the human, mouse and rat genomes is associated with an increased frequency of exon creation and/or loss." Nature genetics **34**(2): 177-180.

Montuenga, L. M. and R. Pio (2007). "Tumour-associated macrophages in nonsmall cell lung cancer: the role of interleukin-10." The European respiratory journal : official journal of the European Society for Clinical Respiratory Physiology **30**(4): 608-610.

Mouland, A. J., H. Xu, et al. (2001). "RNA trafficking signals in human immunodeficiency virus type 1." Molecular and cellular biology **21**(6): 2133-2143.

Mulder, M. P., W. Keijzer, et al. (1989). "Activated ras genes in human seminoma: evidence for tumor heterogeneity." Oncogene **4**(11): 1345-1351.

Munoz, M. J., M. S. Perez Santangelo, et al. (2009). "DNA damage regulates alternative splicing through inhibition of RNA polymerase II elongation." Cell **137**(4): 708-720.

Muro, A. F., M. Caputi, et al. (1999). "Regulation of fibronectin EDA exon alternative splicing: possible role of RNA secondary structure for enhancer display." Molecular and cellular biology **19**(4): 2657-2671.

Nakai, K. and H. Sakamoto (1994). "Construction of a novel database containing aberrant splicing mutations of mammalian genes." Gene **141**(2): 171-177.

Narla, G., A. Difeo, et al. (2005). "A germline DNA polymorphism enhances alternative splicing of the KLF6 tumor suppressor gene and is associated with increased prostate cancer risk." Cancer research **65**(4): 1213-1222.

Nilsen, T. W. and B. R. Graveley (2010). "Expansion of the eukaryotic proteome by alternative splicing." Nature **463**(7280): 457-463.

Oberstrass, F. C., S. D. Auweter, et al. (2005). "Structure of PTB bound to RNA: specific binding and implications for splicing regulation." Science **309**(5743): 2054-2057.

Okunola, H. L. and A. R. Krainer (2009). "Cooperative-binding and splicing-repressive properties of hnRNP A1." Molecular and cellular biology **29**(20): 5620-5631.

Olshavsky, N. A., C. E. Comstock, et al. (2010). "Identification of ASF/SF2 as a critical, allele-specific effector of the cyclin D1b oncogene." Cancer research **70**(10): 3975-3984.

Ousingsawat, J., J. R. Martins, et al. (2009). "Loss of TMEM16A causes a defect in epithelial Ca2+-dependent chloride transport." The Journal of biological chemistry **284**(42): 28698-28703.

Ousingsawat, J., M. Mirza, et al. (2011). "Rotavirus toxin NSP4 induces diarrhea by activation of TMEM16A and inhibition of Na+ absorption." Pflugers Archiv : European journal of physiology **461**(5): 579-589.

Pagani, F., E. Buratti, et al. (2002). "A new type of mutation causes a splicing defect in ATM." Nat Genet **30**(4): 426-429.

Pagani, F. and F. E. Baralle (2004). "Genomic variants in exons and introns: identifying the splicing spoilers." Nat Rev Genet **5**(5): 389-396.

Pagani, F., E. Buratti, et al. (2003). "Missense, nonsense, and neutral mutations define juxtaposed regulatory elements of splicing in cystic fibrosis transmembrane regulator exon 9." J Biol Chem **278**(29): 26580-26588.

Pagani, F., E. Buratti, et al. (2000). "Splicing factors induce cystic fibrosis transmembrane regulator exon 9 skipping through a nonevolutionary conserved intronic element." J Biol Chem **275**(28): 21041-21047.

Pagani, F., C. Stuani, et al. (2003). "New type of disease causing mutations: the example of the composite exonic regulatory elements of splicing in CFTR exon 12." Hum Mol Genet **12**(10): 1111-1120.

Pagani, F., C. Stuani, et al. (2003). "New type of disease causing mutations: the example of the composite exonic regulatory elements of splicing in CFTR exon 12." Human molecular genetics **12**(10): 1111-1120.

Pagani, F., C. Stuani, et al. (2003). "Promoter architecture modulates CFTR exon 9 skipping." The Journal of biological chemistry **278**(3): 1511-1517.

Pastor, T., G. Talotti, et al. (2009). "An Alu-derived intronic splicing enhancer facilitates intronic processing and modulates aberrant splicing in ATM." Nucleic acids research **37**(21): 7258-7267.

Pajares, M. J., T. Ezponda, et al. (2007). "Alternative splicing: an emerging topic in molecular and clinical oncology." The lancet oncology **8**(4): 349-357.

Pan, Q., O. Shai, et al. (2008). "Deep surveying of alternative splicing complexity in the human transcriptome by high-throughput sequencing." Nature genetics **40**(12): 1413-1415.

Pardo, L. A. and W. Stuhmer (2008). "Eag1: an emerging oncological target." Cancer research **68**(6): 1611-1613.

Park, E., J. Han, et al. (2006). "Cooperative actions of Tra2alpha with 9G8 and SRp30c in the RNA splicing of the gonadotropin-releasing hormone gene transcript." The Journal of biological chemistry **281**(1): 401-409.

Park, J. W., K. Parisky, et al. (2004). "Identification of alternative splicing regulators by RNA interference in Drosophila." Proceedings of the National Academy of Sciences of the United States of America **101**(45): 15974-15979.

Paronetto, M. P., M. Cappellari, et al. (2010). "Alternative splicing of the cyclin D1 proto-oncogene is regulated by the RNA-binding protein Sam68." Cancer research **70**(1): 229-239.

Pascual, M., M. Vicente, et al. (2006). "The Muscleblind family of proteins: an emerging class of regulators of developmentally programmed alternative splicing." Differentiation; research in biological diversity **74**(2-3): 65-80.

Patry, C., L. Bouchard, et al. (2003). "Small interfering RNA-mediated reduction in heterogeneous nuclear ribonucleoparticule A1/A2 proteins induces apoptosis in human cancer cells but not in normal mortal cell lines." Cancer research **63**(22): 7679-7688.

Peng, T., C. Xue, et al. (2008). "Functional importance of different patterns of correlation between adjacent cassette exons in human and mouse." BMC genomics **9**: 191.

Perez, I., C. H. Lin, et al. (1997). "Mutation of PTB binding sites causes misregulation of alternative 3' splice site selection in vivo." RNA **3**(7): 764-778.

Perrotti, D., V. Cesi, et al. (2002). "BCR-ABL suppresses C/EBPalpha expression through inhibitory action of hnRNP E2." Nature genetics **30**(1): 48-58.

Pettigrew, C., N. Wayte, et al. (2005). "Evolutionary conservation analysis increases the colocalization of predicted exonic splicing enhancers in the BRCA1 gene with missense sequence changes and in-frame deletions, but not polymorphisms." Breast Cancer Res **7**(6): R929-939.

Pettigrew, C. A. and M. A. Brown (2008). "Pre-mRNA splicing aberrations and cancer." Frontiers in bioscience : a journal and virtual library **13**: 1090-1105.

Piecyk, M., S. Wax, et al. (2000). "TIA-1 is a translational silencer that selectively regulates the expression of TNF-alpha." The EMBO journal **19**(15): 4154-4163.

Pinol-Roma, S. and G. Dreyfuss (1992). "Shuttling of pre-mRNA binding proteins between nucleus and cytoplasm." Nature **355**(6362): 730-732.

Pio, R. and L. M. Montuenga (2009). "Alternative splicing in lung cancer." Journal of thoracic oncology : official publication of the International Association for the Study of Lung Cancer **4**(6): 674-678.

Piper, A. S. and W. A. Large (2003). "Multiple conductance states of single Ca2+-activated Cl- channels in rabbit pulmonary artery smooth muscle cells." The Journal of physiology **547**(Pt 1): 181-196.

Pleiss, J. A., G. B. Whitworth, et al. (2007). "Rapid, transcript-specific changes in splicing in response to environmental stress." Molecular cell **27**(6): 928-937.

Qu, Z. and H. C. Hartzell (2008). "Bestrophin Cl- channels are highly permeable to HCO3." American journal of physiology. Cell physiology **294**(6): C1371-1377.

Radisky, D. C., D. D. Levy, et al. (2005). "Rac1b and reactive oxygen species mediate MMP-3-induced EMT and genomic instability." Nature **436**(7047): 123-127.

Ram, O. and G. Ast (2007). "SR proteins: a foot on the exon before the transition from intron to exon definition." Trends Genet **23**(1): 5-7.

Ram, O. and G. Ast (2007). "SR proteins: a foot on the exon before the transition from intron to exon definition." Trends in genetics : TIG **23**(1): 5-7.

Raponi, M., E. Buratti, et al. (2009). "Low U1 snRNP dependence at the NF1 exon 29 donor splice site." The FEBS journal **276**(7): 2060-2073.

Reed, R. (1989). "The organization of 3' splice-site sequences in mammalian introns." Genes & development **3**(12B): 2113-2123.

Reed, R. (1996). "Initial splice-site recognition and pairing during pre-mRNA splicing." Current opinion in genetics & development **6**(2): 215-220.

Reed, R. and T. Maniatis (1985). "Intron sequences involved in lariat formation during pre-mRNA splicing." Cell **41**(1): 95-105.

Ring, H. Z. and J. T. Lis (1994). "The SR protein B52/SRp55 is essential for Drosophila development." Mol Cell Biol **14**(11): 7499-7506.

Robberson, B. L., G. J. Cote, et al. (1990). "Exon definition may facilitate splice site selection in RNAs with multiple exons." Molecular and cellular biology **10**(1): 84-94.

Rock, J. R., C. R. Futtner, et al. (2008). "The transmembrane protein TMEM16A is required for normal development of the murine trachea." Developmental biology **321**(1): 141-149.

Rock, J. R., W. K. O'Neal, et al. (2009). "Transmembrane protein 16A (TMEM16A) is a Ca2+-regulated Cl- secretory channel in mouse airways." The Journal of biological chemistry **284**(22): 14875-14880.

Rooke, N., V. Markovtsov, et al. (2003). "Roles for SR proteins and hnRNP A1 in the regulation of c-src exon N1." Molecular and cellular biology **23**(6): 1874-1884.

Roscigno, R. F., M. Weiner, et al. (1993). "A mutational analysis of the polypyrimidine tract of introns. Effects of sequence differences in pyrimidine tracts on splicing." The Journal of biological chemistry **268**(15): 11222-11229.

Rothrock, C. R., A. E. House, et al. (2005). "HnRNP L represses exon splicing via a regulated exonic splicing silencer." The EMBO journal **24**(15): 2792-2802.

Ruskin, B., A. R. Krainer, et al. (1984). "Excision of an intact intron as a novel lariat structure during pre-mRNA splicing in vitro." Cell **38**(1): 317-331.

Russell, I. D. and D. Tollervey (1992). "NOP3 is an essential yeast protein which is required for pre-rRNA processing." The Journal of cell biology **119**(4): 737-747.

Rybak, J. N., C. Roesli, et al. (2007). "The extra-domain A of fibronectin is a vascular marker of solid tumors and metastases." Cancer research **67**(22): 10948-10957.

Ryner, L. C. and B. S. Baker (1991). "Regulation of doublesex pre-mRNA processing occurs by 3'-splice site activation." Genes & development **5**(11): 2071-2085.

Saltzman, A. L., Q. Pan, et al. (2011). "Regulation of alternative splicing by the core spliceosomal machinery." Genes & development **25**(4): 373-384.

Sambrook, J., Fritsch, E.F. & Maniatis, T. (1989). Molecular Cloning - A Laboratory Manual, Cold Spring Harbor Laboratory Press.

Sanchez, G., O. Delattre, et al. (2008). "Coupled alteration of transcription and splicing by a single oncogene: boosting the effect on cyclin D1 activity." Cell cycle **7**(15): 2299-2305.

Sanford, J. R., J. Ellis, et al. (2005). "Multiple roles of arginine/serine-rich splicing factors in RNA processing." Biochem Soc Trans **33**(Pt 3): 443-446.

Schaal, T. D. and T. Maniatis (1999). "Multiple distinct splicing enhancers in the protein-coding sequences of a constitutively spliced pre-mRNA." Molecular and cellular biology **19**(1): 261-273.

Scheid, M. P. and J. R. Woodgett (2001). "PKB/AKT: functional insights from genetic models." Nature reviews. Molecular cell biology **2**(10): 760-768.

Schroeder, B. C., T. Cheng, et al. (2008). "Expression cloning of TMEM16A as a calcium-activated chloride channel subunit." Cell **134**(6): 1019-1029.

Sharma, S. (2008). "Isolation of a sequence-specific RNA binding protein, polypyrimidine tract binding protein, using RNA affinity chromatography." Methods in molecular biology **488**: 1-8.

Sharp, P. A. (1994). "Split genes and RNA splicing." Cell **77**(6): 805-815.

Sheen-Chen, S. M., H. S. Chen, et al. (2003). "Circulating soluble Fas in patients with breast cancer." World journal of surgery **27**(1): 10-13.

Shen, H. and M. R. Green (2004). "A pathway of sequential arginine-serine-rich domain-splicing signal interactions during mammalian spliceosome assembly." Mol Cell **16**(3): 363-373.

Sheridan, J. T., E. N. Worthington, et al. (2011). "Characterization of the oligomeric structure of the Ca(2+)-activated Cl- channel Ano1/TMEM16A." The Journal of biological chemistry **286**(2): 1381-1388.

Shimizu, K., N. Hirose, et al. (2008). "Relationship between physical and cognitive function, blood pressure and serum lipid concentration in centenarians." Geriatrics & gerontology international **8**(4): 300-302.

Shimizu, T., E. L. Lee, et al. (2008). "Volume-sensitive Cl(-) channel as a regulator of acquired cisplatin resistance." Anticancer research **28**(1A): 75-83.

Simpson C. G., G. Thow, G. P. Clark, et al. (2002). “Mutational analysis of a plant branchpoint and polypyrimidine tract required for constitutive splicing of a mini-

exon.” RNA journal (8):47–56

Singh, N. N., E. J. Androphy, et al. (2004). "In vivo selection reveals combinatorial controls that define a critical exon in the spinal muscular atrophy genes." RNA **10**(8): 1291-1305.

Singh, N. N., J. Seo, et al. (2011). "TIA1 prevents skipping of a critical exon associated with spinal muscular atrophy." Molecular and cellular biology **31**(5): 935-954.

Singh, R., J. Valcarcel, et al. (1995). "Distinct binding specificities and functions of higher eukaryotic polypyrimidine tract-binding proteins." Science **268**(5214): 1173-1176.

Smith, C. W. and J. Valcarcel (2000). "Alternative pre-mRNA splicing: the logic of combinatorial control." Trends in biochemical sciences **25**(8): 381-388.

Solier, S., E. Logette, et al. (2005). "Nonsense-mediated mRNA decay among human caspases: the caspase-2S putative protein is encoded by an extremely short-lived mRNA." Cell death and differentiation **12**(6): 687-689.

Solomon, D. A., Y. Wang, et al. (2003). "Cyclin D1 splice variants. Differential effects on localization, RB phosphorylation, and cellular transformation." The Journal of biological chemistry **278**(32): 30339-30347.

Sontheimer, H. (2008). "An unexpected role for ion channels in brain tumor metastasis." Experimental biology and medicine **233**(7): 779-791.

Sorek, R., G. Ast, et al. (2002). "Alu-containing exons are alternatively spliced." Genome research **12**(7): 1060-1067.

Sorek, R., G. Lev-Maor, et al. (2004). "Minimal conditions for exonization of intronic sequences: 5' splice site formation in alu exons." Molecular cell **14**(2): 221-231.

Srebrow, A. and A. R. Kornblihtt (2006). "The connection between splicing and cancer." Journal of cell science **119**(Pt 13): 2635-2641.

Srebrow, A. and A. R. Kornblihtt (2006). "The connection between splicing and cancer." J Cell Sci **119**(Pt 13): 2635-2641.

Stamm, S. (2008). "Regulation of alternative splicing by reversible protein phosphorylation." J Biol Chem **283**(3): 1223-1227.

Stanek, D. and K. M. Neugebauer (2006). "The Cajal body: a meeting place for spliceosomal snRNPs in the nuclear maze." Chromosoma **115**(5): 343-354.

Stephan, A. B., E. Y. Shum, et al. (2009). "ANO2 is the cilial calcium-activated chloride channel that may mediate olfactory amplification." Proceedings of the National Academy of Sciences of the United States of America **106**(28): 11776-11781.

Stohr, H., J. B. Heisig, et al. (2009). "TMEM16B, a novel protein with calcium-dependent chloride channel activity, associates with a presynaptic protein

complex in photoreceptor terminals." The Journal of neuroscience : the official journal of the Society for Neuroscience **29**(21): 6809-6818.

Storey, S. and G. Wald (2008). "Novel agents in cystic fibrosis." Nature reviews. Drug discovery **7**(7): 555-556.

Skoko, N., M. Baralle, et al. (2008). "The pathological splicing mutation c.6792C>G in NF1 exon 37 causes a change of tenancy between antagonistic splicing factors." FEBS letters **582**(15): 2231-2236.

Sultan, M., M. H. Schulz, et al. (2008). "A global view of gene activity and alternative splicing by deep sequencing of the human transcriptome." Science **321**(5891): 956-960.

Sun, H. and L. A. Chasin (2000). "Multiple splicing defects in an intronic false exon." Molecular and cellular biology **20**(17): 6414-6425.

Talerico, M. and S. M. Berget (1990). "Effect of 5' splice site mutations on splicing of the preceding intron." Molecular and cellular biology **10**(12): 6299-6305.

Tarran, R., M. E. Loewen, et al. (2002). "Regulation of murine airway surface liquid volume by CFTR and Ca2+-activated Cl- conductances." J Gen Physiol **120**(3): 407-418.

Tazi, J., N. Bakkour, et al. (2009). "Alternative splicing and disease." Biochimica et biophysica acta **1792**(1): 14-26.

Takahashi, N., N. Sasagawa, et al. (2000). "The CUG-binding protein binds specifically to UG dinucleotide repeats in a yeast three-hybrid system." Biochemical and biophysical research communications **277**(2): 518-523.

Thiery, J. P., H. Acloque, et al. (2009). "Epithelial-mesenchymal transitions in development and disease." Cell **139**(5): 871-890.

Thiery, J. P. and J. P. Sleeman (2006). "Complex networks orchestrate epithelial-mesenchymal transitions." Nature reviews. Molecular cell biology **7**(2): 131-142.

Tian, M. and T. Maniatis (1992). "Positive control of pre-mRNA splicing in vitro." Science **256**(5054): 237-240.

Tian, Q., M. Streuli, et al. (1991). "A polyadenylate binding protein localized to the granules of cytolytic lymphocytes induces DNA fragmentation in target cells." Cell **67**(3): 629-639.

Tilgner, H., C. Nikolaou, et al. (2009). "Nucleosome positioning as a determinant of exon recognition." Nature structural & molecular biology **16**(9): 996-1001.

Tomonaga, T. and D. Levens (1995). "Heterogeneous nuclear ribonucleoprotein K is a DNA-binding transactivator." The Journal of biological chemistry **270**(9): 4875-4881.

Tsutsumi, S., N. Kamata, et al. (2004). "The novel gene encoding a putative transmembrane protein is mutated in gnathodiaphyseal dysplasia (GDD)." American journal of human genetics **74**(6): 1255-1261.

Turner, I. A., C. M. Norman, et al. (2004). "Roles of the U5 snRNP in spliceosome dynamics and catalysis." Biochemical Society transactions **32**(Pt 6): 928-931.

Valadkhan, S., A. Mohammadi, et al. (2009). "Protein-free small nuclear RNAs catalyze a two-step splicing reaction." Proceedings of the National Academy of Sciences of the United States of America **106**(29): 11901-11906.

Valcarcel, J. and F. Gebauer (1997). "Post-transcriptional regulation: the dawn of PTB." Current biology : CB **7**(11): R705-708.

Venables, J. P. (2007). "Downstream intronic splicing enhancers." FEBS letters **581**(22): 4127-4131.

Vezain, M., P. Saugier-Veber, et al. (2010). "A rare SMN2 variant in a previously unrecognized composite splicing regulatory element induces exon 7 inclusion and reduces the clinical severity of spinal muscular atrophy." Hum Mutat **31**(1): E1110-1125.

Villaz, M., J. C. Cinniger, et al. (1995). "A voltage-gated chloride channel in ascidian embryos modulated by both the cell cycle clock and cell volume." The Journal of physiology **488 (Pt 3)**: 689-699.

Vivanco, I. and C. L. Sawyers (2002). "The phosphatidylinositol 3-Kinase AKT pathway in human cancer." Nature reviews. Cancer **2**(7): 489-501.

Wagner, E. J., A. P. Baraniak, et al. (2005). "Characterization of the intronic splicing silencers flanking FGFR2 exon IIIb." The Journal of biological chemistry **280**(14): 14017-14027.

Wagner, E. J. and M. A. Garcia-Blanco (2001). "Polypyrimidine tract binding protein antagonizes exon definition." Molecular and cellular biology **21**(10): 3281-3288.

Wahl, M. C., C. L. Will, et al. (2009). "The spliceosome: design principles of a dynamic RNP machine." Cell **136**(4): 701-718.

Wang, B. B., M. O'Toole, et al. (2008). "Cross-species EST alignments reveal novel and conserved alternative splicing events in legumes." BMC plant biology **8**: 17.

Wang, E. T., R. Sandberg, et al. (2008). "Alternative isoform regulation in human tissue transcriptomes." Nature **456**(7221): 470-476.

Wang, L., M. Miura, et al. (1994). "Ich-1, an Ice/ced-3-related gene, encodes both positive and negative regulators of programmed cell death." Cell **78**(5): 739-750.

Wang, Y., J. L. Dean, et al. (2008). "Cyclin D1b is aberrantly regulated in response to therapeutic challenge and promotes resistance to estrogen antagonists." Cancer research **68**(14): 5628-5638.

Wang, Z. and C. B. Burge (2008). "Splicing regulation: from a parts list of regulatory elements to an integrated splicing code." RNA **14**(5): 802-813.

Wang, Z., M. E. Rolish, et al. (2004). "Systematic identification and analysis of exonic splicing silencers." Cell **119**(6): 831-845.

Warzecha, C. C., S. Shen, et al. (2009). "The epithelial splicing factors ESRP1 and ESRP2 positively and negatively regulate diverse types of alternative splicing events." RNA biology **6**(5): 546-562.

Watermann, D. O., Y. Tang, et al. (2006). "Splicing factor Tra2-beta1 is specifically induced in breast cancer and regulates alternative splicing of the CD44 gene." Cancer research **66**(9): 4774-4780.

West, R. B., C. L. Corless, et al. (2004). "The novel marker, DOG1, is expressed ubiquitously in gastrointestinal stromal tumors irrespective of KIT or PDGFRA mutation status." The American journal of pathology **165**(1): 107-113.

Witten, J. T. and J. Ule (2011). "Understanding splicing regulation through RNA splicing maps." Trends in genetics : TIG **27**(3): 89-97.

Will, C. L. and R. Luhrmann (2001). "Spliceosomal UsnRNP biogenesis, structure and function." Curr Opin Cell Biol **13**(3): 290-301.

Wu, J. Y. and T. Maniatis (1993). "Specific interactions between proteins implicated in splice site selection and regulated alternative splicing." Cell **75**(6): 1061-1070.

Wu, J. Y., H. Tang, et al. (2003). "Alternative pre-mRNA splicing and regulation of programmed cell death." Prog Mol Subcell Biol **31**: 153-185.

Wu, S., C. M. Romfo, et al. (1999). "Functional recognition of the 3' splice site AG by the splicing factor U2AF35." Nature **402**(6763): 832-835.

Xiao, Q., K. Yu, et al. (2011). "Voltage- and calcium-dependent gating of TMEM16A/Ano1 chloride channels are physically coupled by the first intracellular loop." Proceedings of the National Academy of Sciences of the United States of America **108**(21): 8891-8896.

Xing, Y. and C. Lee (2005). "Evidence of functional selection pressure for alternative splicing events that accelerate evolution of protein subsequences." Proceedings of the National Academy of Sciences of the United States of America **102**(38): 13526-13531.

Xing, Y. and C. Lee (2006). "Alternative splicing and RNA selection pressure--evolutionary consequences for eukaryotic genomes." Nature reviews. Genetics **7**(7): 499-509.

Xing, Y., A. Resch, et al. (2004). "The multiassembly problem: reconstructing multiple transcript isoforms from EST fragment mixtures." Genome research **14**(3): 426-441.

Xing, Y., A. Resch, et al. (2004). "The multiassembly problem: reconstructing multiple transcript isoforms from EST fragment mixtures." Genome Res **14**(3): 426-441.

Xu, N., C. Y. Chen, et al. (2001). "Versatile role for hnRNP D isoforms in the differential regulation of cytoplasmic mRNA turnover." Molecular and cellular biology **21**(20): 6960-6971.

Yang, Y. D., H. Cho, et al. (2008). "TMEM16A confers receptor-activated calcium-dependent chloride conductance." Nature **455**(7217): 1210-1215.

Yeo, G. W., N. G. Coufal, et al. (2009). "An RNA code for the FOX2 splicing regulator revealed by mapping RNA-protein interactions in stem cells." Nature structural & molecular biology **16**(2): 130-137.

Yeo, G. W., E. Van Nostrand, et al. (2005). "Identification and analysis of alternative splicing events conserved in human and mouse." Proceedings of the National Academy of Sciences of the United States of America **102**(8): 2850-2855.

Young, P. J., C. J. DiDonato, et al. (2002). "SRp30c-dependent stimulation of survival motor neuron (SMN) exon 7 inclusion is facilitated by a direct interaction with hTra2 beta 1." Hum Mol Genet **11**(5): 577-587.

Zeitlin, P. L., M. P. Boyle, et al. (2004). "A phase I trial of intranasal Moli1901 for cystic fibrosis." Chest **125**(1): 143-149.

Zhang, L., G. M. Vincent, et al. (2004). "An intronic mutation causes long QT syndrome." Journal of the American College of Cardiology **44**(6): 1283-1291.

Zhang, X., L. Sun, et al. (2011). "[Advances of LKB1-AMPK-mTOR Signaling Pathway in Tumor]." Zhongguo fei ai za zhi = Chinese journal of lung cancer **14**(8): 685-688.

Zhang, Y., J. C. Qi, et al. (2006). "[The animal research of recombinant adenovirus controlled by human telomerase reverse transcriptase promoter in the treatment of human prostate cancer]." Zhonghua wai ke za zhi [Chinese journal of surgery] **44**(18): 1252-1255.

Zheng, C. L., X. D. Fu, et al. (2005). "Characteristics and regulatory elements defining constitutive splicing and different modes of alternative splicing in human and mouse." RNA **11**(12): 1777-1787.

Zhong, X. Y., P. Wang, et al. (2009). "SR proteins in vertical integration of gene expression from transcription to RNA processing to translation." Molecular cell **35**(1): 1-10.

Zhu, M. H., T. W. Kim, et al. (2009). "A Ca(2+)-activated Cl(-) conductance in interstitial cells of Cajal linked to slow wave currents and pacemaker activity." The Journal of physiology **587**(Pt 20): 4905-4918.

Zuo, P. and T. Maniatis (1996). "The splicing factor U2AF35 mediates critical protein-protein interactions in constitutive and enhancer-dependent splicing." Genes Dev **10**(11): 1356-1368.

ABBREVIATIONS

The standard abbreviations used in this dissertation follow IUPAC rules. All the abbreviations are defined also in the text when they are introduced for the first time. The abbreviations mentioned only once are not included in this list.

3'SS	3' splice site
5'SS	5' splice site
ANO1	Anoctamin 1
AS	Alternative splicing
ASE	Alternative splicing events
bp	Base pairs
BP	Branch point
BS	Branch site
cDNA	complementary DNA
CE	capillary electrophoresis
CERES	Composite Exonic Regulatory Elements of Splicing gene
CFTR	Cystic Fibrosis Transmembrane conductance Regulator
CUG	Elav-like family member 1
DMEM	Dulbecco's modified Eagle medium
DNA	Deoxyribonucleic acid
dsDNA	double.stranded DNA
dNTPs	Deoxynucleoside triphosphate (A, C, G and T)
DTT	Dithiothreitol
EDTA	Ethylenediamine tetra-acetic acid
ESE	Exonic Splicing Enhancer
EST	Expressed sequence tag
ESS	Exonic Splicing Silencer
ESRP1FF	Epithelial Splicing Regulatory Protein 1FF
ESRP2FF	Epithelial Splicing Regulatory Protein 2FF
ETR3	Elav-like family member-3

hnRNP	Heterogenous nuclear ribonucleoprotein
HEK293	Human Embryonic Kidney 293
ISC	Intragenic Splicing Coordination
IPTG	Isopropyl-d-thiogalactopyranoside
ISE	Intronic Splicing Enhancer
ISS	Intronic Splicing Silencer
kb	Kilobase
kDa	Kilodalton
mRNA	messenger RNA
nt	Nucleotides
N	Nucleotide (A or C or G or T)
NMD	nonsense-mediated (mRNA) decay
NOVA2	Neuro-oncological ventral antigen 2
PBS	Phosphate buffer saline
PCR	Polymerase Chain Reaction
PESE	putative exonic splicing enhancer
PESS	putative exonic splicing silencer
PIP3	phosphatidylinositol-3,4,5-trisphosphate
Pol II	polymerase II
Pre-mRNA	precursor messenger RNA
PTB	polypyrimidine track binding protein
Pu	Purine (G or A)
Py	Pyrimidine (T or C)
RbFOX	Feminizing locus on X
RBP	RNA-binding protein
RNA	Ribonucleic acid
RNase	ribonuclease
RNA Pol II	RNA polymerase II
RRM	RNA Recognition Motif
RS	arginine-serine-rich
RT	reverse transcriptase
RT-PCR	reverse transcription and polymerase chain reaction

SDS	N-lauroylsarcosine sodium salt
SFs	splicing factors
shRNA	short hairpin RNA
SMN	Survival of Motor Neuron
snRNA	small nuclear RNA
snRNP	small nuclear RiboNucleoProtein
SR protein	Serine-arginine-rich protein
SS	splice site
ssDNA	single-stranded DNA
Taq	*Thermus aquaticus*
TBE	Tris-borate-EDTA
TIA1	T-cell Intracellular Antigen 1
TMEM16A	Trasmembran protein 16A gene
TRA2	Transformer 2
U	uridine
U2AF	U2 snRNP Auxiliary Factor
USCS	University of California, Santa Cruz
WB	wash buffer
WT	wild type

APPENDIX

Table 2. Oligonucleotides List. List of the primers used for PCR reactions. The DNA oligonucleotides were purchased form IDT (integrated DNA Technologies).

OLIGONUCLEOTIDES FOR REVERSE TRANSCRIPTION	
ALPHA 2-3	CAA CTT CAA GCT CCT AAG CCA CTG C
BRA2	TAG GAT CCG GTC ACC AGG AAG TTG GTT AAA TCA
OLIGONUCLEOTIDES FOR ENDOGENOUS RNAs AMPLIFICATION	
HUMAN:	
hTME_803Dir	CGG AGC ACG ATT GTC TAT GA
hTME_1385Rev	GGG CCA TGA AGA CAG AGA AG
hTME_1368Dir	TCT CTG TCT TCA TGG CCC TC
hTME_1525Rev	CTC CAA GAC TCT GGC TTC GT
hTME_1506Dir	ACG AAG CCA GAG TCT TGG AG
hTME_1894Rev	GGC TAT GCA GCC ATA CAC CT
MOUSE:	
mTME_915Dir	CGA CCT GAC TGA CTG ACA GGG ACT
mTME_1379Rev	GGG ATG TTT TCG TCC ACA GT
mTME_1167Dir	GGA GAT GTG TGA CCA GAG ATA CAA
mTME_1668Rev	TCT GGC TTC ATA CTC TGC TCT G
mTME_1646Dir	CCA GAG CAG AGT ATG AAG CCA
mTME_2121Rev	CAG GAA GGC CTT GAA GGT TA
OLIGONUCLEOTIDES FOR INTRAGENIC ALTERNATIVE SPLICING COORDINATION	
HUMAN:	
hANO1_Fam_803Dir*	[6FAM]CGG AGC ACG ATT GTC TAT GA
hTME_1894Rev	GGC TAT GCA GCC ATA CAC CT
Human NORMALIZZATION:	
hANO1_HEX_2335DIR-II	[HEX]AAC ATC ATC GAG ATC CGC CT
hANO1_2923REV-II	GCT CCT TCT CCA TCC AGG TT
MOUSE:	
mANO1_681dir	GAA GCA ACA CCT ATT CGA CCT GA
mANO1_Fam_1602rev*	[6FAM]CGG TCC CTC CAG GTC AGC TTC A

OLIGONUCLEOTIDES FOR MINIGENES CONSTRUCTS

ANO1ex6bNde2482DIR	TAC ATA TGA AAC CCT TCC CCA CAC AT
ANO1ex6bNde3117REV	TAC ATA TGT GCT CGA TTG GCA GAA TTA G
ANO1ex13Nde2595DIR	TAC ATA TGC CTG CTC AAT AGA GCA AGA CTC C
ANO1ex13Nde3060REV	TAC ATA TGC AGC CAT GAA CTG GCC CTG AGA AC
ANO1ex15Nde2585DIR	GGT TCA TAT GGG CAT GAC GCG GTC CAG TG
ANO1ex15Nde3197REV	GGT TCA TAT GCA CTT GCA GGC AGT TGT GAC A

Exon 6b minigene constructs:

MUT2A_ex6bmt2E_1aDIR	AGG CGA GGG AAA AAA AAA GGA CTC CGC CCT TCT AAG T
MUT2A_ex6bmt2E_1aREV	GGG CGG AGT CCT TTT TTT TTC CCT CGC CTT GCC CTG TTT
MUT2B_ex6bmt2E_1aDIR	AAG GCG AGG GAG AAG GAC TCC GCC CTT CTA A
MUT2B_ex6bmt2E_1aREV	GGG CGG AGT CCT TCT CCC TCG CCT TGC CCT GTT TA
MUT2C_ex6bmt2E_1aDIR	AGG CGA GGG AAG AAG GAC TCC GCC CTT CTA AGT A
MUT2C_ex6bmt2E_1aREV	GGC GGA GTC CTT CTT CCC TCG CCT TGC CCT G
MUT2D_ex6bmt2E_1aDIR	AAG GCG AGG GAG GAC TCC GCC CTT CTA AGT AA
MUT2D_ex6bmt2E_1aREV	GGG CGG AGT CCT CCC TCG CCT TGC CCT GTT TA
MUT2E_ex6bmt2E_1aDIR	AGG CGA GGG AAG AAA AAA GGA CTC CGC CCT TCT AAG TAA
MUT2E_ex6bmt2E_1aREV	GGC GGA GTC CTT TTT CCT TCC CTC GCC
MUT2F_ex6bmt2E_1aDIR	AGG CGA GGG AAA AAA GAA GGA CTC CGC CCT TCT AAG T
MUT2F_ex6bmt2E_1aREV	GCG GAG TCC TTC TTT TTT CCC TCG CCT TGC CCT GTT TAT
MUT2G_ex6bmt2E_1aDIR	AGG GCA AGG CGA AGA AAG AAG GAC TCC GCC CTT
MUT2G_ex6bmt2E_1aREV	GGA GTC CTT CTT TCT TTC GCC TTG CCC TGT TTA TAC A
MUT2H_ex6bmt2E_1aDIR	GAG GGA AGA AAG ACT CCG CCC TTC TAA GTA AAA G
MUT2H_ex6bmt2E_1aREV	AAG GGC GGA GTC TTT CTT CCC TCG CCT TGC C
MUT2I_ex6bmt2E_1aDIR	GCA AGG CGA AAG AAA GAA CTC CGC CCT TCT AAG TAA AGG
MUT2I_ex6bmt2E_1aREV	GAA GGG CGG AGT TCT TTC TTT CGC CTT GCC CTG TTT ATA CA
MUT2L_ex6bmt2E_1aDIR	GAG GGA AGA AAG AAC CAC TCC GCC CTT CTA AGT A
MUT2L_ex6bmt2E_1aREV	AAG GGC GGA GTG GTT CTT TCT TCC CTC GCC TTG CCC T
MUT2M_ex6bmt2E_1aDIR	GGC AAG GCG ACC CAA GAA AGA AGG ACT CCG CCC T
MUT2M_ex6bmt2E_1aREV	GTC CTT CTT TCT TGG GTC GCC TTG CCC TGT TTA TAC A
MUT-7_ex15_1aDIR	AAG TAT GGT AAG TGT GGG CAA CCT AAA ATC
MUT-7_ex15_1bREV	TTG GAA TTA GAT TTT AGG TTG CCC ACA CTT
MUT-8_ex15_1aDIR	CTC CTC CGG CTT TCC CAA TCT TCC AAA TTG TA
MUT-8_ex15_1bREV	AAA CAC ACA TAC AAT TTG GAA ATT GGG AAA G
MUT-9_ex15_1aDIR	CCC AAT CAA CCT AAA ATC TAA CTG ACA CCA T
MUT-9_ex15_1bREV	TGG AAA AAT TGA TGG TGT CAG TTA GAT TTT AG

MUT-10_ex15_1aDIR	ATT CCA AAT TGT ATG TGT GTT TTA CCA CTT ACA
MUT-10_ex15_1bREV	GAA GGT GGA TTG TAA GTG GTA AAA CAC ACA

Exon 13 minigene constructs:

MUT1_ex13_DIR	TGG GAG AGG GAC CTT CTC TCC TAA TCT CTT TCT
MUT1_ex13_REV	AGA AAG AGA TTA GGA GAG AAG GTC CCT CTC CAA

Exon 15 minigene constructs:

MUT-10_ex15_1aDIR	CGGGGGTGAAATTGGTACTTGCGGGCAGCGC
MUT-10_ex15_1aREV	TCAAGACGCGCGCTGCCCGCAAGTACCAAT
MUT-11_ex15_1bDIR	TTGCAGGCAATCAAAGTCGACCTCAACAAA
MUT-11_ex15_1bREV	TATACAACAGTTTGTTGAGGTCGACTTTGA
MUT-12_ex15_1cDIR	GTGTTTTTCCTCAACAAACTGACATTCACAT
MUT-12_ex15_1cREV	AGAAACACGGATGTGAATGTCAGTTTGTTG
MUT-13_ex15_1aDIR	CGGGGGTGAAATTGGTACTTGCACCCAGTGAGCCCAGCATG
MUT-13_ex15_1aREV	CATGCTGGGCTCACTGGGTGCAAGTACCAATTTCACCCCCG
MUT-14_ex15_1dDIR	TTCGGCACCCAGTGAGCCCATTGCGATGGC
MUT-14_ex15_1dREV	AGCCATGCAGTGCCATCGCAATGGGCTCACT
MUT-15_ex15_1eDIR	AGCCCAGCATGTTGCGATGGCACGCTATGGTGG
MUT-15_ex15_1eREV	CCACCGCAGACCCACCATAGCGTGCCATCGC
MUT-16_ex15_1aDIR	CTTCGGCACCCAGTGAGCCCACTATGGTGGGTCTGCGGTGGC
MUT-16_ex15_1aREV	GCCACCGCAGACCCACCATAGTGGGCTCACTGGGTGCCGAAG

RNA OLIGONUCLEOTIDES

WT	cagGGCAAGGCGAGGGAAGAAAGAAGGACUCCGCCCUUCUA
MUT2-A	cagGGCAAGGCGAGGGAAAAAAAAGGACUCCGCCCUUCUA
MUT2-E	cagGGCAAGGCGAGGGAAGAAAAAAGGACUCCGCCCUUCUA
MUT2-G	cagGGCAAGGCGAAAGAAAGAAGGACUCCGCCCUUCUAA
MUT2-H	cagGGCAAGGCGAGGGAAGAAAGAAACUCCGCCCUUCUAA
MUT2-I	cagGGCAAGGCGAAAGAAAGAAACUCCGCCCUUCUAA

FIGURES AND TABLES LEGEND

The Acknowledgement page of my PhD. Thesis